Organotechnetium complexes with nitrosyl ligands

Inaugural-Dissertation

to obtain the academic degree

Doctor rerum naturalium (Dr. rer. nat.)

submitted to the Department of Biology, Chemistry, Pharmacy

of Freie Universität Berlin

by

Abdullah Abdulkader

Berlin, 27.07.2020

This thesis was done in the period 03.2016 - 07.2020 in the research group of Prof. Dr. Ulrich Abram at the Institute of Chemistry and Biochemistry. It was independently done without the help of other sources than the ones cited and acknowledged and it was not submitted to any prior doctoral procedure.

1. Supervisor: Prof. Dr. Ulrich Abram
2. Supervisor: Prof. Dr. Christian Müller

Date of defense: __02.10.2020_____

Acknowledgment

I would like to express my gratitude and thankfulness to Prof. Dr. Ulrich Abram who gave me the opportunity to be one of his students, to introduce me to the radiochemistry field and to his superior supervision. His ideas, his patience, his kindness guided this thesis to the success.

I am gratefully thanking Prof. Dr. Christian Müller for being my second supervisor.

I would like to extend my gratitude and appreciation to Dr. Adelheid Hagenbach, for a lot of help during the lab work, for solving many crystallographic problems and for being so friendly to me, she was always ready to support and to give her helpful hand.

I sincerely thank Prof. Dr. Ernesto Schulz Lang for the chance to work in the Lab of his group and for the fantastic time I had in Brazil. Many thanks go to his group members for their technical helps in the lab and the time we had it together after the work. I will not forget the generous hospitality from Prof. Dr. Ricardo Schumacher and his wife Prof. Dr. Roberta Cargnelutti during my residency in Santa Maria, you were my family in Brazil.

I want to express my heartily thankfulness for my colleagues in the group, those who graduated and who are still working hard to achieve their goals, and who organize all what we need in the Lab. Thank you all for your countless helps and for every nice minute we had together during these four years, without your help I could not be able to finish this thesis: Jacqueline, Detlef, Falk, Eswari, Thang, Bruno, Janine, Sarah, Christelle, Suelen, Clemens, Li Bo, Domenik, Anna, Federico, Max, Guilhem, Carlos, Bruna, Felipe, Camila, Jessica, Janos and Till.

I would like to thank the Institute of Chemistry and Biochemistry of the Freie Universität Berlin and the analytical services. I thank Dr. Simon Steinhauer, who took care about the NMR facility.

This thesis is dedicated to my father and to my mother, to my brother Ali and my sister Sara, to my beloved wife Nour and to our little princess Maria. Your encouragement, support and love made all difficulties easier. There are no words that express my gratitude for all of you. Many thanks, you turned my dream into reality.

ربي ماتوفيقي إلا بك , وماهذا إلا فضل جديد من أفضالك ... فلك الحمد والشكر.

أعوذ بك أن يكون هذا العمل لِمَفخَرَةٍ أو عُجبٍ أو كِبرٍ, وأعني يارب على أن يكون في ماينفعني وينفع الناس.

Translation: Thank you my God almighty. I am sure that this work is entirely another gift from your uncountable grants. Hope I can use this knowledge for what is good for me and for your creatures.

Table of contents:

Abbreviations

Å	Ångstrom
A	Hyperfine coupling (EPR)
EPR	Electron paramagnetic resonance
g	g tensor
DMF	Dimethylformamide
DMSO	Dimethylsulfoxide
THF	Tetrahydrofuran
HTFA	Trifluoroacetic acid
Py	Pyridine
MeOH/MeO/Me	Methanol/Methoxy/Methyl
Cp	Cyclopentadienyl
CpMe	Methylcyclopentadienyl
CpCOOMe	Cyclopentadienyl methyl ester
NBu_4^+	Tetrabutylammonium
IR	Infrared
w	Weak (IR)
m	Medium (IR), multiplet (NMR)
s	Strong (IR), singlet (NMR)
vs	Very strong (IR)
NMR	Nuclear magnetic resonance
ppm	Parts per million
b	Broad
d	Doublet
t	Triplet
RT	Room temperature
UV/Vis	Ultraviolet/Visible
$\Delta\nu_{1/2}$	Line width

1 Introduction

The efficacy of techniques such as SPECT (single-photon emission computed tomography) and PET (positron emission tomography) in the clinical usage, as molecular imaging instruments drew the attention to gamma- and positron emitting radionuclides. Many reasons qualify the pure γ-emitter ^{99m}Tc (E_γ = 140 keV, $t_{1/2}$ = 6 h) to be the "workhorse" in diagnostic nuclear medicine.[1] Its short half-life minimizes the radiation exposure to the patient. Moreover, it is permanently available from ^{99}Mo/^{99m}Tc nuclide generators, and lastly no organ actively accumulates technetium, which ensures the fast release of non-targeted compounds from the human body.[2]

To extend and even improve the clinical application of ^{99m}Tc for an effective imaging of human organs, more information about the coordination chemistry of technetium is very beneficial. For such research studies, the long-lived β^- radioactive isotope ^{99}Tc (E_{max} = 294 keV, $t_{1/2}$ = 210.000 years) is available in macroscopic amounts. On the other hand, the homologous element rhenium, which has similar chemical properties, is frequently used as a model for technetium.

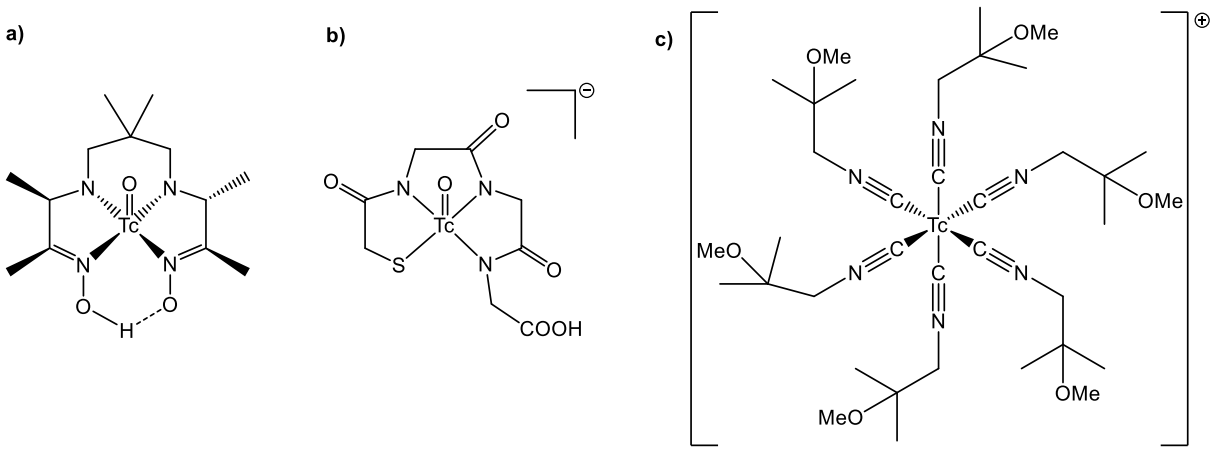

Figure 1.1: a) Ceretec®, b) ^{99m}Tc-MAG3 c) Cardiolite®

Examples for Tc-containing products, which are commonly used as radiopharmaceuticals are listed in Figure 1.1.[3] The first example is the neutral complex Ceretec® (Figure. 1.1), which was the first compound that passed the blood brain barrier and showed a good retention in the brain. Moreover, it possesses a reasonable lipophilicity, thus it is widely used for imaging of the brain. The anionic Tc(V) oxido complex ^{99m}Tc-MAG3 (MAG3: Mercaptoacetyltriglycin) is a key agent for nuclear imaging of the kidneys (Figure. 1.1). The high hydrophilicity of

^{99m}Tc-MAG3 makes it suitable for this purpose. The third complex is Cardiolite®, which proved to be the most successful imaging agent shown in Figure. 1.1. Cardiolite® is a cationic complex, in which technetium adopts the oxidation state "+I". It is specifically used for heart scans, in which a period of 5 minutes is enough to observe almost 5% heart uptake.

In fact, the use of Cardiolite as a radiopharmaceutical has drawn the attention to technetium complexes in the oxidation state "+I", which are very often stabilized by carbonyl or nitrosyl ligands. Thus, the focus of the present thesis is set on the usage of the nitrosyl ligand for the stabilization of low-valent technetium complexes.

The high stability of the nitrosyl-metal bond originates from the strong σ-bond and π-back bonding. Three bonding modes of nitrosyl ligands to metal ions are known: i) as nitrosonium ion (NO^+), ii) in their neutral form (NO) or iii) as nitroxide anion (NO^-) (Figure 1.2). While the nitrosonium (NO^+) molecule is linearly coordinating to the metal ion, NO and NO^- ligands usually coordinate in a bent mode. The coordination style of the NO molecule to the metal can be easily proved by crystal structure analysis and IR spectroscopy. The stretching mode of the linear NO^+ in the IR spectra occurs at wavenumbers between 1650 - 1900 cm^{-1} for Tc-NO complexes.[4]

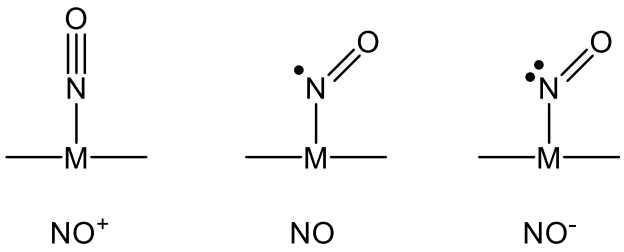

Figure 1.2: Types of bonding for NO ligands.

In addition to the "simple" coordination complexes of technetium, also organotechnetium compounds are of big interest and considered as potential building blocks in bioconjugates.[5-8] Promising attempts have been recently reported, describing cyclopentadienyl (Cp^-) derivatives of the $\{^{99m}Tc(CO)_3\}^+$ core, which can be readily accessed using the IsoLink Kit. In general, the chemistry of cyclopentadienyltechnetium complexes is still poorly developed.[9-13] This is particularly true for nitrosyltechnetium complexes with cyclopentadienyl units. On the other hand, there are many papers and a lot of crystal structures describing the fascinating chemistry of rhenium compounds of the general composition $[Re(NO)(L)(Cp)(PPh_3)]^{0,+1}$, where L can be almost any monodentate ligand.[14-18] A convenient synthesis of the analogous technetium

complex [Tc(NO)Cl(Cp)(PPh_3)] and some reactions of this novel precursor were successfully done, and some compounds of the general composition $[Tc(NO)(L)(Cp)(PPh_3)]^{0,+1}$ have been described (Fig. 1.3).[19,20]

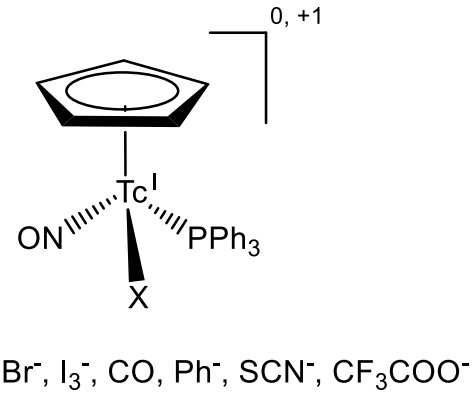

Figure 1.3: [Tc(NO)(L)(Cp)(PPh_3)] complexes.[19,20]

As a continuation of these promising results, the present thesis describes attempts concerning:

i) a further investigation of the reactivity of [Tc(NO)Cl(Cp)(PPh_3)] towards other monodentate ligands.

ii) the synthesis of new organotechnetium precursors in the lower oxidation state "+I" of this element.

iii) the extension of the former work to substituted derivatives of cyclopentadienyl, which in turn may open an access for coupling reactions with biologically active species.

iv) the extension of our knowledge about the less-explored cyclopentadienyl chemistry of technetium.

2 Results and discussion

The key compound of this dissertation, [Tc(NO)Cl(Cp)(PPh_3)], was prepared via a facile, two-step synthesis starting from the technetium (II) complex (NBu_4)[Tc(NO)Cl_4(MeOH)] (Fig. 2.1). The reaction of this compound with PPh_3 in acetonitrile gives [Tc(NO)Cl_2(PPh_3)$_2$(CH_3CN)], where technetium adopts the oxidation state "+1". The latter product reacts with KCp in boiling toluene to give [Tc(NO)Cl(Cp)(PPh_3)].[19]

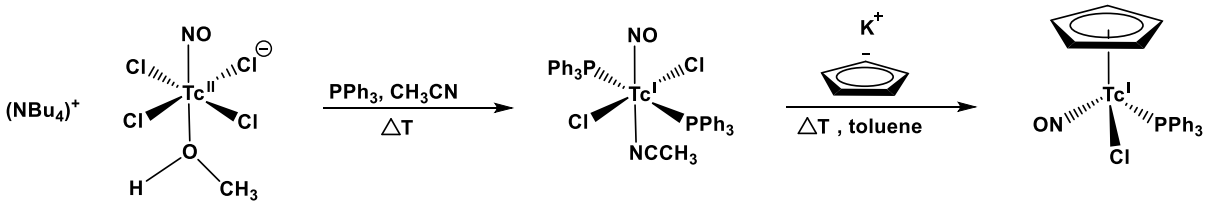

Fig. 2.1: Synthesis of [Tc(NO)Cl(Cp)(PPh_3)].[19]

[Tc(NO)Cl(Cp)(PPh_3)] is finally formed as dark red crystals, which are air stable and can be dissolved readily in almost all organic solvents. The compound shows a ^{99}Tc NMR signal at -234 ppm, while its ^{31}P NMR signal is at 29 ppm. Moreover, it shows a very strong IR absorption band of the NO ligand at 1681 cm^{-1}. These spectroscopic parameters are helpful tools for reactivity studies of [Tc(NO)Cl(Cp)(PPh_3)], since an exchange of only one of the ligands is indicated by large NMR shifts or a shift of the ν(NO) IR band.

Preliminary reactions of [Tc(NO)Cl(Cp)(PPh_3)] with a series of monodentate ligands L (L = Br^-, I_3^-, Ph^-, CO, CF_3COO^- or SCN^-) resulted in a ready replacement of the chlorido ligand and the formation of complexes of the general composition [Tc(NO)(L)(Cp)(PPh_3)]$^{0,+1}$. Technetium retains its oxidation state "+1" and its pseudotetrahedral coordination environment.[19][20] These results qualify [Tc(NO)Cl(Cp)(PPh_3)] as a suitable precursor for the further investigation of the chemistry of the {Tc(NO)(Cp)(PPh_3)}$^+$ core.

2.1 [Tc(NO)(L)(Cp)(PPh$_3$)] complexes (L = I$^-$, I$_3^-$, SCN$^-$) and their reactions

During reactions of [Tc(NO)Cl(Cp)(PPh$_3$)] with monodentate ligands such as halides or pseudohalides preferably the chlorido ligand is exchanged. This comes not completely unexpected with regard to the related rhenium chemistry and the previously reported reactions of [Tc(NO)Cl(Cp)(PPh$_3$)] with Me$_3$SiBr or HBr, which both gave the corresponding bromido complex in good yields.[19] Nevertheless, some of the reaction products with iodide or pseudohalides possess remarkable structural features or an unexpected reactivity. Figure 2.2 contains a summary of the performed reactions and the obtained products.

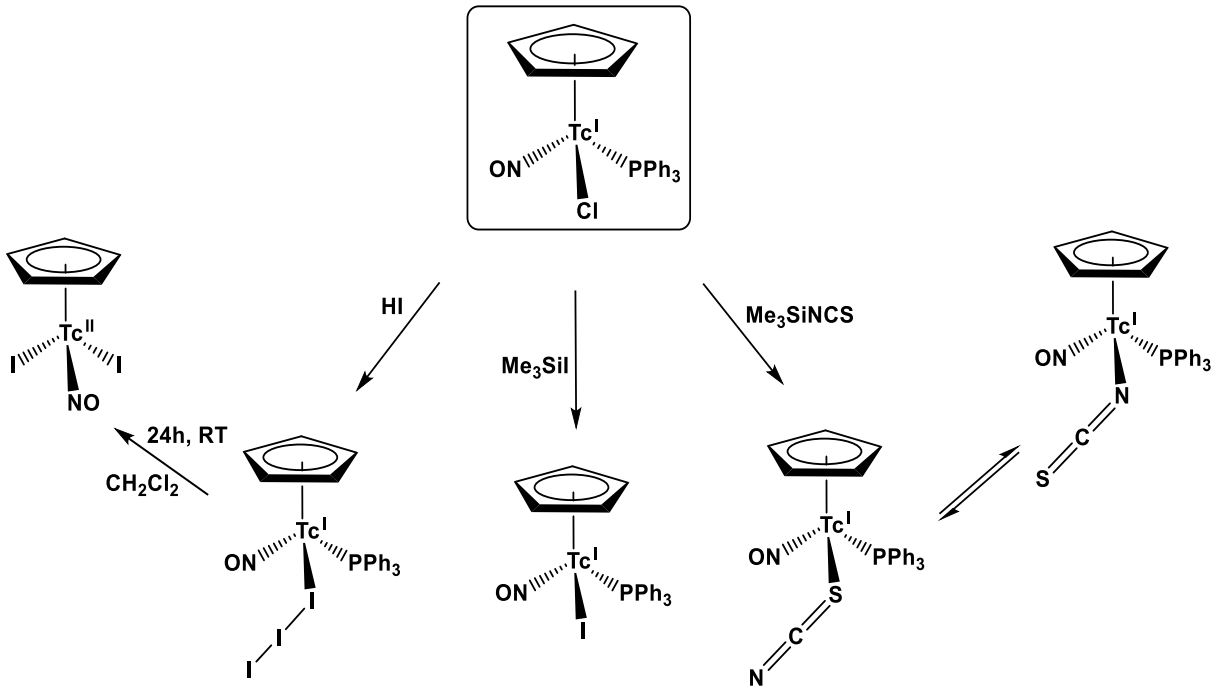

Figure 2.2: The synthesis and reactivity of [Tc(NO)(L)(Cp)(PPh$_3$)] complexes with L = I$^-$, I$_3^-$, or SCN$^-$.

The reaction of [Tc(NO)Cl(Cp)(PPh$_3$)] with Me$_3$SiNCS is straightforward and the red solid, which is formed after evaporation of the solvent, could be characterized as [Tc(NO)(SCN)(Cp)(PPh$_3$)].[20] Surprisingly, the SCN$^-$ ligand is *S*-bonded in this complex, while it is *N*-bonded in all other hitherto structurally characterized technetium complexes.[21-29] Thus, [Tc(NO)(SCN)(Cp)(PPh$_3$)] is the first example of a thiocyanato complex of technetium. The molecular structure of the compound is shown in Fig. 2.3. Clearly, the expected bent coordination of the SCN$^-$ ligand with a Tc-S20-C20 angle of 108.5(3)° is seen, which is in

contrast to the linearly bonded isothiocyanato ligands.[21-29] As in the other complexes of this thesis, the nitrosyl ligand is almost linearly coordinated (Tc-N10-O10 angle: 168.4(6)°) and can formally be regarded as NO^+.

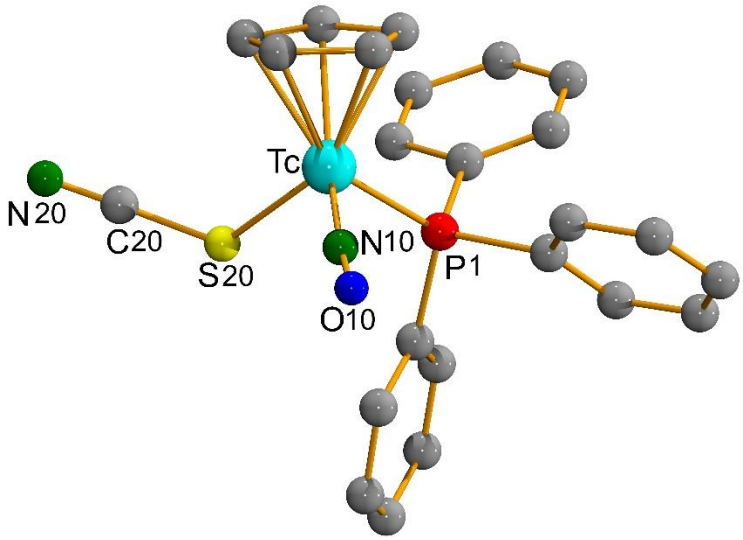

Fig. 2.3: Molecular structure of [Tc(NO)(SCN)(Cp)(PPh_3)].

The formation of coordination isomers with thiocyanato ligands is reported for many metals including the heavier homolog of technetium, rhenium. In some rhenium complexes, also isomerization reactions were observed.[30-32] Since the formation of a thiocyanato complex was unexpected and the reason for the preferred formation of the *S*-bonded complex in this particular ligand exchange on [Tc(NO)Cl(Cp)(PPh_3)] is not clear, some DFT calculations were done on the *S*- and *N*-bonded isomers. Indeed, there is a preference in total energy as well as in the Gibb's energy of about 22 kJ/mol for the isothiocyanato complex and the crystallized thiocyanato species should be regarded as a 'kinetic' product.[33]

The preference of [Tc(NO)(NCS)(Cp)(PPh_3)] over [Tc(NO)(SCN)(Cp)(PPh_3)] was a motivation to study a potential isomerization reaction on [Tc(NO)(SCN)(Cp)(PPh_3)]. For this, [Tc(NO)(SCN)(Cp)(PPh_3)] was dissolved in toluene and heated on reflux for a prolonged time (Fig. 2.4).

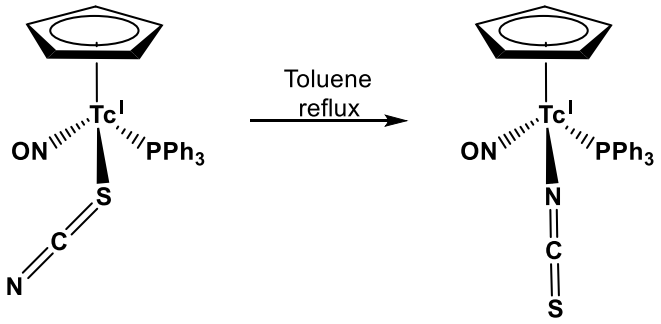

Fig. 2.4: Isomerization of [Tc(NO)(SCN)(Cp)(PPh_3)].

^{99}Tc NMR spectroscopy proved to be a perfect tool to monitor the course of this reaction. Figure 2.5 shows the ^{99}Tc NMR spectra obtained from such a solution of [Tc(NO)(SCN)-(Cp)(PPh_3)] in boiling toluene. The initially dominating signal at -816 ppm is assigned to the fully characterized *S*-bonded compound, but a second signal appears at -453 ppm, which can be assigned to the isothiocyanato species. This compound dominates after a heating period of 6 h. Prolonged heating, however, did not result in the formation of the pure *N*-bonded complex, but decomposition of the compounds becomes dominating, which goes along with a decrease of the overall intensities of both signals. Nevertheless, from the solution obtained after 6 h reflux in toluene, two different species could be isolated by fractionation: the red starting material and the orange-red isothiocyanato compound. Unfortunately, no single crystals of the orange-red complex suitable for X-ray diffraction could be obtained, but it shows the expected ^{99}Tc NMR resonance at -453 ppm and the ν_{CN} stretch in the IR spectrum is shifted by a value of 30 cm^{-1} to higher wavenumbers compared with the value of [Tc(NO)(SCN)(Cp)(PPh_3)].

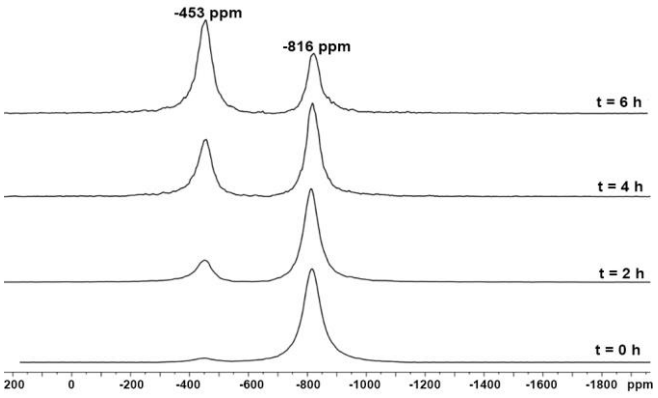

Figure 2.5: ^{99}Tc NMR spectra obtained from a solution of [Tc(NO)(SCN)(Cp)(PPh_3)] in boiling toluene.

The exchange of the chlorido ligand in [Tc(NO)Cl(Cp)(PPh_3)] by Br^- works straightforward and the corresponding bromido complex is readily formed during reactions with HBr or Me_3SiBr.[19] An analog reaction with HI, however, gives an unexpected result: the formation of

the triiodido complex [Tc(NO)(I_3)(Cp)(PPh_3)], the first structurally characterized technetium complex with a I_3^- ligand.[33] The triiodide ion is formed by oxidation of I^- in the reaction mixture and was also observed when carefully purified HI was used. The molecular structure of [Tc(NO)(I_3)(Cp)(PPh_3)] shows an I_3^- ligand: I1-I2-I3: angle 179.59(3)°). The I_3^- ligand is bent coordinated with a Tc-I1-I2 angle of 124.38(3)°. The I1-I2 bond of 3.060(1) Å is slightly longer than the I2-I3 bond (2.808(1) Å), which gives a bonding situation similar to that in the rhenium(I) complex [$Re(CO)_3(I_3)$(DPPE)] (DPPE = 1,2-diphenylphosphino ethane).[34]

[Tc(NO)(I_3)(Cp)(PPh_3)] is stable as solid, but CH_2Cl_2 solutions of this compound show already at room temperature a gradual change of their color from red to green. Parallelly, the intensity of the ^{99}Tc NMR signal decreases and disappears completely after approximately 24 h. A UV/Vis monitoring of the decomposition shows an isosbestic point at 594 nm (Fig. 2.6).

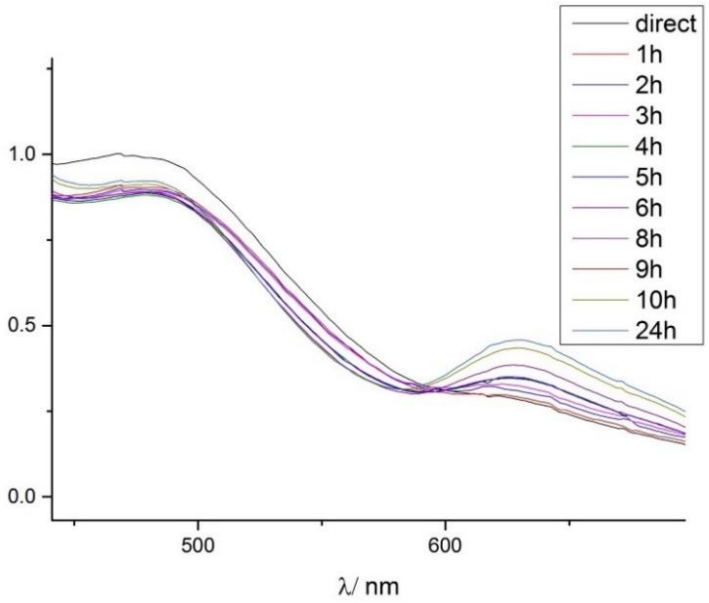

Figure 2.6: UV/Vis Spectra of a solution of [Tc(NO)(I_3)(Cp)(PPh_3)] in CH_2Cl_2 over 24 h.

The loss of the NMR signal and the detected color change are strong hints for a change of the oxidation state of technetium and indeed the resulting green solution gives intense, well-resolved EPR spectra, which prove the product as a Tc(II) compound. Figure 2.7 shows the EPR spectra of the compound in CH_2Cl_2 at room temperature and in frozen solution at T = 77 K. In the room-temperature spectrum, no ^{99}Tc hyperfine interactions are resolved, also that of a frozen solution has no clear separation of parallel and perpendicular parts, suggesting a non-axial coordination environment of technetium.

The spectrum of the compound obtained by the decomposition of [Tc(NO)(I_3)(Cp)(PPh_3)] can be described by a rhombic spin-Hamiltonian with the following parameters: g_x = 2.240, g_y =1.886, g_z =2.240, $A_x^{Tc} = 50 \cdot 10^{-4}$ cm^{-1}, $A_y^{Tc} = 70 \cdot 10^{-4}$ cm^{-1}, $A_z^{Tc} = 136 \cdot 10^{-4}$ cm^{-1}. The formation of a technetium(II) complex and the 'non-axial' symmetry of the observed EPR spectrum is readily understood by a view to the structure of the green oxidation product: [Tc(NO)(I_2)(Cp)]. Single crystals of the compound suitable for X-ray diffraction were obtained by storing a CH_2Cl_2/diethyl ether solution of the complex in a refrigerator.

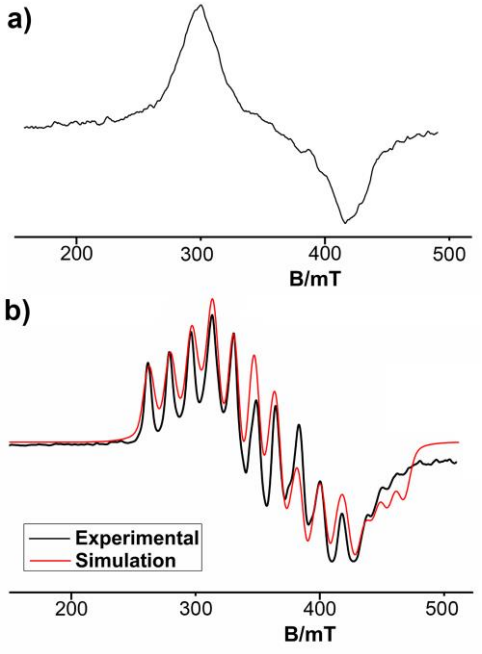

Figure 2.7: X-band EPR spectra of [Tc(NO)(I_2)(Cp)] in CH_2Cl_2 a) at room temperature and b) at T =77 K.

Figure 2.8 depicts the molecular structure of the reaction product. It becomes evident that the triiodide is cleaved, and the technetium ion is oxidized by the formally released iodine. Parallelly, the PPh_3 ligand is replaced by a second iodido ligand. The Tc-I bond lengths of 2.6731(3) and 2.677(3) Å are somewhat smaller than in the triiodo complex. The nitrosyl ligand in the Tc(II) complex is linearly bonded as those in the Tc(I) compounds, but the ν_{NO} stretch in the IR spectrum appears at 1746 cm^{-1}, which is clearly at higher wave numbers than the bands for the Tc(I) complexes, which appear between 1674 and 1710 cm^{-1}. This can be understood by a lower degree of back-donation into anti-bonding ligand orbitals by the d^5 system compared with the d^6 complexes.

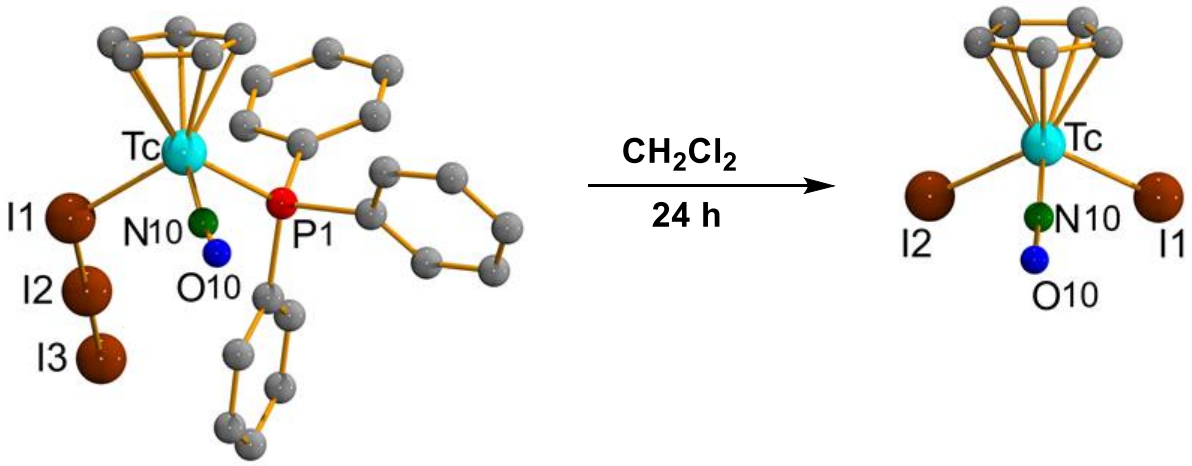

Figure 2.8: Molecular structures of [Tc(NO)(Cp)(I_3)(PPh_3)] and [Tc(NO)$(I)_2$(Cp)].

The synthesis of the corresponding monoiodido complex [Tc(NO)I(Cp)(PPh_3)] (Fig. 2.9) succeeded with the use of Me_3SiI as I^- source. The crystal structure of [Tc(NO)I(Cp)(PPh_3)] is of relatively low quality and could only be refined with isotropic thermal parameters, but clearly confirms the nature of the compound as an iodido complex. The Tc-I bond is approximately 2.70 Å, which is close to the value in the triiodo complex (2.704(1) Å). The ^{99}Tc NMR resonance is almost identical to that of the triiodido complex (-668 ppm), while a sharp signal was seen for the ^{31}P NMR resonance at 44 ppm. The complex shows a ν_{NO} stretch in the IR spectrum at 1682 cm^{-1}.

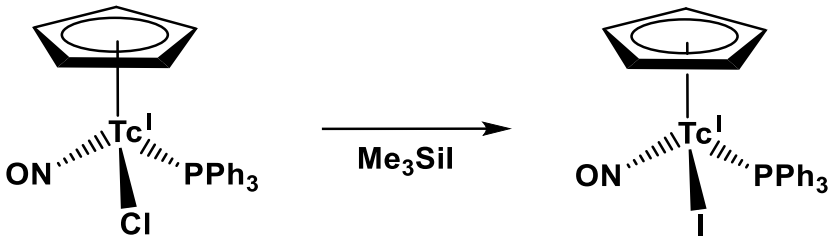

Figure 2.9. Synthesis of [Tc(NO)I(Cp)(PPh_3)].

Summarizing, it can be concluded that the ‘pseudotetrahedral’ technetium(I) complex [Tc(NO)Cl(Cp)(PPh_3)] possesses a robust {Tc(NO)(Cp)(PPh_3)}$^+$ core, which means that the chlorido ligand can readily be replaced by other monoanionic ligands such as halides or pseudohalides without replacement of other ligands.

The products are stable as long as the oxidation state of the transition metal is not changed. Oxidation of the technetium results in the loss of the PPh_3 ligand.

In solution, a slow isomerization of the thiocyanato compound [Tc(NO)(SCN)(Cp)(PPh_3)] into the thermodynamically more stable isothiocyanato species is observed, while solutions of [Tc(NO)(I_3)(Cp)(PPh_3)] undergo an internal oxidation under formation of the technetium(II) complex [Tc(NO)$(I)_2$(Cp)].

2.2 Dimerization of [Tc(NO)Cl(Cp)(PPh$_3$)] via a bridging chloride: [{Tc(NO)(Cp)(PPh$_3$)}$_2$Cl](PF$_6$) and synthesis of the phosphine complexes [Tc(NO)(Cp)(PPh$_3$)(L)](PF$_6$) (L = PPh$_3$, PMe$_3$)

A reaction of [Tc(NO)Cl(Cp)(PPh$_3$)] with AgPF$_6$ and PPh$_3$ in CH_2Cl_2 at room temperature did not result in the formation of the simple ligand exchange product [Tc(NO)(Cp)(PPh$_3$)$_2$](PF$_6$). Instead, a dimerization of the starting material was observed and a bridging chlorido ligand was established giving [{Tc(NO)(Cp)(PPh$_3$)}$_2$Cl](PF$_6$). Meanwhile, the usage of PMe$_3$ in boiling CH_2Cl_2 for 4h formed the complex [Tc(NO)(Cp)(PPh$_3$)(PMe$_3$)](PF$_6$). Thus, the first reaction with the PPh$_3$ was repeated in boiling toluene. After a reflux period of 6h, also the introduction of a second PPh$_3$ ligand and the formation of [Tc(NO)(Cp)(PPh$_3$)$_2$](PF$_6$) was observed.

The three new complexes where synthesized from the same starting complex [Tc(NO)Cl(Cp)(PPh$_3$)] (Fig. 2.10). Technetium remained in its original core ({Tc(NO)(Cp)(PPh$_3$}$^+$) and retained the oxidation state "+1".

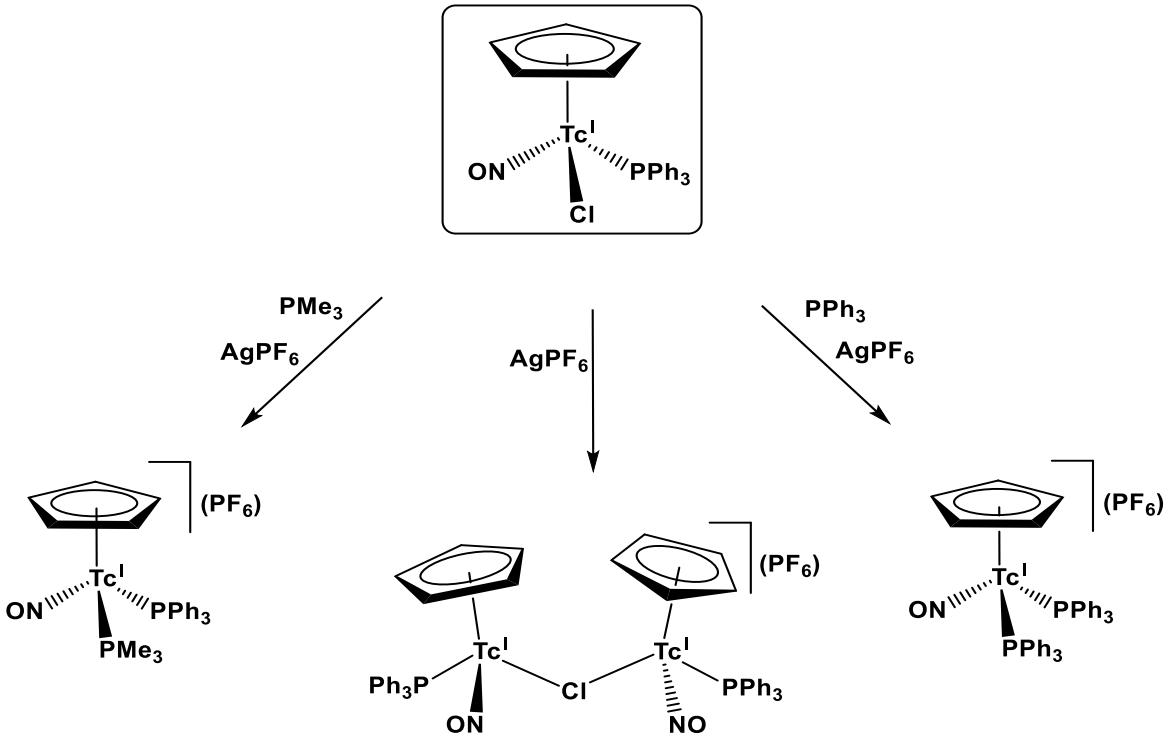

Figure 2.10: Syntheses of [{Tc(NO)(Cp)(PPh$_3$)}$_2$Cl](PF$_6$), [Tc(NO)(Cp)(PPh$_3$)$_2$](PF$_6$) and [Tc(NO)(Cp)(PPh$_3$)(PMe$_3$)](PF$_6$).

Also the corresponding rhenium unit $\{Re(NO)(Cp)(PPh_3)\}^+$ successfully coordinated to a second PPh_3 ligand. The corresponding complex $[Re(NO)(Cp)(PPh_3)_2](PF_6)$ was prepared by the treatment of $[Re(NO)(Cp)(PPh_3)(CO)]^+$ with $(CH_3)_3N^+O^-$ in the presence of PPh_3.[35]

The motivation for the performed reactions was to explore the ability of technetium, the lighter congener of rhenium, to bind a second bulky PPh_3 ligand on the $\{Tc(Cp)(NO)(PPh_3)\}^+$ moiety. Thus, first the reactivity of $[Tc(NO)Cl(Cp)(PPh_3)]$ was tested towards PPh_3 in CH_2Cl_2 at room temperature. The starting material was treated with $AgPF_6$ and an excess amount of PPh_3 was added. Surprisingly, no reaction with the added triphenylphosphine ligand was noticed under such conditions and instead, a dimerization of the starting complex was observed. The formed silver chloride precipitate was filtered off and the red residue was recrystallized from CH_2Cl_2/diethyl ether giving red crystals. An X-ray measurement of the crystals confirmed the formation of a dimeric complex with two $\{Tc(Cp)(NO)(PPh_3)\}^+$ units, which are bridged by a chlorido ligand. The repetition of the reaction in boiling dichloromethane also exclusively gave this compound. Since there is no consumption of PPh_3 during the reaction described above, it has been repeated without the addition of the phosphine, and $[\{Tc(NO)(Cp)(PPh_3)\}_2Cl](PF_6)$ was also obtained in a yield of approximately 50% (Fig. 2.11).

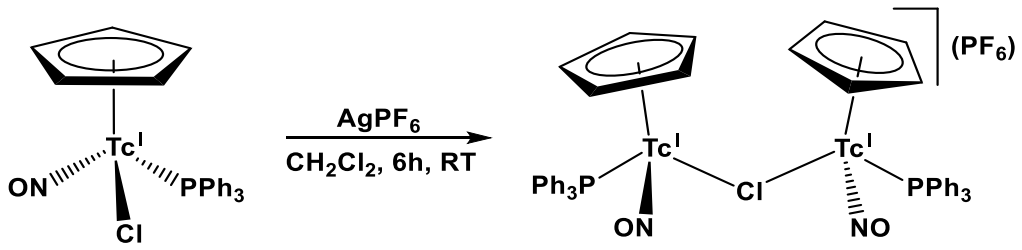

Figure 2.11: The synthesis of $[\{Tc(NO)(Cp)(PPh_3)\}_2Cl](PF_6)$.

The ^{99}Tc NMR spectrum of the dimeric complex shows a signal at -220 ppm, which is 15 ppm shifted to lower field in comparison to that of $[Tc(NO)Cl(Cp)(PPh_3)]$. No significant differences of the values for the ^{31}P NMR chemical shifts and the IR-spectral data have been observed between the monomeric and dimeric complexes. The crystal structure presents the two cyclopentadienyl rings in a gauche conformation to each other and a linear coordination mode for the NO^+ molecule has been adopted (Fig. 2.12).

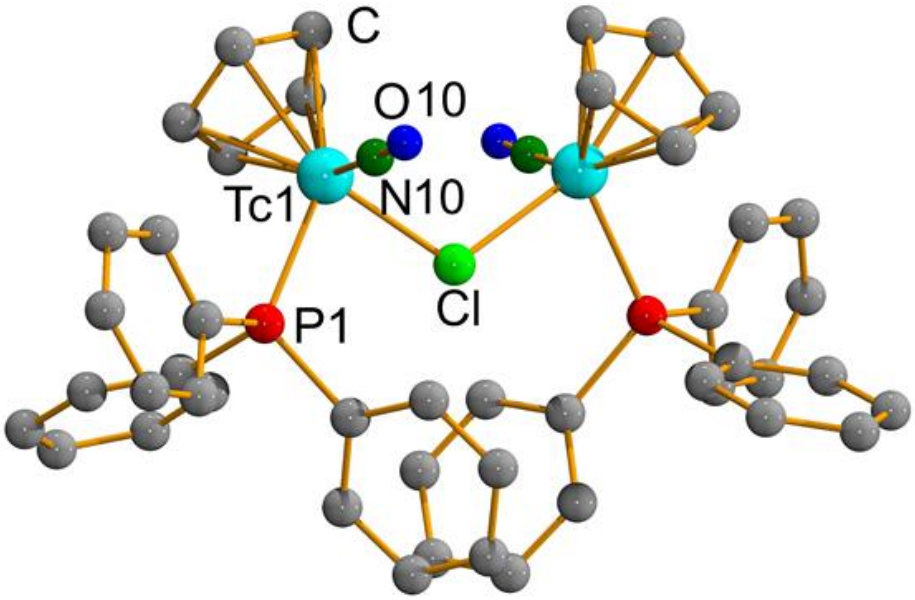

Figure 2.12: Structure of the complex cation of [{Tc(NO)(Cp)(PPh_3)}$_2$Cl](PF_6).

The analogous rhenium species, [{Re(NO)(Cp)(PPh_3)}$_2$Cl](BF_4) was made by the group of John Gladysz.[36] It was isolated from a reaction of [Re(NO)Cl(Cp)(PPh_3)] with $AgBF_4$ in boiling benzene, but only the corresponding iodido dimer [{Re(NO)(Cp)(PPh_3)}$_2$I](BF_4) was studied crystallographically.[36] The obtained structure is similar to the chlorido dimer [{Tc(NO)(Cp)(PPh_3)}$_2$Cl](PF_6).

Due to the initially supposed steric hindrance between two PPh_3 ligands on one metal center, a reaction with the smaller and more basic PMe_3 was performed. For this, [Tc(NO)Cl(Cp)(PPh_3)] was heated with $AgPF_6$ and PMe_3 in CH_2Cl_2 for 4 h. The reaction mixture turned gradually its color from red to light orange-red and a ^{99}Tc NMR measurement of the solution showed a new resonance for technetium at -1420 ppm. This significant shift in the ^{99}Tc resonance, from -235 (for [Tc(NO)Cl(Cp)(PPh_3)]) to -1420 ppm, and the appearance of two resonances in ^{31}P NMR spectra at 32 and 28 ppm, which are related to two different phosphine ligands, were strong hints for the formation of the [Tc(NO)(Cp)(PPh_3)(PMe_3)](PF_6) complex. This was confirmed by an X-ray diffraction study of the isolated yellow crystals. The molecular structure of [Tc(NO)(Cp)(PPh_3)(PMe_3)](PF_6) is shown in Fig. 2.13.

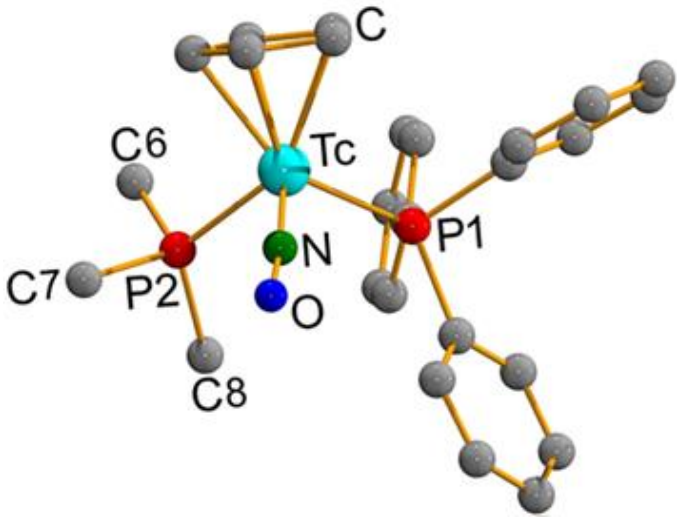

Figure 2.13: Structure of the complex cation of $[Tc(NO)(Cp)(PPh_3)(PMe_3)](PF_6)$.

The IR spectrum of the product shows an absorption for NO at 1718 cm^{-1}. The Tc-P1 and Tc-P2 bond lengths are similar: 2.383(1) and 2.390(1) Å. The angle P1-Tc-P2 is 95.50(5)º.

Similar reactions with the analogous rhenium core $\{Re(Cp)(NO)(PPh_3)\}^+$ were done with PPh_2H, PEt_2H and P*t*-Bu_2H. The secondary phosphine complexes $[Re(NO)(Cp)(PPh_3)(PR_2H)]^+$ (R = Ph, Et, *t*-Bu) were synthesized and subsequent treatment with BuO^-K^+ was made. This resulted in hydrogen cleavage from the (PR_2H) ligands and gave the corresponding phosphide complexes $[Re(NO)(Cp)(PPh_3)(PR_2)]$.[37]

With the isolation of $[Tc(NO)(Cp)(PPh_3)(PMe_3)](PF_6)$, it was demonstrated that a second phosphine ligand can in principle be coordinated to the $\{Tc(Cp)(NO)(PPh_3)\}^+$ core. Finally, this also succeeded with PPh_3. But harsh reaction conditions were required. Heating of $[Tc(NO)Cl(Cp)(PPh_3)]$ with $AgPF_6$ and PPh_3 in boiling toluene for a prolonged time (6h) gave the expected product $[Tc(NO)(Cp)(PPh_3)_2](PF_6)$. A new ^{99}Tc NMR signal was observed at -1219 ppm and the color of the initially red solution turned to orange-yellow. The residual product was recrystallized from a CH_2Cl_2/toluene mixture giving orange-yellow crystals. The X-ray structural analysis of the crystals confirms the presence of a second triphenylphosphine ligand as is shown in Figure 2.14.

The Tc1-P1 and Tc1-P2 bond lengths are 2.389 and 2.433 (Å). An intense, sharp signal at 22 ppm in the ^{31}P NMR spectrum of the product is related to the magnetically equivalent PPh_3 ligands. The IR spectrum shows a ν_{NO} stretch at 1720 cm^{-1}.

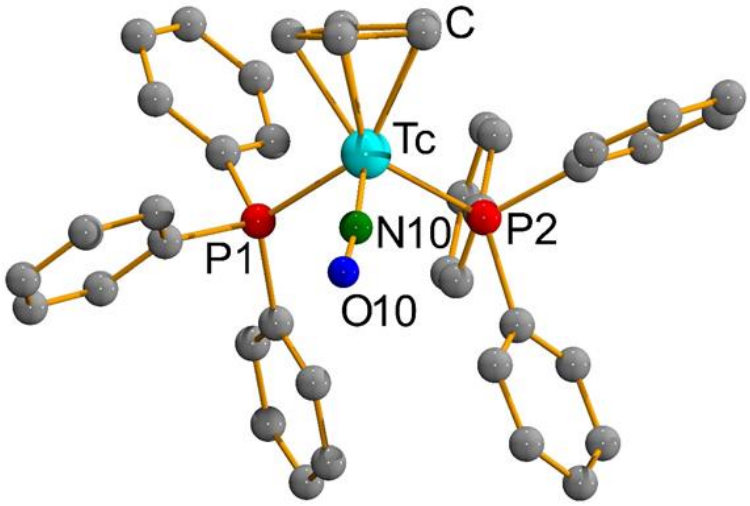

Figure 2.14: Structure of the complex cation of $[Tc(NO)(Cp)(PPh_3)_2](PF_6)$.

$[Tc(NO)(Cp)(PPh_3)_2](PF_6)$ is stable on air and was obtained in a reasonable yield (45%).

It is important to mention that particularly ^{31}P and ^{99}Tc NMR analysis of the reaction mixtures was an efficient tool to observe the course of the reactions and to optimize the elevation of the heating. The ^{99}Tc resonances for the three complexes, which are described in this chapter are shown in Figure 2.15.

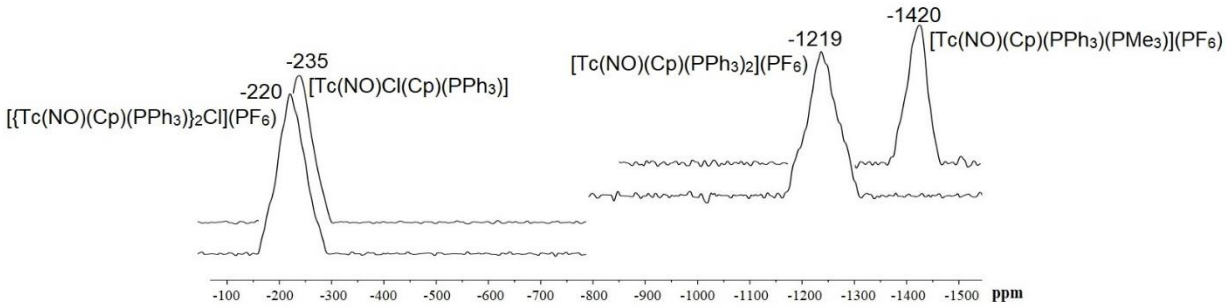

Figure 2.15: ^{99}Tc NMR resonances for the complexes $[\{Tc(NO)(Cp)(PPh_3)\}_2Cl](PF_6)$, $[Tc(NO)Cl(Cp)(PPh_3)]$, $[Tc(NO)(Cp)(PPh_3)_2](PF_6)$ and $[Tc(NO)(Cp)(PPh_3)(PMe_3)](PF_6)$.

Summarizing, it can be concluded that $[Tc(NO)Cl(Cp)(PPh_3)]$ showed again its potential as a precursor molecule for the synthesis of interesting species and derivatives of this robust core. The abstraction of the chlorido ligands from $[Tc(NO)Cl(Cp)(PPh_3)]$ with $AgPF_6$ without the addition of another ligand, is not quantitative and results in a dimerization of the starting complex. The $\{Tc(NO)(Cp)(PPh_3)\}^+$ core can accommodate a second bulky PPh_3 ligand, when prolonged reaction times at elevated temperature are applied.

2.3 Synthesis of the carbene complex $[Tc^{I}(NO)(Cp)(PPh_3)\{C(OMe)\text{-}C_2H_4PPh_3\}](PF_6)_2$ and related compounds

The treatment of $[Tc(NO)Cl(Cp)(PPh_3)]$ with $AgPF_6$ and the symmetrical alkynes RC≡CR [R = CH_3, C_2H_5] did not give the intended products $[Tc(NO)(Cp)(PPh_3)(RC{\equiv}CR)](PF_6)$. In contrary, no reactivity could be observed between the used alkynes and the technetium precursor and consequently no products with coordinated alkynes could be isolated or at least detected spectroscopically. This behavior is clearly in contrast to the behavior of the analogous rhenium complexes, which show an extended chemistry with alkynes or alkenes. Previous work of Gladysz demonstrated the versatility of these ligands and a large number of reactions has been performed particularly with alkynes.[38,39]

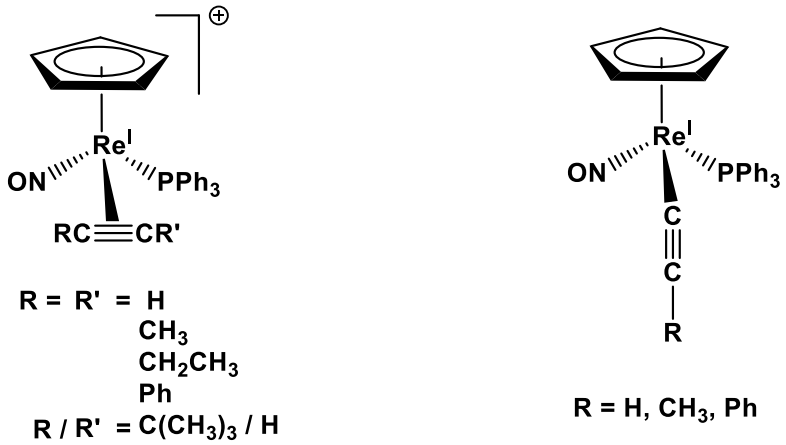

Figure 2.16: $[Re(NO)(Cp)(PPh_3)(RC{\equiv}CR)]^+$ and $[Re(NO)(C{\equiv}CR)(Cp)(PPh_3)]$ complexes. [38,39]

As shown in Figure 2.16, the $[Re(NO)Cl(Cp)(PPh_3)]$ readily forms products with symmetrical (2-butyne, 3-hexyne) and unsymmetrical alkynes (2-hexyne, tert-butyl-acetylene). A side on coordination mode was observed between the former alkynes and the metal center. The structure of the 3-hexyne complex $[Re(NO)(Cp)(PPh_3)(C_2H_5C{\equiv}CC_2H_5)](BF_4)$ (Fig. 2.17) shows a kind of cleft opened between two phenyl rings of the PPh_3 ligand to accommodate the ethyl group. This observation proved that the alkyne molecule adjusted to fit close to the bulky triphenylphosphine ligand with no real influence of the steric hindrance of this large ligand.

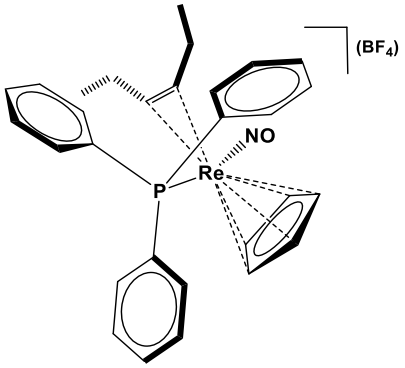

Figure 2.17: Structure of [Re(NO)(Cp)(PPh_3)($C_2H_5C{\equiv}CC_2H_5$)](BF_4).[38]

The rhenium core $\{Re(Cp)(NO)(PPh_3)\}^+$ can also coordinate to alkynes in an end-on-mode. In this case, the alkyne acts as a negatively charged ligand. [39]

Attempted reactions of [Tc(NO)Cl(Cp)(PPh_3)] with symmetrical alkynes gave no hints for the formation of alkyne-containing products (Fig. 2.18). The parallel addition of $AgPF_6$ resulted in a partial Cl^- abstraction. Finally, red crystals could be isolated, which were characterized spectroscopically and by X-ray diffraction as the dimeric complex [{Tc(NO)(Cp)(PPh_3)}$_2$Cl]-(PF_6). This compound has been isolated as well in good yields, when [Tc(NO)Cl(Cp)(PPh_3)] was treated with $AgPF_6$ without the presence of any other ligand (see also the discussion in the previous chapter).

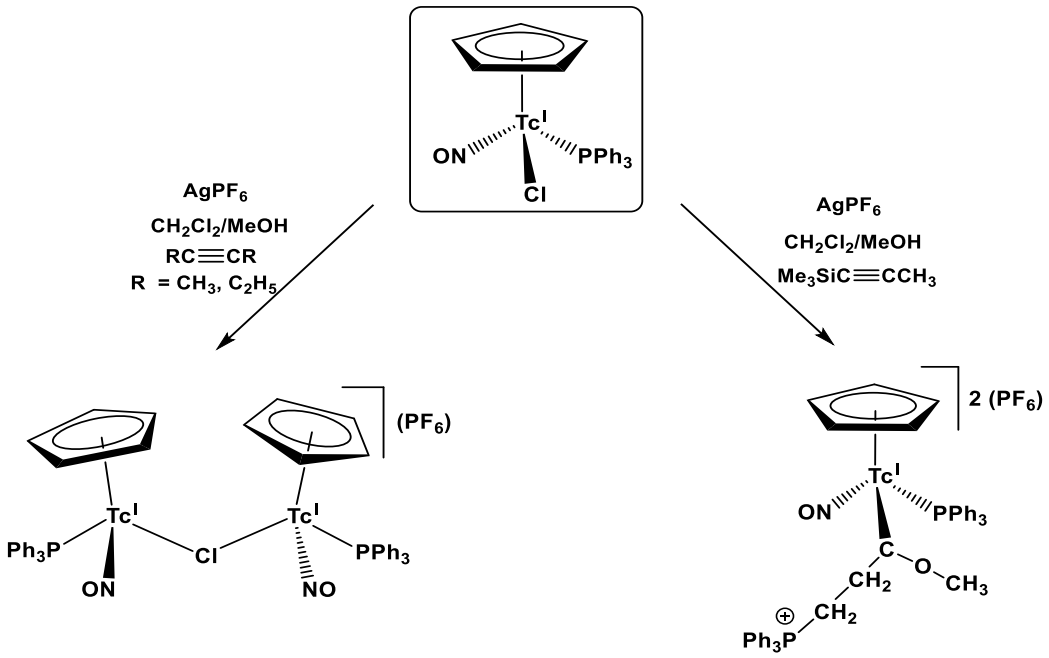

Figure 2.18: Attempted reactions of [Tc(NO)Cl(Cp)(PPh_3)] with the alkynes and synthesis of the complex [Tc(NO)(Cp)(PPh_3){$C(OMe)C_2H_4PPh_3$}](PF_6)$_2$.

So far, it was clear that no reactivity have been recognized between [Tc(NO)Cl(Cp)(PPh_3)] and the symmetrical alkynes (Fig. 2.18). On the other hand, it was shown previously in Figure 2.17 how the bulky PPh_3 ligand could adjust to allow the side part of the alkyne to fit in the molecular structural of the $[Re(NO)(Cp)(PPh_3)(C_2H_5C{\equiv}CC_2H_5)]^+$ with no steric hindrance. Consequently, it is not very probable that the bulky PPh_3 ligand blocks the alkyne and avoid its coordination to the technetium atom.

Next, trimethylsilylalkynes were used as alkyne sources. Such reactions were more promising in a way that clearly a change of the color of the reaction mixtures was observed upon the addition of $Ag(PF_6)$, which was dissolved in a CH_2Cl_2/MeOH, 2:1 mixture. The reaction was stirred in toluene for 5h at room temperature. The ^{99}Tc NMR spectrum of the resulting reaction mixture showed a new signal at -1375 ppm, which was not $[\{Tc(NO)(Cp)(PPh_3)\}_2Cl]^+$ (chem. shift -220 ppm) or $[\{Tc(NO)(Cp)(PPh_3)_2]^+$ (chem. shift -1219 ppm) (see Fig. 2.19).

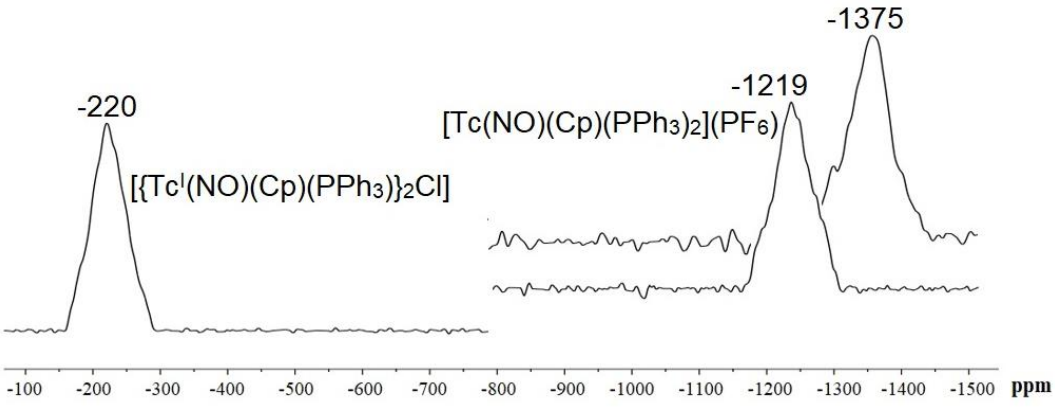

Figure 2.19: ^{99}Tc NMR spectra for $[\{Tc^I(NO)(Cp)(PPh_3)\}_2Cl](PF_6)$ (-220 ppm), $[Tc(NO)(Cp)(PPh_3)_2](PF_6)$ (-1219 ppm) , and the reaction product between [Tc(NO)Cl(Cp)(PPh_3)] and trimethylsilylacetylene in dichloromethane (-1375 ppm).

Although several attempts were performed, no pure and crystalline compound could be isolated. More successful was the related reaction with trimethylsilylpropyne (Fig. 2.18). It resulted in a product with a ^{99}Tc NMR signal at -1371 ppm. Crystals suitable for an X-ray structure were grown from the resulting brown product. The X-ray diffraction analysis (Fig. 2.20) indicates the formation of an unusual carbene complex of technetium: $[Tc(NO)(Cp)(PPh_3)\text{-}\{C(OMe)C_2H_4PPh_3\}](PF_6)_2$.

The product is one of the very few examples of Fischer-type carbenes of technetium and the first cationic one. Hitherto, only one of such compounds has been isolated in pure form and studied by X-ray crystallography: $[Tc(Cp)(CO)_2\{C(OEt)Ph\}]$.[40] It has been prepared in the classical way by treatment of $[Tc(CO)_3(Cp)]$ with LiPh and subsequent addition of $(Et_3O)BF_4$.

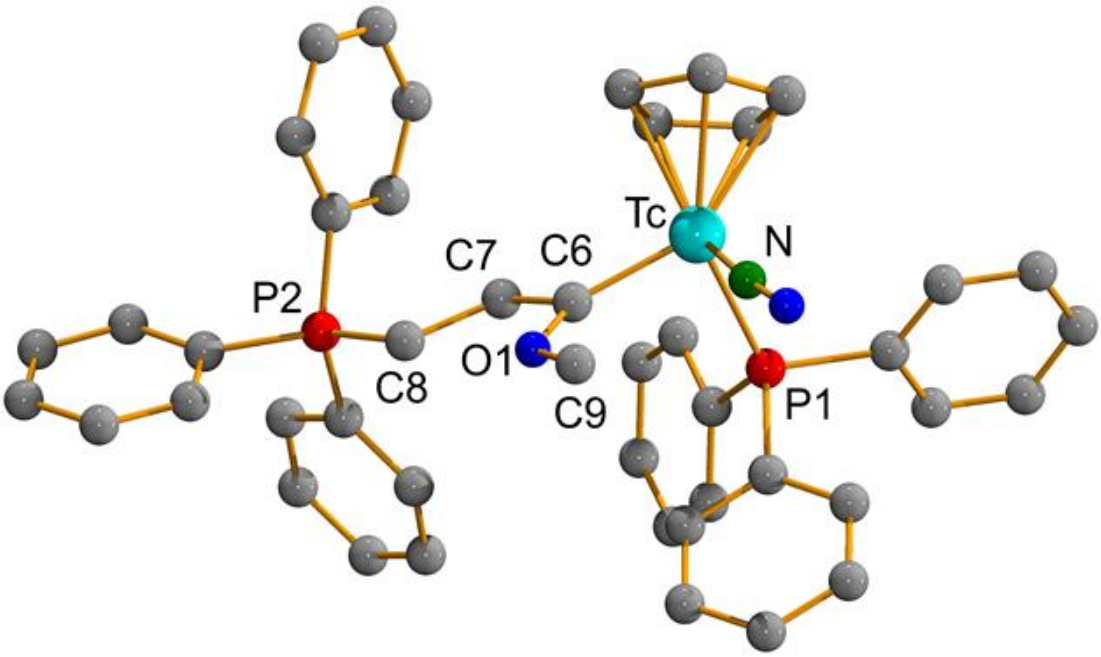

Figure 2.20: Structure of the complex cation of $[Tc(NO)(Cp)(PPh_3)\{C(OMe)C_2H_4PPh_3\}](PF_6)_2$.

The formation of $[Tc(NO)(Cp)(PPh_3)\{C(OMe)C_2H_4PPh_3\}](PF_6)_2$ from $[\{Tc(NO)(Cp)(PPh_3\}_2Cl](PF_6)$, which is with respect to the ^{99}Tc NMR spectra the dominant species in the starting solution, requires a kind of a programmed assembly of the species inside the reaction mixture. The process may involve the liberation of a C_3 building block, which coordinates first in a carbide-type fashion on technetium. A subsequent attack of MeOH and PPh_3 finally gives the cationic carbene complex with a peripheral phosphonio substituent (Fig. 2.21). The ^{31}P NMR spectrum of the complex shows a sharp signal at 29 ppm related to the PPh_3 ligand. This value is similar to resonances of the related technetium complexes. The phosphonio moiety gives a broad signal at 11 ppm. The IR-spectrum of the complex shows a strong ν_{NO} stretch at 1721 cm^{-1}.

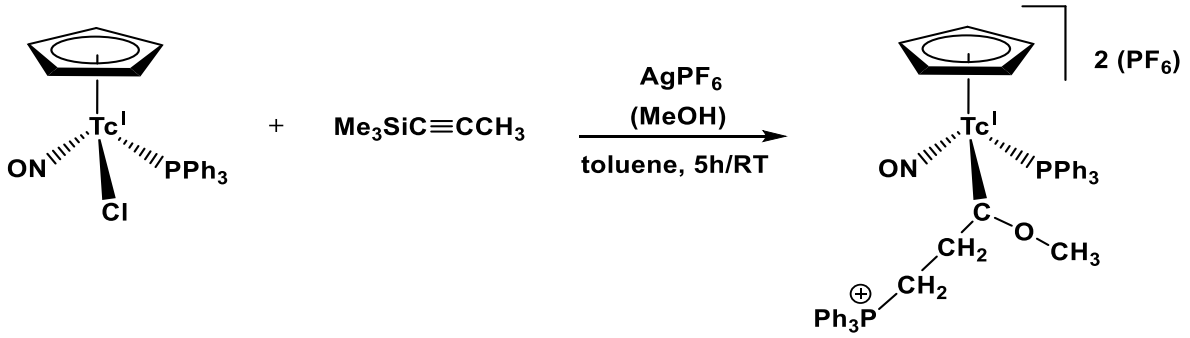

Figure 2.21: The synthesis of $[Tc(NO)(Cp)(PPh_3)\{C(OMe)C_2H_4PPh_3\}](PF_6)_2$.

Structurally similar carbene complexes have produced for manganese and rhenium (Figure 2.22).[41-42] They do not contain the phosphonio substituent, but there are also examples, where such compounds have been formed with released PPh_3 ligands. The example of a corresponding ruthenium complex has been added to Figure 2.22.[43-44] It is important to note, that the addition of an extra amount of the PPh_3 to the reaction mixture from which the latter compound was isolated, increases the yield of the ruthenium carbene significantly.

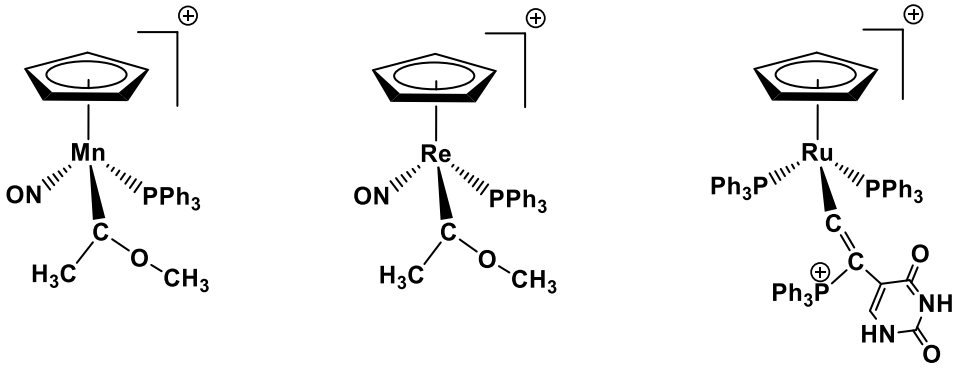

Figure 2.22: $[M(Cp)(NO)(PPh_3)\{C(OMe)CH_3\}](PF_6)$ complexes (M = Mn, Re) and $[Ru(E\text{-}CH{=}C\{PPh_3\}uracil)(Cp)(PPh_3)_2](PF_6)$.[41-44]

The structure of $[Tc(NO)(Cp)(PPh_3)\{C(OMe)C_2H_4PPh_3\}](PF_6)_2$ (Figure 2.20) can be discussed as a Fischer-type carbene with an extra triphenylphosphonio group bonded to the terminal methylene group. The observed bond lengths are in accordance with those of related manganese and rhenium carbenes (Table 2.1). On the other hand, the carbon-phosphorus bond lengths for the triphenylphosphonio units of $[Tc(NO)(Cp)(PPh_3)\{C(OMe)C_2H_4PPh_3\}](PF_6)_2$ and the related ruthenium carbene $[Ru(E\text{-}CH{=}C\{PPh_3\}uracil)(Cp)(PPh_3)_2](PF_6)$ are also similar (Tc: C-PPh_3 = 1.804(2)Å, Ru: C-PPh_3 = 1.788(5) Å.[44]

	[Tc(NO)(Cp)(PPh_3)-{C(OMe)$C_2H_4PPh_3$}](PF_6)$_2$	**[Mn(Cp)(NO)(PPh_3)-{C(OMe)CH_3}](PF_6)**	**[Re(Cp)(NO)(PPh_3)-{C(OMe)CH_3}](PF_6)**
M-C (carbene)	2.013(4) Å	1.901(4) Å	1.990(2) Å
C-O (carbene-OCH_3)	1.303(4) Å	1.320(5) Å	1.335(3) Å
O-C (O-CH_3)	1.439(4) Å	1.465(6) Å	1.464(1) Å

Table 2.1: Comparison of the bond lengths in the complexes [Tc(NO)(Cp)(PPh_3){C(OMe)$C_2H_4PPh_3$}]-(PF_6)$_2$, [Mn(Cp)(NO)(PPh_3){C(OMe)CH_3}](PF_6)[41] and [Re(Cp)(NO)(PPh_3){C(OMe)CH_3}]-(PF_6).[42]

The yields of [Tc(NO)(Cp)(PPh_3){C(OMe)$C_2H_4PPh_3$}](PF_6)$_2$ were in several independent experiments in the range of only 20 %. ^{99}Tc NMR spectra of the reaction solutions indicate that several Tc(I) species are formed in addition to the carbene species. In general, a yield of less than 50 percent must be expected with regard to the fact that the PPh_3, which is used for the formation of the triphenylphosphonio group must be taken from a {Tc(NO)(Cp)(PPh_3)}$^+$ unit. But also the addition of an excess of PPh_3 did not increase the yield. This fact is an indicator that the formation of the Ph_3P^+-C bond is one integrated step of the concerted reaction and most probably metal-controlled.

Lastly, the origin of the methoxy species in the carbene ligand was confirmed to be the methanol, in which Ag(PF_6) was dissolved. Indeed, when the reaction has been performed without any traces of MeOH, no signal for the carbene formation has been observed in the ^{99}Tc NMR spectrum and the dimeric complex [{Tc(NO)(Cp)(PPh_3)}$_2$Cl](PF_6) was the only isolated product. The usage of 2-propanol, gave a compound with a ^{99}Tc NMR resonance at -1370 ppm, which is similar to that observed for the methoxy-carbene. Due to this ^{99}Tc NMR signal and considering the work of Struchkov and Aleksandrov[45] on the synthesis of 2-propoxy-carbeneplatinum(II) complexes, it is highly probable that a similar technetium carbene complex has been produced but with a (2-propoxy) residue as well (Fig. 2.23). The ^{31}P NMR spectrum of [Tc(NO)(Cp)(PPh_3){C(OCH(CH_3)$_2$))$C_2H_4PPh_3$}](PF_6)$_2$ is almost identical to that of the methoxy-substituted carbene. Two signals are observed at 29 and 10 ppm and can be attributed to the triphenylphosphine and triphenylphosphonio phosphorus atoms.

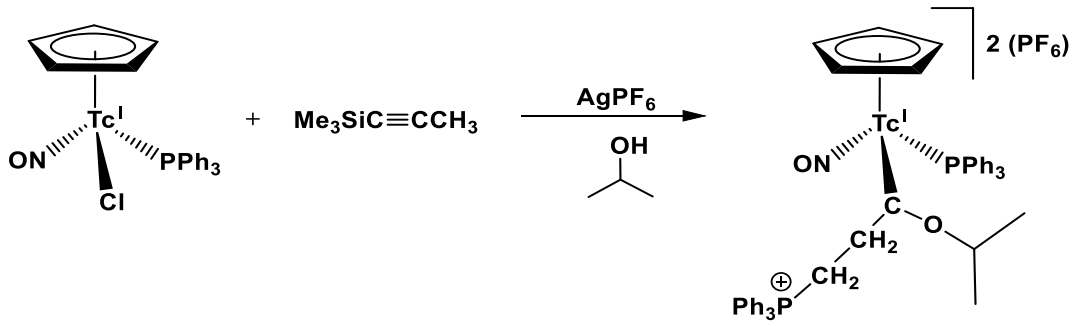

Figure 2.23: Synthesis of $[Tc(NO)(Cp)(PPh_3)\{C(OCH(CH_3)_2))C_2H_4PPh_3\}](PF_6)_2$.

Summarizing, it can be concluded that no alkyne or related complexes were found during reactions of $[Tc(NO)Cl(Cp)(PPh_3)]$ and symmetrical alkynes. This result is in contrast to the analogous $[Re(NO)Cl(Cp)(PPh_3)]$ chemistry, where $[Re(NO)(Cp)(PPh_3)(RC{\equiv}CR)]^+$ complexes were effectively synthesized.[38-39]

A stable Fischer-type technetium carbene was synthesized via a one-pot reaction between $[Tc(NO)Cl(Cp)(PPh_3)]$, $AgPF_6$, MeOH and $Me_3SiC{\equiv}C\text{-}CH_3$.

2.4 Synthesis and reactivity of [Tc(NO)(Cp)(PPh$_3$)(CH$_3$CN)](PF$_6$)

The treatment of [Tc(NO)Cl(Cp)(PPh$_3$)] with AgPF$_6$ in refluxing CH$_3$CN forms the ionic complex [Tc(NO)(Cp)(PPh$_3$)(CH$_3$CN)](PF$_6$). This new acetonitrile species shows reactivity towards neutral ligands such as pyridine or 1,4-thioxane, where the acetonitrile group was readily replaced by the corresponding ligands. On the other hand, the species is less reactive towards other donor solvents like tetrahydrofuran (THF) or dimethyl sulfoxide (DMSO) and alkynes (Fig. 2.24). The respective reactions can effectively be followed by ^{99}Tc NMR measurements, where the resonance of the starting complex [Tc(NO)(Cp)(PPh$_3$)(CH$_3$CN)](PF$_6$) either shifts to another position in the case of successful exchange reactions or stays unchanged when no reactivity occurs. [Tc(NO)(Cp)(PPh$_3$)(CH$_3$CN)](PF$_6$) can be prepared by the addition of AgPF$_6$ to a solution of [Tc(NO)Cl(Cp)(PPh$_3$)] in acetonitrile. The reaction is straightforward, but is faster when the reaction mixture is heated under reflux for a while. After removal of the precipitated AgCl, the product is formed as an orange-red crystalline solid after concentration of the acetonitrile solution.

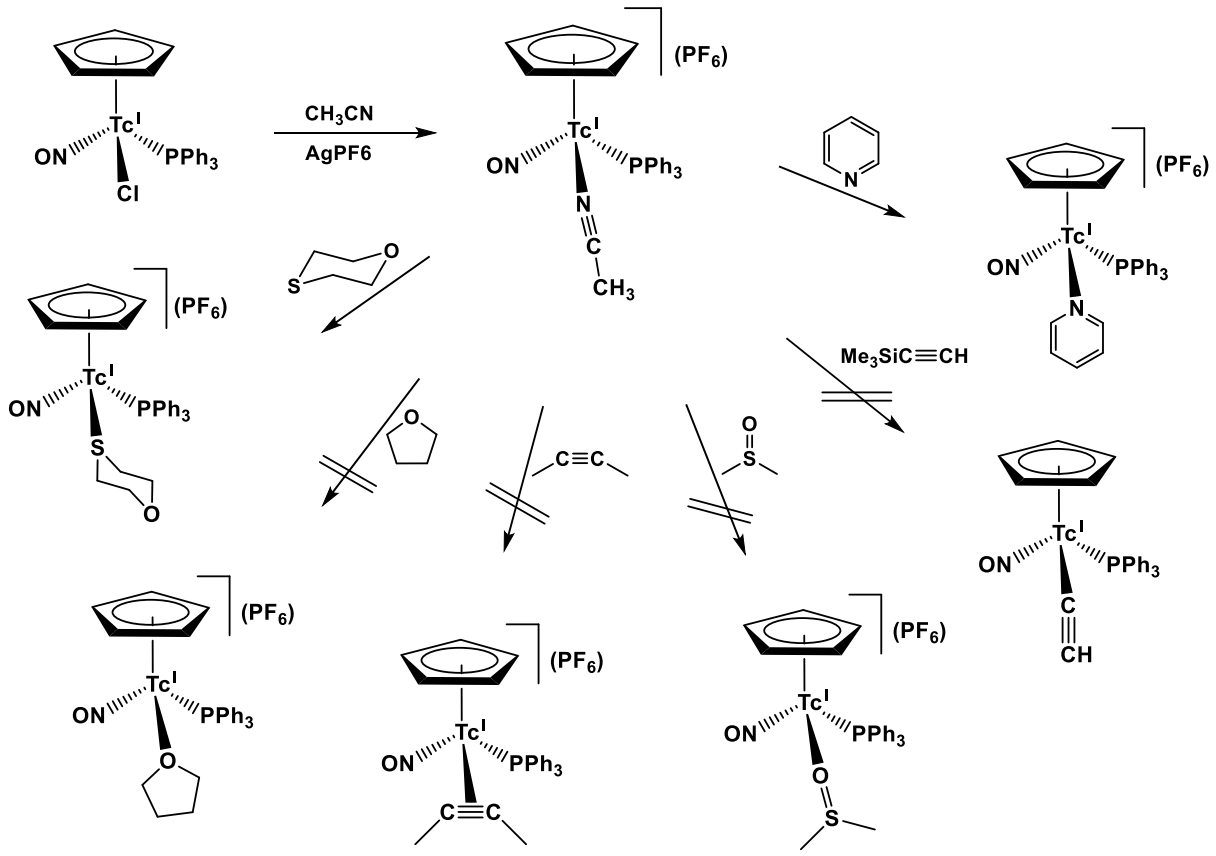

Figure 2.24: Synthesis of [Tc(NO)(Cp)(PPh$_3$)(CH$_3$CN)](PF$_6$) and its reactions.

The X-ray diffraction study was of low quality and refinement could only performed with isotropic thermal parameters. Nevertheless, the structure of the complex is clearly confirmed (Fig. 2.25).

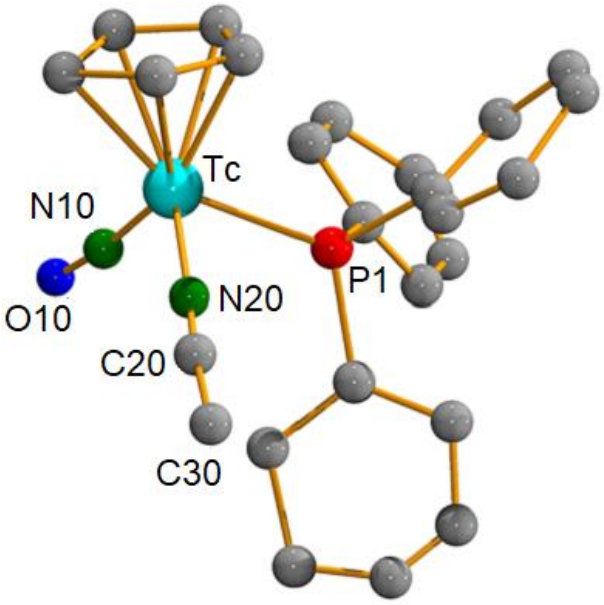

Figure 2.25: Structure of the complex cation of $[Tc(NO)(Cp)(PPh_3)(CH_3CN)](PF_6)$.

The chlorido ligand of $[Tc(NO)Cl(Cp)(PPh_3)]$ was successfully replaced by the linearly coordinated acetonitrile ligand. The analogous rhenium species $[Re(NO)(Cp)(PPh_3)(CH_3CN)](PF_6)$ was reported by Gladysz and his coworkers, but no information about its crystal structure is available.[46] Nevertheless, the structure of $[Tc(NO)(Cp)(PPh_3)(CH_3CN)](PF_6)$ can be compared with that of $[Re(NO)(Cp)(PPh_3)(NCCH(C_6H_5)CH_2CH_3)](PF_6)$, another nitrile complex having the $\{Re(NO)(Cp)(PPh_3)\}^+$ core (Fig. 2.26).[47]

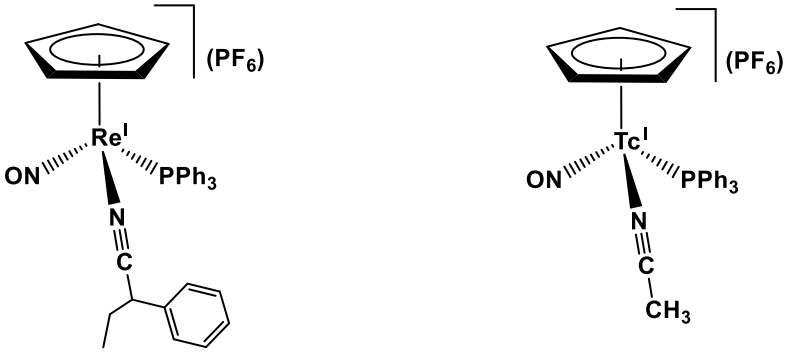

Figure 2.26: $[Re(NO)(Cp)(PPh_3)(NCCH(C_6H_5)CH_2CH_3)](PF_6)$ and $[Tc(NO)(Cp)(PPh_3)(CH_3CN)](PF_6)$.[47]

A comparison of the bond lengths and angles of the two nitrile complexes is given in Table 2.2.

	[Tc(NO)(Cp)(PPh_3)(CH_3CN)](PF_6)	[Re(NO)(Cp)(PPh_3)(NCCH(C_6H_5)CH_2CH_3)](PF_6)
M-N (nitrile)	2.037(1) Å	2.089(8) Å
N≡C (Å)	1.145(7) Å	1.131(10) Å
M-N≡C (º)	178.23(1)	168.5(6)

Table 2.2: Selected bond lengths and angles in [Tc(NO)(Cp)(PPh_3)(CH_3CN)](PF_6) and [Re(NO)(Cp)-(PPh_3)(NCCH(C_6H_5)CH_2CH_3)](PF_6)

The ^{99}Tc NMR signal of [Tc(NO)(Cp)(PPh_3)(CH_3CN)](PF_6) appears at -540 ppm, and, thus shows a significant shift compared to that of [Tc(NO)Cl(Cp)(PPh_3)] (-235 ppm). The ^{31}P NMR resonance is found at 31 ppm. The NO molecule remains in the linear coordination mode and shows a ν_{NO} stretch at 1710 cm^{-1}.

Unfortunately, the use of [Tc(NO)(Cp)(PPh_3)(CH_3CN)](PF_6) as starting molecule for ongoing ligand-exchange reactions is limited. The complex was treated with a series of donor solvents such as tetrahydrofuran (THF) or dimethyl sulfoxide (DMSO) and it was also mixed with alkynes. However, all these attempts did not show ligand exchange and the acetonitrile ligand kept bonded to the technetium (Fig. 2.24). These results were proved through ^{99}Tc NMR measurements, where only the precursor resonance (-540 ppm) could be detected and no hint for any exchange reactions could be observed.

Also this behavior of the studied Tc^{I}(NO) complexes is in contrast to their rhenium analogs, where cationic complexes with THF, alkyl sulfoxides and side-on bonded butyne are well-known and completely characterized (Fig. 2.27).[46,48,38] Interestingly, their technetium analogs could also not be isolated when other synthetic routes were attempted. While the dimeric complex [{Tc(NO)(Cp)(PPh_3)}$_2$Cl]$^+$ results from the reaction of [Tc(NO)Cl(Cp)(PPh_3)] with $AgPF_6$ in THF, DMSO or neat butyne, frequently decomposition was observed in other donor solvents.

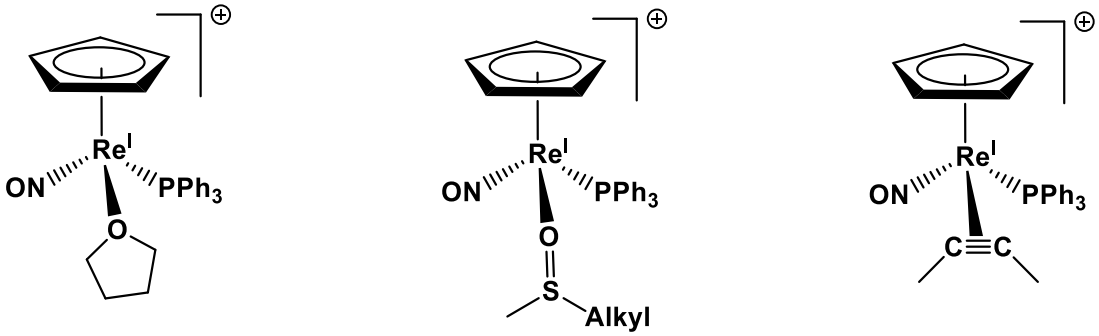

Figure 2.27: $[Re(NO)(Cp)(PPh_3)(THF)]^+$, $[Re(NO)(Cp)(PPh_3)(O=S(Me)R))]^+$ and $[Re(NO)(Cp)(PPh_3)(R{\equiv}R)]^+$ as examples for complexes with donor solvents. [46,48,38]

More successful were reactions with neutral ligands such as pyridine or thioxane. When these compounds were added to $[Tc(NO)(Cp)(PPh_3)(CH_3CN)](PF_6)$ at room temperature, a color change was gradually observed. Upon stirring the reaction mixtures for 2 hours, the ^{99}Tc NMR signal of the starting compound disappeared and the resonances of the formed products were apparent at -285 ppm for $[Tc(NO)(Cp)(PPh_3)(pyridine)]^+$ and -860 ppm for $[Tc(NO)(Cp)(PPh_3)(thioxane)]^+$ (Fig. 2.28).

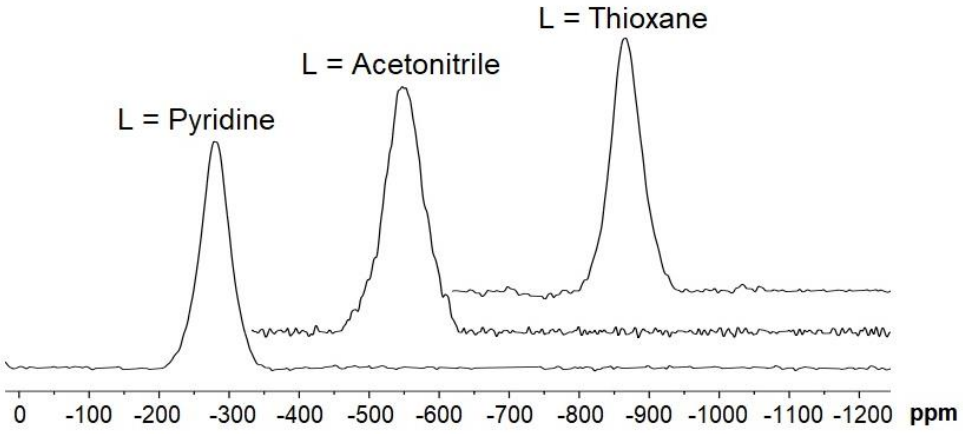

Figure 2.28: ^{99}Tc NMR signals of the $[Tc(NO)(Cp)(PPh3)(L)]^+$ complexes (L = pyridine, acetonitrile, thioxane.

The pyridine and 1,4-thioxane complexes were isolated as orange-red or red crystals, which were suitable for X-ray diffraction. The acetonitrile ligand of $[Tc(NO)(Cp)(PPh_3)(CH_3CN)](PF_6)$ was replaced by a pyridine or a thioxane ligand. The NO ligands are linear and show ν_{NO} stretches at 1724 cm^{-1} ($[Tc(NO)(Cp)(PPh_3)(pyridine)](PF_6)$) and 1737 cm^{-1} ($[Tc(NO)(Cp)(PPh_3)(thioxane)](PF_6)$). Technetium kept its pseudotetrahedral coordination mode and the oxidation state "+1".

No significant differences were observed for the ^{31}P NMR resonances of the new complexes. They appear at 29 ppm for the pyridine complex and at 34 ppm for [Tc(NO)(Cp)(PPh_3)-(thioxane)](PF_6).

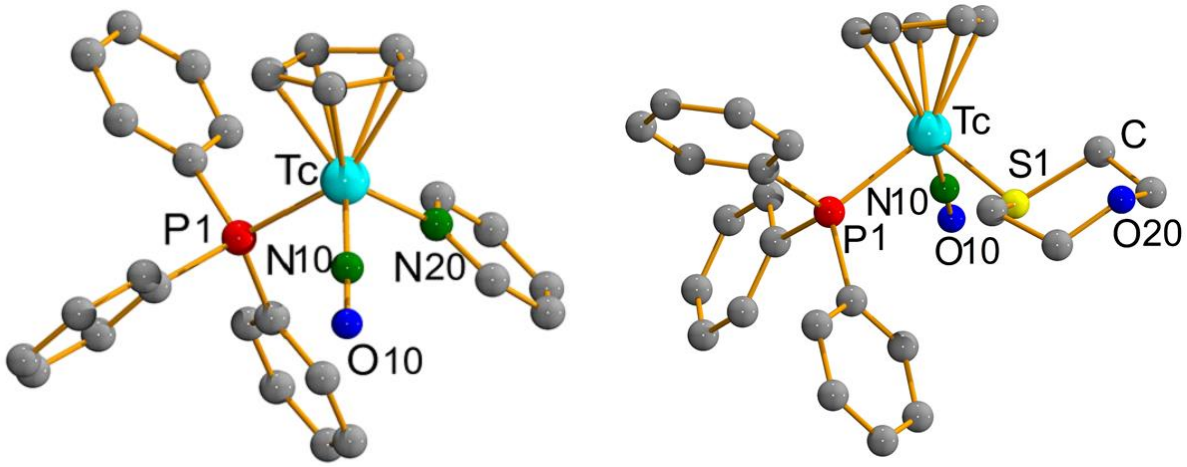

Figure 2.29: Structures of the complex cations of [Tc(NO)(Cp)(PPh_3)(pyridine)](PF_6) and [Tc(NO)-(Cp)(PPh_3)(thioxane)](PF_6).

The bonding situation in [Tc(NO)(Cp)(PPh_3)(pyridine)](PF_6) is similar to that in the analogous rhenium complex, with Tc-N(Py) and Re-N(Py) bond lengths of 2.145(3) ppm and 2.147(3) ppm.[49] No information about a similar rhenium thioxane structure is available. Nevertheless, 1,4-thioxane is a well-known ambidentate ligand, and is mostly coordinated through the sulfur atom.[50-51] This coordination mode was also observed in the *trans*-[$TcCl_4$(thioxane)$_2$], where two thioxane molecules are *S*-bonded to technetium.[52] The Tc-S bond lengths in this complex is 2.476(1) ppm, which is in accordance with the Tc-S bond length (2.407(1) ppm) measured in [Tc(NO)(Cp)(PPh_3)(thioxane)](PF_6).

Summarizing, it can be concluded that a new ionic species [Tc(NO)(Cp)(PPh_3)(CH_3CN)](PF_6) can readily be prepared from [Tc(NO)Cl(Cp)(PPh_3)], but is only limited suitable as precursor for ongoing ligand exchange reactions. [Tc(NO)(Cp)(PPh_3)(CH_3CN)](PF_6) only reacts with strong donor ligands such as pyridine or 1,4-thioxane, while corresponding reactions with THF, DMSO or alkynes fail.

2.5 Reactivity of [Tc(NO)Cl(Cp)(PPh_3)] towards triphenylphosphine chalcogenides Ph_3PX (X = O, S, Se)

Treatment of [Tc(NO)Cl(Cp)(PPh_3)] with $AgPF_6$ and Ph_3PO, Ph_3PS or Ph_3PSe results in the formation of three new species possessing the general formula [Tc(NO)(Cp)(PPh_3)-($XPPh_3$)](PF_6) (X = O, S, Se). The chlorido ligand is expectedly replaced by the phosphine chalcogenides and technetium keeps its piano stool coordination system (Fig. 2.30).

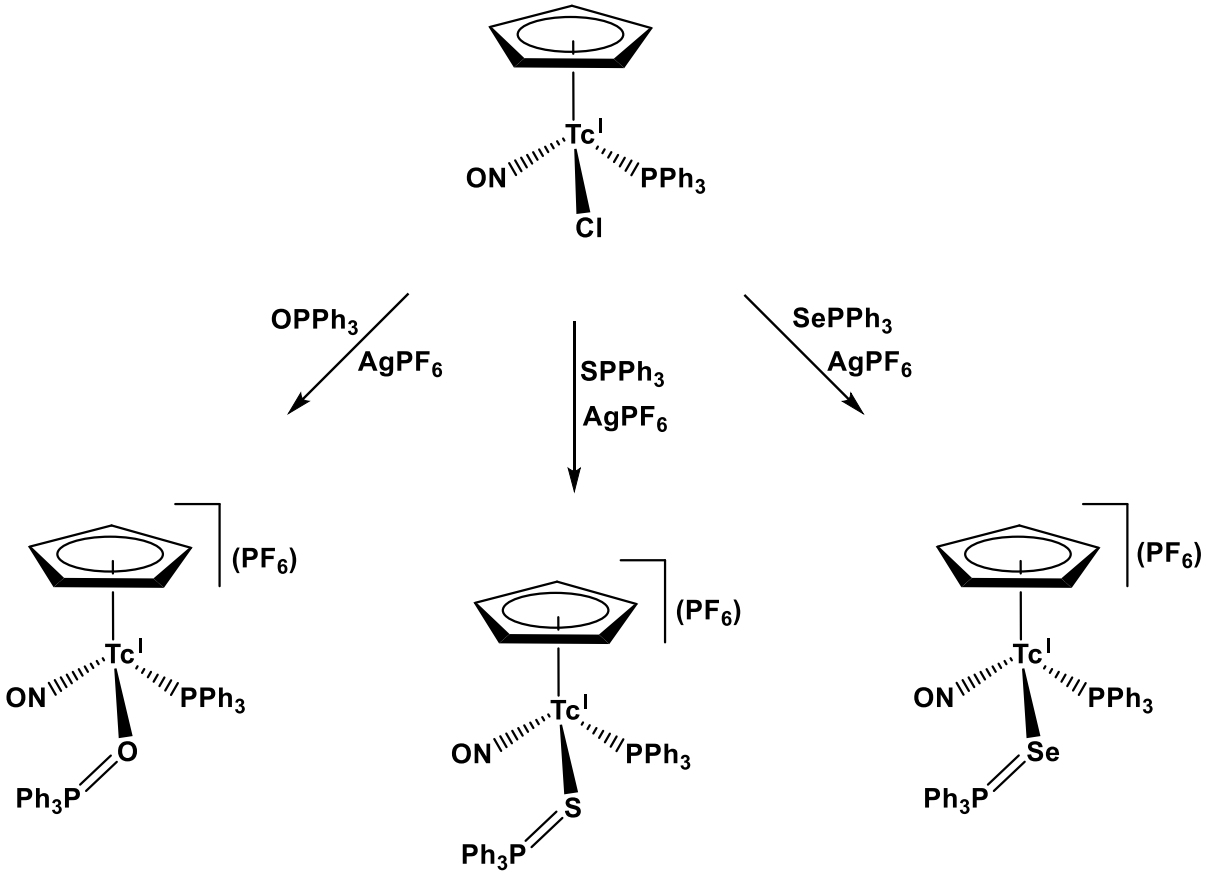

Figure 2.30: Synthesis of [Tc(NO)(Cp)(PPh_3)($XPPh_3$)](PF_6) complexes (X= O, S, Se).

In fact, the coordination chemistry of triphenylphosphine chalcogenides and different metal ions can be regarded as well-studied.[53-56] Most of the research focused on the triphenylphosphine oxide, while less examples discuss corresponding triphenylphosphine sulfides and selenides.[54-55] The instability of triphenylphosphine telluride excludes the extension of these studies to Ph_3PTe. There are only a few examples of stable complexes with trialkylphosphine telluride ligands (R_3PTe: R = $_t$-Bu, $_i$-Pr).[57-58]

In general, the nature of the bonds and angles inside of such compounds are influenced by both the metal ion (the Lewis acid) and the chalcogen. A comprehensive work about these coordination compounds and their bond lengths was made by Neil Burford, who listed in his review many phosphine chalcogenide complexes, in which the phosphine oxide moiety showed a wide range of Ph_3P-O-M angles (130-180º), while the sulfides and selenides were constrained to sharp angles (91-117º).[59]

$[Tc(NO)(Cp)(PPh_3)(OPPh_3)]^+$, $[Tc(NO)(Cp)(PPh_3)(SPPh_3)]^+$ and $[Tc(NO)(Cp)(PPh_3)(SePPh_3)]^+$ were synthesized by the treatment of $[Tc(NO)Cl(Cp)(PPh_3)]$ with $AgPF_6$ and an equivalent amount of the triphenylphosphine chalcogenide (Ph_3PX; X = O, S, Se) in CH_2Cl_2 at room temperature for 4 h. The ^{99}Tc NMR measurements of the reaction mixtures proved clearly the formation of the products, while the resonance of the starting complex disappeared and new shifts for the related new species appear (Fig. 2.31).

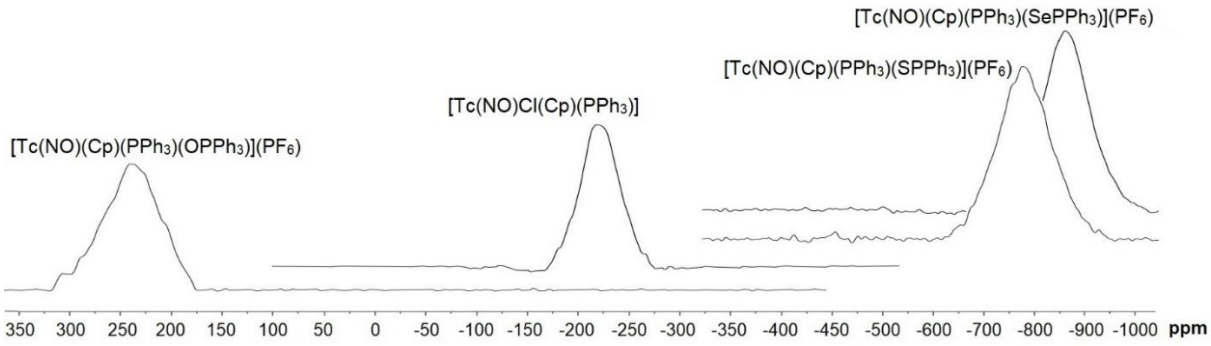

Figure 2.31: ^{99}Tc NMR signals of the $[Tc(NO)(Cp)(PPh_3)(XPPh_3)](PF_6)$ (X = O, S, Se) complexes.

Interestingly, the resonance for $[Tc(NO)(Cp)(PPh_3)(OPPh_3)](PF_6)$ was observed at significantly lower field (+241 ppm). This result is in accordance with the values seen for the complexes: $[Tc(NO)(OOCCF_3)(Cp)(PPh_3)]$ (+20 ppm) and $[Tc(NO)(Cp)(PPh_3)(OOOSCF_3)]$ (+245 ppm), where the $\{Tc^I(NO)(Cp)(PPh_3)\}^+$ core is also oxygen-bonded to the introduced ligands ($O_2CCF_3^-$, $O_3SCF_3^-$).[33]

On the other hand, the resonances of the sulfide and selenide species were shifted to the upper field (-783 ppm, -876 ppm) respectively. The resonance of the phosphine sulfide complex $[Tc(NO)(Cp)(PPh_3)(SPPh_3)](PF_6)$ appears in the same range as that of $[Tc(NO)(Cp)(PPh_3)$-(thioxane)$](PF_6)$ (860 ppm). A comparison of ^{99}Tc NMR spectra of phosphine selenide complex with related compounds is not possible since there are hitherto no related Tc(I) complexes with selenium bonded ligands. The $[Tc(NO)(Cp)(PPh_3)(XPPh_3)](PF_6)$ complexes (X = O, S, Se)

were studied by X-ray diffraction. Their structures are shown in Figure 2.32. Selected bond lengths and angles are summarized in Table 2.3.

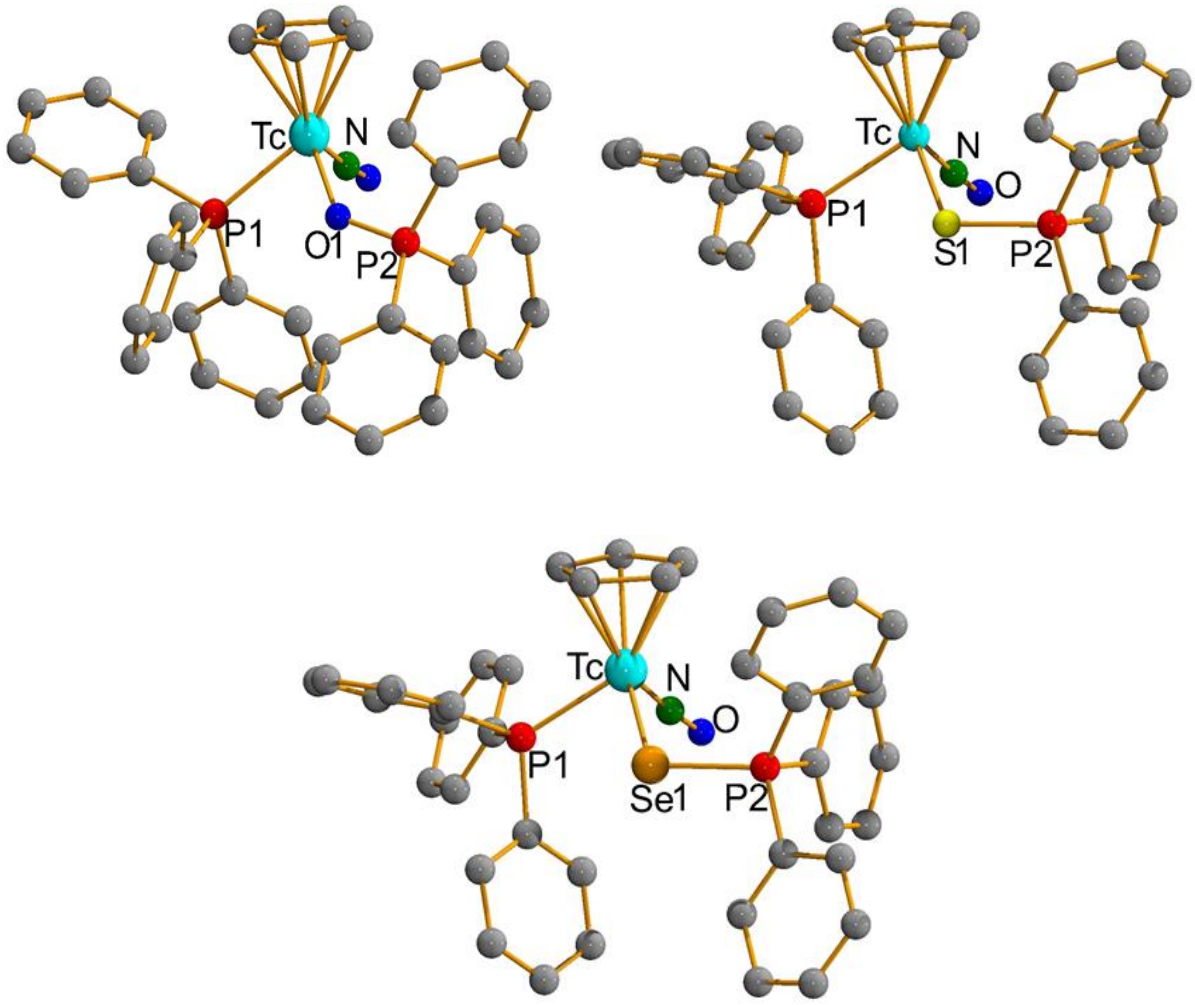

Figure 2.32: Structures of the complex cations of the $[Tc(NO)(Cp)(PPh_3)(XPPh_3)](PF_6)$ complexes (X = O, S, Se).

The products contain the phosphine chalcogenides in their typical bent coordination mode. The Tc-X-P angels vary between 133º for $[Tc(NO)(Cp)(PPh_3)(OPPh_3)](PF_6)$ and 109º or 107º for its sulfur or selenium analogs. Simultaneously, the bond lengths Tc-X increase expectedly from oxygen to selenium. These observations are in accordance with the values mentioned in other samples of $XPPh_3$ (X = O, S, Se) complexes.[59]

	[Tc(NO)(Cp)(PPh$_3$)-(OPPh$_3$)](PF$_6$)	**[Tc(NO)(Cp)(PPh$_3$)-(SPPh$_3$)](PF$_6$)**	**[Tc(NO)(Cp)(PPh$_3$)-(SePPh$_3$)](PF$_6$)**
Tc-X	2.149(3) Å	2.424(6) Å	2.530(3) Å
Tc-P1	2.398(2) Å	2.372(3) Å	2.381(2) Å
Tc-N	1.755(4) Å	1.768(2) Å	1.757(7) Å
X-P2	1.519(3) Å	2.024(5) Å	2.183(2) Å
N-O	1.184(6) Å	1.177(3) Å	1.186(8) Å
Tc-X-P2	133.28(2) º	109.22(3) º	107.36(7) º

Table 2.3: Selected bond lengths and angles of the complexes [Tc(NO)(Cp)(PPh$_3$)(XPPh$_3$)](PF$_6$) (X = O, S, Se).

The observed differences in the bond lengths and angles between the phosphine oxide complex and both the sulfide and selenide complexes agree with the valence shell electron pair repulsion (VSEPR) model.[59]

Consequently, the differences in the structural bonding between the phosphine oxide and its heavier analogs can be accounted for the diversity in the ^{31}P NMR resonances observed for the three [Tc(NO)(Cp)(PPh$_3$)(XPPh$_3$)](PF$_6$) complexes (X= O, S, Se). In fact, the ^{31}P NMR shift of the uncoordinated PPh$_3$O (25.7 ppm) was significantly affected by the complexation of this moiety to technetium (57.8 ppm). Meanwhile, the impact on the ^{31}P NMR shift of the heavier triphenylphosphine chalcogenides (PPh$_3$S, PPh$_3$Se) was obviously lower (Table 2.4).

Non-coordinated PPh_3X **(**X= O, S, Se)	**$[Tc(NO)(Cp)(PPh_3)(XPPh_3)](PF_6)$** (X = O, S, Se)
25.7	57.8
41.6	51.8
32.3	34.2

Table 2.4: ^{31}P NMR resonances in CD_2Cl_2 of the non-coordinated and complexed phosphine chalcogenides.

The complexes show ν_{NO} stretches at 1699 cm^{-1} (O), 1686 cm^{-1} (S) and 1705 cm^{-1} (Se), which are very similar to that of the starting complex $[Tc(NO)Cl(Cp)(PPh_3)]$ (1681 cm^{-1}).

Summarizing, it can be concluded that complexes of the general formula $[Tc(NO)(Cp)(PPh_3)(XPPh_3)](PF_6)$ (X = O, S, Se) can effectively be prepared from $[Tc(NO)Cl(Cp)(PPh_3)]$.

The three products were studied by ^{99}Tc NMR spectroscopy, where the resonances for the oxide and sulfide species could be estimated by the consideration of other *S* and *O*-bonded complexes to the $\{Tc(NO)(Cp)(PPh_3)\}^+$ unit.

The ^{99}Tc NMR chemical shift of the complexes with phosphine sulfide and phosphine selenide are very similar, but shifted 1000 ppm from the corresponding signal of $[Tc(NO)(Cp)(PPh_3)(OPPh_3)](PF_6)$.

2.6 Synthesis of [Tc(NO)Cl(CpR)(PPh_3)] (R = CH_3, $COOCH_3$) complexes

Reactions between [Tc(NO)Cl_2(PPh_3)$_2$(CH_3CN)] and Na(CpR) (R= CH_3, $COOCH_3$) in refluxing toluene form the organotechnetium compounds [Tc(NO)Cl(CpMe)(PPh_3)] and [Tc(NO)Cl(CpCOOMe)(PPh_3)]. The products show a ligand exchange reactivity as reported for the unsubstituted [Tc(NO)Cl(Cp)(PPh_3)]. This has been proved by a reaction of [Tc(NO)Cl(CpMe)(PPh_3)] with pyridine, which results in the replacement of the chlorido ligand and the formation of the complex [Tc(NO)(CpMe)(PPh_3)(pyridine)](PF_6). The performed reactions are depicted in Figure 2.33.

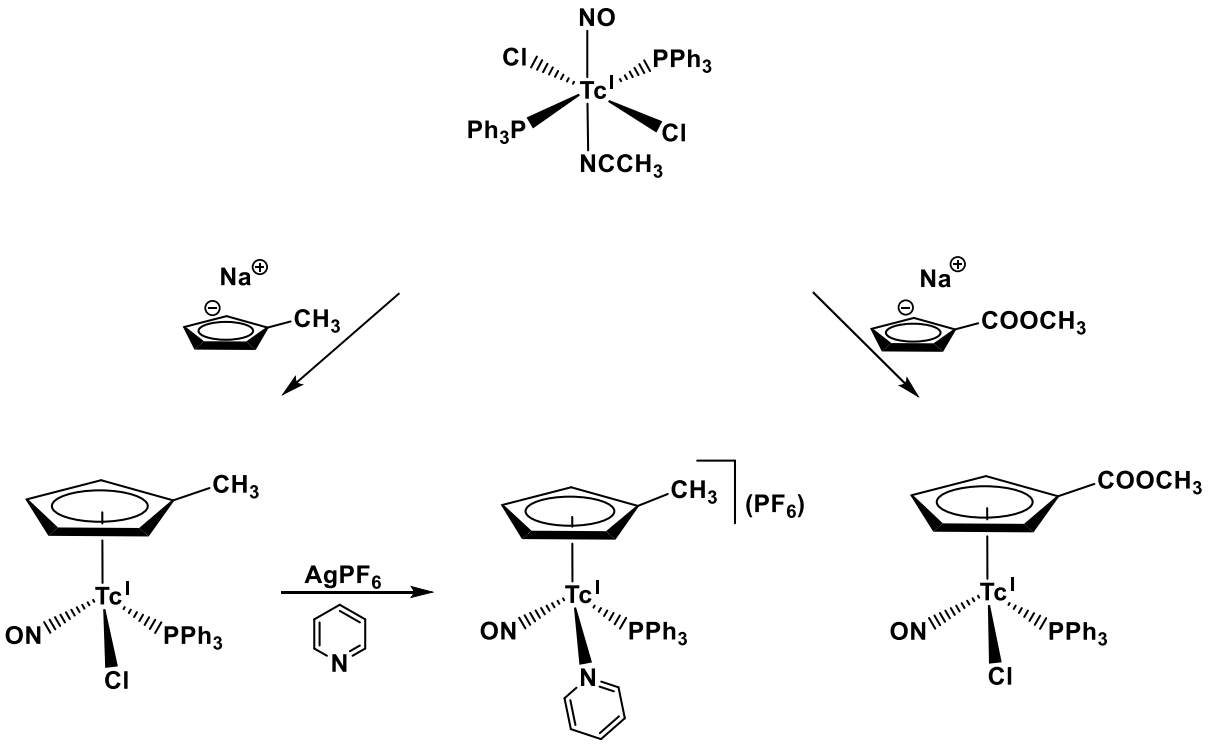

Figure 2.33: The synthesis of the complexes [Tc(NO)Cl(CpR)(PPh_3)] (R = Me, COOMe) and [Tc(NO)-(CpMe)(PPh_3)(Py)](PF_6).

Substituted cyclopentadiene (Cp-X) rings and their complexes are well studied in the literature and variable substituents have been described.[60-64] The interest in the presence of a functional group on the cyclopentadienyl ring is due to the offered access for coupling a biologically active species, which can then be used for medical purposes. Coming from this background, Alberto and his co-workers synthesized a series of cyclopentadienyl derivatives of both rhenium and technetium having a fac-tricarbonyl unit, $\{M(CO)_3\}^+$ (M = Re, Tc), and tested their biological activities towards nuclear imaging applications.[65-67] Two examples of these complexes with substituents ready for biolabeling are shown in Figure 2.34.

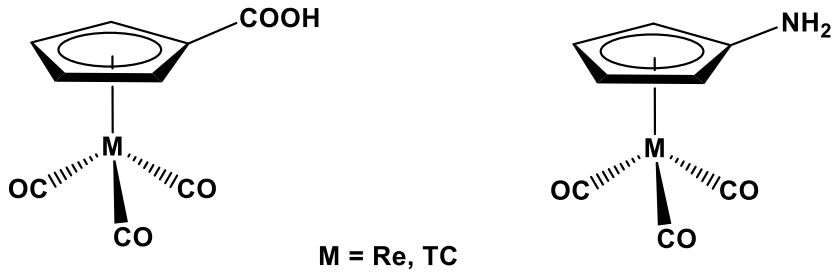

Figure 2.34: $[M(CpCOOH)(CO)_3]$, $[M(CpNH_2)(CO)_3]$ complexes as potential precursors for medical applications, M = Re, Tc.[65-67]

Conducting the chemical potential of compounds having a $\{Tc(NO)(Cp)(PPh_3)\}^+$ core, which has been described in the previous chapters of this thesis, it could be interesting to extend the work to compounds with coupling positions for biomolecules. First, a methylcyclopentadienyl (CpMe) derivative was synthesized.

Since the procedure described for a similar rhenium complex resulted frequently in the formation of a dimethyl substituted derivative as a side-product [68], another procedure has been chosen for the planned technetium derivative. Since the procedure for the synthesis of $[Tc(NO)Cl(Cp)(PPh_3)]$ is more straightforward than that of the rhenium analog and can be performed via $[Tc(NO)Cl_2(PPh_3)_2(CH_3CN)]$ in a two-step synthesis starting from $(NBu_4)[Tc(NO)Cl_4(MeOH)]$, a direct synthesis appeared to be more favorable than an alkylation on the organometallic compound as has been done for rhenium (Fig. 2.35).

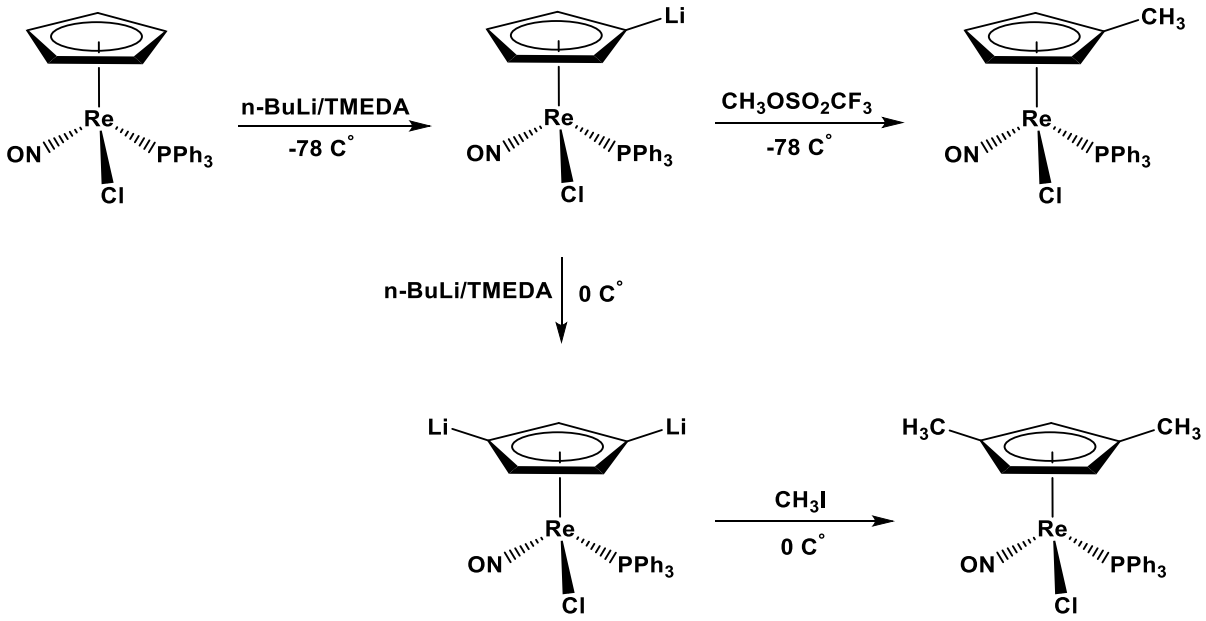

Figure 2.35: Routes for the synthesis of methylated Cp complexes of rhenium.[68]

The change in the procedure seems also mandatory having in mind that the target of this synthesis is ^{99m}Tc, where other requirements for the timescale and solvents are given.

A one-pot reaction of Na(CpMe) with [Tc(NO)Cl_2(PPh_3)$_2$(CH_3CN)] in boiling toluene gives a dark red solid of [Tc(NO)Cl(CpMe)(PPh_3)] within 2 hours (Fig. 2.36).

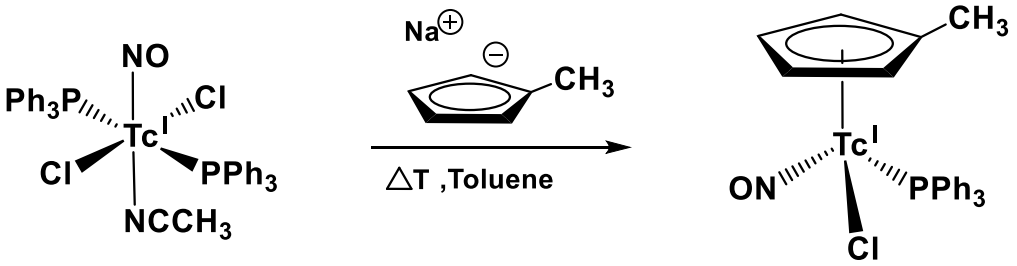

Figure 2.36: Synthesis of [Tc(NO)Cl(CpMe)(PPh_3)].

The identity of the product was confirmed by ^{1}H, ^{31}P and ^{99}Tc NMR and IR spectroscopy. Table 2.5 shows the spectroscopic data of the new CpMe product in comparison to those of [Tc(NO)Cl(Cp)(PPh_3)].

	[Tc(NO)Cl(Cp)(PPh_3)]	**[Tc(NO)Cl(CpMe)(PPh_3)]**
^{99}Tc NMR (ppm)	-235	-295
^{31}P NMR (ppm)	29	27
^{1}H NMR (ppm)	5.12 (s, 5H, Cp)	5.13, 4.96, 4.62, 4,48 (4H, Cp) 1.81 (3H, Cp-CH_3)
ν_{NO} stretch (cm^{-1})	1681	1684

Table 2.5: Spectroscopic data for [Tc(NO)Cl(Cp)(PPh_3)] and [Tc(NO)Cl(CpMe)(PPh_3)].

To analyze the ^{1}H and ^{13}C NMR spectra of [Tc(NO)Cl(CpMe)(PPh_3)], the work made by Coville and his coworkers was reviewed, who revealed the synthesis and the ^{1}H and ^{13}C NMR spectra of a series of [(η^5-CpMe)Fe(CO)(L)I] complexes (L = phosphine, phosphite).[69-70] They showed that a substituent on the cyclopentadienyl ring decreases the fivefold symmetry of the ring and in turn makes its four protons magnetically non-equivalent. Thus, the observed resonances of these protons could be interpreted up to four different signals. Moreover, if the ring has an electron donating substituent like CH_3, the protons of the adjacent protons to substituent are shifted downfield. In contrast, the other two protons are expected to be shifted upfield.

In an achiral complex as [(η^5-CpMe)Fe(A)$_2$(B)], where it is supposed that each two protons are equivalent, two different proton resonances can be expected. This can be explained by either the symmetry impact (fast rotation of the ring) or preferable ligands conformation (slow rotation). On the other hand, a chiral complex as [(η^5-CpMe)Fe(A)(B)(C)] (or the technetium complex under study) has four nonequivalent protons on the Cp ring and they are expected to show four distinct resonances in the proton NMR spectra.

The former considerations made for the ^{1}H NMR spectra can be extended to the ^{13}C NMR spectra of [Tc(NO)Cl(CpMe)(PPh_3)]. But the poor solubility of the compound did not allow the registration of ^{13}C spectra of sufficient quality.

The ^{1}H NMR spectrum of [Tc(NO)Cl(CpMe)(PPh_3)] shows the four separated signals (as expected for a chiral complex) for the four protons of the CpMe ring (Fig. 2.37).

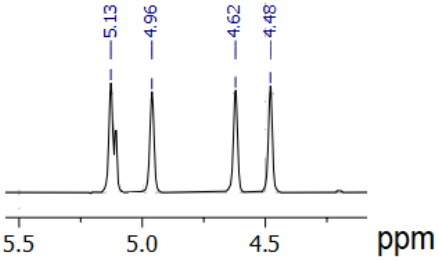

Figure 2.37: Cp part of the ^{1}H NMR spectrum of [Tc(NO)Cl(CpMe)(PPh_3)] in $CDCl_3$.

The ready synthetic approach to [Tc(NO)Cl(CpMe)(PPh_3)] opened the door for the preparation of corresponding ligand exchange products having methylcyclopentadienyl units. For a 'proof of principles', [Tc(NO)Cl(CpMe)(PPh_3)] we treated with $AgPF_6$ and pyridine. The reaction resulted in the precipitation of silver chloride and the replacement of the chlorido ligand by the neutral pyridine one (Fig. 2.38).

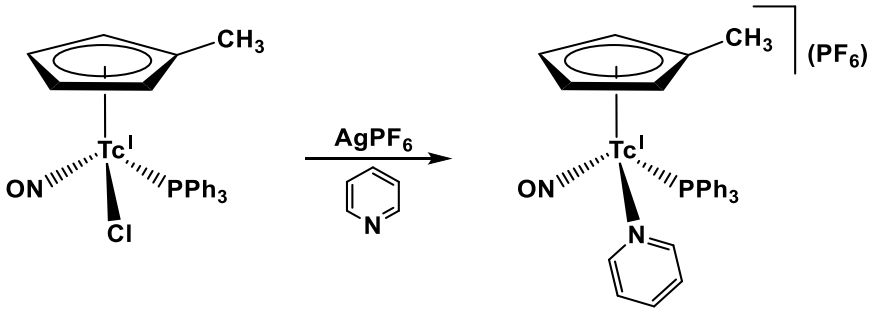

Figure 2.38: Synthesis of [Tc(NO)(CpMe)(PPh_3)(pyridine)](PF_6).

The IR spectrum of the product shows a ν_{NO} stretch at 1708 cm^{-1} and no significant change for the ^{99}Tc NMR resonance (-300 ppm) in comparison to that of the starting complex (-295 ppm). The ^{31}P NMR resonance of the PPh_3 ligand is found at 29 ppm and that of the counter ion PF_6^- at -145 ppm. The ^{1}H- and ^{13}C NMR measurements shows the expected four resonances of the four cyclopentadienyl protons (5.40, 5.29, 5.18, 4.97 ppm) and five resonances of the five carbon atoms (107.2, 97.5, 94.1, 91.1, 90.3 ppm) of the CpMe ring. The methyl substituent on the Cp ring gives a singlet at 1.65 ppm and a signal at 13.2 ppm in the ^{13}C NMR spectrum.

A single-crystal X-ray structure determination on [Tc(NO)(CpMe)(PPh_3)(pyridine)](PF_6) shows the expected pseudotetrahedral coordination around the technetium atom and a linear

nitrosyl ligand (Fig. 2.39). The methylcyclopentadienyl ring is η^5-bonded to the technetium atom and the methyl group of the ring points away from the bulky PPh_3 ligand.

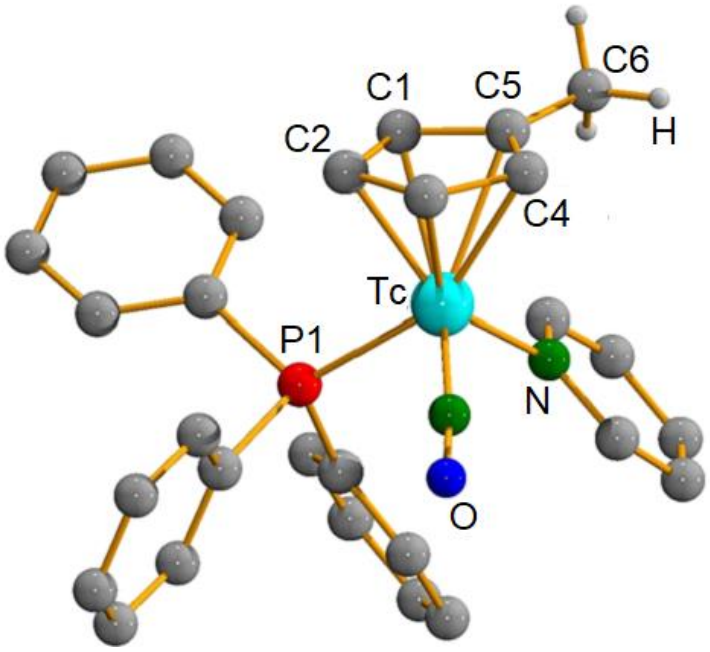

Figure 2.39: Structure of the cation of [Tc(NO)(CpMe)(PPh_3)(pyridine)](PF_6).

In a similar way as [Tc(NO)Cl(Cp)(PPh_3)] and [Tc(NO)Cl(CpMe)(PPh_3)], the ester-substituted derivative [Tc(NO)Cl(CpCOOMe)(PPh_3)] was prepared from [Tc(NO)Cl_2(PPh_3)$_2$(CH_3CN)] (Fig. 2.40). The resulting residue was dried and isolated as a red solid. Attempts to grow single crystals for X-ray measurements were unsuccessful. However, the crude product was characterized by IR and NMR spectroscopy, which proved the composition of [Tc(NO)Cl(CpCOOMe)(PPh_3)].

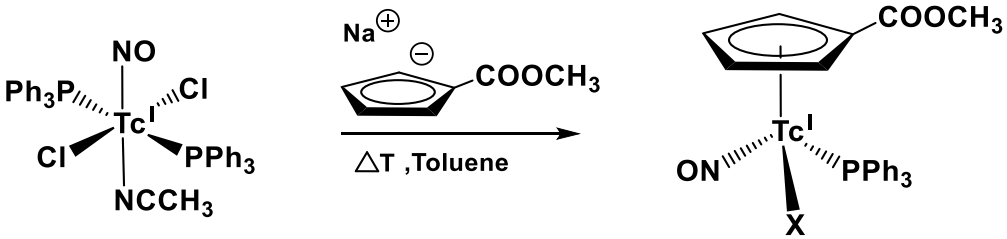

Figure 2.40: Synthesis of [Tc(NO)Cl(CpCOOMe)(PPh_3)].

The IR spectrum shows a medium absorption at 1786 cm^{-1} and a very strong one at 1697 cm^{-1}, related to the C=O bond of the ester group and the NO ligand. The ^{99}Tc NMR resonance of the

product is observed at -255 ppm. Figure 2.41 shows the ^{99}Tc NMR resonances of the complexes [Tc(NO)Cl(CpMe)(PPh_3)], [Tc(NO)Cl(CpCOOMe)(PPh_3)] and [Tc(NO)Cl(Cp)(PPh_3)].

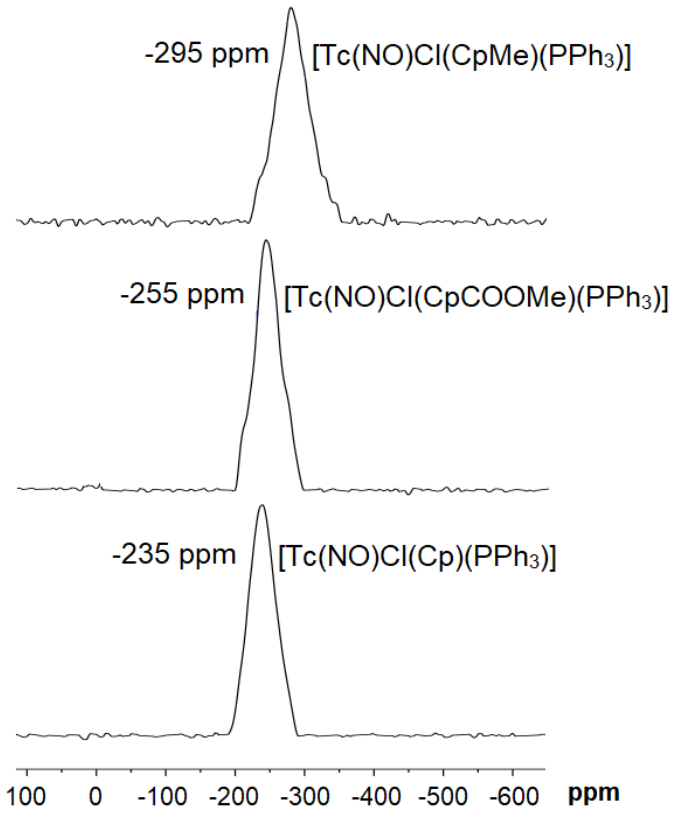

Figure 2.41: ^{99}Tc NMR spectra ($CDCl_3$, ppm) of [Tc(NO)Cl(CpMe)(PPh_3)], [Tc(NO)Cl(CpCOOMe)-(PPh_3)] and [Tc(NO)Cl(Cp)(PPh_3)].

The ^{31}P NMR spectrum of [Tc(NO)Cl(CpCOOMe)(PPh_3)] shows a singlet peak at 28 ppm and the ^{1}H NMR spectrum is consistent with that of the [Tc(NO)Cl(CpMe)(PPh_3)] complex. The separated four proton resonances of the ring are registered in the ^{1}H NMR spectrum at 5.76, 5.38, 5.03 and 4.92 ppm.

It is essential to state, that [Tc(NO)Cl(CpCOOMe)(PPh_3)] suffers from slow decomposition within some days in solution. This was evident by a color change from red into black and by the decrease of the intensity of the ^{99}Tc NMR resonance. This behavior was not observed with the related complexes [Tc(NO)Cl(Cp)(PPh_3)] and [Tc(NO)Cl(CpMe)(PPh_3)]. Both complexes show a high stability on air conditions as solid and in solution.

Summarizing, it can be concluded that three complexes with substituted Cp rings ([Tc(NO)Cl-(CpMe)(PPh_3)], [Tc(NO)(CpMe)(PPh_3)(pyridine)](PF_6) and [Tc(NO)Cl(CpCOOMe)(PPh_3)] could be synthesized and fully characterized.

Particularly, the $COOCH_3$ groups at the Cp ring, provided a promising approach for bioconjugation.

3 Experimental Part

3.1 Starting Materials

All chemicals were reagent grade and used without further purification. Solvents were dried and distilled prior to use. $(NBu_4)[Tc(NO)Cl_4(MeOH)]$, $[Tc(NO)Cl_2(PPh_3)_2(MeCN)]$, $[Tc(NO)Cl(Cp)(PPh_3)]$, $[Tc(NO)(I_3)(Cp)(PPh_3)]$, $[Tc(NO)(SCN)(Cp)(PPh_3)]$, KCp, Na(CpMe) and Na(CpCOOMe) were prepared as described in the literature.[71,72,19,73,74,33,75]

3.2 Physical measurements

IR spectra were measured from KBr pellets on a Shimadzu FTIR 8300 spectrometer between 400 and 4000 cm^{-1}. NMR spectra were recorded on a JEOL 400 MHz spectrometer. Tc values were determined by liquid scintillation counting. EPR spectra were measured on a Miniscope MS400 spectrometer (Magnetech). The simulated spectra were prepared by using the WinEPR and SimFonia programs.[76]

3.3 Radiation Precautions

^{99}Tc is a long-lived weak β^- emitter (E_{max} = 0.292 MeV). Normal glassware provides adequate protection against the weak beta radiation when milligram amounts are used. Secondary X-rays (bremsstrahlung) play a significant role only when larger amounts of ^{99}Tc are handled. All manipulations were done in a laboratory approved for the handling of radioactive materials.

3.4 X-Ray crystallography

The intensities for the X–ray determinations were collected on a Bruker APEX II instrument or a STOE IPDS with Mo Kα or Cu Kα radiation. The space groups were determined by the detection of systematic absences. Absorption corrections were carried out by SADABS or integration via the Gaussian method.[77,78] Structure solutions were performed with the programs SHELXS 97 and SHELXS 2014, structure refinements were done with the SHELXL 2014 program.[79,80] Hydrogen atoms were placed at calculated positions and treated with the 'riding model' option of SHELXL. The representation of molecular structures was done using the program DIAMOND 4.2.2.[81]

3.5 Syntheses of the complexes

[Tc^{I}(NO)I(Cp)(PPh_3)]:

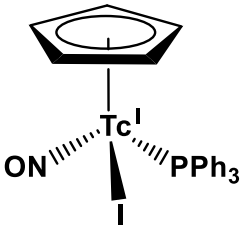

[Tc(NO)Cl(Cp)(PPh_3)] (49 mg, 0.1 mmol) was dissolved in 2 mL CH_2Cl_2. Me_3SiI (0.1 mL) was added. The reaction mixture was stirred for 2 h at room temperature. The solvent was removed under vacuum and the residue was dissolved in 0.5 mL CH_2Cl_2 and overlayered with 3 mL diethyl ether. Red-brown microcrystals deposited after slow diffusion of the solvents. Yield 39 % (23 mg). Elemental analysis: Calcd. for $C_{23}H_{20}NOPITc$: Tc 17 %, Found: Tc 16.3 %. IR (KBr, cm^{-1}): 3049 (w), 3050 (w), 2920 (w), 1681 (vs), 1475 (m), 1429 (m), 1311 (w), 1182 (w), 1157 (w), 1089 (s), 999 (m), 918 (w), 833 (m), 806 (m), 746 (m), 696 (s), 617 (w), 582 (m), 522 (s), 493 (m), 441 (w), 428 (w). ^{1}H NMR (CD_2Cl_2, ppm): 7.33 - 7.67 (m, 15H, Ph), 5.23 (s, 5H, Cp). $^{31}P\{^{1}H\}$ NMR (CD_2Cl_2, ppm): 44.9. ^{99}Tc NMR (CD_2Cl_2, ppm): -668 ($\nu_{1/2}$ = 4200 Hz). The resonances in the ^{13}C NMR spectra were of low intensities and no accurate values could be assigned.

[Tc^{II}(NO)$(I)_2$(Cp)]:

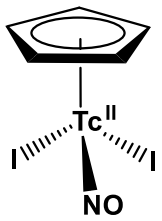

[Tc(NO)(I_3)(Cp)(PPh_3)] (45 mg, 0.1 mmol) was dissolved in 5 mL CH_2Cl_2 and kept in solution for 2 days. The red-brown solution slowly changed its color to bright green. After concentration of the green solution to 1 mL, diethyl ether (2 mL) was added. Standing overnight in a refrigerator gave green crystals. Yield 60 % (20 mg). Elemental analysis: Calcd. for $C_5H_5NOI_2Tc$: Tc 22.1 %, Found: Tc 21.5 %. IR (KBr, cm^{-1}): 3447 (w), 2961 (w), 2923 (w), 1746 (m), 1431 (w), 1262 (m), 1161 (w), 1113 (s), 1096 (s), 1022 (m), 802 (s), 721 (m), 691 (m), 538 (s). ^{1}H NMR (CD_2Cl_2, ppm): 4.88 (s, 5H, Cp). ^{13}C NMR (CD_2Cl_2, ppm): 99.9 (s, 5C, Cp). EPR (CH_2Cl_2, 77 K): $g_x = g_z = 2.240$, $g_y = 1.886$, $A_x^{Tc} = 50 \cdot 10^{-4}$ cm^{-1}, $A_y^{Tc} = 70 \cdot 10^{-4}$ cm^{-1}, $A_z^{Tc} = 136 \cdot 10^{-4}$ cm^{-1}.

[{Tc^{I}(NO)(Cp)(PPh_3)}Cl](PF_6):

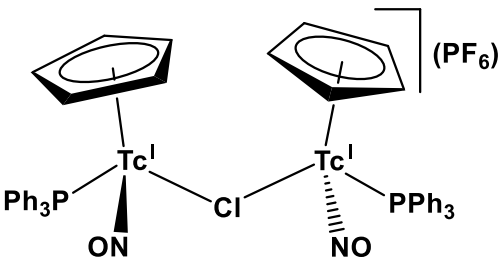

[Tc(NO)Cl(Cp)(PPh_3)] (50 mg, 0.1 mmol) was dissolved in 10 mL CH_2Cl_2 and treated with a solution of $AgPF_6$ (25 mg, 0.1 mmol) in 2 mL CH_2Cl_2/MeOH (2/1, v/v). A dark grey precipitate was formed. The reaction mixture was stirred at room temperature for 5 h. The solution was filtered and the solvent was removed under vacuum. The

residue was suspended in 1 mL CH_2Cl_2 and covered with 3 mL diethyl ether. Red crystals were formed after slow diffusion of the solvents. Yield 44 % (48 mg). Elemental analysis: Calcd. for $C_{46}H_{40}ClN_2O_2P_3F_6Tc_2$: Tc 16.8 %, Found: Tc 15.4 %. IR (KBr, cm^{-1}): 3440 (w), 2918 (w), 1885 (vs), 1520 (w), 1490 (s), 1295 (w), 1240 (w), 1189 (m), 1176 (m), 855 (vs), 758 (m), 701 (s). ^1H NMR (CD_2Cl_2, ppm): 7.53 - 7.59 (m, 9H, Ph), 7.39 - 7.46 (m, 6H, Ph), 5.29 (s, 5H, Cp). $^{31}P\{^1H\}$ NMR (CD_2Cl_2, ppm): 29.0 (s, P, PPh_3), 144.5 (m, P, PF_6). ^{99}Tc NMR (CD_2Cl_2, ppm): -220 ($\nu_{1/2}$ = 4150 Hz). The resonances in the ^{13}C NMR spectra were of low intensities and no accurate values could be assigned.

$[Tc^I(NO)(Cp)(PPh_3)(PMe_3)](PF_6)$:

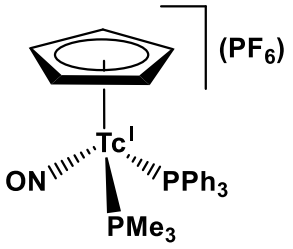

[Tc(NO)Cl(Cp)(PPh_3)] (50 mg, 0.1 mmol) was dissolved in 10 mL CH_2Cl_2 and treated with a solution of $AgPF_6$ (25 mg, 0.1 mmol) in 2 mL CH_2Cl_2/MeOH (2/1, v/v). Trimethylphosphine (0.5 mL) was added to the reaction mixture, which was heated under reflux for 4 h. The solution was filtered and the solvent was removed under vacuum. The residue was dissolved in 1 mL CH_2Cl_2 and covered with 4 mL diethyl ether. Yellow crystals were formed after diffusion of the solvents. Yield 47 % (38 mg). Elemental analysis: Calcd. for $C_{26}H_{29}NOP_3F_6Tc$: Tc 14.7 %, Found: Tc 13.2 %. IR (KBr, cm^{-1}): 3435 (w), 2975 (w), 2932 (w), 1718 (vs), 1487 (w), 1445 (m), 1295 (m), 1078 (m), 971 (s), 810 (vs), 748 (m), 710 (m), 543 (s), 495 w). ^1H NMR ($CDCl_3$, ppm): 7.14 - 7.31 (m, 15H, Ph), 5.17 (s, 5H, Cp), 1.44 (d, 9H, PMe_3). ^{13}C NMR ($CDCl_3$, ppm): 128 - 131.7 (Ph), 93.2 (Cp). ^{31}P NMR ($CDCl_3$, ppm): 32.1 (s, P, PMe_3), 27.9 (s, p, PPh_3), 147 (m, p, PF_6). ^{99}Tc NMR ($CDCl_3$, ppm): -1420 ($\nu_{1/2}$ = 4100 Hz).

$[Tc^I(NO)(Cp)(PPh_3)_2](PF_6)$:

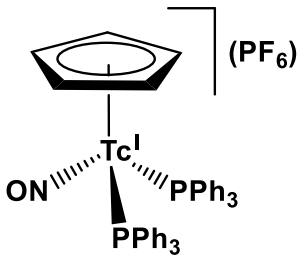

[Tc(NO)Cl(Cp)(PPh_3)] (50 mg, 0.1 mmol) was dissolved in 10 mL CH_2Cl_2/toluene (5:95) and treated with a solution of $AgPF_6$ (25 mg, 0.1 mmol) in 2 mL CH_2Cl_2/MeOH (2/1, v/v). Triphenylphosphine (40 mg, 0.15 mmol) was added to the reaction mixture, which was heated under reflux for 6 h. The solution was filtered and the solvent was removed under vacuum. The residue was dissolved in 1 mL CH_2Cl_2 and covered with 3 mL toluene. Orange-red crystals were formed after diffusion of the solvents. Yield 45 % (39 mg). Elemental analysis: Calcd. for $C_{41}H_{35}NOP_3F_6Tc$: Tc 11.5 %, Found: Tc 13.1 %. IR (KBr, cm^{-1}): 3440 (w), 3057 (w), 2962 (s), 2924 (m), 2854 (w), 1720 (s), 1481 (w), 1436 (m), 1261 (vs), 1095 (vs), 1020 (vs), 800 (vs), 748 (m), 696 (s). ^1H NMR

($CDCl_3$, ppm): 7.14 - 7.67 (m, 30H, Ph), 5.18 (s, 5H, Cp). ^{31}P NMR ($CDCl_3$, ppm): 22.4 (s, 2p, PPh_3), 150 (m, p, PF_6) ^{99}Tc NMR ($CDCl_3$, ppm): -1219 ($\nu_{1/2}$ = 6600 Hz). The resonances in the ^{13}C NMR spectra were of low intensities and no accurate values could be assigned.

$[Tc^{I}(NO)(Cp)(PPh_3)\{C(OMe)C_2H_4PPh_3\}](PF_6)_2$:

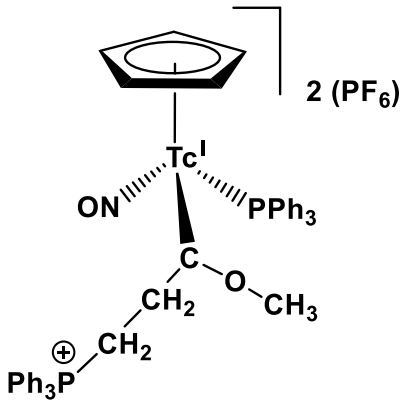

[Tc(NO)Cl(Cp)(PPh_3)] (50 mg, 0.1 mmol) was dissolved in 5 mL toluene and treated with a solution of $AgPF_6$ (37 mg, 0.15 mmol) in 1 mL CH_2Cl_2/MeOH (2/1, v/v). 1-Trimethylsilylpropyne (0.25 mL, 1.5 mmol) was added to the deep red solution and the reaction mixture was stirred at room temperature for 6 h. The solution was filtered and the solvent was removed under vacuum to give a brown residue, which was dissolved in a small quantity of CH_2Cl_2 and chromatographed on silica gel. Elution with hexane/CH_2Cl_2 (1/2, v/v) resulted in the separation of an orange-red band containing the carbene complex. After the evaporation of the solvent, the residue was dissolved in 1 mL CH_2Cl_2 and covered with 4 mL toluene. Brown crystals were formed. Yield is about 19 % (25 mg). IR (KBr, cm^{-1}): 3440 (w), 2918 (w), 1721 (vs), 1477 (m), 1433 (s), 1251 (s), 1210 (s), 1125 (s), 1072 (m), 835 (vs), 690 (s), 525 (s) 446 (w), 424 (w). $^{31}P\{^1H\}$ NMR ($CDCl_3$, pm): 29.2 (s, 1P, PPh_3), 11.2 (broad, 1P, PPh_3^+), 144.6 (m, 1P, PF_6). ^{99}Tc NMR ($CDCl_3$, ppm): -1371 ($\nu_{1/2}$ = 3900 Hz). High quality ^1H and ^{13}C NMR spectra of the pure product could not be obtained, since minor traces of the dimer complex could not be removed.

$[Tc^{I}(NO)(Cp)(PPh_3)(CH_3CN)](PF_6)$:

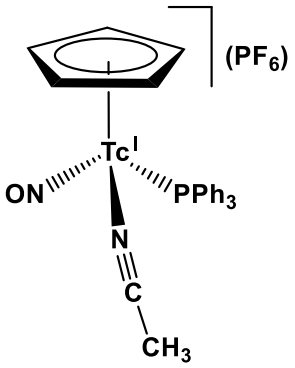

[Tc(NO)Cl(Cp)(PPh_3)] (25 mg, 0.05 mmol) was dissolved in 2 mL CH_2Cl_2 and treated with a solution of $AgPF_6$ (25 mg, 0.1 mmol) in 2 mL CH_2Cl_2/MeOH (2/1, v/v). CH_3CN (15 mL) was added to the deep red solution and the reaction mixture was heated under reflux for 3 h. The solution was filtered and the solvent was removed under vacuum. The residue was dissolved in 1 mL CH_2Cl_2 and covered with 4 mL *n*-hexane. Orange-red crystals were formed after slow diffusion of the solvents. Yield 52 % (17 mg). Elemental analysis: Calcd. for $C_{25}H_{23}N_2OP_2F_6Tc$: Tc 15.4 %, Found: Tc 13.9 %. IR (KBr, cm^{-1}): 3055 (w), 2910 (w), 2815 (w), 1710 (vs), 1507 (w), 1485 (m), 1310 (w), 1244 (w), 1180 (m), 1159 (w), 816 (vs), 748 (m), 694 (m), 578 (m), 546 (m), 525 (w), 500 (m). ^1H NMR ($CDCl_3$, ppm): 6.69 - 7.19 (m, 15H, Ph), 4.91

(s, 5H, Cp), 1.67 (s, 3H, CH_3). $^{31}P\{^1H\}$ NMR ($CDCl_3$, ppm): 37.5 (s, PPh_3), 146.4 (m, PF_6). ^{99}Tc NMR ($CDCl_3$, ppm): -538 ($\nu_{1/2}$ = 5900 Hz). The resonances in the ^{13}C NMR spectra were of low intensities and no accurate values could be assigned.

[Tc^I(NO)(Cp)(PPh_3)(Py)](PF_6):

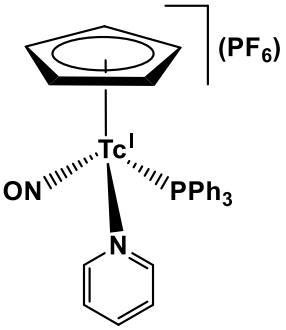

[Tc(NO)(Cp)(PPh_3)(CH_3CN)](PF_6) (32 mg, 0.05 mmol) was dissolved in 2 mL CH_2Cl_2 and treated with pyridine (0.5 mL). The reaction mixture was stirred for 1 h at room temperature. The solvent was removed under vacuum. The residue was dissolved in 1 mL CH_2Cl_2 and covered with 4 mL diethyl ether. Orange-red crystals were formed after slow diffusion of the solvents. Yield 64 % (22 mg). Elemental analysis: Calcd. for $C_{28}H_{25}N_2OP_2F_6Tc$: Tc 14.5 %, Found: Tc 13.1 %. IR (KBr, cm^{-1}): 3124 (w), 3074 (w), 1724 (vs), 1674 (w), 1514 (m), 1495 (m), 1242 (vs), 1170 (vs), 1089 (vs), 814 (vs), 708 (s), 692 (s), 518 (s). ^1H NMR ($CDCl_3$, ppm): 8.24 (d, 2h, Py), 7.68 (t, 1H, Py), 7.63 (t, 2H, Py), 7.12 - 7.56 (m, 15H, Ph), 5.41 (s, 5H, cp). ^{13}C NMR ($CDCl_3$, ppm): 154.6 (Py), 149.0 (Py), 138.2 (Py), 126.1 - 133.6 (Ph), 129.1 (Ph), 95.4 (Cp). $^{31}P\{^1H\}$ NMR ($CDCl_3$, ppm): 29.6 (s, PPh_3), 144.5 (m, PF_6). ^{99}Tc NMR ($CDCl_3$, ppm): -287 ($\nu_{1/2}$ = 4700 Hz).

[Tc^I(NO)(Cp)(PPh_3)(thioxane)](PF_6):

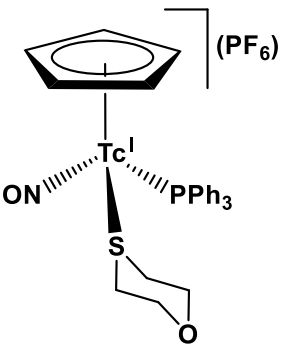

[Tc(NO)(Cp)(PPh_3)(CH_3CN)](PF_6) (32 mg, 0.05 mmol) was dissolved in 2 mL CH_2Cl_2 and treated with 0.5 mL thioxane. The reaction mixture was stirred for 2 h at room temperature. The solvent was removed under vacuum. The residue was dissolved in 1 mL CH_2Cl_2 and covered with 4 mL diethyl ether. Red crystals were formed after slow diffusion of the solvents. Yield 55 % (19 mg). Elemental analysis: Calcd. for $C_{27}H_{28}NOP_2F_6STc$: Tc 14.4 %, Found: Tc 12.9 %. IR (KBr, cm^{-1}): 3445 (w), 2912 (w), 2852 (w), 1737 (vs), 1481 (w), 1435 (m), 1311 (w), 1278 (w), 1192 (m), 1097 (m), 997 (w), 839 (vs), 745 (m), 694 (s), 574 (m), 526 (s), 497 (m). ^1H NMR ($CDCl_3$, ppm): 7.28 - 7.60 (m, 15, Ph), 5.29 (s, 5H, Cp), 3.68 - 3.87 (m, 4H, thioxane), 2.39 - 2.66 (m, 4H, thioxane). ^{13}C NMR ($CDCl_3$, ppm): 133.7 - 128.8 (Ph), 95.4 (Cp), 68.8 (CH_2, thioxane), 27.7 (CH_2, thioxane). $^{31}P\{^1H\}$ NMR ($CDCl_3$, ppm): 34.3 (s, PPh_3), 144.5 (m, PF_6). ^{99}Tc NMR ($CDCl_3$, ppm): -860 ($\nu_{1/2}$ = 5400 Hz).

[Tc^{I}(NO)(Cp)(PPh_3)($OPPh_3$)](PF_6):

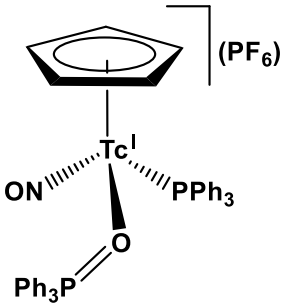

[Tc(NO)Cl(Cp)(PPh_3)] (50 mg, 0.1 mmol) was dissolved in 10 mL CH_2Cl_2 and treated with a solution of $AgPF_6$ (25 mg, 0.1 mmol) in 2 mL CH_2Cl_2/MeOH (2/1, v/v). A grey precipitate was formed. Triphenylphosphine oxide (28 mg, 0.1 mmol) was added to the reaction mixture, which was then heated under reflux for 3 h. The solution was filtered and the solvent was removed under vacuum. The residue was dissolved in 1 mL CH_2Cl_2 and covered with 3 mL diethyl ether. Red crystals were formed after slow diffusion of the solvents. Yield 49 % (42 mg). Elemental analysis: Calcd. for $C_{41}H_{35}NO_2P_3F_6Tc$: Tc 11.3 %, Found: Tc 10.1 %. IR (KBr, cm^{-1}): 3446 (w), 3055 (w), 2924 (w), 1699 (vs), 1585 (w), 1479 (m), 1435 (vs), 1309 (w), 1263 (w), 1180 (m), 1120 (vs), 839 (vs), 750 (m), 723 (s), 540 (vs). ^{1}H NMR (CD_2Cl_2, ppm): 7.25 - 7.73 (m, 30H, PPh_3, $OPPh_3$), 5.29 (s, 5H, Cp). ^{13}C NMR (CD_2Cl_2, ppm): 126.5 - 133.9 (36C, Ph), 93.2 (s, 5C, Cp). $^{31}P\{^{1}H\}$ NMR (CD_2Cl_2, ppm): 57.8 (s, P, $OPPh_3$), 31.7 (s, P, PPh_3), 144.5 (m, P, PF_6). ^{99}Tc NMR (CD_2Cl_2, ppm): 241 ($\nu_{1/2}$ = 6200 Hz).

[Tc^{I}(NO)(Cp)(PPh_3)($SPPh_3$)](PF_6):

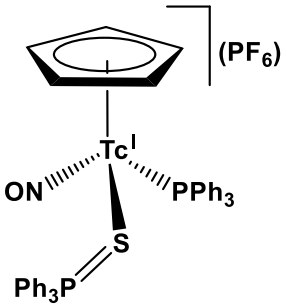

[Tc(NO)Cl(Cp)(PPh_3)] (50 mg, 0.1 mmol) was dissolved in 10 mL CH_2Cl_2 and treated with a solution of $AgPF_6$ (25 mg, 0.1 mmol) in 2 mL CH_2Cl_2/MeOH (2/1, v/v). A grey precipitate was formed. Triphenylphosphine sulfide (30 mg, 0.1 mmol) was added to the reaction mixture, which was then heated under reflux for 3 h. The solution was filtered and the solvent was removed under vacuum. The residue was dissolved in 1 mL CH_2Cl_2 and covered with 3 mL diethyl ether. Red crystals were formed after slow diffusion of the solvents. Yield 43 % (39 mg). Elemental analysis: Calcd. for $C_{41}H_{35}NOP_3F_6STc$: Tc 11.1 %, Found: Tc 9.7 %. IR (KBr, cm^{-1}): 3406 (w), 2902 (w), 1686 (s), 1579 (w), 1433 (vs), 1182 (m), 1099 (vs), 1024 (w), 997 (w), 839 (vs), 748 (s), 711 (vs), 603 (m), 553 (w), 511 (vs). ^{1}H NMR (CD_2Cl_2, ppm): 7.09 - 7.66 (m, 30H, PPh_3, $SPPh_3$), 5.29 (s, 5H, Cp) ppm. ^{13}C NMR (CD_2Cl_2, ppm): 128.2 - 133.6 (36C, Ph), 94.3 (s, 5C, Cp) ppm. $^{31}P\{^{1}H\}$ NMR (CD_2Cl_2, ppm): 51.8 (s, P, $SPPh_3$), 27.9 (s, P, PPh_3), 142.2 (m, P, PF_6). ^{99}Tc NMR (CD_2Cl_2, ppm): -781 ($\nu_{1/2}$ = 5800 Hz).

[Tc^{I}(NO)(Cp)(PPh_3)($SePPh_3$)](PF_6):

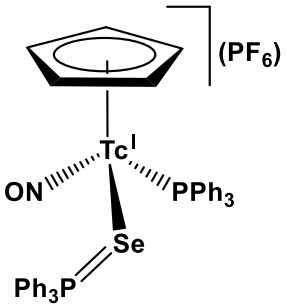

[Tc(NO)Cl(Cp)(PPh_3)] (50 mg, 0.1 mmol) was dissolved in 10 mL CH_2Cl_2 and treated with a solution of $AgPF_6$ (25 mg, 0.1 mmol) in 2 mL CH_2Cl_2/MeOH (2/1, v/v). A grey precipitate was formed. Triphenylphosphine selenide (35 mg, 0.1 mmol) was added to the reaction mixture, which was heated under reflux for 4 h. The solution was filtered and the solvent was removed under vacuum. The residue was dissolved in 1 mL CH_2Cl_2 and covered with 3 mL diethyl ether. Orange-red crystals were formed after slow diffusion of the solvents. Yield 38 % (35 mg). Elemental analysis: Calcd. for $C_{41}H_{35}NOP_3F_6SeTc$: Tc 10.5 %, Found: Tc 9.1 %. IR (KBr, cm^{-1}): 3425 (m), 1705 (vs), 1479 (m), 1435 (vs), 1195 (w), 1099 (vs), 997 (w), 839 (vs), 784 (s), 690 (vs), 549 (vs), 507 (vs). ^{1}H NMR (400 MHz, CD_2Cl_2, ppm): 6.99 - 7.71 (m, 30H, PPh_3, $SePPh_3$), 5.29 (s, 5H, Cp). $^{31}P\{^{1}H\}$ NMR (CD_2Cl_2, ppm): 34.2 (s, P, $SePPh_3$), 31.7 (s, P, PPh_3), 144.5 (m, P, PF_6). ^{99}Tc NMR (CD_2Cl_2, ppm): -876 ($\nu_{1/2}$ = 4850 Hz). The resonances in the ^{13}C NMR spectra were of low intensities and no accurate values could be assigned.

[Tc^{I}(NO)Cl(CpMe)(PPh_3)]:

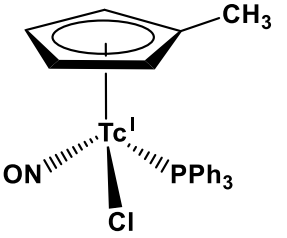

[Tc^{I}(NO)Cl_2(PPh_3)$_2$(MeCN)] (230 mg, 0.3 mmol) was suspended in 5 mL toluene. Na(CpMe) (102 mg, 1 mmol) was dissolved in 5 mL toluene and added to the light orange-red suspension. The reaction mixture was heated under reflux for 2 h. The solvent was removed under vacuum and the red residue was dissolved in CH_2Cl_2 (2 mL) and filtered over a 2 cm layer of silica gel. Hexane (2 mL) was added and the solvents were slowly evaporated, which resulted in the formation of a red solid of [Tc(NO)Cl(CpMe)(PPh_3)], which was isolated by filtration. Yield 66 % (110 mg). Elemental analysis: Calcd. for $C_{24}H_{22}NOPClTc$: Tc 19.5 %. Found: Tc 18.1 %. IR (KBr, cm^{-1}): 3442 (w), 3052 (w), 2978 (m), 2911 (w), 1684 (vs), 1488 (m), 1435 (s), 1268 (vs), 1203 (m), 1107 (vs), 1054 (vs), 926 (w), 999 (m), 810 (vs), 541 (m), 527 (m), 503 (m). ^{1}H NMR ($CDCl_3$, ppm): 7.40 - 7.67 (m, 15H, Ph), 5.13 (1H, Cp), 4.96 (1H, Cp), 4.62 (1H, Cp), 4.48 (1H, Cp), 1.81 (3H, Cp-CH_3). $^{31}P\{^{1}H\}$ NMR ($CDCl_3$, ppm): 27.3 (s, PPh_3). ^{99}Tc NMR ($CDCl_3$, ppm): -295 ($\nu_{1/2}$ = 4750 Hz). The resonances in the ^{13}C NMR spectra were of low intensities and no accurate values could be assigned.

[Tc^{I}(NO)(CpMe)(PPh_3)(Py)](PF_6):

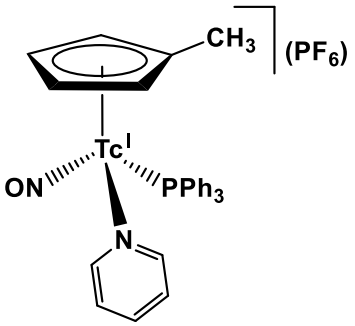

[Tc^{I}(NO)Cl(CpMe)(PPh_3)] (55 mg, 0.1 mmol) was dissolved in 2 mL CH_2Cl_2 and treated with a solution of $AgPF_6$ (25 mg, 0.1 mmol) in 2 mL CH_2Cl_2/MeOH (2/1, v/v). A grey precipitate was formed. Pyridine (0.5 mL) was added and the reaction mixture was stirred at room temperature for 2 h. The solution was filtered and the solvent was removed under vacuum. The residue was dissolved in 1 mL CH_2Cl_2 and covered with 4 mL diethyl ether. Orange-red crystals were formed after slow diffusion of the solvents. Yield 62 % (44 mg). Elemental analysis: Calcd. for $C_{29}H_{27}N_2OP_2F_6Tc$: Tc 14.2 %. Found: Tc 12.7 %. IR (KBr, cm^{-1}): 3449 (s), 2968 (m), 2901 (w), 1708 (vs), 1488 (m), 1439 (s), 1268 (w), 1245 (m), 1201 (m), 1112 (s), 1064 (m), 817 (vs), 768 (m), 751 (s), 740 (vs), 537 (vs). ^{1}H NMR ($CDCl_3$, ppm): 8.30 (d, 2h, Py), 7.72 (t, 1h, Py), 7.13 - 7.62 (m, 17H, Ph, Py), 5.38 (1H, Cp), 5.30 (1H, Cp), 5.14 (1H, Cp), 4.88 (1H, Cp), 1.65 (3H, Cp-CH_3). ^{13}C NMR ($CDCl_3$, ppm): 155.4 (Py), 149.9 (Py), 136.8 (Py), 124.2 - 133.3 (Ph, PPh_3), 107.2 (Cp), 97.5 (Cp), 94.1 (Cp), 91.7 (Cp), 90.7 (Cp), 13.2 (CH_3). ^{31}P{^{1}H} NMR ($CDCl_3$, ppm): 28.9 (S, PPh_3), 145.1 (m, PF_6). ^{99}Tc NMR ($CDCl_3$, ppm): -298 ($\nu_{1/2}$ = 4850 Hz).

[Tc^{I}(NO)Cl(CpCOOMe)(PPh_3)].

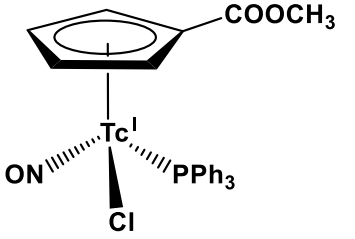

[Tc^{I}(NO)Cl_2(PPh_3)$_2$(MeCN)] (150 mg, 0.2 mmol) was suspended in 5 mL toluene. Na(CpCOOMe) (100 mg, 0.7 mmol) was dissolved in 5 mL toluene and added to the light orange-red suspension. The reaction mixture was heated under reflux for 2 h. The solvent was removed under vacuum. The red residue was dissolved in CH_2Cl_2 (2 mL) and filtered over a 2 cm layer of silica gel. Hexane (2 mL) was added and the solvents were slowly evaporated, which resulted in the formation of a deep red solid of [Tc(NO)Cl(CpCOOMe)(PPh_3)], which was isolated by filtration. Yield 63 % (70 mg). Elemental analysis: Calcd. for $C_{25}H_{22}NO_3PClTc$: Tc 17.9 %. Found: Tc 16.2 %. IR (KBr, cm^{-1}): 3392 (w), 3053 (m), 2958 (w), 2920 (w), 1786 (m), 1697 (vs), 1479 (s), 1433 (vs), 1286 (s), 1190 (s), 1143 (m), 1116 (m), 1093 (m), 1026 (m), 804 (m), 756 (s), 723 (m), 694 (vs), 540 (vs), 449 (w). ^{1}H NMR (CD_2Cl_2, ppm): 7.37 - 7.65 (m, 15H, PPh_3), 5.76 (1H, Cp), 5.38 (1H, Cp), 5.03 (1H, Cp), 4.92 (1H, Cp), 3.67 (3H, $COOCH_3$). ^{31}P{^{1}H} NMR (CD_2Cl_2, ppm): 28.1 (PPh_3). ^{99}Tc NMR (CD_2Cl_2, ppm): -253 ($\nu_{1/2}$ = 3350 Hz). The resonances in the ^{13}C NMR spectra were of low intensities and no accurate values could be assigned.

4 Summary

[Tc(NO)Cl(Cp)(PPh_3)] shows a considerable reactivity for ligand exchange reactions. Different monodentate ligands were used and a variety of donor atoms (O, Cl, I, N, S, Se, P, C) could successfully be coordinated to the robust {Tc(NO)(Cp)(PPh_3)}$^+$ core.

Most of the resulting complexes are stable as solids and in solution. However two exceptions were observed: (i) the dissolution of [Tc(NO)(I_3)(Cp)(PPh_3)] in CH_2Cl_2 for 24 h results in an internal oxidation of the technetium center and gives the complex [Tc(NO)(I_2)(Cp)] and (ii) a prolonged heating of [Tc(NO)(SCN)(Cp)(PPh_3)] in toluene forces an isomerization of this compound and gives the thermodynamically more stable complex [Tc(NO)(NCS)(Cp)(PPh_3)].

The treatment of [Tc(NO)Cl(Cp)(PPh_3)] with $AgPF_6$ forms in absence of any other ligand the dimeric complex [{Tc(NO)(Cp)(PPh_3)}$_2$Cl](PF_6), where two units of the {Tc(NO)(Cp)(PPh_3)}$^+$ core are bridged via the chlorido ligand.

The {Tc(NO)(Cp)(PPh_3)}$^+$ core can accommodate a second bulky PPh_3 ligand and gives the complex [Tc(NO)(Cp)(PPh_3)$_2$](PF_6) after prolonged heating of [Tc(NO)Cl(Cp)(PPh_3)], $AgPF_6$ and PPh_3 in boiling toluene.

The carbene complex [Tc(NO)(Cp)(PPh_3){C(OMe)$C_2H_4PPh_3$}](PF_6)$_2$ can be prepared by treating [Tc(NO)Cl(Cp)(PPh_3)] with $AgPF_6$, MeOH and $Me_3SiC{\equiv}C\text{-}CH_3$. The resulting complex is a Fischer-type carbene and is stable on air.

The ionic complex [Tc(NO)(Cp)(PPh_3)(CH_3CN)](PF_6) is formed by refluxing [Tc(NO)Cl(Cp)(PPh_3)] in an acetonitrile solution, which contains an equivalent amount of $AgPF_6$. [Tc(NO)(Cp)(PPh_3)(CH_3CN)](PF_6) readily reacts with strong donor ligands such as pyridine or 1,4-thioxane.

The {Tc(NO)(Cp)(PPh_3)}$^+$ core coordinates successfully to the three phosphine chalcogenide ligands Ph_3PO, Ph_3PS and Ph_3PSe. Consequently, three complexes of the general formula [Tc(NO)(Cp)(PPh_3)($XPPh_3$)](PF_6) (X = O, S, Se) were prepared and fully characterized.

All complexes synthesized for the present thesis are shown in Figure 4.1.

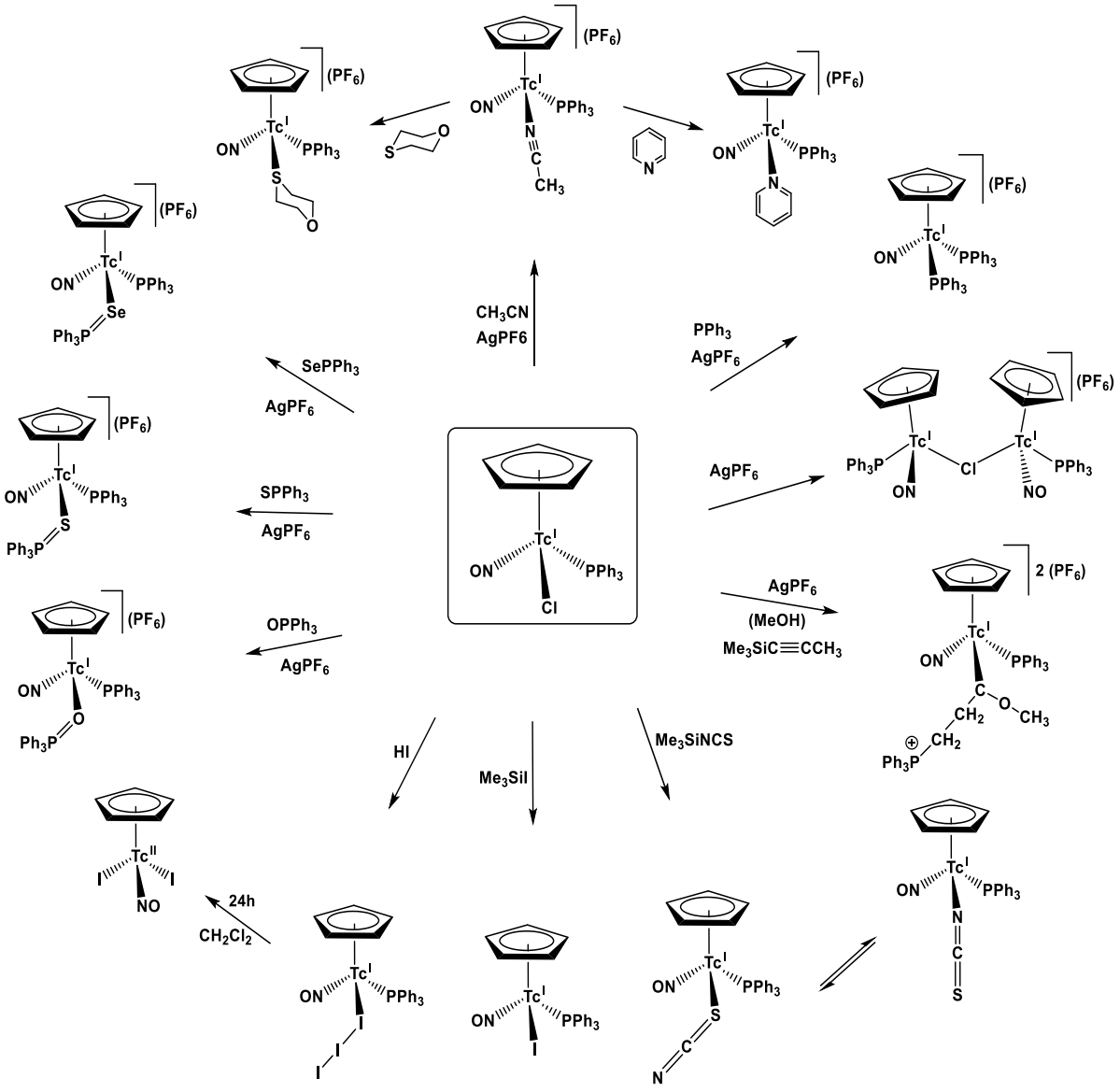

Figure 4.1: Complexes formed starting from [Tc(NO)Cl(Cp)(PPh_3)].

In the last part of this thesis, the syntheses of two substituted cyclopentadienyl species of the general formula [Tc(NO)Cl(Cp-X)(PPh_3)] (X = CH_3, $COOCH_3$) are described. These complexes were prepared following the same synthetic route, which was used for the preparation of [Tc(NO)Cl(Cp)(PPh_3)]. The reactivity of [Tc(NO)Cl(CpMe)(PPh_3)] was tested toward a ligand exchange reaction, where the chlorido ligand was readily replaced by a pyridine ligand and gave the complex [Tc(NO)(CpMe)(PPh_3)(pyridine)](PF_6). Particularly, the complex [Tc(NO)Cl(CpCOOMe)(PPh_3)] with the $COOCH_3$ group at the Cp ring can be considered as a promising precursor for bioconjugate labeling reactions. Figure 4.2 shows the complexes prepared in this part.

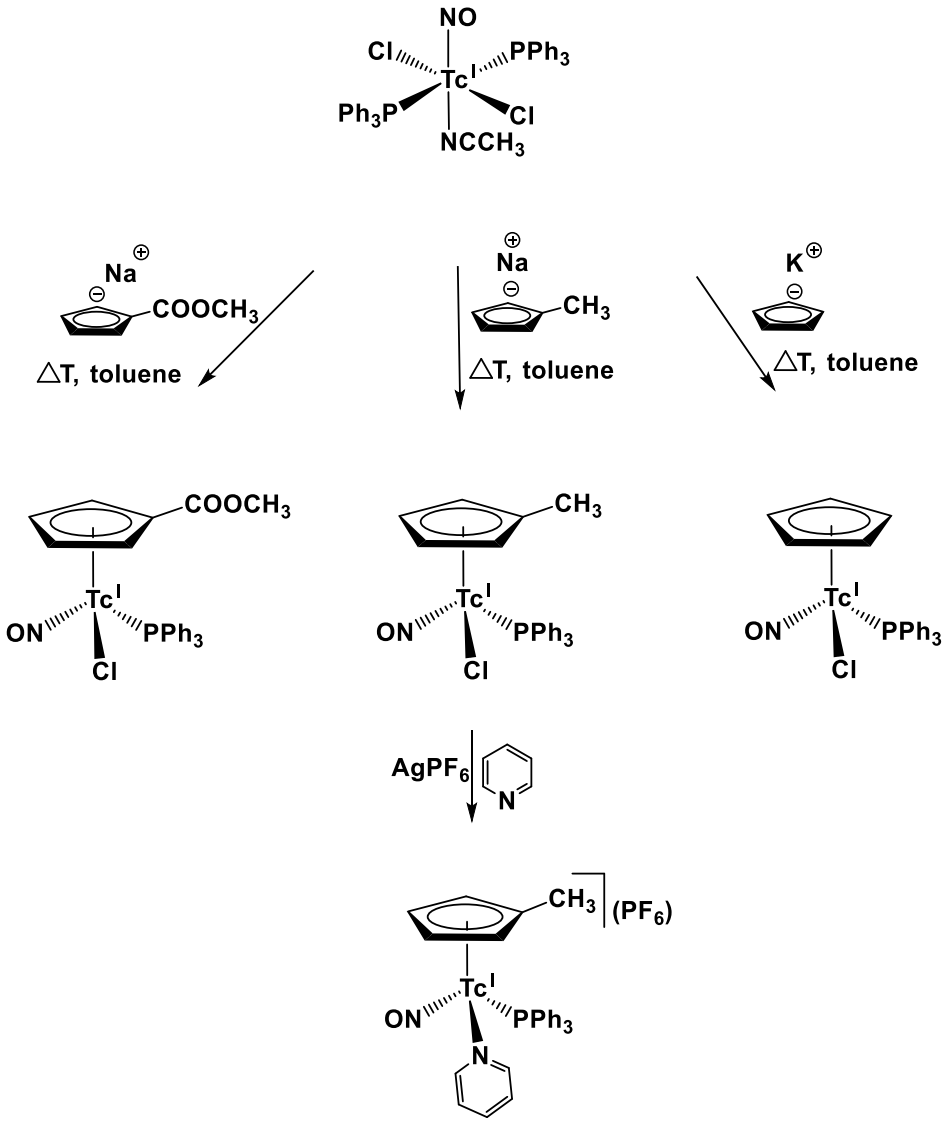

Figure 4.2: Synthesis of the complexes [Tc(NO)Cl(Cp-X)(PPh_3)] (X = CH_3, $COOCH_3$) and [Tc(NO)-Cl(Cp)(PPh_3)].

The complexes of this thesis possess pseudotetrahedral structures, in which the cyclopentadienyl rings (Cp, Cp-Me, Cp-COOMe) are η^5-coordinated. The NO ligands are linearly coordinated to technetium and show very strong absorption ν(NO) bands in the range between 1680 and1750 cm^{-1} for the resulting Tc(I) and Tc(II) complexes.

It is important to note, that the lead analytic method during the preparation of the complexes mentioned above was ^{99}Tc NMR spectroscopy. It proved to be an effective tool to monitor the course of the previous reactions. The chemical shifts for all NO-Cp, NO-CpMe and NO-CpCOOMe complexes appeared in the range between +250 ppm and -1800 ppm. In fact, the ^{99}Tc NMR shifts are solvent dependent with chemical shift differences up to 30 ppm.

Table 4.1 lists the ^{99}Tc resonances for all complexes having the $\{Tc(NO)(Cp\text{-}X)(PPh_3)\}^+$ core.

Compound	Solvent	δ	$\Delta\nu_{1/2}$	ref.
$[Tc(NO)(Cp)(PPh_3)(OPPh_3)]PF_6$	CD_2Cl_2	245	6231	This thesis
$[Tc(NO)(Cp)(OSO_2CF_3)(PPh_3)]$	$CDCl_3$	242	7070	33
$[Tc(NO)(OOCCF_3)(Cp)(PPh_3)]$	$CDCl_3$	19	4690	33
$[\{Tc(NO)(Cp)(PPh_3)\}_2Cl](PF_6)$	CD_2Cl_2	-220	4142	This thesis
$[Tc(NO)Cl(Cp)(PPh_3)]$	$CDCl_3$	-231	7170	19
$[Tc(NO)Cl(CpCOOMe)(PPh_3)]$	$CDCl_3$	-253	3350	This thesis
$[Tc(NO)Cl(CpMe)(PPh_3)]$	$CDCl_3$	-295	4750	This thesis
$[Tc(NO)(Cp)(PPh_3)(Py)]PF_6$	$CDCl_3$	-284	4679	This thesis
$[Tc(NO)Br(Cp)(PPh_3)]$	$CDCl_3$	-359	6500	19
$[Tc(NO)(Cp)(PPh_3)(CH_3CN)]PF_6$	$CDCl_3$	-538	5928	This thesis
$[Tc(NO)(I_3)(Cp)(PPh_3)]$	CD_2Cl_2	-679	6860	33
$[Tc(NO)I(Cp)(PPh_3)]$	CD_2Cl_2	-668	4200	33
$[Tc(NO)(Cp)(PPh_3)(SPPh_3)]PF_6$	CD_2Cl_2	-783	5783	This thesis
$[Tc(NO)(SCN)(Cp)(PPh_3)]$	$CDCl_3$	-820	6580	33
$[Tc(NO)(Cp)(PPh_3)(thioxane)]PF_6$	$CDCl_3$	-860	5412	This thesis
$[Tc(NO)(Cp)(PPh_3)(SePPh_3)]PF_6$	CD_2Cl_2	-876	4851	This thesis
$[Tc(NO)(Ph)(Cp)(PPh_3)]$	$CDCl_3$	-1201	8820	19
$[Tc(NO)(Cp)(PPh_3)_2]PF_6$	$CDCl_3$	-1219	6591	This thesis
$[Tc(NO)(Cp)(PPh_3)\{C(OMe)C_2H_4PPh_3\}](PF_6)_2$	$CDCl_3$	-1371	3927	This thesis
$[Tc(NO)(Cp)(PPh_3)(PMe_3)]PF_6$	$CDCl_3$	-1420	4100	This thesis
$[Tc(NO)(Cp)(PPh_3)(CO)]BF_4$	$CDCl_3$	-1753	3900	19

Table 4.1: Chemical shifts for all known complexes having the $\{Tc(NO)(Cp\text{-}X)(PPh_3)\}^{0,+1}$ cores.

Figure 4.3 shows the ^{99}Tc NMR chemical shifts observed for the known {Tc(NO)(Cp-X)(PPh_3)}$^{0,+1}$ complexes.

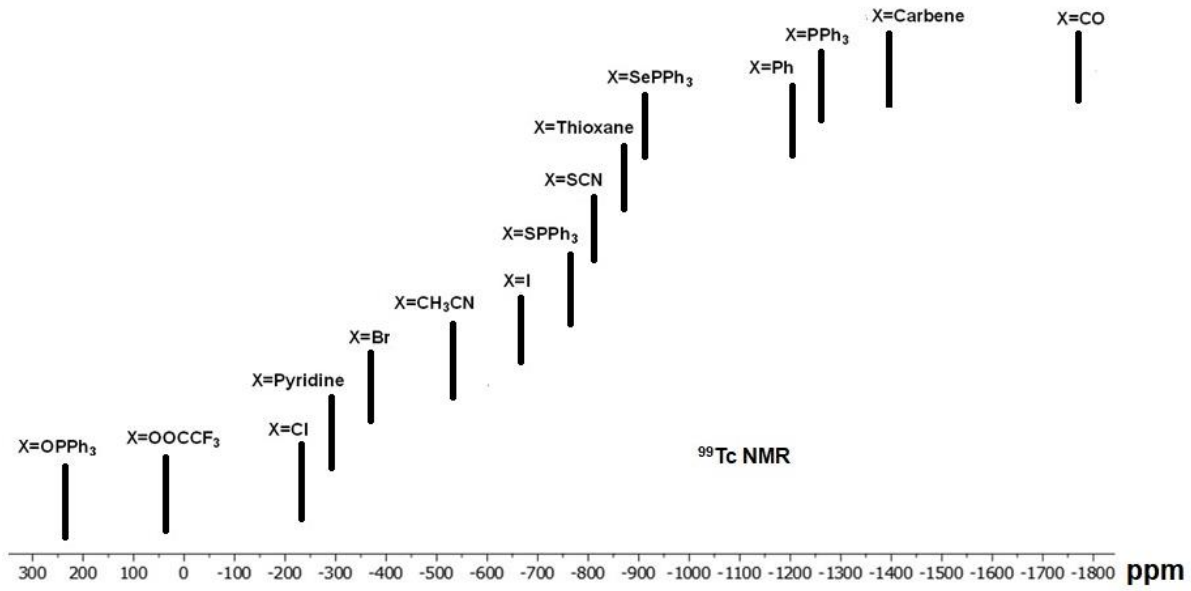

Figure 4.3: The ^{99}Tc NMR chemical shifts of the [Tc(NO)(L)(Cp)(PPh_3)]$^{0,+1}$ complexes.

It can be seen that the ligand L in the [Tc(NO)(L)(Cp)(PPh_3)]$^{0,+1}$ complexes has a large impact on the chemical shift values of the ^{99}Tc NMR data, which in turn reflect the influence of the electronic environment around technetium. It is interesting to see that the electronegativity of the donor atoms (ligand L) has a strong influence on the ^{99}Tc NMR chemical shift. The rule which was applicable in all earlier cases of L is, the more electronegative the bonded atom is, the weaker the shielding around the technetium nucleus is, and consequently the more the signal is shifted to the down-field.

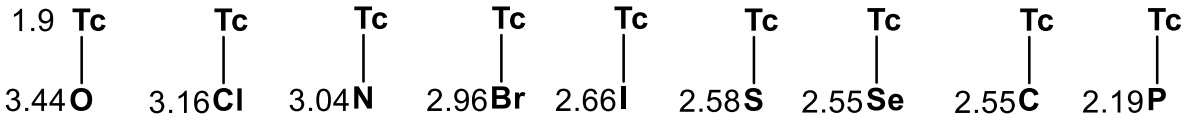

Figure 4.4: Comparison of the electronegativities of the donor atoms of the ligands used.

Lastly, there is no big difference in the observed ^{99}Tc NMR resonances by the replacement of the cyclopentadienyl ring with substituted ones (CpMe and CpOOCMe).

Zusammenfassung

[Tc(NO)Cl(Cp)(PPh_3)] zeigt vielfältige Ligandenaustauschreaktionen. So konnte eine Vielzahl einzähniger Liganden mit unterschiedlichsten Donoratomen (O, Cl, I, N, S, Se, P, C) an die stabile $\{Tc(NO)(Cp)(PPh_3)\}^+$-Einheit koordiniert werden.

Die meisten der entstandenen Komplexe sind sowohl als Feststoff als auch in gelöster Form stabil. Zwei Ausnahmen wurden hierbei beobachtet: erstens entsteht in einer CH_2Cl_2-Lösung von [Tc(NO)(I_3)(Cp)(PPh_3)] innerhalb von 24h durch intramolekulare Oxidation des Technetiums der Komplex [Tc(NO)($I)_2$(Cp)] und zweitens führt längeres Erhitzen von [Tc(NO)(SCN)(Cp)(PPh_3)] in Toluol zu einer Isomerisierung zum thermodynamisch stabileren Komplex [Tc(NO)(NCS)(Cp)(PPh_3)].

Die Reaktion von [Tc(NO)Cl(Cp)(PPh_3)] mit $AgPF_6$ führt in Abwesenheit weiterer Liganden zur Dimerisierung des Startkomplexes. Dabei werden zwei $\{Tc(NO)(Cp)(PPh_3)\}^+$-Einheiten über einen Chlorido-Liganden verbrückt.

Die Koordination eines zweiten sterisch anspruchsvollen Triphenylphosphan-Liganden an ein $\{Tc(NO)(Cp)(PPh_3)\}^+$-Zentrum, das heißt die Bildung von [Tc(NO)(Cp)($PPh_3)_2$](PF_6), gelingt bei längeren Reaktionszeiten und hohen Temperaturen.

Der Carbenkomplex [Tc(NO)(Cp)(PPh_3){$C(OMe)C_2H_4PPh_3$}]($PF_6)_2$ wurde durch ein Reaktion von [Tc(NO)Cl(Cp)(PPh_3)] mit $AgPF_6$, MeOH und $Me_3SiC{\equiv}C\text{-}CH_3$ erhalten. Dieser Komplex vom Fischer-Carben-Typ ist an der Luft stabil.

Wird [Tc(NO)Cl(Cp)(PPh_3)] in Acetonitril am Rückfluss erhitzt und ein Äquivalent $AgPF_6$ zugegeben, so wird der Chloridoligand durch ein Acetonitril-Molekül ersetzt und es entsteht der Komplex [Tc(NO)(Cp)(PPh_3)(CH_3CN)](PF_6). [Tc(NO)(Cp)(PPh_3)(CH_3CN)](PF_6) reagiert mit starken Donor-Liganden wie Pyridin oder 1,4-Thioxan unter Austausch des Acetonitril-Liganden.

Die $\{Tc(NO)(Cp)(PPh_3)\}^+$-Einheit konnte erfolgreich an drei Phosphinchalkogenide, Ph_3PO, Ph_3PS und Ph_3PSe koordiniert werden. Die drei Komplexe der allgemeinen Formel [Tc(NO)(Cp)(PPh_3)($XPPh_3$)(PF_6) (X=O, S, Se) wurden vollständig charakterisiert.

Alle Komplexe, die in dieser Dissertation vorgestellt wurden, sind in Abbildung 4.5 dargestellt.

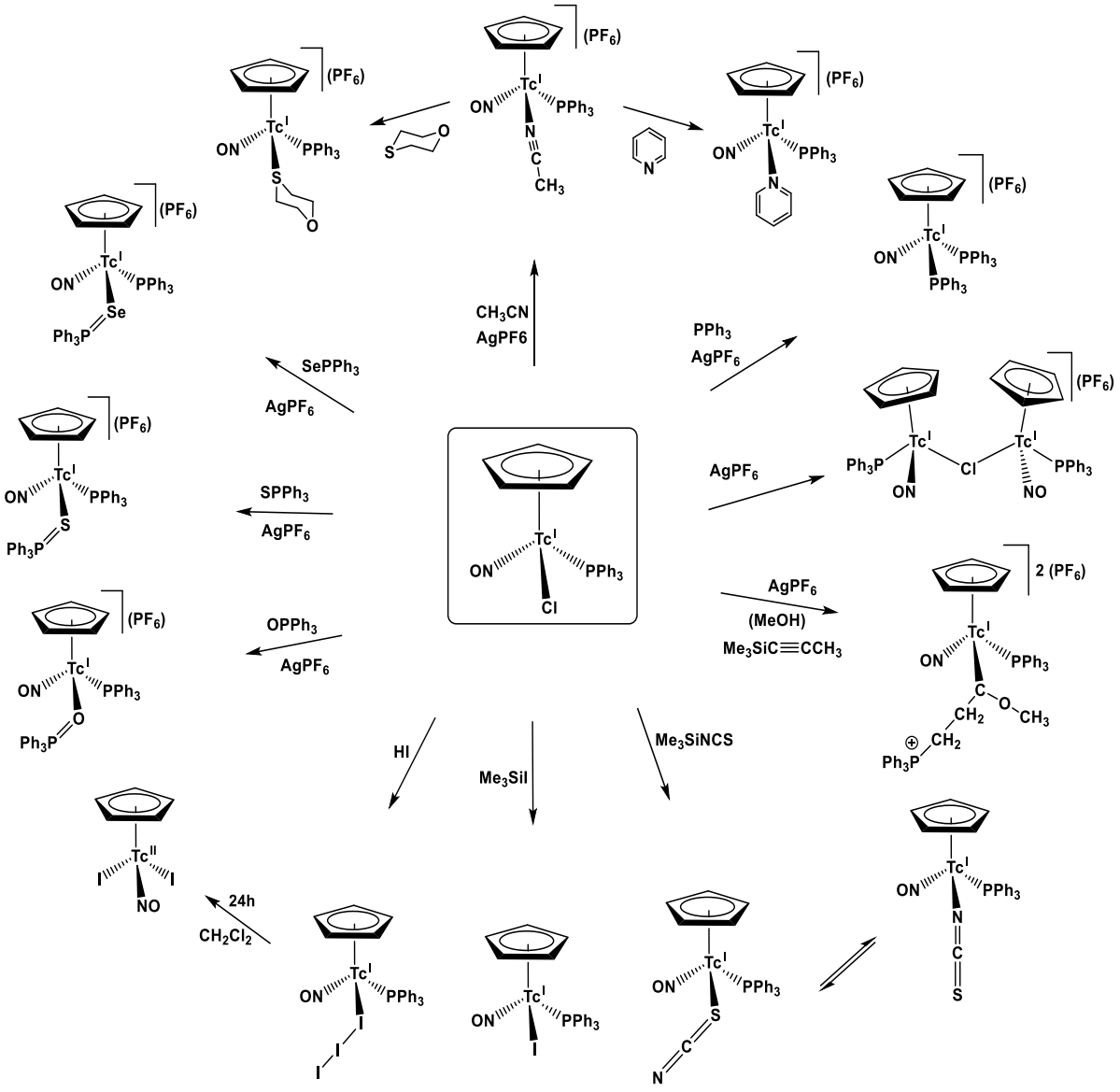

Abbildung 4.5: Komplexe, die ausgehend von [Tc(NO)Cl(Cp)(PPh_3)] hergestellt wurden und ihre Reaktionen.

Im letzten Teil dieser Dissertation wird die Synthese zweier Technetiumkomplexe mit substituierten Cyclopentadienyl-Liganden der allgemeinen Formel [Tc(NO)Cl(Cp-X)(PPh_3)] (X = CH_3, $COOCH_3$) beschrieben. Diese Komplexe wurden über den gleichen Syntheseweg, der zur Herstellung des Komplexes [Tc(NO)Cl(Cp)(PPh_3)] verwendet wurde, hergestellt. Eine Untersuchung der Reaktivität des Komplexes [Tc(NO)Cl(CpMe)(PPh_3)] zeigt, dass der Chlorido-Ligand in dieser Verbindung ebenfalls leicht durch einen Pyridin-Liganden ausgetauscht werden kann. Der Komplex [Tc(NO)Cl(CpCOOMe)(PPh_3)] kann somit als Startkomplex für die Biokonjugation betrachtet werden. Eine Zusammenstellung dieser Versuche wird in Abb. 4.6. gezeigt.

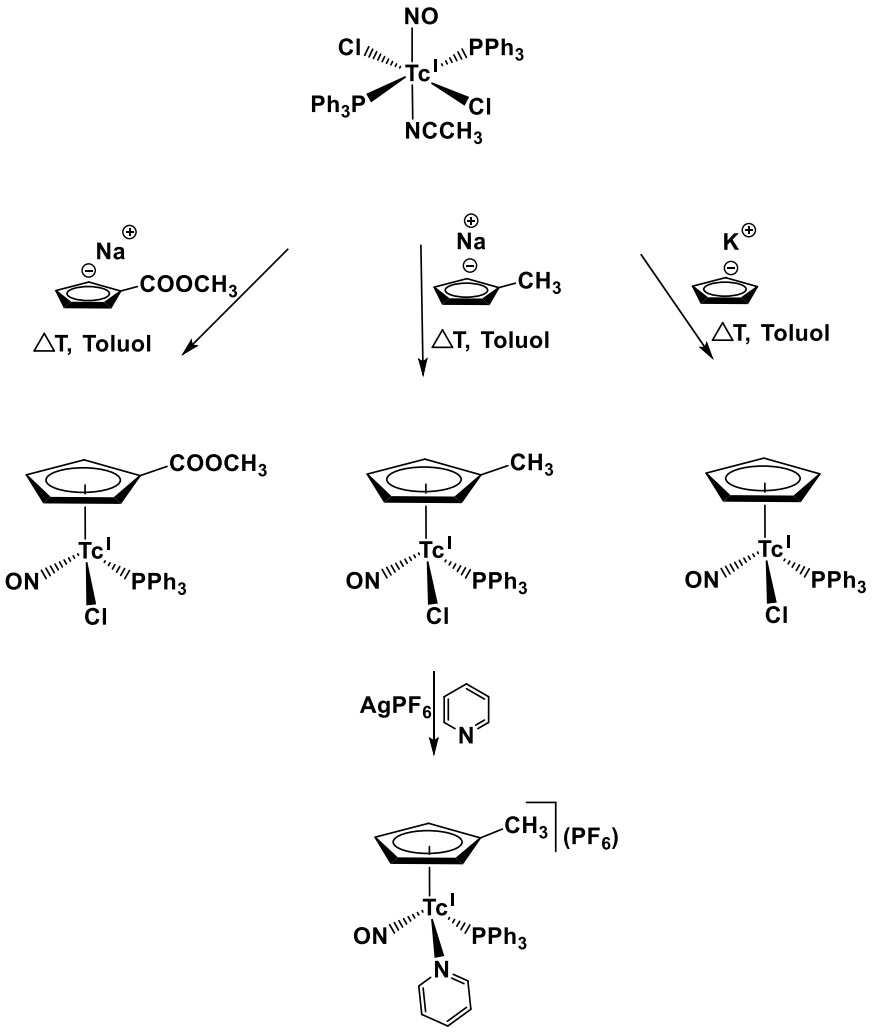

Abbildung 4.6: Synthese der Komplexe [Tc(NO)Cl(Cp-X)(PPh_3)] (X = CH_3, $COOCH_3$) und [Tc(NO)Cl-(Cp)(PPh_3)].

Alle in dieser Dissertation vorgestellten neuen Komplexe haben eine pseudotetraedrische Struktur, bei der die Cyclopentadienyl-Ringe zum Metallion η^5-koordiniert sind. Der NO-Ligand ist linear an das Technetiumatom koordiniert, es resultieren starke ν(NO)-Absorptionsbanden im Bereich von 1680 - 1750 cm^{-1} für die entsprechenden Tc(I) und Tc(II) Komplexe.

Bei der Kontrolle der Synthese der Komplexe spielte die ^{99}Tc-NMR-Spektroskopie eine wichtige Rolle. Diese Methode ist sehr gut geeignet, den Verlauf der beschriebenen Reaktionen zu verfolgen. Die chemischen Verschiebungen aller beschriebenen NO-Cp, NO-CpMe und NO-CpCOOMe Komplexe mit Technetium wurden im Bereich von +250 bis -1800 ppm nachgewiesen. Die ^{99}Tc-NMR-chemischen Verschiebungen sind stark lösungsmittelabhängig. Es treten dabei Unterschiede von bis zu 30 ppm auf. Eine Zusammenstellung der ^{99}Tc-NMR-

chemischen Verschiebungen von Komplexen mit einer zentralen $\{Tc(NO)(Cp\text{-}X)(PPh_3)\}^+$ Einheit sind in Tabelle 4.2 zu finden.

Komplex	Lösungsmittel	δ	$\Delta\nu_{1/2}$	Lit.
$[Tc(NO)(Cp)(PPh_3)(OPPh_3)]PF_6$	CD_2Cl_2	245	6231	diese Dissertation
$[Tc(NO)(Cp)(OSO_2CF_3)(PPh_3)]$	$CDCl_3$	242	7070	33
$[Tc(NO)(OOCCF_3)(Cp)(PPh_3)]$	$CDCl_3$	19	4690	33
$[\{Tc(NO)(Cp)(PPh_3)\}_2Cl](PF_6)$	CD_2Cl_2	-220	4142	diese Dissertation
$[Tc(NO)Cl(Cp)(PPh_3)]$	$CDCl_3$	-231	7170	19
$[Tc(NO)Cl(CpCOOMe)(PPh_3)]$	$CDCl_3$	-253	3350	diese Dissertation
$[Tc(NO)Cl(CpMe)(PPh_3)]$	$CDCl_3$	-295	4750	diese Dissertation
$[Tc(NO)(Cp)(PPh_3)(Py)]PF_6$	$CDCl_3$	-284	4679	diese Dissertation
$[Tc(NO)Br(Cp)(PPh_3)]$	$CDCl_3$	-359	6500	19
$[Tc(NO)(Cp)(PPh_3)(CH_3CN)]PF_6$	$CDCl_3$	-538	5928	diese Dissertation
$[Tc(NO)(I_3)(Cp)(PPh_3)]$	CD_2Cl_2	-679	6860	33
$[Tc(NO)I(Cp)(PPh_3)]$	CD_2Cl_2	-668	4200	33
$[Tc(NO)(Cp)(PPh_3)(SPPh_3)]PF_6$	CD_2Cl_2	-783	5783	diese Dissertation
$[Tc(NO)(SCN)(Cp)(PPh_3)]$	$CDCl_3$	-820	6580	33
$[Tc(NO)(Cp)(PPh_3)(Thioxan)]PF_6$	$CDCl_3$	-860	5412	diese Dissertation
$[Tc(NO)(Cp)(PPh_3)(SePPh_3)]PF_6$	CD_2Cl_2	-876	4851	diese Dissertation
$[Tc(NO)(Ph)(Cp)(PPh_3)]$	$CDCl_3$	-1201	8820	19
$[Tc(NO)(Cp)(PPh_3)_2]PF_6$	$CDCl_3$	-1219	6591	diese Dissertation
$[Tc(NO)(Cp)(PPh_3)\{C(OMe)C_2H_4PPh_3\}](PF_6)_2$	$CDCl_3$	-1371	3927	diese Dissertation
$[Tc(NO)(Cp)(PPh_3)(PMe_3)]PF_6$	$CDCl_3$	-1420	4100	diese Dissertation
$[Tc(NO)(Cp)(PPh_3)(CO)]BF_4$	$CDCl_3$	-1753	3900	19

Tabelle 4.2: Chemische Verschiebungen von Komplexen mit einer $\{Tc(NO)(Cp\text{-}X)(PPh_3)\}^+$-Einheit.

Abbildung 4.7 zeigt eine graphische Übersicht der Lage der ^{99}Tc-NMR-Signale der bislang bekannten {Tc(NO)(Cp-X)(PPh_3)}$^{0,+1}$-Komplexe.

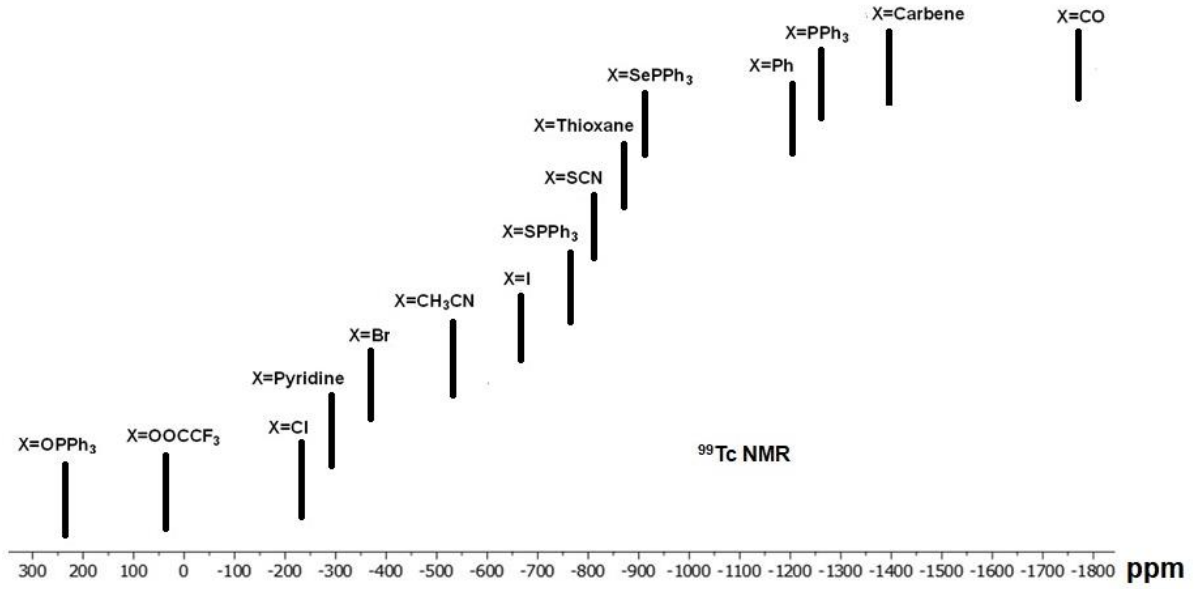

Abbildung 4.7: Lage von ^{99}Tc-NMR-Signalen von Komplexen der Zusammensetzung [Tc(NO)(L)-(Cp)(PPh_3)]$^{0,+1}$.

Es ist klar ersichtlich, dass der Ligand L in den [Tc(NO)(L)(Cp)(PPh_3)]-Komplexen einen großen Einfluss auf die chemische Verschiebung der ^{99}Tc-NMR-Signale hat. Das spiegelt den Einfluss der Liganden auf die elektronische Umgebung am Technetium wieder. Hierbei ist interessant, dass die Elektronegativität der Donoratome der Liganden einen starken Einfluss auf die chemische Verschiebung im ^{99}Tc-NMR-Spektrum hat. Für alle bisher untersuchten Komplexe gilt, dass je elektronegativer das gebundene Atom ist, desto schwächer ist die Abschirmung des Technetiumatoms und folglich umso stärker ist die Verschiebung ins Niedrigfeld.

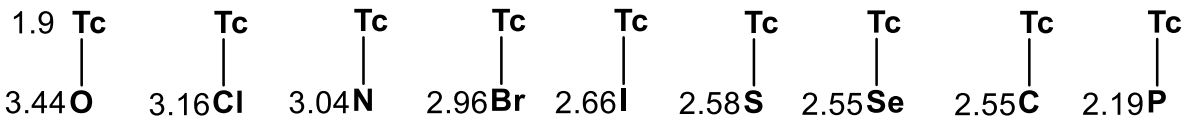

Abbildung 4.8: Vergleich der Elektronegativitäten der verwendeten Donoratome.

Der Austausch der unsubstituierten gegen substituierte Cyclopentadienyl-Ringe (CpMe und CpOOCMe) führt zu keinen signifikanten Unterschieden bei den beobachteten ^{99}Tc-NMR-Resonanzen.

5 References

[1] Alberto, R. 'Technetium', in *Comprehensive coordination chemistry II* (Eds.: McCleverty, A. J.; A., Meyer, J. T. *Elsevier*, Amsterdam, **2004**.

[2] Abram, U.; Alberto, R. Technetium and rhenium: coordination chemistry and nuclear medical applications. *J. Braz. Chem. Soc.* **2006,** *17*, 1486-1500.

[3] Alberto, R. Application of technetium and rhenium in nuclear medicine. *COSMOS* **2012**, *8*, 83-101.

[4] Linder, E. K.; Davison, A.; Dewan, C. J.; Costello, E. C.; Maleknia, S. synthesis and characterization of $[TcI(NO)(CNCMe_3)_5](PF_6)_2$ and $Tc(NO)Br_2(CNCMe_3)_3$ and the crystal structure of $Tc(NO)Br_2(CNCMe_3)_3$. *Inorg. Chem*. **1986**, *25*, 2085-2089.

[5] Abram, U.; Alberto, R. ^{99m}Tc: Labeling chemistry and labeled compounds. in *Handbook of Nuclear Chemistry*. Springer, **2011**, pp, 2073-2120.

[6] Bhattacharyya, S.; Dixit, M. Metallic radionuclides in the development of diagnostic and therapeutic radiopharmaceuticals. *Dalton Trans*. **2011,** *40*, 6112-6128.

[7] Cutler, C. S.; Hennkens, H. M.; Sisay, N.; Huclier-Markai, S.; Jurisson, S. S. Radiometals for Combined Imaging and Therapy. *Chem. Rev.* **2013,** *113*, 858-883.

[8] Price, E. W.; Orvig, C. Matching chelators to radiometals for radiopharmaceuticals. *Chem. Soc. Rev.* **2014,** *43*, 260-290.

[9] Liu, Y.; Spingler, B.; Schmutz, P.; Alberto, R., Metal-mediated *retro* Diels−Alder of dicyclopentadiene derivatives: a convenient synthesis of $[(Cp\text{-}R)M(CO)_3]$(M = ^{99m}Tc, Re) complexes. *J. Am. Chem. Soc.* **2008,** *130*, 1554-1555.

[10] Morais, G. R.; Paulo, A.; Santos, I. Organometallic complexes for SPECT imaging and/or radionuclide therapy. *Organometallics* **2012,** *31*, 5693-5714.

[11] N'Dongo, H. W. P.; Raposinho, P. D.; Fernandes, C.; Santos, I.; Can, D.; Schmutz, P.; Spingler, B.; Alberto, R. Preparation and biological evaluation of cyclopentadienyl-based ^{99m}Tc-complexes $[(Cp\text{-}R)^{99m}Tc(CO)_3]$ mimicking benzamides for malignant melanoma targeting. *Nucl. Med. and Biol*. **2010,** *37*, 255-264.

[12] Sulieman, S.; Can, D.; Mertens, J.; N'Dongo, H. W. P.; Liu, Y.; Schmutz, P.; Bauwens, M.; Spingler, B.; Alberto, R. Cyclopentadienyl-based amino acids (Cp-aa) as phenylalanine analogues for tumor targeting: syntheses and biological properties of $[(Cp\text{-}aa)M(CO)_3]$(M = Mn, Re, ^{99m}Tc). *Organometallics* **2012,** *31*, 6880-6886.

[13] Wang, X.; Li, D.; Deuther-C, W.; Lu, J.; Xie, Y.; Jia, B.; Cui, M.; Steinbach, J.; Brust, P.; Liu, B.; Jia, H. Novel cyclopentadienyl tricarbonyl ^{99m}Tc complexes containing

1-piperonylpiperazine moiety: potential imaging probes for sigma-1 receptors. *J. Med. Chem.* **2014,** *57*, 7113-7125.

[14] Agbossou, F.; O'Connor, J. E.; Garner, M. C.; Mendez, Q. N.; Fernandez, M. J.; Patton, T. A.; Ramsden, A. J.; Gladysz. A. J. Cyclopentadienyl Rhenium Complexes. In *Inorg. Synth*. **1992**, *29*, 211-225.

[15] Dembinski, R.; Lis, T.; Szafert, S.; Mayne, C. L.; Bartik, T.; Gladysz, A. J. Appreciably bent sp carbon chains: synthesis, structure, and protonation of organometallic 1, 3, 5-triynes and 1, 3, 5, 7-tetraynes of the formula (η^5-C_5Me_5) Re (NO)(PPh_3)(($C\equiv C)_n$-*p*-C_6H_4Me). *J. Organomet. Chem*. **1999,** *578*, 229-246.

[16] Eichenseher, S.; Delacroix, O.; Kromm, K.; Hampel, F.; Gladysz, A. J. Rhenium-containing phosphorus donor ligands for palladium-catalyzed Suzuki cross-coupling reactions: A new strategy for high-activity systems. *Organometallics* **2005,** *24*, 245-255.

[17] Quirós Méndez, N.; Arif, A. M.; Gladysz, A. J. Synthesis, structure, and dynamic behavior of rhenium sulfide and sulfoxide complexes of the formula [(η^5-C_5H_5)Re(NO)(L)(XRR')]$^+X'^-$ (X= S, SO). *Organometallics* **1991,** *10*, 2199-2209.

[18] Seidel, S. N.; Prommesberger, M.; Eichenseher, S.; Meyer, O.; Hampel, F.; Gladysz, J. A. Syntheses and structural analyses of chiral rhenium containing amines of the formula (η^5-C_5H_5)Re(NO)(PPh_3)(($CH_2)_n$NRR′)(n= 0, 1). *Inorg. Chim. Acta* **2010,** *363*, 533-548.

[19] Ackermann, J.; Hagenbach, A.; Abram, U. {Tc(NO)(Cp)(PPh_3)}$^+$ – a novel technetium(I) core. *Chem. Comm.* **2016,** *52*, 10285-10288.

[20] Ackermann, Janine. *Dissertation* FU Berlin **2016**.

[21] Trop, H. S.; Davison, A.; Jones, A. G.; Davis, M. A.; Szalda, D. J.; Lippard, S. J. Synthesis and physical properties of hexakis(isothiocyanato)technetate(III) and -(IV) complexes. Structure of the $[Tc(NCS)_6]^{3-}$ ion. *Inorg. Chem*. **1980**, *19*, 1105-1010.

[22] Baldas, J.; Bonnyman, J.; Williams, G. A. J. Structural studies of technetium complexes. Part 4. The crystal structure of *trans*,*trans*-acetonitriledi-isothiocyanato(nitrido) bis(triphenylphosphine)-technetium(V)-acetonitrile (1/0.5). *J. Chem. Soc., Dalton Trans*. **1984**, 833-837.

[23] Bandoli, G.; Mazzi, U.; Ichimura, A.; Libson, K.; Heineman, W. R.; Deutsch, E. An isothiocyanato complex of technetium(II). Spectroelectrochemical and single-crystal x-ray structural studies on trans-$[Tc(DPPE)_2(NCS)_2]^0$, where DPPE = 1,2-bis(diphenylphosphino)-ethane. *Inorg. Chem*. **1984**, *23*, 2898-2901.

[24] Williams, G. A.; Bonnyman, J.; Baldas, J. Structural Studies of Technetium Complexes. X. The Crystal Structure of Tetraphenylarsonium Hexakis (Isothiocyanat)Technetate(IV) -

Dichloromethane (1/1). *Aust. J. Chem*. **1987**, *40*, 27-33.

[25] Rochon, F. D.; Melanson, R.; Kong, P.-C. Synthesis of new mixed-ligands Tc complexes containing monodentate phosphine and isothiocyanato ligands: Crystal structures of complexes $Tc(P(C_3H_7)_3)_2(NCS)_4$, $Tc(P(CH_3)_2Ph)_4(NCS)_2$ and $Tc(P(OCH_3)Ph_2)_4(NCS)_2 \cdot 1/2CH_2Cl_2$. *Inorg. Chim. Acta* **2000***, 300,* 43-48.

[26] Hauck, J.; Schwochau, K.; Bucksch, R. Zur Kristallstruktur komplexer Technetiumverbindungen II. $[(CH_3)_4N][Tc^V(NCS)_6]$. *Inorg. Nucl. Chem. Lett.* **1973**, *9*, 927-927.

[27] Roodt, A.; Leipoldt, J. G.; Deutsch, E. A.; Sullivan, J. G. Kinetic and structural studies on the oxotetracyanotechnetate(V) core: protonation and ligation of dioxotetracyanotechnetate(V) ions and crystal structure of 2,2'-bipyridinium trans-oxothiocyanatotetracyanotechnetate(V). *Inorg. Chem.* **1992**, *31*, 1080-1085.

[28] Jurisson, S.; Hallhan, M. M.; Lydon, J. D.; Barnes, C. L.; Nowotnik, D. P.; Nunn, A. D. Linkage Isomerization of $MSCN(CDOH)_2(CDO)BMe$ to $MNCS(CDOH)_2(CDO)BMe$ (M= Tc, Re). Crystal Structures of $TcNCS(CDOH)_2(CDO)BMe$, $ReNCS(CDOH)_2(CDO)BMe$, and $ReSCN(CDOH)_2(CDO)BMe$. *Inorg. Chem.* **1998**, *37*, 1922-1928.

[29] Abram, U.; Abram, S.; Dilworth, J. R. Mixed-Ligand Complexes of Technetium. XIV. Structure of trans-$[TcCl_2(NCS)(Me_2PhP)_3]$. *Acta Cryst*. **1996**, *C52*, 605-607.

[30] Homolya, L.; Preetz, W. Kristallstrukturen, Schwingungsspektren und Normalkoordinaten-analyse von cis-$(n\text{-}Bu_4N)_2[ReBr_4(NCS)(SCN)]$, trans-$(n\text{-}Bu_4N)_2[ReBr_4(NCS)(SCN)]$ und trans-$(n\text{-}Bu_4N)_2[ReBr_4(NCSe)(SeCN)]$. *Z. Naturforsch.* **1999**, *B54*, 1009-1014.

[31] Gonzalez, R.; Barboza, N.; Chiozzone, R.; Kremer, C.; Armentano, D.; De Munno, G.; Faus, J. Linkage isomerism in the metal complex hexa(thiocyanato)rhenate(IV): Synthesis and crystal structure of $(NBu_4)_2[Re(NCS)_6]$ and $[Zn(NO_3)(Me_2phen)_2]_2[Re(NCS)_5(SCN)]$. *Inorg. Chim. Acta*, **2008**, *361*, 2715-2720.

[32] Gonzalez, R.; Acosta, A.; Chiozzone, R.; Kremer, C.; Armentano, D.; De Munno, G.; Julve, M.; Lloret, F.; Faus, J. New family of thiocyanate-bridged Re(IV)-SCN-M(II) (M = Ni, Co, Fe, and Mn) heterobimetallic compounds: synthesis, crystal structure, and magnetic properties. *Inorg. Chem*. **2012**, *51*, 5737-5747.

[33] Ackermann, J.; Abdulkader, A.; Scholtysik, C.; Roca Jungfer, M.; Hagenbach, A.; Abram, U. $[Tc^I(NO)X(cp)(PPh_3)]$ Complexes ($X^- = I^-, I_3^-, SCN^-, CF_3SO_3^-$ or CF_3COO^-) and Their Reactions. *Organometallics,* **2019**. *38,* 4471-4478.

[34] Ambrosetti, R.; Baratta, W.; Dell'Amico, D. B.; Calderazzo, F.; Marchetti, F. Adducts of diiodine and other dihalogens with halo metal complexes. I. Reactions with iodo complexes of

group 7 metals. Spectroscopic studies, formation constants and crystal and molecular structure of the triiodo complex $Re(I_3)(CO)_3(Me_2PCH_2CH_2PMe_2)$. *Gazz. Chim. Ital.* **1990**, *120*, 511-525.

[35] Tam, W.; Lin, G-Y.; Wong, W-K.; Kiel, A. W.; Wong, K. V.; Gladysz, A. J. Synthesis and Electrophile-Induced Disproportionation of the Neutral Formyl [(η^5-C_5H_5)Re(NO)(PPh_3)(CHO)]. *J. Am. Chem. Soc*. **1982**, *104*, 141-152.

[36] Winter, H. C.; Arif, A. M.; and Gladysz, A. J. Synthesis, Structure, and Reactivity of Bridging Halide Complexes of the Formula [(η^5-C_5H_5)Re(NO)(PPh_3)]$_2X^+BF_4$". Preferential Binding of One Enantiomer of Halide Complexes (η^5-C_5H_5)Re(NO)(PPh_3)(X) by the Chiral Lewis Acid [(η^5-C_5H_5)Re(NO)(PPh_3)]$^+$. *Organometallics* **1989**, *8*, 219-225.

[37] Buhro, E. W.; Zwick, D. B.; Georgiou, S.; Hutchinson, P. J.; Gladysz, A. J. Synthesis, Structure, Dynamic Behavior, and Reactivity of Rhenium Phosphido Complexes (η^5-C_5H_5)Re(NO)(PPh_3)(PR_2): The "Gauche Effect" in Transition-Metal Chemistry. *J. Am. Chem. Soc.* **1988**, *110*, 2427-2439.

[38] Kowalczyk, J. J.; Arif, A. M.; Gladysz, J. A. Synthesis, Structure, and Reactivity of Chiral Rhenium Alkyne Complexes of the Formula [(η^5-C_5H_5)Re(NO)(PPh_3)(RC=CR')](BF_4)]. *Organometallics* **1991**, *10*, 1079-1088.

[39] Senn, R. D.; Wong, A.; Patton, T. A.; Marsi, M.; Strouse, E. C.; Gladysz, A. J. Synthesis, Structure, and Reactions of Chiral Rhenium Vinylidene and Acetylide Complexes of the Formula [(η^5-C_5H_5)Re(NO)(PPh_3)(X)]$^{n+}$': Vinylidene Complexes That Are Formed by Stereospecific C_β Electrophilic Attack, Exist as Two Re=C=C Geometric Isomers, and Undergo Stereospecific C_α Nucleophilic Attack. *J. Am. Chem. Soc.* **1988**, *110*, 6096-6109.

[40] Fischer, O. E.; Apostolidis, C.; Dornberger, E.; Filippou, C. A.; Kanellakopulos, B.; Lungwitz, B.; Müller, J.; Powietzka, B.; Rebizant, J.; Roth, W. Carbene and Carbyne Complexes of Technetium and Rhenium - Synthesis, Structure and Reactions. *Z. Natuforsch*. **1995**, *50b*, 1382-1395.

[41] Semmelhack, F. M.; Lindenschmidt, A.; Ho, D. Preparation and Structure of Chiral Carbene Complexes of Manganese and Iron from Terminal Alkynes. *Organometallics* **2001**, *20*, 4114-4117.

[42] Buhro, E. W.; Wong, A.; Merrifield, H. J.; Lin, Y. G.; Constable, C. A.; Gladysz, A. J. Synthesis and Chemistry of Chiral Rhenium Acyls (η^5-C_5H_5)Re(NO)(PPh_3)(COR). *Organometallics* **1983**, *2*, 1852-1859.

[43] Ogata, K.; Seta, J.; Yamamoto, Y.; Kuge, K.; Tatsumi, K. One-pot syntheses of alkenyl-phosphonio complexes of ruthenium(II), rhodium(III) and iridium(III) bearing *p*-cymene or pentamethylcyclopentadienyl groups. *Inorg. Chim. Acta* **2007**, *10*, 3296-3303.

[44] Cowley, J. M.; Lynam, M. J.; Moneypenny, S. R.; Whitwood, C. A.; Wilson, J. A. Ruthenium alkynyl, carbene and alkenyl complexes containing pendant uracil groups: an investigation into the formation of alkenyl-phosphonio complexes. *Dalton Trans.* **2009**, 9529-9542.

[45] Struchkov, T. Y.; Aleksandrov, G. G. X-ray Crystal structure of some new alkoxy-carbeneplatinum(II) complexes. *J. Organomet. Chem.* **1979**, *172*, 269-272.

[46] Kowalczyk, J. J.; Agbossou, K. S.; Gladysz, A. J. Generation and reactivity of the chiral rhenium chlorobenzene complex $[(\eta^5\text{-}C_5H_5)Re(NO)(PPh_3)(ClC_6H_5)]^+BF_4^-$: an improved functional equivalent of the chiral Lewis acid $[(\eta^5\text{-}C_5H_5)Re(NO)(PPh_3)]^+BF_4^-$. *J. Organomet. Chem*. **1990**, *397*, 333-346.

[47] Merrifield, H. J.; Lin, Y. G.; Kiel, A. W.; Gladysz, A. J. Mechanism of Coupling of $=CH_2$ to $H_2C=CH_2$ at a Homogeneous $(\eta^5\text{-}C_5H_5)Re(NO)(PPh_3)^+$ Center. Remarkable Enantiomer Self-Recognition. *J. Am. Chem. Soc*. **1983**, *105*, 5811-5819.

[48] Otto, M.; Boone, J. B.; Arif, M. A.; Gladysz, A. J. Synthesis, structure, and interconversion of chiral rhenium oxygenand sulfur-bound sulfoxide complexes of formula $[(\eta^5\text{-}C_5H_5)\text{-}Re(NO)(PPh_3)(OS(Me)R)]\ X^-$; diastereoselective oxidations of coordinated methyl alkyl sulfides. *J. Chem. Soc., Dalton Trans*. **2001**, 1218-1229.

[49] Dewey, A. M.; Knight, A. D.; Arif, M. Atta.; Gladysz, A. J. Synthesis and Structure of σ Complexes of the Chiral Rhenium Lewis Acid $[(\eta^5\text{-}C_5H_5)Re(NO)(PPh3)]^+$ and Aromatic Nitrogen Heterocycles. *Z. Naturforsch*. **1992,** *47b*, 1175-1184.

[50] Olmstead, M. M.; Musker, K. W.; Kessler, M. R. Differences in the Coordinating Ability of Water, Perchlorate and Tetrafluoroborate toward Copper(I). The X-ray Crystal Structures of $[Cu(1,4\text{-thioxane})_3OC1O_3]$, $[Cu(1,4\text{-thioxane})_3OH_2]BF_4$ and $[Cu(1,4\text{-thioxane})_4BF_4$. *Transition Met. Chem.* **1982**, *7*, 140-146.

[51] Barnes, C. J., and Paton, D. J. Structures of Three Polymeric Complexes [Silver(l) Nitrate]$_x$-l,4-Oxathiane, $(AgNO_3)_x.C_4H_8OS$ [X= 1(I), 2(II), 6(III)]. *Acta Cryst.* **1984**. *40*, 72-78.

[52] Hagenbach, A.; Yegen, E.; Abram, U. Technetium Tetrachloride as A Precursor for Small Technetium(IV) Complexes. *Inorg. Chem*. **2006**, *45*, 7331-7338.

[53] Boorman, M. P.; Reimer, J. K. Complexes of Tungsten Halides with Group VI Donors: Adducts with Triphenylphosphine Chalcogenides. *Can. J. Chem.* **1971**, *49*, 2926-2930.

[54] Burford, N.; Royan, W. B.; Spence, E. v. H. R. Nuclear Magnetic Resonance Spectroscopic Characterisation and the Crystal and Molecular Structures of $Ph_3PS.AICI_3$ and $Ph_3PSe.AICI_3$: A Classification of the Co-ordinative Bonding Modes of the Phosphine Chalcogenides. *J. Chem. Soc., Dalton Trans*. **1990,** 2111-2117.

[55] Taouss, C.; Jones, G. P.; Upmann, D.; Bockfeld. D. Phosphanchalkogenide und ihre Metallkomplexe. III. Halogenierungsprodukte der Gold(I)komplexe Ph_3PEAuX (E = S oder Se; X = Cl, Br oder I). *Z. Naturforsch*. **2015**, *70*, 911-927.

[56] Thöne, C.; Jones, O. P. Tricarbonyl(cyclopentadienyl)(selenotriphenylphosphonium)-tungsten(I) Perchlorate, $[W(C_5H_5)(C_{18}H_{15}PSe)(CO)_3](ClO_4)$. *Acta Cryst.* **1996**. *C52*, 1084-1086.

[57] Kuhn, N.; Schumann, H,; Wolmershauser, G. $M(CO)_5(R_3PTe)$ (M = Cr, Mo, W; R = Bu^t): the First Stable Tellurophosphorane Complexes. *J. Chem. Soc., Chem. Commun.* **1985**, *22*, 1595-1597.

[58] Daniliuc, C.; Druckenbrodt, C.; Hrib, G. C.; Ruthe, F.; Blaschette, A.; Jones, G.; du Mont, W-W. The first trialkylphosphane telluride complexes of Ag(I): molecular, ionic and supramolecular structural alternatives. *Chem. Commun*. **2007**, *20*, 2060-2062.

[59] Burford, N. Modes of coordination for the phosphorylic unit. *Coord. Chem. Rev.* **1992,** *112*, 1-18.

[60] Scapens, D.; Adams, H.; Johnson, R. T.; Mann, E. B.; Sawle, P.; Aqil, R.; Perrior, T.; Motterlini, R. $[(\eta\text{-}C_5H_4R)Fe(CO)_2X]$, X= Cl, Br, I, NO_3, CO_2Me and $[(\eta\text{-}C_5H_4R)Fe(CO)_3]^+$, R=$(CH_2)_nCO_2Me$ (*n* =0–2), and $CO_2CH_2CH_2OH$: a new group of CO-releasing molecules. *Dalton Trans*. **2007**, 4962-4973.

[61] Nantz, H. M.; Radisson, X.; Fuchs, L.P. Efficient 4 + 1 Syntheses of Highly Functionalized Cyclopentenes. *Synth. Commun.* **1987**, *17*, 55-69.

[62] Chong, D.; Laws, R. D.; Nafady, A.; Costa, J. P.; Rheingold, L. A.; Calhorda, J. M.; Geiger, E. W. $[Re(\eta^5\text{-}C_5H_5)(CO)_3]^+$ Family of 17-Electron Compounds: Monomer/Dimer Equilibria and Other Reactions. *J. Am. Chem. Soc*. **2008**, *130*, 2692-2703.

[63] Top, S.; Lehn, J.-S.; Morel, P.; Jaouen, G. Synthesis of cyclopentadienyl-tricarbonylrhenium(I) carboxylic acid from perrhenate. *J. Organomet. Chem*. **1999**, *583*, 63-68.

[64] Cais, M.; Kozikowski, J. The Chemistry of Cyclopentadienyhnanganese Tricarbonyl Compounds. II. Sulfonation and Metallated Derivatives. *J. Am. Chem. Soc.* **1960**, *82*, 5667-5670.

[65] Cana, D.; Peindy N'Dongo W. H.; Spingler. B.; Schmutza, P.; Raposinhob, P.; Santosb, I.; Alberto, R. The $[(Cp)M(CO)_3]$ (M= Re, ^{99m}Tc) Building Block for Imaging Agents and Bioinorganic Probes: Perspectives and Limitations. *Chemistry & Biodiversity* **2012**, *9*, 1849-1865.

[66] Can, D.; Schmutz, P.; Sulieman, S.; Spingler, B.; Alberto, R. $[(Cp\text{-}R)M(CO)_3]$ (M= Re or ^{99m}Tc) Conjugates for Theranostic Receptor Targeting. *Chimia* **2013**, *67*, 267-270.

[67] Ursillo, S.; Can, D.; Peindy N'Dongo W. H.; Schmutz, P.; Spingler. B.; Alberto, R. Cyclopentadienyl Chemistry in Water: Synthesis and Properties of Bifunctionalized [(η^5-C_5H_3{COOR}$_2$)M(CO)$_3$] (M=Re and ^{99m}Tc) Complexes. *Organometallics* **2014**, *33*, 6945-6952.

[68] Crocco, L. G.; Gladysz, A. J. Reactions of (Cyclopentadieny1)rhenium Halide Complexes (η^5-C_5H_5)Re(NO)(PPh,)(X) with n-BuLi/TMEDA; Generation and Methylation of Lithio- and Dilithiocyclopentadienyl Ligands. *Chem. Ber*. **1988**, *121*, 375-377.

[69] Johnston, P.; Loonat, S. M.; Ingham, L.W.; Carlton, L.; Coville, J. N. Substituted Cyclopentadienyl Complexes. 1. The Proton Nuclear Magnetic Resonance Spectra off [(η^5-C_5H_4Me)Fe(CO)(L)I] and [(η^5-C_9H_7)Fe(CO)(L)I]. *Organometallics* **1987**, *6*, 2121-2127.

[70] Carlton, L.; Johnston, P.; Coville, J. N. Substituted cyclopentadienyl complexes II. ^{13}C NMR spectra of some [(η^5-C_5H_4Me)Fe(CO)(L)I] complexes. *J. Organomet. Chem*, **1988**, *339*, 339-343.

[71] Ackermann, J.; Noufele, C. N.; Hagenbach, A.; Abram, U. Nitrosyltechnetium(I) Complexes with 2-(Diphenylphosphanyl)aniline. *Z. Anorg. Allg. Chem*. **2019**, *645*, 8-13.

[72] Blanchard, S. S.; Nicholson, T. L.; Davison, A.; Davis, W. M.; Jones, A. G. The synthesis, characterization and substitution reactions of the mixed ligand technetium(I) nitrosyl complex trans–trans-[(NO)(NCCH$_3$)Cl$_2$(PPh$_3$)$_2$Tc]. *Inorg. Chim. Acta* **1996**, *244*, 121-130.

[73] Panda, T. K.; Gamer, M. T.; Roesky, P. W.; Yoo, H.; Berry, H. H. Sodium and Potassium Cyclopentadienide. *Inorg. Synth*. **2014**, *36*, 35-37.

[74] Jana, R.; Kumar, M. S.; Singh, N.; Elias, A. J. Synthesis, reactivity and structural studies of (η^5-methylcyclopentadienyl)(η^4-tetraphenylcyclopentadiene)cobalt and its derivatives. *J. Organomet. Chem*. **2008,** *693*, 3780-3786.

[75] Hart, P. W.; Shihua, D.; Rausch, D. M. The formation and reactions of (η^5-carboxycyclopentadienyl)dicarbonylcobalt. *J. Organomet. Chem*. **1985**, *282*, 111-121.

[76] WinEPR SimFonia, Bruker Instruments, Inc.: Billerica, MA USA, **1995**.

[77] Sheldrick, G. M.; SADABS, University of Göttingen, Germany, **2014**.

[78] Coppens, P.; The evaluation of absorption and extinction in single crystal structure analysis. In 'Crystallographic Computing', ed. Ahmed, R. F.; Hall, R. S and Huber, P. C.; Munksgaard, **1979**, 255-270.

[79] Sheldrick, G. M.; A short history of SHELX, *Acta Crystallogr*. Sect. A, **2008**, *64*, 112-122.

[80] Sheldrick, G. M.; Crystal structure refinement with SHELXL, *Acta Crystallogr*. Sect. C, **2015**, 71, 3-8.

[81] Brandenburg, K., Diamond - Crystal and Molecular Structure Visualization, Crystal impact GbR, vers. 4.5.1, **2018**, Bonn (Germany).

6 Appendix

6.1 Crystallographic data

Table 6.1.1: Crystal data and structure refinement for $[Tc^{II}(NO)(I)_2(Cp)]$.

Empirical formula	$C_5H_5I_2NOTc$	
Formula weight	446.90	
Temperature	100(2) K	
Wavelength	0.71073 Å	
Crystal system	Triclinic	
Space group	$P\bar{1}$	
Unit cell dimensions	a = 7.1478(6) Å	α= 74.839(2)º
	b = 7.1590(5) Å	β= 88.069(2)º
	c = 10.3936(8) Å	γ = 6.956(2)°
Volume	470.96(6) $Å^3$	
Z	2	
Density (calculated)	3.151 g/cm^3	
Absorption coefficient	8.023 mm^{-1}	
F(000)	398	
Crystal size	0.26 x 0.18 x 0.11 mm^3	
Theta range for data collection	3.106 to 27.946°.	
Index ranges	-9<=h<=9, -9<=k<=9, -13<=l<=13	
Reflections collected	15237	
Independent reflections	2268 [R(int) = 0.0304]	
Completeness to theta = 25.242°	99.8 %	
Absorption correction	Semi-empirical from equivalents	
Refinement method	Full-matrix least-squares on F^2	
Data / restraints / parameters	2268 / 0 / 91	
Goodness-of-fit on F^2	1.276	
Final R indices [I>2sigma(I)]	R1 = 0.0188, wR2 = 0.0439	
Final R indexes [all data]	R1 = 0.0198, wR2 = 0.0443	
Diffractometer	CCD, Bruker	

Table 6.1.2: Atomic coordinates (x 10^4) and equivalent isotropic displacement parameters ($Å^2$ x 10^3) for $[Tc^{II}(NO)(I)_2(Cp)]$**.** U(eq) is defined as one third of the trace of the orthogonalized U^{ij} tensor.

	x	y	z	U(eq)
C(1)	5401(5)	2268(5)	8577(4)	19.4(1)
C(2)	3556(6)	2759(5)	9182(3)	19.4(1)
C(3)	2035(5)	2924(5)	8257(4)	18.5(1)
C(4)	2978(6)	2466(5)	7103(3)	18.0(6)
C(5)	5054(5)	2108(5)	7272(3)	18.2(6)
I(1)	6213.0(3)	6746.4(3)	6821.0(2)	14.95(6)
I(2)	803.3(1)	8175.8(3)	8612.2(2)	14.06(6)
N(10)	1695(4)	6982(4)	5718(2)	14.1(5)
O(10)	720(4)	7785(4)	4708(2)	23.6(5)
Tc(1)	3117.8(1)	5498.2(3)	7261.2(2)	8.07(6)

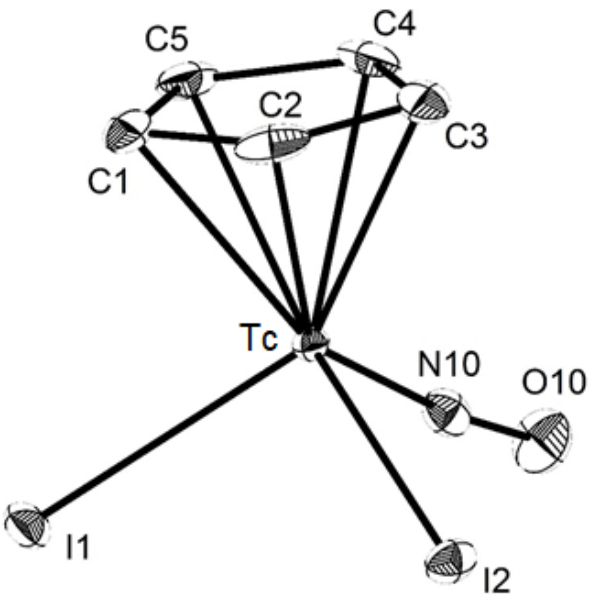

Figure 6.1.1: Ellipsoid plot (50% probability) of $[Tc^{II}(NO)(I)_2(Cp)]$.

Table 6.1.3: Crystal data and structure refinement for $[\{Tc^{I}(NO)(Cp)(PPh_3)\}_2Cl](PF_6) \cdot CH_2Cl_2$.

Empirical formula	$C_{47}H_{42}Cl_3F_6N_2O_2P_3Tc_2$	
Formula weight	1176.08	
Temperature	100(2) K	
Wavelength	0.71073 Å	
Crystal system	Monoclinic	
Space group	C 2/c	
Unit cell dimensions	a = 20.416(1) Å	α = 90°
	b = 17.6776(9) Å	β = 118.182(2)°
	c = 14.9263(7) Å	γ = 90°
Volume	4748.4(4) $Å^3$	
Z	4	
Density (calculated)	1.645 g/cm^3	
Absorption coefficient	0.917 mm^{-1}	
F(000)	2360	
Crystal size	0.60 x 0.02 x 0.02 mm^3	
Theta range for data collection	2.263 to 27.540°.	
Index ranges	-26<=h<=26, -22<=k<=22, -19<=l<=18	
Reflections collected	37811	
Independent reflections	5447 [R(int) = 0.0601]	
Completeness to theta = 25.242°	99.8 %	
Absorption correction	None	
Refinement method	Full-matrix least-squares on F^2	
Data / restraints / parameters	5448 / 138 / 309	
Goodness-of-fit on F^2	1.440	
Final R indices [I>2sigma(I)]	R1 = 0.1258, wR2 = 0.3027	
Final R indexes [all data]	R1 = 0.1327, wR2 = 0.3054	
Diffractometer	CCD, Bruker	

Table 6.1.4: Atomic coordinates (x 10^4) and equivalent isotropic displacement parameters (Å^2 x 10^3) for [{Tc^I(NO)(Cp)(PPh_3)}$_2$Cl](PF_6) · CH_2Cl_2. U(eq) is defined as one third of the trace of the orthogonalized U^{ij} tensor.

	x	**y**	**z**	**U(eq)**
Tc(1)	3895.8(1)	5327.4(6)	6444.1(7)	14.0(3)
Cl(1)	5000	4594(2)	7500	17.1(8)
P(1)	3315.0(17)	4152(2)	5769(2)	16(1)
O(10)	4147(6)	5580(6)	4682(7)	31(2)
N(10)	4067(5)	5469(6)	5412(7)	18(2)
C(11)	2629(6)	4190(8)	4417(9)	19(2)
C(31)	3926(7)	3383(7)	5812(9)	20(3)
C(16)	2248(7)	4878(6)	4021(9)	18(2)
C(26)	2067(7)	3636(7)	5936(10)	20(2)
C(12)	2473(6)	3576(6)	3775(9)	14(2)
C(14)	1556(7)	4285(8)	2393(9)	21(3)
C(36)	4423(7)	3503(7)	5435(9)	19(3)
C(2)	3241(8)	6381(9)	6285(12)	34(4)
C(15)	1706(8)	4909(7)	3014(10)	27(3)
C(21)	2822(7)	3765(9)	6398(9)	23(3)
C(13)	1932(7)	3628(8)	2760(9)	23(3)
C(32)	3925(8)	2664(7)	6209(10)	27(3)
C(25)	1718(7)	3348(7)	6467(10)	21(3)
C(35)	4905(8)	2949(8)	5463(10)	27(3)
C(23)	2885(8)	3312(10)	7976(11)	34(4)
C(22)	3217(8)	3620(10)	7446(11)	36(4)
C(3)	2896(8)	5779(11)	6520(11)	39(4)
C(34)	4901(9)	2246(8)	5883(11)	34(4)
C(5)	4034(9)	5969(14)	7870(12)	59(7)
C(24)	2127(8)	3180(8)	7484(12)	28(3)
C(4)	3397(8)	5512(12)	7505(11)	45(5)
C(33)	4415(9)	2113(9)	6253(13)	41(4)
C(1)	3955(9)	6491(12)	7157(16)	56(6)
P(2)	4215(5)	8288(5)	5936(6)	28(2)
F(5)	4141(13)	7407(15)	5677(17)	57(3)
F(2)	4399(13)	8102(14)	7093(17)	57(3)

F(4)	4014(12)	8443(15)	4786(16)	58(7)
F(6)	4508(13)	9177(17)	6268(18)	57(3)
F(1)	5076(11)	8231(15)	6264(18)	60(7)
F(3)	3352(13)	8306(15)	5656(17)	57(3)
C(6)	4170(30)	9150(30)	6110(40)	62(2)
Cl(3)	4478(6)	9937(6)	5473(8)	62(2)
Cl(2)	3862(8)	8474(7)	5541(9)	62(2)

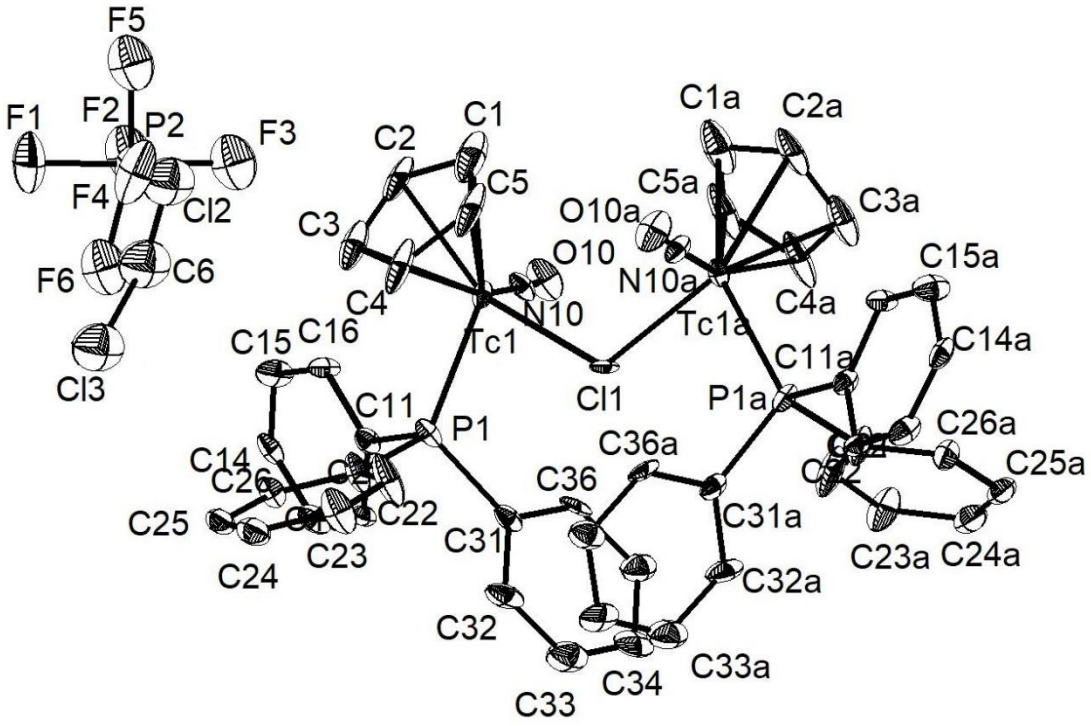

Figure 6.1.2: Ellipsoid plot (50% probability) of [{Tc^{I}(NO)(Cp)(PPh_3)}Cl](PF_6) · CH_2Cl_2.

Table 6.1.5: Crystal data and structure refinement for $[Tc^{I}(NO)(Cp)(PPh_3)(PMe_3)](PF_6)$.

Empirical formula	$C_{26}H_{29}F_6NOP_3Tc$	
Formula weight	676.41	
Temperature	100(2) K	
Wavelength	0.71073 Å	
Crystal system	Orthorhombic	
Space group	$P\ 2_12_12_1$	
Unit cell dimensions	a = 11.564(1) Å	α = 90°
	b = 13.600(1) Å	β = 90°
	c = 17.659(2) Å	γ = 90°
Volume	2777.1(5) $Å^3$	
Z	4	
Density (calculated)	1.618 g/cm^3	
Absorption coefficient	0.753 mm^{-1}	
F(000)	1368	
Crystal size	0.40 x 0.15 x 0.03 mm^3	
2Θ range for data collection/°	2.312 to 27.177°.	
Index ranges	-14<=h<=14, -14<=k<=17, -22<=l<=22	
Reflections collected	82273	
Independent reflections	6154 [R(int) = 0.0723]	
Completeness to theta = 25.242°	99.8 %	
Absorption correction	None	
Refinement method	Full-matrix least-squares on F^2	
Flack parameter	-0.01(1) (Pearson's method)	
Data / restraints / parameters	6154 / 0 / 343	
Goodness-of-fit on F^2	1.133	
Final R indices [I>2sigma(I)]	R1 = 0.0390, wR2 = 0.0970	
Final R indexes [all data]	R1 = 0.0456, wR_2 = 0.1013	
Diffractometer	CCD, Bruker	

Table 6.1.6: Atomic coordinates (x 10^4) and equivalent isotropic displacement parameters ($Å^2$ x 10^3) for $[Tc^I(NO)(Cp)(PPh_3)(PMe_3)](PF_6)$. U(eq) is defined as one third of the trace of the orthogonalized U^{ij} tensor.

	x	y	z	U(eq)
C(1)	8992(5)	8372(4)	2633(3)	18(1)
C(2)	8388(5)	8907(4)	3195(3)	20(1)
C(3)	8452(5)	8386(5)	3894(3)	22(1)
C(4)	9140(4)	7518(5)	3752(3)	19(1)
C(5)	9466(4)	7527(5)	2986(3)	20(1)
C(6)	5154(5)	7377(5)	4283(4)	26(1)
C(7)	7177(6)	6543(6)	4927(4)	33(2)
C(8)	5821(5)	5409(5)	3944(4)	25(1)
C(11)	8513(5)	6287(4)	1438(3)	16(1)
C(12)	8382(5)	7100(5)	970(4)	22(1)
C(13)	9139(6)	7271(4)	369(4)	23(1)
C(14)	10059(6)	6627(5)	250(4)	26(1)
C(15)	10214(5)	5831(5)	721(3)	22(1)
C(16)	9445(5)	5649(4)	1320(3)	18(1)
C(21)	7808(4)	4900(4)	2595(3)	15(1)
C(22)	8563(5)	4840(4)	3214(3)	20(1)
C(23)	8767(5)	3952(5)	3565(3)	21(1)
C(24)	8225(5)	3104(5)	3312(4)	24(1)
C(25)	7490(6)	3159(4)	2687(4)	28(1)
C(26)	7288(5)	4046(4)	2332(3)	21(1)
C(31)	6125(5)	5894(4)	1673(3)	17(1)
C(32)	5048(5)	6060(4)	2013(3)	18(1)
C(33)	4034(5)	5832(4)	1634(4)	21(1)
C(34)	4074(5)	5425(5)	914(4)	22(1)
C(35)	5134(5)	5263(5)	570(3)	23(1)
C(36)	6154(5)	5502(5)	942(3)	20(1)
F(1)	8600(3)	10672(3)	1942(2)	34(1)
F(2)	8662(4)	11179(4)	714(3)	52(1)
F(3)	7049(3)	10342(4)	462(2)	35(1)
F(4)	7001(4)	9792(4)	1677(2)	46(1)

F(5)	8584(4)	9567(3)	975(2)	41(1)
F(6)	7047(5)	11418(4)	1425(3)	61(2)
N(10)	6182(4)	7989(4)	2664(3)	18(1)
O(10)	5368(4)	8394(4)	2413(3)	31(1)
P(1)	7465(1)	6111(1)	2199(1)	13(1)
P(2)	6410(1)	6643(1)	4031(1)	18(1)
P(3)	7824(1)	10503(1)	1203(1)	20(1)
Tc(1)	7451(1)	7470(1)	3050(1)	13(1)

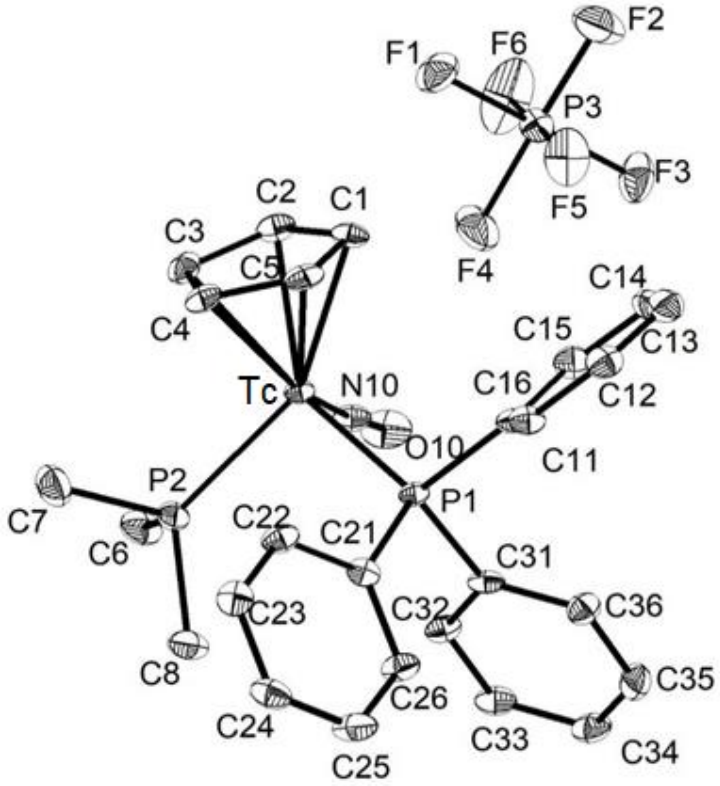

Figure 6.1.3: Ellipsoid plot (50% probability) of $[Tc^{I}(NO)(Cp)(PPh_3)(PMe_3)](PF_6)$.

Table 6.1.7: Crystal data and structure refinement for $[Tc^{I}(NO)(Cp)(PPh_3)_2](PF_6) \cdot 0.75$ toluene.

Empirical formula	$C_{46.25}H_{41}F_6NOP_3Tc$	
Formula weight	931.71	
Temperature	100(2) K	
Wavelength	1.54178 Å	
Crystal system	Monoclinic	
Space group	P $2_1/n$	
Unit cell dimensions	a = 10.0870(4) Å	α = 90°
	b = 19.5184(9) Å	β = 93.568(3)°
	c = 42.094(2) Å	γ = 90°
Volume	8271.4(6) $Å^3$	
Z	8	
Density (calculated)	1.496 g/cm^3	
Absorption coefficient	4.477 mm^{-1}	
F(000)	3804.0	
Crystal size	0.28 x 0.21 x 0.13 mm^3	
2Θ range for data collection/°	4.206 to 145.076°.	
Index ranges	-11<=h<=12, -24<=k<=24, -51<=l<=52	
Reflections collected	138877	
Independent reflections	16402 [R(int) = 0.1200]	
Completeness to theta = 67.679°	100.0 %	
Absorption correction	Semi-empirical from equivalents	
Refinement method	Full-matrix least-squares on F^2	
Data / restraints / parameters	16402 / 1410 / 1069	
Goodness-of-fit on F^2	1.063	
Final R indices [I>2sigma(I)]	R1 = 0.0485, wR2 = 0.0921	
Final R indexes [all data]	R1 = 0.0718, wR_2 = 0.1000	
Diffractometer	CCD, Bruker	

Table 6.1.8: Atomic coordinates (x 10^4) and equivalent isotropic displacement parameters ($Å^2$ x 10^3) for $[Tc^I(NO)(Cp)(PPh_3)_2](PF_6) \cdot 0.75$ toluene. U(eq) is defined as one third of the trace of the orthogonalized U^{ij} tensor.

	x	y	z	U(eq)
C(11)	3739(4)	2276(2)	4647.8(9)	28.0(8)
C(12)	4281(5)	1754(2)	4464.6(10)	39.1(10)
C(13)	3666(6)	1568(3)	4176.5(12)	54.4(14)
C(14)	2503(6)	1892(3)	4066.6(12)	57.3(15)
C(15)	1977(5)	2409(3)	4243.3(12)	49.0(13)
C(16)	2602(4)	2605(2)	4533.3(10)	35.6(10)
C(21)	6151(4)	2859(2)	4939.0(9)	24.7(8)
C(22)	6258(4)	3206(2)	4650.0(9)	30.3(9)
C(23)	7374(4)	3601(2)	4603.4(11)	39.6(10)
C(24)	8373(5)	3672(3)	4840.6(11)	43.4(11)
C(25)	8267(4)	3325(3)	5128.4(10)	37.2(10)
C(26)	7164(4)	2924(2)	5175.3(10)	27.9(8)
C(31)	4940(4)	1634(2)	5193.4(9)	24.8(8)
C(32)	6174(4)	1324(2)	5186.7(11)	37.7(10)
C(33)	6358(5)	665(3)	5311.4(14)	54.2(14)
C(34)	5320(6)	329(3)	5441.6(14)	55.1(14)
C(35)	4092(5)	629(2)	5444.4(12)	46.7(12)
C(36)	3911(4)	1283(2)	5320.7(10)	30.9(9)
C(1)	2587(4)	4281(2)	5108.0(10)	31.9(9)
C(2)	2820(4)	4409(2)	5436.2(10)	32.0(9)
C(3)	4194(4)	4338.0(19)	5508.6(9)	25.9(8)
C(4)	4815(4)	4160(2)	5230.9(9)	25.9(8)
C(5)	3807(4)	4120(2)	4979.0(9)	28.8(8)
C(51)	3485(4)	3459.7(19)	6165.0(9)	22.7(7)
C(52)	2198(4)	3714(2)	6123.2(9)	25.3(8)
C(53)	1670(4)	4132(2)	6350.7(9)	28.8(8)
C(54)	2440(4)	4298(2)	6622.5(10)	32.8(9)
C(55)	3718(4)	4050(2)	6668.9(9)	32.9(9)
C(56)	4248(4)	3625(2)	6441.0(9)	27.5(8)
C(61)	5800(3)	2734(2)	5940.4(8)	22.0(7)
C(62)	6623(4)	3306(2)	5987.5(9)	27.1(8)

C(63)	7984(4)	3220(2)	6027.3(9)	32.2(9)
C(64)	8531(4)	2578(2)	6018.4(10)	34.5(9)
C(65)	7729(4)	2009(2)	5967.5(10)	33.1(9)
C(66)	6359(4)	2085(2)	5928.0(9)	29.0(8)
C(41)	3264(3)	2077(2)	6021.8(9)	22.7(7)
C(42)	2044(4)	1832(2)	5898.4(9)	28.9(8)
C(43)	1442(4)	1278(2)	6040.7(10)	34.3(9)
C(44)	2065(4)	967(2)	6306.2(10)	33.1(9)
C(45)	3254(4)	1215(2)	6430.8(11)	39.8(11)
C(46)	3851(4)	1772(2)	6294.3(10)	33.4(9)
C(81)	4106(4)	6614.2(19)	6413.4(8)	22.4(7)
C(82)	5393(4)	6756(2)	6324.1(9)	27.0(8)
C(83)	6067(4)	6280(2)	6148.9(9)	29.5(9)
C(84)	5470(4)	5663(2)	6061.2(9)	29.3(8)
C(85)	4210(4)	5518(2)	6148.9(9)	30.4(9)
C(86)	3527(4)	5993(2)	6327.0(9)	24.4(8)
C(91)	2665(4)	7880(2)	6335.4(9)	26.3(8)
C(92)	2145(4)	8499(2)	6427.0(11)	37.2(10)
C(93)	1652(5)	8967(3)	6200.7(13)	51.9(13)
C(94)	1682(6)	8814(3)	5879.7(13)	58.2(14)
C(95)	2177(5)	8194(3)	5784.3(12)	55.5(14)
C(96)	2679(5)	7729(3)	6011.8(10)	40.9(11)
C(71)	4586(3)	7670(2)	6865.2(9)	22.6(7)
C(72)	5129(3)	7310(2)	7127.4(9)	22.9(8)
C(73)	6168(4)	7583(2)	7317.2(9)	27.2(8)
C(74)	6684(4)	8217(2)	7241.2(10)	30.3(9)
C(75)	6173(4)	8568(2)	6974.4(10)	33.4(9)
C(76)	5127(4)	8297(2)	6785.5(10)	30.0(8)
C(6)	219(4)	6765(2)	6421.5(9)	32.6(9)
C(7)	-107(4)	6157(3)	6578.8(10)	37.6(10)
C(8)	-745(4)	6340(3)	6858.3(10)	43.2(11)
C(9)	-818(4)	7053(3)	6868.2(10)	42.0(11)
C(10)	-220(4)	7325(3)	6603.5(10)	36.2(9)
C(121)	205(4)	7309(3)	7629.5(9)	36.1(10)
C(122)	-124(4)	6640(3)	7698.0(10)	44.2(11)

C(123)	-1058(4)	6498(4)	7921.0(11)	58.7(15)
C(124)	-1670(4)	7035(4)	8066.9(12)	67.7(16)
C(125)	-1386(4)	7691(4)	7994.9(12)	65.5(16)
C(126)	-420(4)	7848(3)	7779.1(10)	47.8(12)
C(111)	2938(3)	7265(2)	7693.5(8)	20.8(7)
C(112)	3593(3)	6640(2)	7715.2(9)	23.1(7)
C(113)	4501(4)	6503(2)	7971.9(9)	25.3(8)
C(114)	4731(3)	6983(2)	8209.1(9)	24.6(8)
C(115)	4065(4)	7599(2)	8191.1(9)	27.7(8)
C(116)	3161(4)	7743(2)	7937.2(9)	27.8(9)
C(101)	1715(4)	8349(2)	7301.9(9)	28.7(8)
C(106)	2924(4)	8699(2)	7329.6(9)	28.8(8)
C(105)	3001(5)	9383(2)	7239.1(11)	40.5(11)
C(104)	1881(5)	9721(3)	7116.7(12)	51.9(13)
C(103)	685(5)	9380(3)	7083.9(12)	53.8(13)
C(102)	591(4)	8703(3)	7172.7(11)	43.3(11)
C(141)	6309(5)	5521(3)	7435.9(13)	53.5(13)
C(142)	7069(4)	5105(2)	7218.9(11)	40.2(10)
C(143)	6671(5)	5059(3)	6896.5(10)	40.1(10)
C(144)	7379(5)	4681(3)	6699.3(13)	47.1(12)
C(145)	8525(5)	4327(3)	6806.0(12)	51.3(12)
C(146)	8941(5)	4375(3)	7119.3(13)	55.5(13)
C(147)	8209(4)	4770(2)	7330.0(11)	39.1(10)
F(1)	6996(4)	785.7(17)	6394.4(8)	67.8(9)
F(2)	6376(3)	-320.5(18)	6368.9(7)	58.7(8)
F(3)	8471(3)	-650.2(16)	6452.4(7)	57.4(8)
F(4)	9139(3)	447(2)	6472.4(9)	75.3(10)
F(5)	7904(4)	75(2)	6045.4(7)	74.1(10)
F(6)	7613(3)	73.6(13)	6796.3(6)	40.8(6)
F(7)	8724(2)	5052.9(14)	6072.1(6)	37.2(6)
F(8)	8586(2)	5855.9(13)	5679.9(7)	44.2(6)
F(9)	9658(2)	5135.0(14)	5361.3(6)	40.4(6)
F(10)	9792(2)	4343.2(12)	5745.9(6)	34.6(5)
F(11)	7782(2)	4792.1(13)	5587.6(6)	37.4(6)
F(12)	10586(2)	5412.9(13)	5849.2(6)	37.1(6)

N(10)	1889(3)	2802.6(18)	5264.2(8)	29.3(7)
N(20)	2342(3)	6045.9(18)	7038.7(7)	28.5(7)
O(10)	885(3)	2511.5(18)	5192.4(8)	47.2(9)
O(20)	2909(4)	5528.7(16)	7112.1(7)	47.8(9)
P(1)	4575.1(9)	2484.6(5)	5034.5(2)	19.73(19)
P(2)	4007.0(9)	2854.2(5)	5860.9(2)	19.61(19)
P(3)	7748.6(11)	76.2(6)	6418.6(3)	34.3(2)
P(4)	3216.5(9)	7254.9(5)	6635.3(2)	19.66(19)
P(5)	1624.1(9)	7434.4(6)	7381.2(2)	23.7(2)
P(6)	9182.3(9)	5102.8(5)	5715.0(2)	26.2(2)
Tc(1)	3359.0(3)	3286.2(2)	5331.7(2)	19.04(7)
Tc(2)	1399.7(3)	6754.4(2)	6899.1(2)	21.39(7)
C(131)	8894(13)	-954(6)	5312(3)	72(4)
C(133)	9780(11)	225(4)	5314(3)	56(3)
C(132)	9542(9)	-388(3)	5151(3)	48(2)
C(137)	9841(8)	-445(4)	4835(3)	55(3)
C(136)	10377(9)	109(5)	4680(3)	65(3)
C(135)	10615(11)	722(4)	4842(4)	72(4)
C(134)	10316(12)	779(3)	5159(4)	79(4)

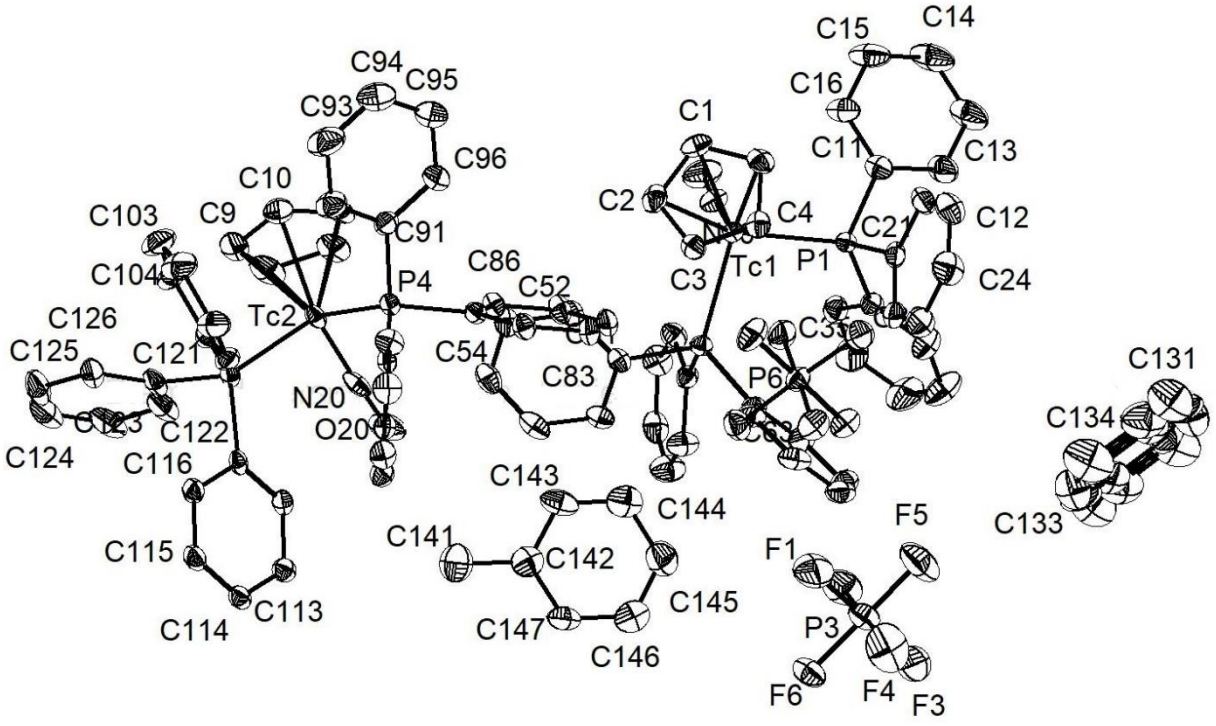

Figure 6.1.4: Ellipsoid plot (50% probability) of $[Tc^{I}(NO)(Cp)(PPh_3)_2](PF_6) \cdot 0.75$ toluene.

Table 6.1.9: Crystal data and structure refinement for $[Tc^{I}(NO)(Cp)(PPh_3)\{C(OMe)\text{-}C_2H_4PPh_3\}](PF_6)_2 \cdot$ toluene**.**

Empirical formula	$C_{52}H_{50}F_{12}NO_2P_4Tc$	
Formula weight	1170.81	
Temperature	100(2) K	
Wavelength	1.54178 Å	
Crystal system	Monoclinic	
Space group	C 2/c	
Unit cell dimensions	a = 50.442(2) Å	α = 90º
	b = 11.5575(4) Å	β = 105.257(2)º
	c = 17.9876(6) Å	γ = 90º
Volume	10116.8(6) $Å^3$	
Z	8	
Density (calculated)	1.537 g/cm^3	
Absorption coefficient	4.269 mm^{-1}	
F(000)	4768.0	
Crystal size	0.25 x 0.18 x 0.12 mm^3	
2Θ range for data collection/°	7.266 to 159.512°.	
Index ranges	-64<=h<=62, -14<=k<=14, -19<=l<=22	
Reflections collected	87306	
Independent reflections	10321 [R(int) = 0.1131]	
Completeness to theta = 67.679°	99.9 %	
Absorption correction	Semi-empirical from equivalents	
Refinement method	Full-matrix least-squares on F^2	
Data / restraints / parameters	10855 / 0 / 688	
Goodness-of-fit on F^2	1.054	
Final R indices [I>2sigma(I)]	R1 = 0.0551, wR2 = 0.1103	
Final R indexes [all data]	R1 = 0.0780, wR2 = 0.1211	
Diffractometer	CCD, Bruker	

Table 6.1.10: Atomic coordinates (x 10^4) and equivalent isotropic displacement parameters ($Å^2$x 10^3) for $[Tc^I(NO)(Cp)(PPh_3)\{C(OMe)C_2H_4PPh_3\}](PF_6)_2 \cdot$ toluene. U(eq) is defined as one third of the trace of the orthogonalized U^{ij} tensor.

	x	y	z	U(eq)
Tc(1)	6379.7(2)	4279.6(3)	6807.4(2)	20.12(8)
P(1)	6718.5(2)	4963.5(8)	7919.7(5)	19.76(19)
P(2)	5796.3(2)	8727.7(8)	6461.6(5)	18.03(19)
P(3)	6725.1(2)	9964.5(9)	6203.1(6)	27.7(2)
P(4)	5634.9(2)	5872.9(10)	4214.3(6)	30.8(2)
F(10)	5621.9(6)	7241(2)	4335.9(15)	38.5(6)
O(1)	6395.0(5)	6463(2)	5876.9(15)	21.5(5)
F(2)	7028.2(5)	9696(3)	6130.3(16)	43.3(7)
F(4)	6419.3(5)	10233(2)	6268.9(18)	45.9(7)
F(11)	5524.2(8)	6029(3)	3316.7(17)	67.6(10)
F(6)	6662.9(6)	8617(2)	6167(2)	58.9(9)
F(12)	5750.6(7)	5742(3)	5119.7(16)	58.3(9)
F(8)	5645.2(8)	4492(3)	4114.9(19)	64.5(10)
F(1)	6832.0(6)	9893(4)	7107.9(17)	65.1(10)
F(3)	6617.7(8)	10028(3)	5292.5(18)	65.3(9)
F(9)	5331.5(6)	5755(3)	4290(2)	66.8(10)
O(10)	6835.1(6)	3636(3)	6151.7(19)	36.9(7)
F(5)	6786.0(7)	11307(3)	6236(2)	64.1(9)
F(7)	5941.2(7)	6002(4)	4146(2)	76.4(11)
C(6)	6308.1(7)	5902(3)	6396(2)	18.0(7)
N(10)	6653.9(7)	3941(3)	6396(2)	28.0(8)
C(51)	5523.5(7)	7790(3)	6556(2)	19.9(7)
C(21)	6875.9(8)	3811(4)	8591(2)	26.1(8)
C(7)	6106.6(8)	6703(3)	6646(2)	20.8(8)
C(61)	5668.1(8)	9801(3)	5728(2)	23.7(8)
C(8)	6045.0(7)	7825(3)	6180(2)	19.9(7)
C(11)	6610.6(8)	6025(3)	8536(2)	21.8(8)
C(66)	5818.7(8)	10120(3)	5216(2)	24.7(8)
C(36)	6983.9(8)	6717(4)	7330(2)	24.7(8)
C(54)	5168.9(9)	6010(4)	6659(3)	32.6(10)

C(3)	6153.2(9)	3207(4)	7555(2)	27.5(9)
C(15)	6266.4(8)	6656(4)	9163(2)	27.7(9)
C(41)	5942.6(8)	9457(3)	7358(2)	22.5(8)
C(16)	6350.9(8)	5906(3)	8662(2)	23.1(8)
C(22)	7012.5(8)	4079(4)	9353(2)	33.4(10)
C(56)	5343.3(8)	7356(4)	5890(2)	24.9(8)
C(31)	7009.9(8)	5618(3)	7657(2)	22.5(8)
C(42)	6222.2(8)	9369(4)	7725(2)	27.0(8)
C(46)	5773.0(9)	10164(4)	7663(3)	30.2(9)
C(4)	5968.8(8)	4043(4)	7145(2)	27.8(9)
C(14)	6442.8(9)	7518(4)	9537(2)	28.0(9)
C(53)	5347.3(9)	6436(4)	7318(3)	31.4(9)
C(32)	7253.7(8)	5012(4)	7738(2)	29.5(9)
C(55)	5165.0(8)	6462(4)	5949(3)	29.4(9)
C(2)	6222.3(9)	2441(4)	7030(3)	31.9(9)
C(12)	6785.5(8)	6891(4)	8917(2)	26.8(9)
C(5)	5922.1(9)	3799(4)	6351(3)	32.1(10)
C(35)	7199.0(9)	7201(4)	7091(3)	31.1(9)
C(1)	6082.2(9)	2809(4)	6285(3)	33.4(10)
C(44)	6162.6(11)	10703(4)	8693(2)	37.8(11)
C(13)	6699.9(9)	7626(4)	9414(2)	31.4(9)
C(63)	5343.5(11)	11318(5)	5235(3)	49.1(13)
C(62)	5428.2(10)	10391(4)	5734(3)	39.1(11)
C(33)	7467.8(9)	5498(4)	7493(3)	34.8(10)
C(26)	6872.1(9)	2678(4)	8336(3)	35.9(10)
C(52)	5525.9(8)	7334(4)	7275(2)	25.0(8)
C(45)	5883.8(10)	10792(4)	8331(3)	38.2(10)
C(34)	7440.6(9)	6594(4)	7177(3)	32.9(10)
C(9)	6577.6(9)	5978(4)	5465(2)	30.3(9)
C(64)	5495.6(11)	11638(4)	4733(3)	43.1(12)
C(43)	6329.8(9)	9992(4)	8397(2)	33.8(10)
C(65)	5729.4(9)	11037(4)	4713(2)	31.7(9)
C(25)	6992.1(9)	1801(5)	8840(4)	49.2(14)
C(24)	7120.0(10)	2070(5)	9603(3)	48.3(14)
C(23)	7134.4(10)	3201(5)	9853(3)	45.2(13)

C(84)	57(3)	5701(6)	2970(10)	46(5)
C(85)	157.1(19)	4714(9)	3392(6)	40(3)
C(86)	147.6(12)	3653(6)	3021(4)	37(2)
C(81)	37.7(12)	3580(5)	2228(4)	37(2)
C(82)	-62.7(17)	4567(8)	1806(5)	36(3)
C(83)	-53(3)	5628(6)	2177(9)	37(4)
C(87)	64(3)	2472(9)	1814(6)	57(3)
C(75)	2407.3(18)	3931(7)	80(6)	52(3)
C(76)	2417.7(16)	2971(8)	552(4)	36(3)
C(71)	2507.4(17)	1913(7)	343(5)	36(2)
C(72)	2586.8(14)	1815(9)	-338(5)	38(4)
C(73)	2576.4(17)	2775(13)	-810(4)	74(5)
C(74)	2487(2)	3833(10)	-601(5)	79(8)
C(77)	2534(4)	954(16)	870(12)	75(6)

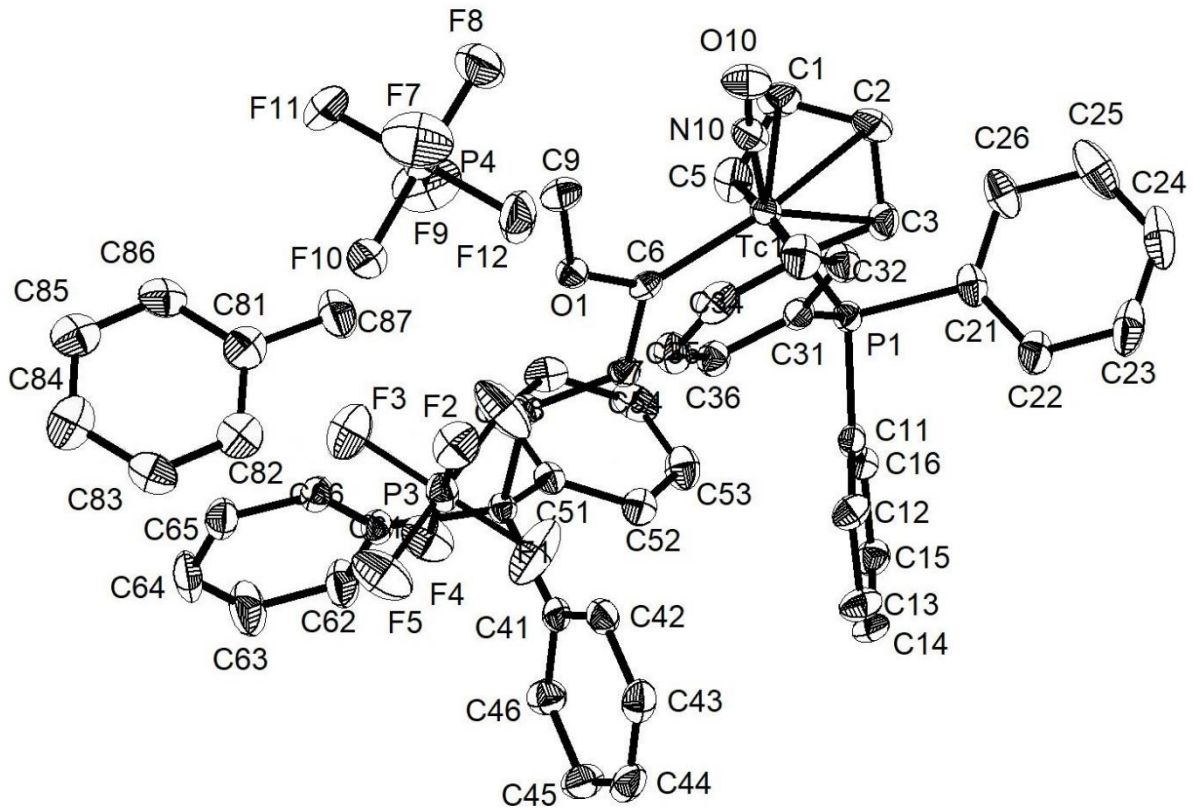

Figure 6.1.5: Ellipsoid plot (50% probability) of $[Tc^{I}(NO)(Cp)(PPh_3)\{C(OMe)C_2H_4PPh_3\}](PF_6)_2 \cdot$ toluene.

Table 6.1.11: Crystal data and structure refinement for $[Tc^{I}(NO)(Cp)(PPh_3)(Py)](PF_6)$.

Empirical formula	$C_{28}H_{25}F_6N_2OP_2Tc$	
Formula weight	679.44	
Temperature	100(2) K	
Wavelength	0.71073 Å	
Crystal system	Orthorhombic	
Space group	$P\ 2_12_12_1$	
Unit cell dimensions	a = 9.9142(6) Å	α = 90º
	b = 17.7475(1) Å	β = 90º
	c = 31.944(2) Å	γ = 90º
Volume	5620.7(6) $Å^3$	
Z	8	
Density (calculated)	1.606 g/cm^3	
Absorption coefficient	0.691 mm^{-1}	
F(000)	2736	
Crystal size	0.42 x 0.18 x 0.12 mm^3	
Theta range for data collection	2.230 to 27.151°.	
Index ranges	-12<=h<=12, -22<=k<=22, -40<=l<=40	
Reflections collected	100174	
Independent reflections	12447 [R(int) = 0.0240]	
Completeness to theta = 25.242°	99.9 %	
Absorption correction	None	
Refinement method	Full-matrix least-squares on F^2	
Flack parameter	-0.02(3) (Pearson's method)	
Data / restraints / parameters	12447 / 0 / 721	
Goodness-of-fit on F^2	1.097	
Final R indices [I>2sigma(I)]	R1 = 0.0238, wR2 = 0.0585	
Final R indexes [all data]	R1 = 0.0246, wR2 = 0.0589	
Diffractometer	CCD, Bruker	

Table 6.1.12: Atomic coordinates (x 10^4) and equivalent isotropic displacement parameters ($Å^2$x 10^3) for $[Tc^I(NO)(Cp)(PPh_3)(Py)](PF_6)$. U(eq) is defined as one third of the trace of the orthogonalized U^{ij} tensor.

	x	y	z	U(eq)
C(1)	10512(4)	8753(3)	7006(2)	40(1)
C(2)	9778(4)	8969(2)	7364(1)	33(1)
C(3)	9603(4)	8315(2)	7619(1)	33(1)
C(4)	10248(4)	7708(3)	7417(1)	38(1)
C(5)	10800(4)	7977(3)	7029(1)	42(1)
C(6)	5694(4)	6133(2)	5691(1)	25(1)
C(7)	7125(4)	6149(2)	5610(1)	26(1)
C(8)	7299(4)	6415(2)	5195(1)	29(1)
C(9)	6025(4)	6553(2)	5018(1)	29(1)
C(10)	5034(4)	6379(2)	5326(1)	27(1)
C(11)	6675(3)	9489(2)	7532(1)	17(1)
C(12)	6886(3)	9491(2)	7965(1)	18(1)
C(13)	7260(3)	10145(2)	8169(1)	24(1)
C(14)	7431(4)	10811(2)	7947(1)	28(1)
C(15)	7225(4)	10816(2)	7518(1)	29(1)
C(16)	6859(3)	10166(2)	7313(1)	23(1)
C(21)	5483(3)	8012(2)	7641(1)	19(1)
C(22)	6080(4)	7392(2)	7834(1)	23(1)
C(23)	5349(4)	6962(2)	8119(1)	26(1)
C(24)	4033(4)	7148(2)	8215(1)	27(1)
C(25)	3427(4)	7762(2)	8027(1)	27(1)
C(26)	4141(3)	8188(2)	7737(1)	23(1)
C(31)	5127(3)	8767(2)	6861(1)	23(1)
C(32)	4351(3)	9419(2)	6830(1)	27(1)
C(33)	3404(4)	9493(3)	6511(1)	39(1)
C(34)	3214(4)	8924(3)	6229(1)	44(1)
C(35)	3952(4)	8264(3)	6261(1)	42(1)
C(36)	4906(4)	8186(2)	6575(1)	33(1)
C(41)	7901(4)	9216(2)	6326(1)	25(1)
C(42)	7516(4)	9488(2)	5940(1)	31(1)
C(43)	7302(4)	8987(2)	5617(1)	34(1)

C(44)	7504(5)	8230(2)	5690(1)	35(1)
C(45)	7880(4)	7989(2)	6084(1)	30(1)
C(51)	4349(3)	3998(2)	5825(1)	14(1)
C(52)	4140(3)	3298(2)	6018(1)	17(1)
C(53)	2852(3)	3082(2)	6135(1)	19(1)
C(54)	1760(3)	3555(2)	6062(1)	19(1)
C(55)	1966(3)	4249(2)	5872(1)	18(1)
C(56)	3257(3)	4470(2)	5754(1)	17(1)
C(61)	6719(3)	3384(2)	5469(1)	17(1)
C(62)	7620(3)	2911(2)	5678(1)	23(1)
C(63)	8039(4)	2240(2)	5483(1)	29(1)
C(64)	7561(4)	2048(2)	5095(1)	29(1)
C(65)	6633(4)	2501(2)	4893(1)	27(1)
C(66)	6218(3)	3167(2)	5079(1)	22(1)
C(71)	6916(3)	4470(2)	6163(1)	17(1)
C(72)	6168(3)	4700(2)	6508(1)	21(1)
C(73)	6797(4)	4928(2)	6873(1)	25(1)
C(74)	8195(4)	4921(2)	6899(1)	26(1)
C(75)	8948(4)	4692(2)	6558(1)	28(1)
C(76)	8320(3)	4470(2)	6189(1)	23(1)
C(81)	7635(4)	4408(2)	4503(1)	24(1)
C(82)	8673(4)	4052(2)	4297(1)	32(1)
C(83)	9957(4)	4067(2)	4465(1)	34(1)
C(84)	10153(4)	4458(2)	4836(1)	31(1)
C(85)	9071(3)	4796(2)	5029(1)	23(1)
N(10)	7744(4)	7194(2)	6949(1)	36(1)
N(20)	8054(3)	8471(2)	6404(1)	22(1)
N(30)	4821(3)	4864(2)	4896(1)	21(1)
N(40)	7802(3)	4773(2)	4871(1)	19(1)
O(10)	7275(5)	6589(2)	6914(1)	72(1)
O(30)	3857(3)	4607(1)	4728(1)	31(1)
F(1)	956(4)	7188(2)	6106(1)	87(1)
F(2)	2490(2)	6278(2)	6021(1)	40(1)
F(3)	1594(3)	5980(1)	5405(1)	50(1)
F(4)	16(3)	6903(2)	5491(1)	55(1)

F(5)	2252(2)	7170(1)	5529(1)	47(1)
F(6)	283(3)	5990(2)	5971(1)	57(1)
F(7)	-146(3)	2053(2)	6646(1)	65(1)
F(8)	-125(4)	905(2)	6961(1)	77(1)
F(9)	484(2)	373(1)	6348(1)	50(1)
F(10)	499(3)	1520(2)	6046(1)	44(1)
F(11)	1734(3)	1310(2)	6619(1)	47(1)
F(12)	-1380(2)	1100(2)	6383(1)	52(1)
P(1)	6405(1)	8595(1)	7263(1)	17(1)
P(2)	1251(1)	6592(1)	5757(1)	22(1)
P(3)	6064(1)	4271(1)	5671(1)	14(1)
P(4)	170(1)	1209(1)	6506(1)	26(1)
Tc(1)	8489(1)	8079(1)	7025(1)	22(1)
Tc(2)	6125(1)	5289(1)	5187(1)	16(1)

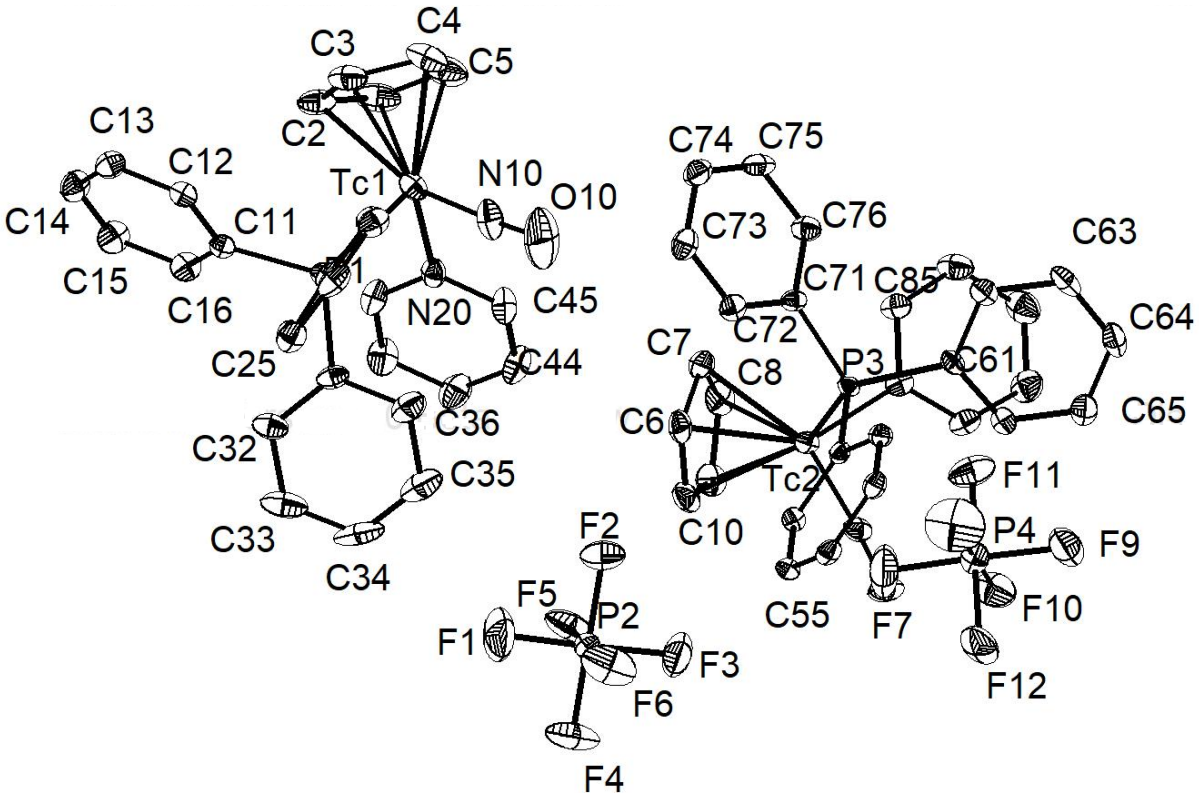

Figure 6.1.6: Ellipsoid plot (50% probability) of $[Tc^{I}(NO)(Cp)(PPh_3)(Py)](PF_6)$.

Table 6.1.13: Crystal data and structure refinement for $[Tc^{I}(NO)(Cp)(PPh_3)(thioxane)](PF_6)$.

Empirical formula	$C_{27}H_{28}F_6NO_2P_2STc$	
Formula weight	704.50	
Temperature	233(2) K	
Wavelength	0.71073 Å	
Crystal system	Triclinic	
Space group	$P\bar{1}$	
Unit cell dimensions	a = 10.5858(8) Å	α = 96.063(3)º
	b = 10.7434(8) Å	β = 102.373(3)º
	c = 13.300(1) Å	γ = 107.210(3)º
Volume	1387.91(2) $Å^3$	
Z	2	
Density (calculated)	1.686 g/cm^3	
Absorption coefficient	0.777 mm^{-1}	
F(000)	712	
Crystal size	0.21 x 0.16 x 0.09 mm^3	
Theta range for data collection	2.274 to 27.270°.	
Index ranges	-13<=h<=13, -13<=k<=13, -17<=l<=17	
Reflections collected	38126	
Independent reflections	6183 [R(int) = 0.0347]	
Completeness to theta = 25.242°	99.9 %	
Absorption correction	None	
Refinement method	Full-matrix least-squares on F^2	
Data / restraints / parameters	6183 / 0 / 365	
Goodness-of-fit on F^2	0.964	
Final R indices [I>2sigma(I)]	R1 = 0.0304, wR2 = 0.0670	
Final R indexes [all data]	R1 = 0.0381, wR2 = 0.0707	
Diffractometer	CCD, Bruker	

Table 6.1.14: Atomic coordinates (x 10^4) and equivalent isotropic displacement parameters ($Å^2$ x 10^3) for $[Tc^I(NO)(Cp)(PPh_3)(thioxane)](PF_6)$. U(eq) is defined as one third of the trace of the orthogonalized U^{ij} tensor.

	x	y	z	U(eq)
C(1)	3800(3)	5942(3)	4508(2)	34(1)
C(2)	3101(3)	6719(3)	4878(2)	29(1)
C(3)	1703(3)	5980(3)	4656(2)	27(1)
C(4)	1527(3)	4694(3)	4147(2)	36(1)
C(5)	2830(4)	4662(3)	4044(2)	39(1)
C(11)	5087(2)	5587(2)	2366(2)	17(1)
C(12)	6082(3)	6690(2)	3040(2)	21(1)
C(13)	7391(3)	6663(3)	3469(2)	24(1)
C(14)	7705(3)	5523(3)	3224(2)	28(1)
C(15)	6733(3)	4420(3)	2570(2)	30(1)
C(16)	5417(3)	4442(3)	2136(2)	24(1)
C(21)	2452(3)	4108(2)	899(2)	20(1)
C(22)	1625(4)	3041(3)	1223(2)	41(1)
C(23)	884(4)	1871(3)	516(3)	58(1)
C(24)	948(4)	1750(3)	-516(3)	45(1)
C(25)	1754(3)	2787(3)	-844(2)	28(1)
C(26)	2493(3)	3962(2)	-148(2)	21(1)
C(31)	3665(2)	6833(2)	906(2)	16(1)
C(32)	2542(3)	7141(2)	368(2)	20(1)
C(33)	2691(3)	7953(3)	-375(2)	25(1)
C(34)	3962(3)	8475(2)	-571(2)	26(1)
C(35)	5078(3)	8196(2)	-30(2)	24(1)
C(36)	4937(3)	7373(2)	706(2)	20(1)
S(1A)	2518(1)	8312(1)	2777(1)	16(1)
C(41A)	4274(2)	9363(2)	2987(2)	24(1)
C(44A)	2144(3)	9250(3)	3819(2)	27(1)
S(1B)	3376(14)	8540(14)	3529(11)	16(1)
C(41B)	4274(2)	9363(2)	2987(2)	24(1)
C(44B)	2144(3)	9250(3)	3819(2)	27(1)
C(42)	4323(3)	10789(3)	2950(2)	26(1)

C(43)	2470(3)	10693(3)	3700(2)	30(1)
N(10)	633(2)	5422(2)	2107(2)	24(1)
O(10)	-437(2)	4863(2)	1516(2)	40(1)
O(20)	3880(2)	11334(2)	3780(2)	33(1)
P(1)	3391(1)	5675(1)	1807(1)	15(1)
P(2)	1398(1)	9220(1)	6781(1)	17(1)
Tc(1)	2211(1)	6083(1)	3075(1)	15(1)
F(1)	2447(2)	9993(2)	7875(1)	36(1)
F(2)	2457(2)	10014(2)	6189(1)	38(1)
F(3)	353(2)	8443(2)	5683(1)	36(1)
F(4)	347(2)	8422(2)	7374(1)	36(1)
F(5)	711(2)	10356(2)	6777(2)	38(1)
F(6)	2086(2)	8077(2)	6795(2)	42(1)

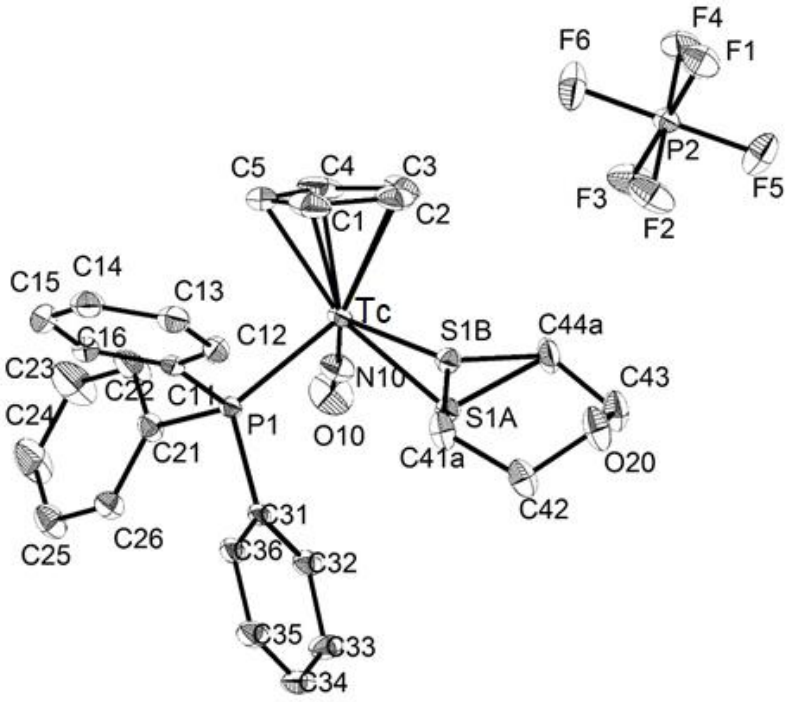

Figure 6.1.7: Ellipsoid plot (50% probability) of [Tc^{I}(NO)(Cp)(PPh_3)(thioxane)](PF_6).

Table 6.1.15: Crystal data and structure refinement for $[Tc^{I}(NO)(Cp)(PPh_3)(OPPh_3)](PF_6) \cdot CH_2Cl_2$.

Empirical formula	$C_{42}H_{37}Cl_2F_6NO_2P_3Tc$	
Formula weight	963.53	
Temperature	100(2) K	
Wavelength	0.71073 Å	
Crystal system	Monoclinic	
Space group	P 2_1/c	
Unit cell dimensions	a = 22.075(2) Å	α = 90º
	b = 10.6519(9) Å	β = 109.277(3)º
	c = 18.7877(2) Å	γ = 90º
Volume	4170.1(7) $Å^3$	
Z	4	
Density (calculated)	1.535 g/cm^3	
Absorption coefficient	0.653 mm^{-1}	
F(000)	1952	
Crystal size	0.27 x 0.19 x 0.09 mm^3	
Theta range for data collection	2.230 to 27.206°.	
Index ranges	-28<=h<=28, -13<=k<=13, -24<=l<=24	
Reflections collected	85431	
Independent reflections	9259 [R(int) = 0.0462]	
Completeness to theta = 25.242°	99.8 %	
Absorption correction	None	
Refinement method	Full-matrix least-squares on F^2	
Data / restraints / parameters	9259 / 0 / 515	
Goodness-of-fit on F^2	1.191	
Final R indices [I>2sigma(I)]	R1 = 0.0690, wR2 = 0.1453	
Final R indexes [all data]	R1 = 0.0775, wR2 = 0.1490	
Diffractometer	CCD, Bruker	

Table 6.1.16: Atomic coordinates (x 10^4) and equivalent isotropic displacement parameters ($Å^2$ x 10^3) for $[Tc^{I}(NO)(Cp)(PPh_3)(OPPh_3)](PF_6) \cdot CH_2Cl_2$. U(eq) is defined as one third of the trace of the orthogonalized U^{ij} tensor.

	x	y	z	U(eq)
C(1)	7268(3)	6034(6)	1385(3)	31(1)
C(2)	6673(3)	6652(6)	1285(3)	28(1)
C(3)	6810(3)	7935(5)	1432(3)	26(1)
C(4)	7468(3)	8111(5)	1639(3)	25(1)
C(5)	7768(3)	6917(6)	1620(3)	30(1)
C(10)	6107(3)	2617(7)	1574(5)	50(2)
C(11)	6537(2)	6566(4)	3905(3)	19(1)
C(12)	7096(3)	5961(5)	4340(3)	24(1)
C(13)	7087(3)	5145(5)	4910(3)	28(1)
C(14)	6516(3)	4936(5)	5056(3)	29(1)
C(15)	5969(3)	5555(6)	4640(3)	30(1)
C(16)	5973(3)	6366(5)	4060(3)	24(1)
C(21)	5733(2)	7711(5)	2526(3)	19(1)
C(22)	5469(3)	6717(5)	2033(3)	25(1)
C(23)	4829(3)	6769(6)	1566(3)	30(1)
C(24)	4459(3)	7805(6)	1585(3)	35(1)
C(25)	4718(3)	8780(6)	2066(4)	34(1)
C(26)	5355(2)	8741(5)	2544(3)	24(1)
C(31)	6784(2)	9114(4)	3561(3)	15(1)
C(32)	6696(2)	9419(5)	4246(3)	20(1)
C(33)	6877(3)	10601(5)	4574(3)	24(1)
C(34)	7148(3)	11467(5)	4220(3)	26(1)
C(35)	7236(3)	11175(5)	3543(3)	24(1)
C(36)	7055(2)	10003(4)	3213(3)	20(1)
C(41)	8827(2)	5748(5)	4196(3)	21(1)
C(42)	8934(3)	5491(5)	4958(3)	27(1)
C(43)	8951(3)	4250(6)	5193(4)	34(1)
C(44)	8859(3)	3288(6)	4680(4)	39(2)
C(45)	8753(3)	3536(5)	3927(4)	36(2)
C(46)	8737(3)	4769(5)	3684(3)	28(1)
C(51)	9150(2)	7647(5)	3249(3)	19(1)

C(52)	8993(2)	8727(5)	2809(3)	23(1)
C(53)	9298(3)	8989(5)	2287(3)	30(1)
C(54)	9770(3)	8194(6)	2214(3)	36(1)
C(55)	9938(3)	7150(6)	2665(4)	40(2)
C(56)	9634(3)	6857(6)	3176(3)	30(1)
C(61)	8968(2)	8366(5)	4661(3)	20(1)
C(62)	8527(3)	9114(5)	4852(3)	24(1)
C(63)	8740(3)	9886(5)	5484(3)	28(1)
C(64)	9381(3)	9892(5)	5920(3)	29(1)
C(65)	9819(3)	9144(6)	5732(3)	32(1)
C(66)	9615(3)	8381(5)	5103(3)	27(1)
F(5)	7504(2)	12636(5)	1012(2)	70(2)
F(6)	8594(2)	11670(4)	2507(2)	57(1)
N(10)	7214(2)	5235(4)	2836(3)	25(1)
O(10)	7115(2)	4178(4)	2956(3)	41(1)
O(1)	7985(2)	7608(3)	3453(2)	19(1)
P(1)	6570(1)	7572(1)	3129(1)	14(1)
P(2)	8691(1)	7339(1)	3860(1)	17(1)
P(3)	8051(1)	12168(2)	1755(1)	31(1)
Tc(1)	7274(1)	6755(1)	2504(1)	15(1)
Cl(1)	5765(1)	1109(2)	1510(1)	39(1)
Cl(2)	5605(1)	3649(2)	895(2)	73(1)
F(1B)	8312(7)	11587(13)	1184(8)	67(1)
F(2A)	7575(6)	11631(11)	2131(7)	47(1)
F(3A)	7801(6)	13148(10)	2210(6)	47(1)
F(4B)	8523(7)	13333(12)	1839(8)	67(1)
F(1A)	8183(3)	10838(6)	1387(4)	47(1)
F(2B)	7494(5)	11259(8)	1860(5)	67(1)
F(3B)	8101(5)	13565(8)	2077(5)	67(1)
F(4A)	8602(3)	12705(6)	1454(4)	47(1)

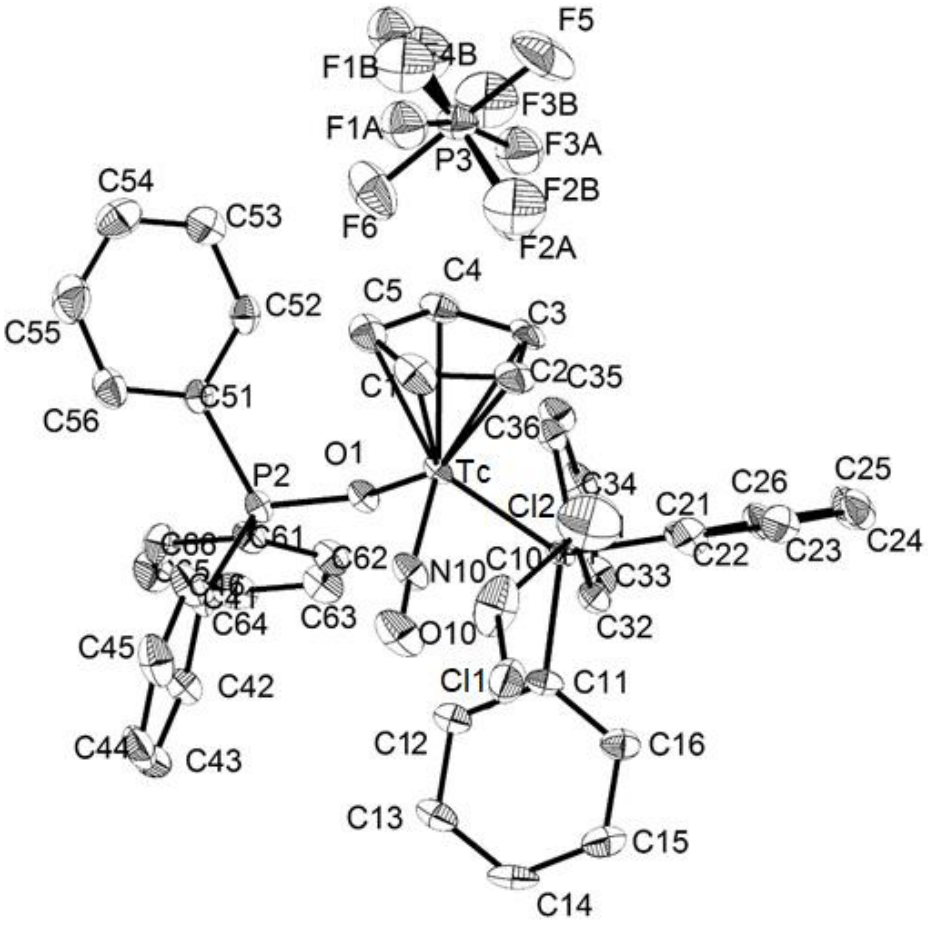

Figure 6.1.8: Ellipsoid plot (50% probability) of $[Tc^{I}(NO)(Cp)(PPh_3)(OPPh_3](PF_6) \cdot CH_2Cl_2$.

Table 6.1.17: Crystal data and structure refinement for $[Tc^{I}(NO)(Cp)(PPh_3)(SPPh_3)](PF_6)$.

Empirical formula	$C_{41}H_{35}F_6NOP_3STc$	
Formula weight	894.67	
Temperature	100(2) K	
Wavelength	0.71073 Å	
Crystal system	Monoclinic	
Space group	P $2_1/c$	
Unit cell dimensions	a = 21.2199(1) Å	α = 90º
	b = 11.1669(5) Å	β = 112.156(2)º
	c = 17.4508(1) Å	γ = 90º
Volume	3829.8(3) $Å^3$	
Z	4	
Density (calculated)	1.552 g/cm^3	
Absorption coefficient	0.620 mm^{-1}	
F(000)	1816	
Crystal size	0.18 x 0.16 x 0.08 mm^3	
Theta range for data collection	2.217 to 27.307°.	
Index ranges	-27<=h<=27, -14<=k<=14, -22<=l<=22	
Reflections collected	119727	
Independent reflections	8570 [R(int) = 0.1050]	
Completeness to theta = 25.242°	100.0 %	
Absorption correction	None	
Refinement method	Full-matrix least-squares on F^2	
Data / restraints / parameters	8570 / 0 / 627	
Goodness-of-fit on F^2	1.033	
Final R indices [I>2sigma(I)]	R1 = 0.0340, wR2 = 0.0649	
Final R indexes [all data]	R1 = 0.0551, wR2 = 0.0715	
Diffractometer	CCD, Bruker	

Table 6.1.18: Atomic coordinates (x 10^4) and equivalent isotropic displacement parameters ($Å^2$ x 10^3) for $[Tc^I(NO)(Cp)(PPh_3)(SPPh_3)](PF_6)$. U(eq) is defined as one third of the trace of the orthogonalized U^{ij} tensor.

	x	y	z	U(eq)
Tc(1)	6873(1)	4656(1)	7283(1)	11(1)
S(1)	7755(1)	3322(1)	8152(1)	15(1)
P(1)	6101(1)	3278(1)	7490(1)	12(1)
P(2)	8599(1)	3526(1)	7889(1)	13(1)
P(3)	1902(1)	1246(1)	4167(1)	22(1)
F(3)	2129(1)	208(1)	4852(1)	39(1)
O(1)	6646(1)	3686(2)	5633(1)	26(1)
F(1)	1681(1)	2289(2)	3498(1)	49(1)
F(2)	1956(1)	339(2)	3496(1)	43(1)
F(5)	2681(1)	1599(2)	4406(1)	47(1)
F(6)	1131(1)	865(2)	3926(1)	50(1)
F(4)	1855(1)	2144(2)	4850(1)	55(1)
N(1)	6752(1)	4016(2)	6311(1)	15(1)
C(21)	6377(1)	1719(2)	7665(2)	14(1)
C(61)	9116(1)	2207(2)	8277(2)	16(1)
C(56)	9039(1)	5250(2)	9107(2)	20(1)
C(42)	8372(1)	2586(2)	6338(2)	19(1)
C(11)	5293(1)	3178(2)	6609(1)	15(1)
C(46)	8289(1)	4736(2)	6393(2)	17(1)
C(26)	6384(2)	1062(2)	8340(2)	26(1)
C(51)	9101(1)	4812(2)	8391(2)	15(1)
C(31)	5874(1)	3608(2)	8374(2)	13(1)
C(22)	6611(1)	1187(2)	7104(2)	23(1)
C(33)	6263(1)	3945(2)	9843(2)	21(1)
C(43)	8213(1)	2658(2)	5491(2)	22(1)
C(45)	8118(1)	4796(2)	5546(2)	22(1)
C(41A)	8418(1)	3631(2)	6797(2)	14(1)
C(32)	6400(1)	3783(2)	9139(2)	17(1)
C(35)	5067(1)	3795(2)	9035(2)	23(1)
C(16)	4907(1)	2130(2)	6431(2)	19(1)
C(44)	8087(1)	3757(3)	5099(2)	24(1)

C(62)	9820(1)	2293(2)	8523(2)	21(1)
C(34)	5598(1)	3938(2)	9793(2)	24(1)
C(36)	5204(1)	3628(2)	8326(2)	18(1)
C(63)	10223(1)	1292(3)	8811(2)	29(1)
C(54)	9896(2)	6712(2)	9236(2)	31(1)
C(15)	4285(1)	2098(3)	5774(2)	25(1)
C(12)	5051(1)	4169(3)	6104(2)	28(1)
C(53)	9963(1)	6278(3)	8531(2)	31(1)
C(24)	6858(2)	-616(2)	7893(2)	32(1)
C(5)	6334(1)	6199(2)	7636(2)	22(1)
C(55)	9437(1)	6208(2)	9520(2)	27(1)
C(66)	8819(2)	1105(2)	8307(2)	29(1)
C(23)	6843(2)	18(2)	7210(2)	30(1)
C(52)	9564(1)	5325(2)	8104(2)	24(1)
C(1)	6991(2)	6099(2)	8253(2)	26(1)
C(3)	7100(2)	6604(2)	7044(2)	25(1)
C(4)	6402(1)	6499(2)	6893(2)	22(1)
C(64)	9931(2)	205(3)	8848(2)	33(1)
C(14)	4047(2)	3087(3)	5288(2)	32(1)
C(2)	7463(1)	6350(2)	7874(2)	30(1)
C(25)	6632(2)	-105(2)	8452(2)	36(1)
C(13)	4427(2)	4118(3)	5444(2)	38(1)
C(65)	9229(2)	104(3)	8590(2)	38(1)

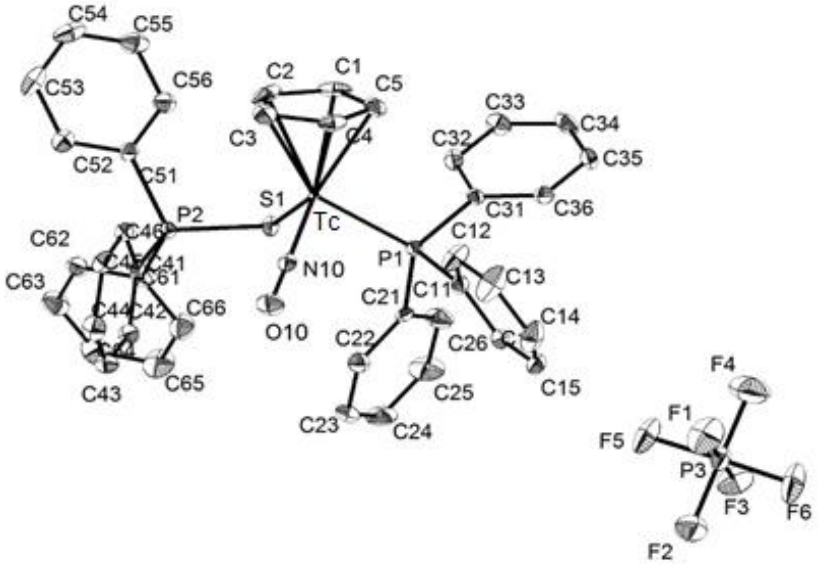

Figure 6.1.9: Ellipsoid plot (50% probability) of $[Tc^{I}(NO)(Cp)(PPh_3)(SPPh_3)](PF_6)$.

Table 6.1.19: Crystal data and structure refinement for $[Tc^{I}(NO)(Cp)(PPh_3)(SePPh_3)](PF_6)$.

Empirical formula	$C_{41}H_{35}F_6NOP_3SeTc$	
Formula weight	941.57	
Temperature	293(2) K	
Wavelength	0.71073 Å	
Crystal system	Monoclinic	
Space group	P 2_1/c	
Unit cell dimensions	a = 21.567(2) Å	α = 90º
	b = 11.2351(9) Å	β = 112.228(5)º
	c = 17.759(1) Å	γ = 90º
Volume	3983.4(5) $Å^3$	
Z	4	
Density (calculated)	1.570 g/cm^3	
Absorption coefficient	1.457 mm^{-1}	
F(000)	1888	
Crystal size	0.18 x 0.14 x 0.08 mm^3	
Theta range for data collection	3.302 to 28.995°.	
Index ranges	-29<=h<=29, -15<=k<=13, -24<=l<=24	
Reflections collected	45560	
Independent reflections	10582 [R(int) = 0.2471]	
Completeness to theta = 25.242°	99.8 %	
Absorption correction	Integration	
Refinement method	Full-matrix least-squares on F^2	
Data / restraints / parameters	10582 / 21 / 479	
Goodness-of-fit on F^2	0.898	
Final R indices [I>2sigma(I)]	R1 = 0.0853, wR2 = 0.1136	
R indices (all data)	R1 = 0.2197, wR2 = 0.1483	
Diffractometer	IPDS, STOE	

Table 6.1.20: Atomic coordinates (x 10^4) and equivalent isotropic displacement parameters ($Å^2$ x 10^3) for $[Tc^{I}(NO)(Cp)(PPh_3)(SePPh_3)](PF_6)$. U(eq) is defined as one third of the trace of the orthogonalized U^{ij} tensor.

	x	y	z	U(eq)
Tc(1)	3155(1)	4642(1)	2711(1)	29(1)
Se(1)	2259(1)	3253(1)	1807(1)	39(1)
P(1)	3931(1)	3272(2)	2532(1)	32(1)
P(2)	1371(1)	3503(2)	2097(1)	36(1)
O(10)	3355(3)	3682(6)	4326(4)	61(2)
N(10)	3262(3)	4018(6)	3659(4)	37(2)
C(11)	4163(4)	3601(7)	1666(5)	30(2)
C(12)	4814(4)	3599(7)	1712(5)	40(2)
C(13)	4955(5)	3765(9)	1020(7)	54(3)
C(14)	4452(5)	3904(8)	287(6)	54(3)
C(15)	3803(5)	3912(8)	228(6)	53(3)
C(16)	3654(4)	3743(7)	912(5)	41(2)
C(21)	4725(4)	3190(8)	3408(5)	36(2)
C(22)	5110(5)	2172(9)	3590(6)	48(2)
C(23)	5717(5)	2138(11)	4238(6)	59(3)
C(24)	5948(5)	3138(13)	4693(6)	69(3)
C(25)	5578(6)	4146(12)	4537(7)	80(4)
C(26)	4967(5)	4191(9)	3894(6)	55(3)
C(31)	3658(3)	1721(7)	2377(5)	33(2)
C(32)	3635(5)	1068(8)	1718(6)	52(2)
C(33)	3360(6)	-78(9)	1602(7)	75(3)
C(34)	3160(5)	-580(9)	2159(8)	73(3)
C(35)	3195(5)	55(8)	2818(8)	65(3)
C(36)	3445(5)	1188(8)	2927(6)	52(2)
C(41)	3598(5)	6481(7)	3082(6)	54(3)
C(42)	3670(5)	6176(8)	2382(7)	47(2)
C(43)	3052(7)	6081(8)	1759(6)	69(3)
C(44)	2564(5)	6336(8)	2127(9)	77(4)
C(45)	2926(6)	6555(7)	2938(7)	58(3)
C(51)	878(4)	4787(7)	1619(5)	37(2)
C(52)	937(4)	5251(9)	915(5)	49(2)

C(53)	553(5)	6203(9)	532(7)	65(3)
C(54)	99(6)	6697(10)	799(8)	76(3)
C(55)	28(6)	6240(12)	1481(9)	86(4)
C(56)	413(4)	5281(9)	1887(6)	57(2)
C(61)	853(4)	2180(8)	1727(5)	41(2)
C(62)	1145(5)	1107(10)	1719(7)	72(3)
C(63)	739(7)	102(10)	1453(9)	98(4)
C(64)	67(6)	213(11)	1158(8)	84(4)
C(65)	-221(5)	1274(10)	1174(7)	70(3)
C(66)	177(4)	2270(9)	1462(6)	56(3)
C(71)	1572(4)	3616(7)	3183(5)	33(2)
C(72)	1621(4)	2576(9)	3632(6)	51(2)
C(73)	1789(5)	2668(11)	4466(6)	61(3)
C(74)	1923(5)	3747(11)	4837(6)	62(3)
C(75)	1880(5)	4761(10)	4401(6)	55(2)
C(76)	1703(4)	4723(9)	3568(6)	47(2)
P(5)	1951(6)	6274(13)	9195(8)	104(2)
F(5)	1839(8)	7204(13)	8498(10)	104(2)
F(6)	2020(7)	5324(15)	9870(10)	104(2)
F(1)	1877(7)	5526(14)	8418(10)	104(2)
F(2)	1185(6)	6146(15)	8990(10)	104(2)
F(3)	2065(8)	7142(13)	9957(9)	104(2)
F(4)	2727(6)	6346(15)	9410(10)	104(2)
P(5A)	1922(3)	6280(6)	9177(4)	25(1)
F(4A)	2601(6)	6921(14)	9431(11)	104(2)
F(1A)	1564(8)	7347(14)	8580(11)	104(2)
F(6A)	2103(8)	5279(15)	8665(11)	104(2)
F(2A)	1238(6)	5610(13)	8875(11)	104(2)
F(3A)	2300(7)	5276(15)	9841(11)	104(2)
F(5A)	1684(8)	7094(14)	9730(11)	104(2)

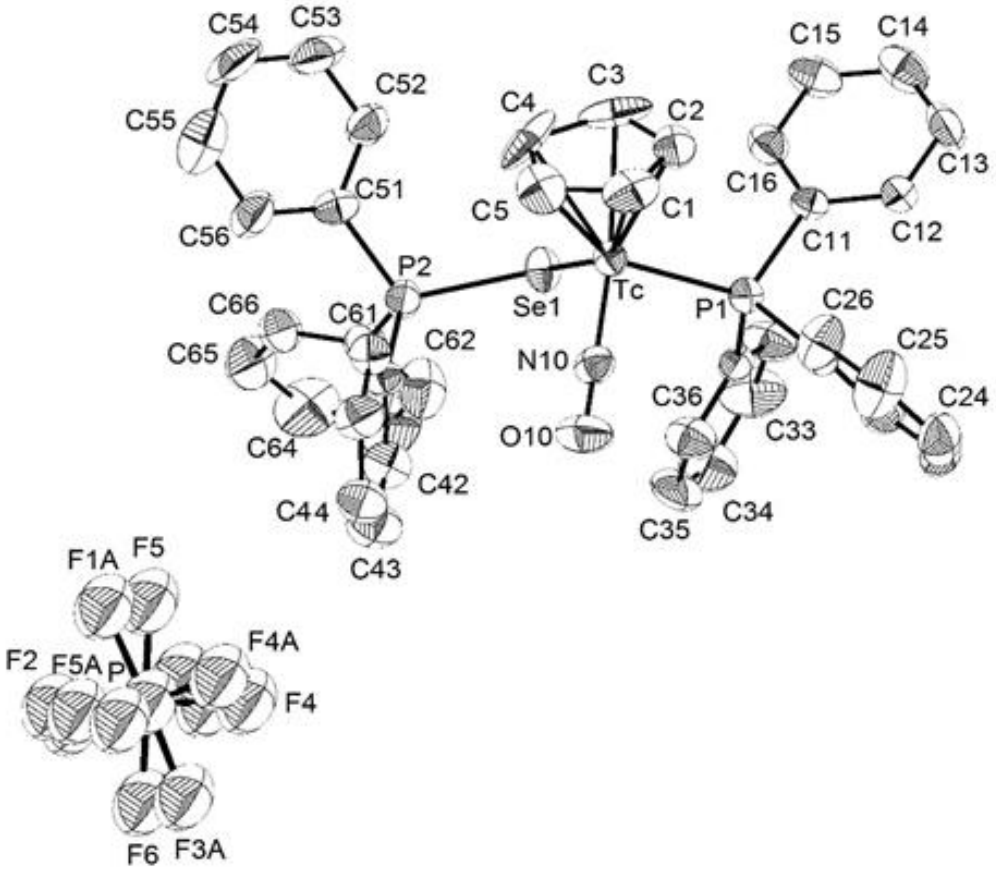

Figure 6.1.10: Ellipsoid plot (50% probability) of [Tc^{I}(NO)(Cp)(PPh_3)($SePPh_3$)](PF_6).

Table 6.1.21: Crystal data and structure refinement for $[Tc^{I}(NO)(CpMe)(PPh_3)(Py)](PF_6)$.

Empirical formula	$C_{29}H_{27}F_6N_2OP_2Tc$	
Formula weight	693.46	
Temperature	100(2) K	
Wavelength	0.71073 Å	
Crystal system	Monoclinic	
Space group	C c	
Unit cell dimensions	a = 17.944(2) Å	α = 90º
	b = 10.9664(2) Å	β = 114.190(5)º
	c = 16.006(3) Å	γ = 90º
Volume	2873.1(8) $Å^3$	
Z	4	
Density (calculated)	1.603 g/cm^3	
Absorption coefficient	0.678 mm^{-1}	
F(000)	1400	
Crystal size	0.28 x 0.23 x 0.12 mm^3	
Theta range for data collection	2.235 to 27.160°.	
Index ranges	-22<=h<=22, -14<=k<=14, -20<=l<=20	
Reflections collected	50841	
Independent reflections	6090 [R(int) = 0.0259]	
Completeness to theta = 25.242°	100.0 %	
Absorption correction	None	
Refinement method	Full-matrix least-squares on F^2	
Flack parameter	-0.014(4) (Pearson's method)	
Data / restraints / parameters	6090 / 2 / 370	
Goodness-of-fit on F^2	1.101	
Final R indices [I>2sigma(I)]	R1 = 0.0154, wR2 = 0.0389	
R indices (all data)	R1 = 0.0155, wR2 = 0.0390	
Diffractometer	CCD, Bruker	

Table 6.1.22: Atomic coordinates (x 10^4) and equivalent isotropic displacement parameters ($Å^2$ x 10^3) for $[Tc^{I}(NO)(CpMe)(PPh_3)(Py)](PF_6)$. U(eq) is defined as one third of the trace of the orthogonalized U^{ij} tensor.

	x	y	z	U(eq)
C(1)	2426(1)	7751(2)	3443(2)	25(1)
C(2)	2683(2)	8977(2)	3735(2)	26(1)
C(3)	3078(1)	9410(2)	3187(2)	27(1)
C(4)	3074(1)	8466(2)	2570(2)	28(1)
C(5)	2653(2)	7448(2)	2723(2)	26(1)
C(6)	2467(2)	6268(3)	2206(2)	37(1)
C(11)	4725(1)	6281(2)	6173(1)	19(1)
C(12)	5499(1)	6260(2)	6167(2)	24(1)
C(13)	6000(2)	5246(2)	6506(2)	32(1)
C(14)	5734(2)	4270(2)	6858(2)	34(1)
C(15)	4973(2)	4295(2)	6881(2)	31(1)
C(16)	4465(2)	5301(2)	6541(1)	25(1)
C(21)	4585(1)	8861(2)	6358(1)	17(1)
C(22)	5183(1)	8702(2)	7246(1)	22(1)
C(23)	5556(1)	9715(2)	7781(2)	26(1)
C(24)	5331(1)	10879(2)	7437(2)	24(1)
C(25)	4730(2)	11041(2)	6558(2)	26(1)
C(26)	4361(1)	10034(2)	6018(2)	22(1)
C(31)	3181(1)	7302(2)	5895(2)	19(1)
C(32)	3090(2)	7904(2)	6618(2)	28(1)
C(33)	2450(2)	7597(3)	6855(2)	37(1)
C(34)	1893(2)	6714(2)	6369(2)	33(1)
C(35)	1976(1)	6107(2)	5648(2)	27(1)
C(36)	2620(1)	6396(2)	5420(2)	22(1)
C(41)	5108(1)	6069(2)	4034(2)	23(1)
C(42)	5500(2)	4972(2)	4076(2)	28(1)
C(43)	5122(2)	3900(2)	4139(2)	31(1)
C(44)	4352(2)	3967(2)	4147(2)	30(1)
C(45)	4004(1)	5100(2)	4116(2)	24(1)
F(1)	6731(1)	6904(1)	3759(1)	30(1)
F(2)	7413(1)	8700(1)	4102(1)	43(1)

F(3)	8115(1)	8064(2)	5561(1)	46(1)
F(4)	7433(1)	6267(1)	5215(1)	36(1)
F(5)	8111(1)	6915(1)	4380(1)	29(1)
F(6)	6727(1)	8046(2)	4929(1)	44(1)
N(10)	4714(1)	8797(2)	4414(1)	22(1)
N(20)	4366(1)	6150(2)	4057(1)	20(1)
O(10)	5225(1)	9547(2)	4602(1)	33(1)
P(1)	4064(1)	7571(1)	5635(1)	15(1)
P(2)	7422(1)	7490(1)	4661(1)	22(1)
Tc(1)	3821(1)	7904(1)	4068(1)	16(1)

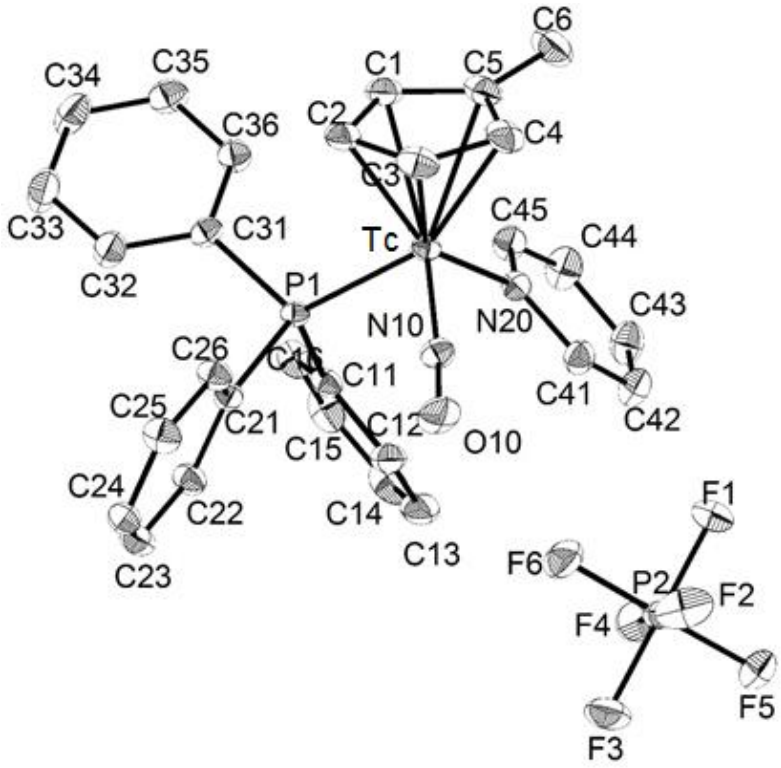

Figure 6.1.11: Ellipsoid plot (50% probability) of [Tc^{I}(NO)(CpMe)(PPh_3)(Py)](PF_6).

6.2 Spectroscopic data

6.2.1 Spectroscopic data of [Tc^{I}(NO)I(Cp)(PPh_3)]

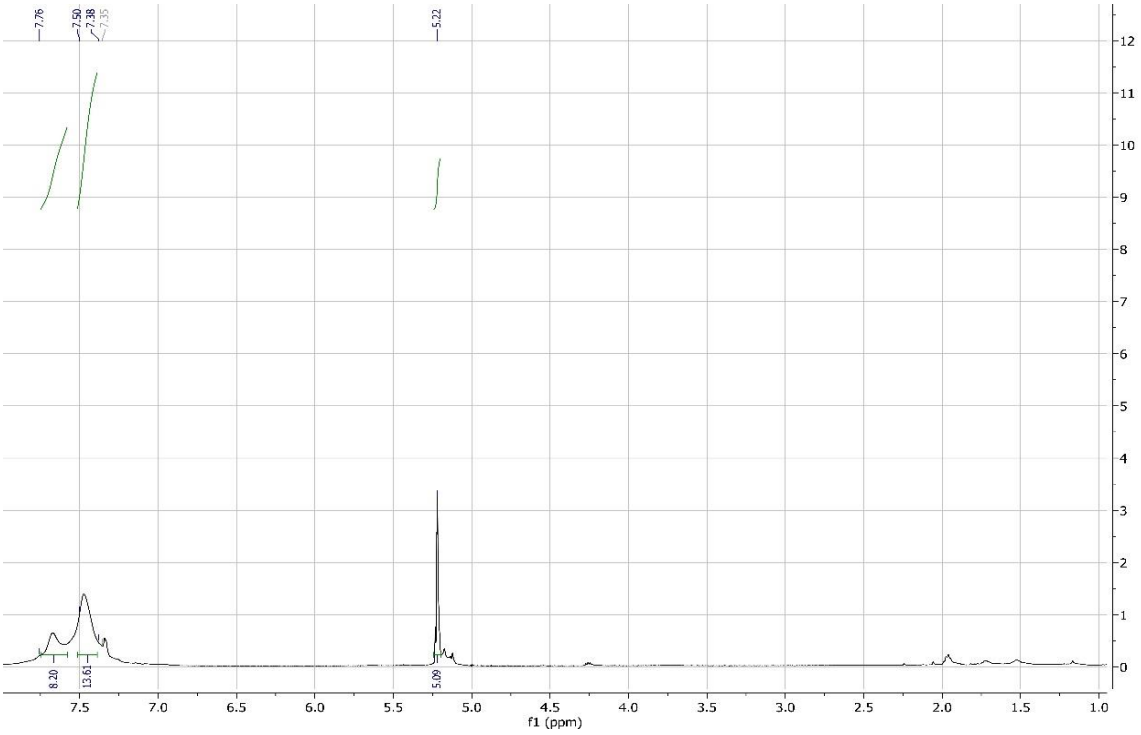

Figure 6.2.1: ^{1}H NMR spectrum of [Tc^{I}(NO)I(Cp)(PPh_3)] in CD_2Cl_2.

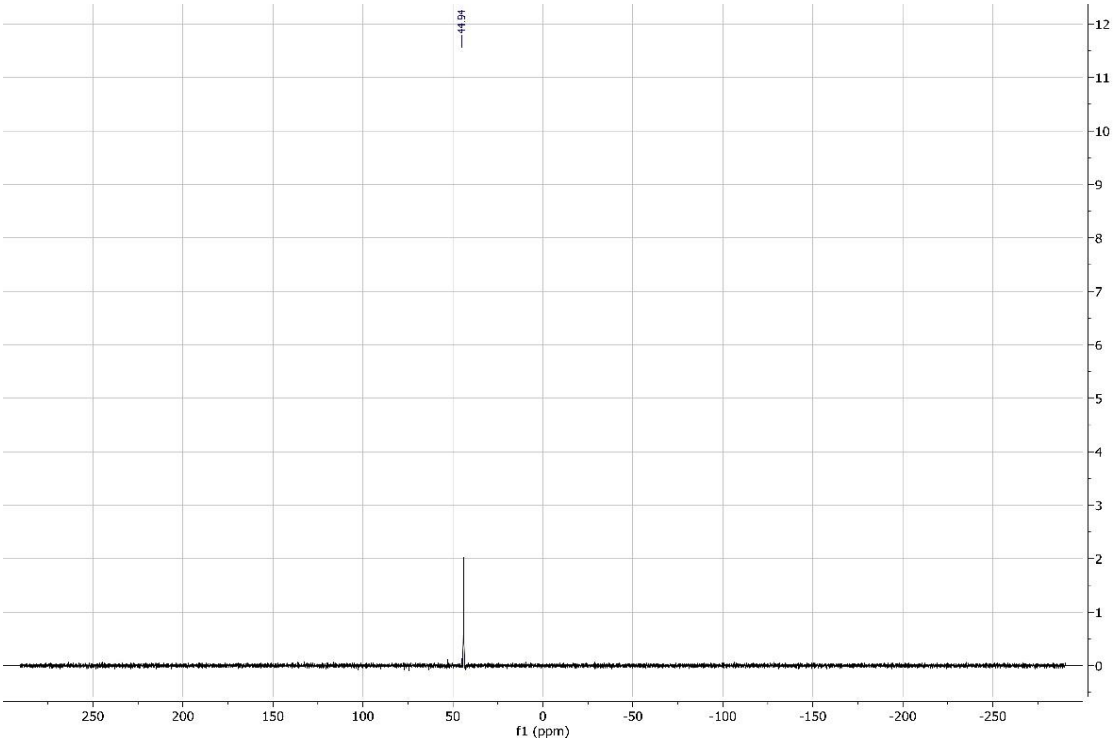

Figure 6.2.2: ^{31}P NMR spectrum of [Tc^{I}(NO)I(Cp)(PPh_3)] in CD_2Cl_2.

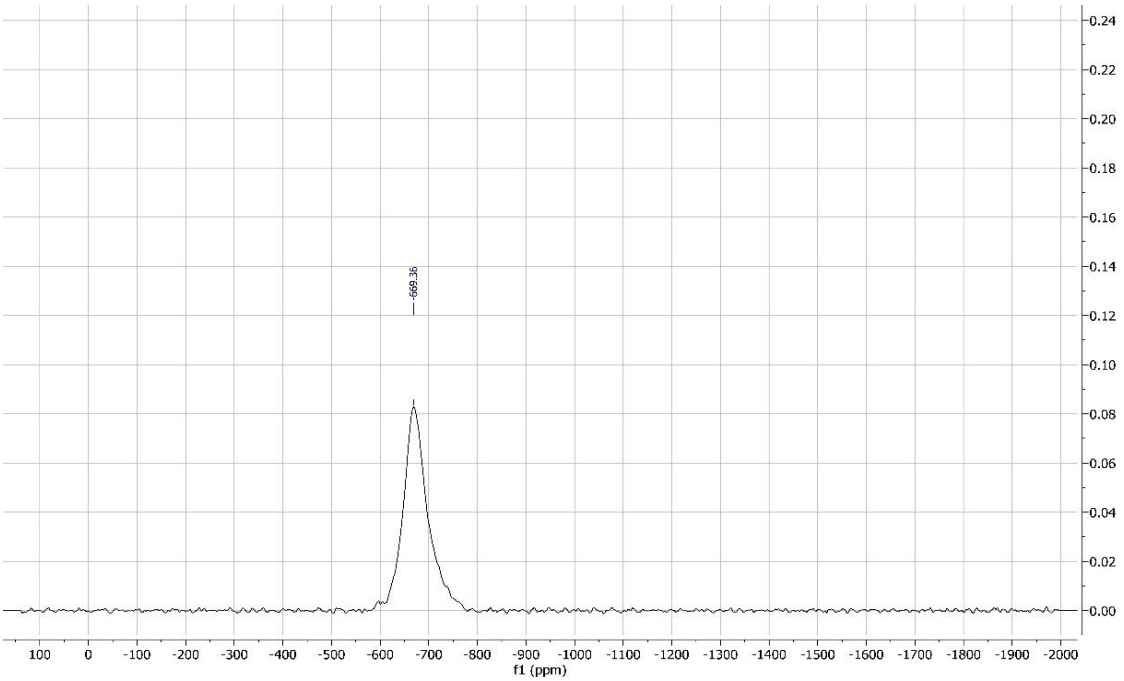

Figure 6.2.3: ^{99}Tc NMR spectrum of [Tc^{I}(NO)I(Cp)(PPh$_3$)] in CD_2Cl_2.

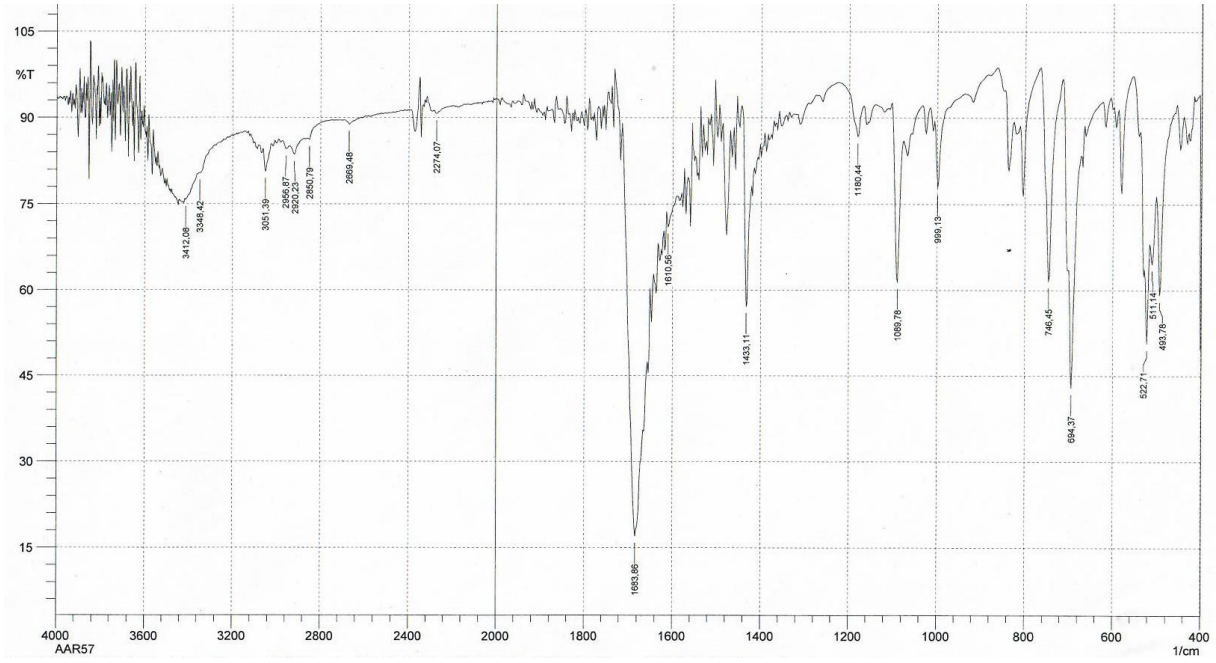

Figure 6.2.4: IR spectrum of [Tc^{I}(NO)I(Cp)(PPh$_3$)].

6.2.2 Spectroscopic data of $[Tc^{II}(NO)(I)_2(Cp)]$

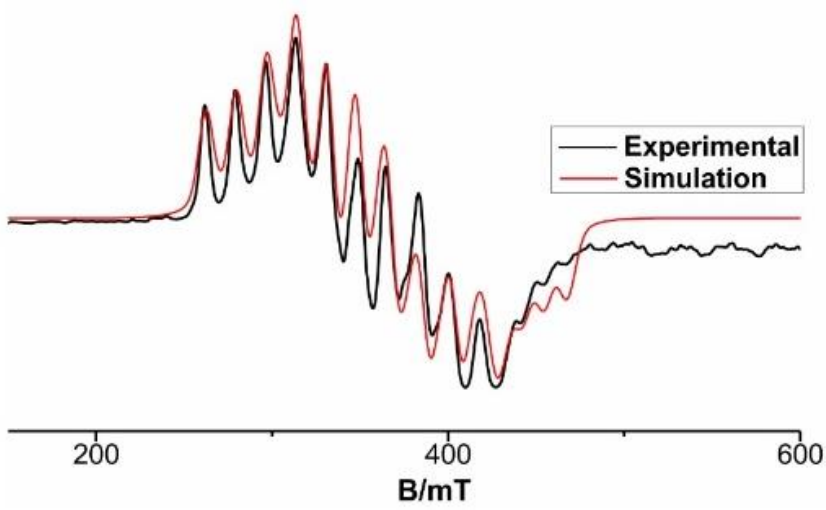

Figure 6.2.5: X- Band EPR spectrum of $[Tc^{II}(NO)(I)_2(Cp)]$ in CH_2Cl_2 at *T = 77* K

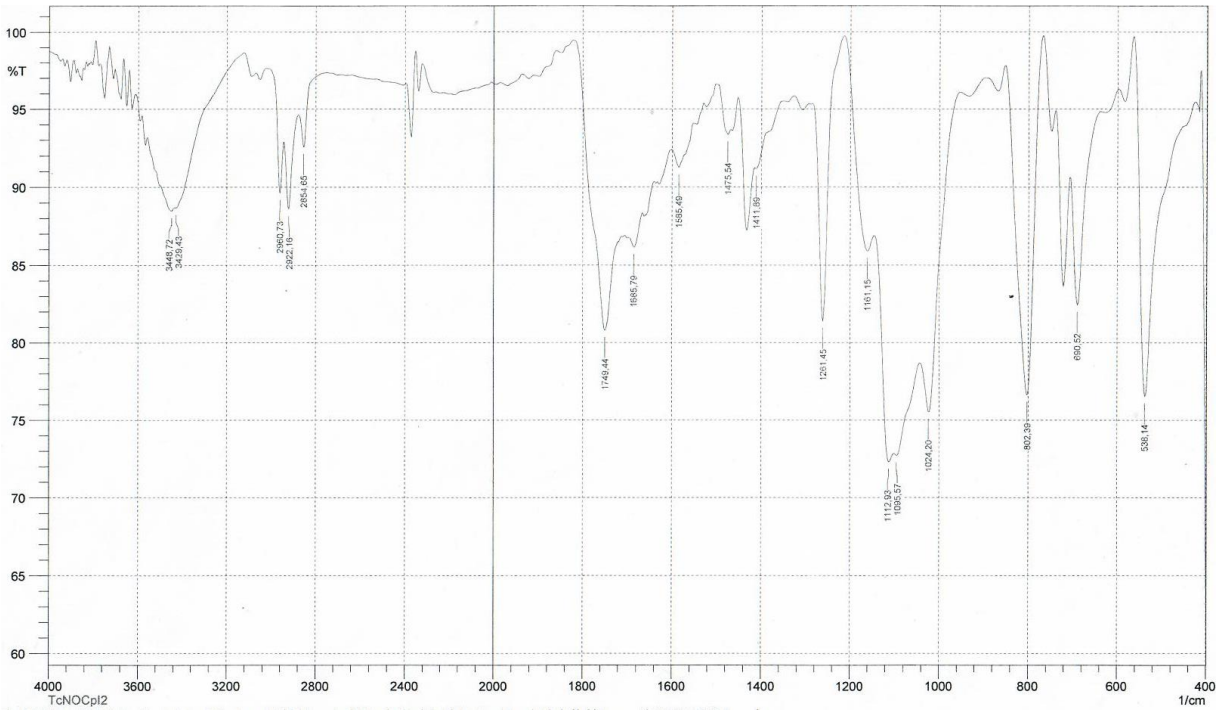

Figure 6.2.6: IR spectrum of $[Tc^{II}(NO)(I)_2(Cp)]$.

6.2.3 Spectroscopic data of [{Tc^{I}(NO)(Cp)(PPh_3)}$_2$Cl](PF_6)

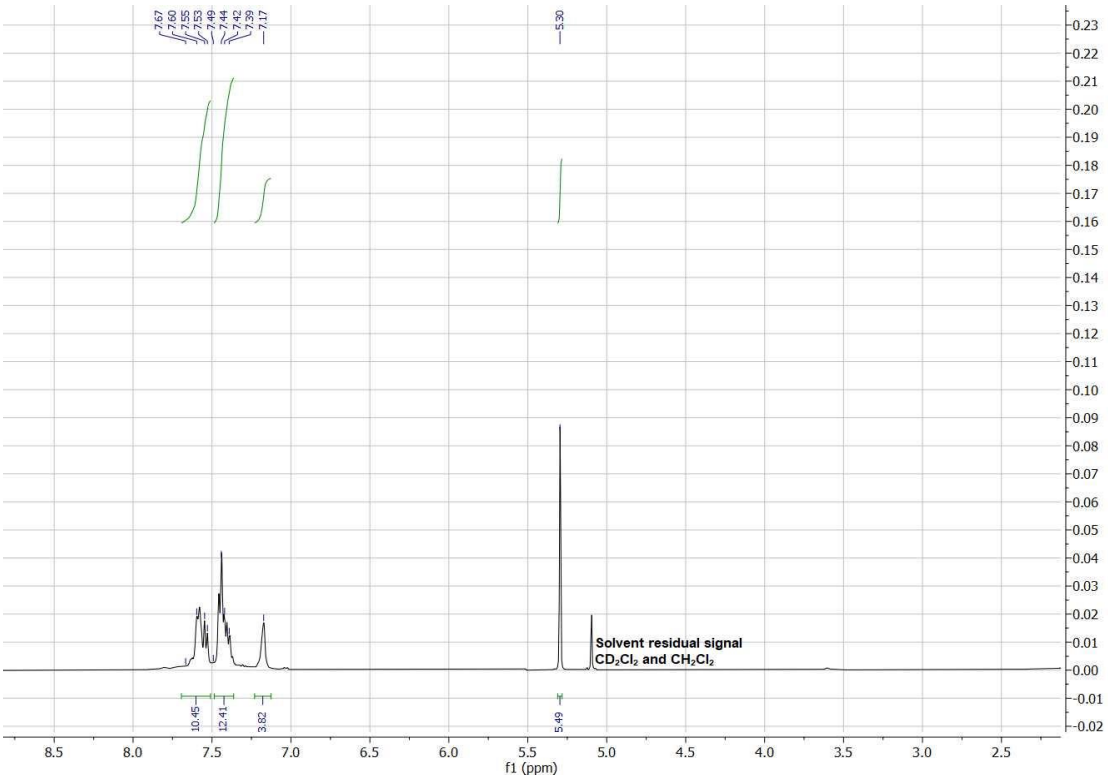

Figure 6.2.7: ^{1}H NMR spectrum of [{Tc^{I}(NO)(Cp)(PPh_3)}$_2$Cl](PF_6) in CD_2Cl_2.

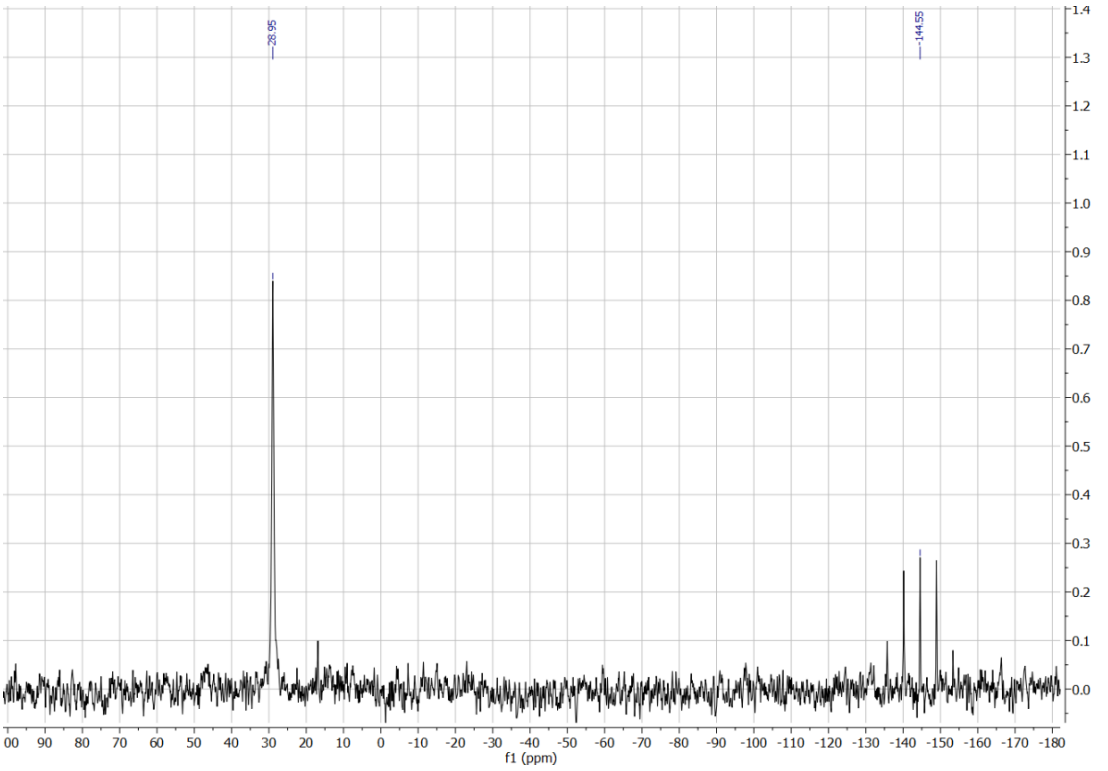

Figure 6.2.8: ^{13}P NMR spectrum of [{Tc^{I}(NO)(Cp)(PPh_3)}$_2$Cl](PF_6) in CD_2Cl_2.

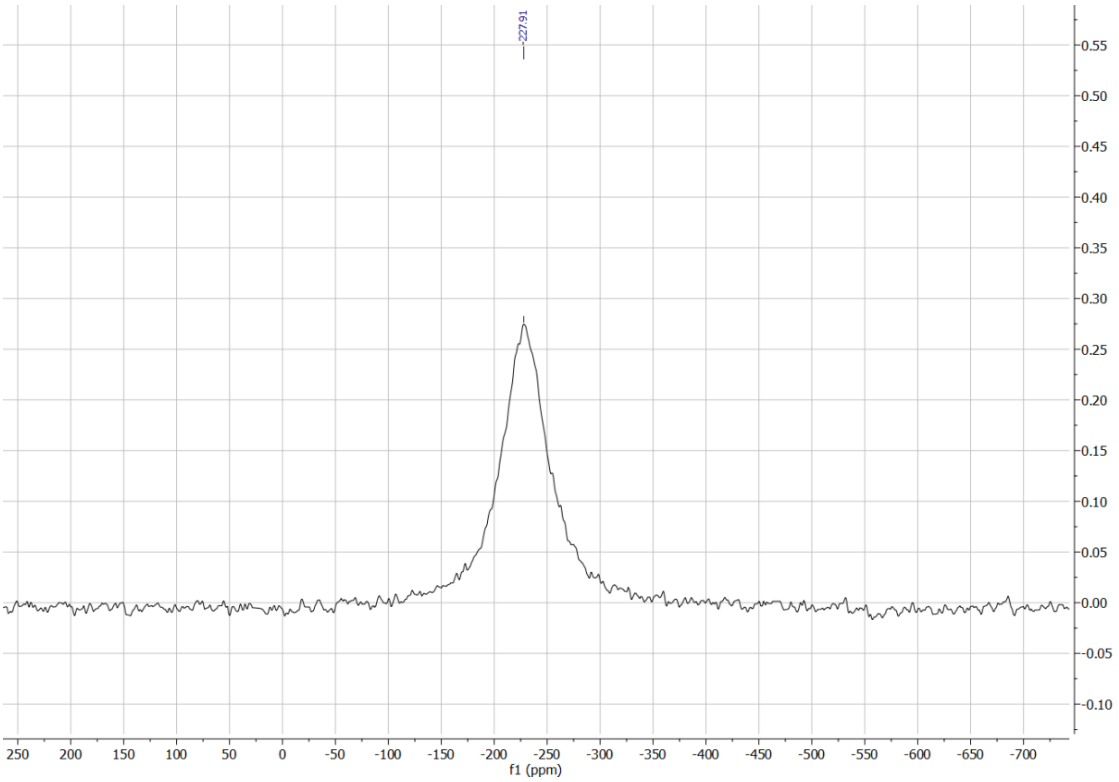

Figure 6.2.9: ^{99}Tc NMR spectrum of [{Tc^{I}(NO)(Cp)(PPh$_3$)}$_2$Cl](PF$_6$) in CD_2Cl_2.

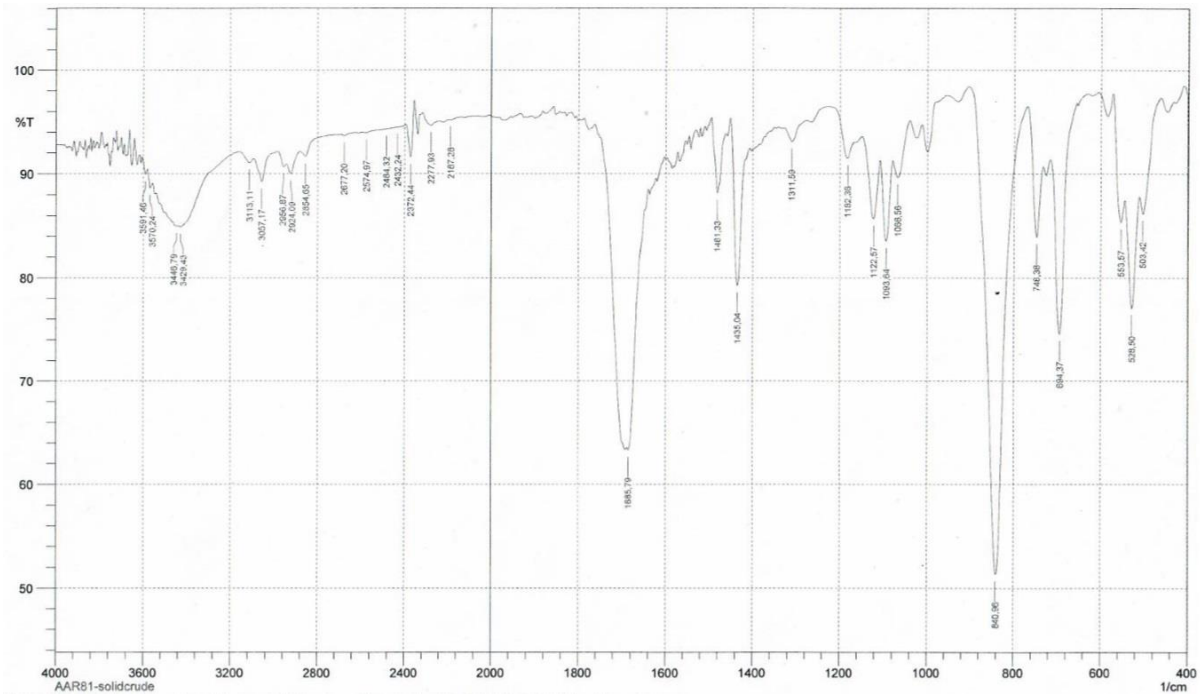

Figure 6.2.10: IR spectrum of [{Tc^{I}(NO)(Cp)(PPh$_3$)}$_2$Cl](PF$_6$).

6.2.4 Spectroscopic data of $[Tc^{I}(NO)(Cp)(PPh_3)(PMe_3)](PF_6)$

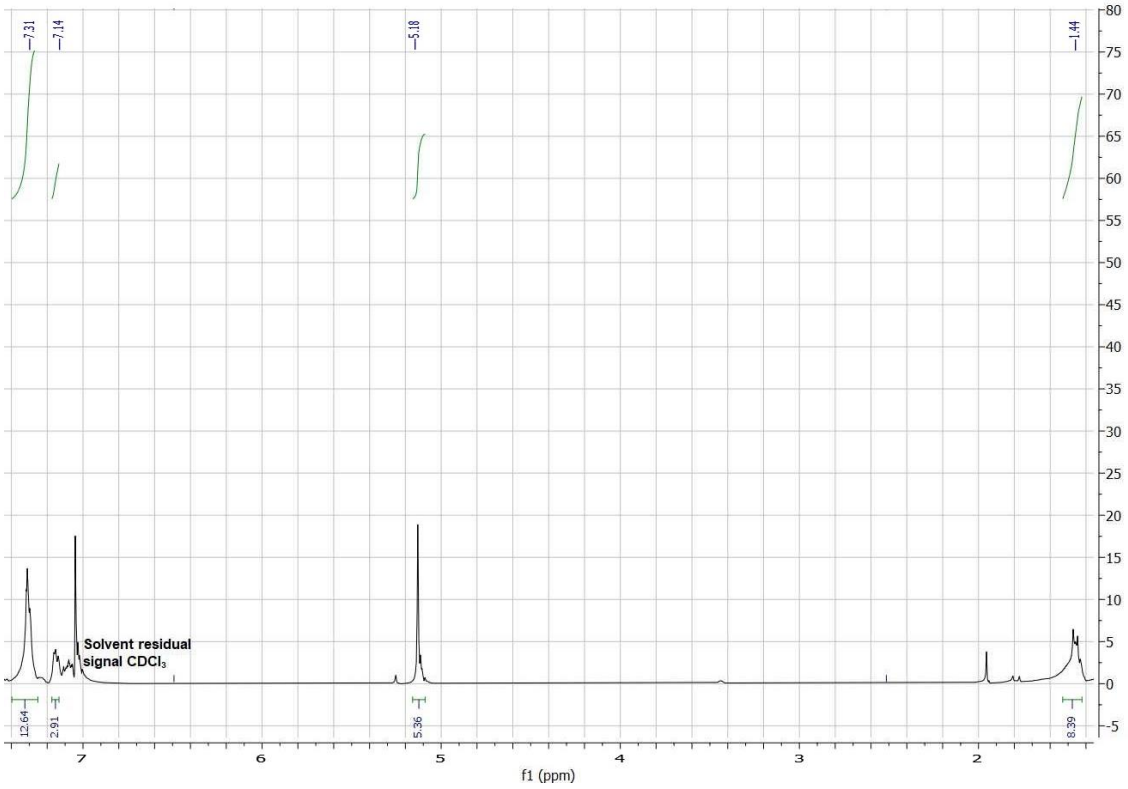

Figure 6.2.11: ^{1}H NMR spectrum of $[Tc^{I}(NO)(Cp)(PPh_3)(PMe_3)](PF_6)$ in $CDCl_3$.

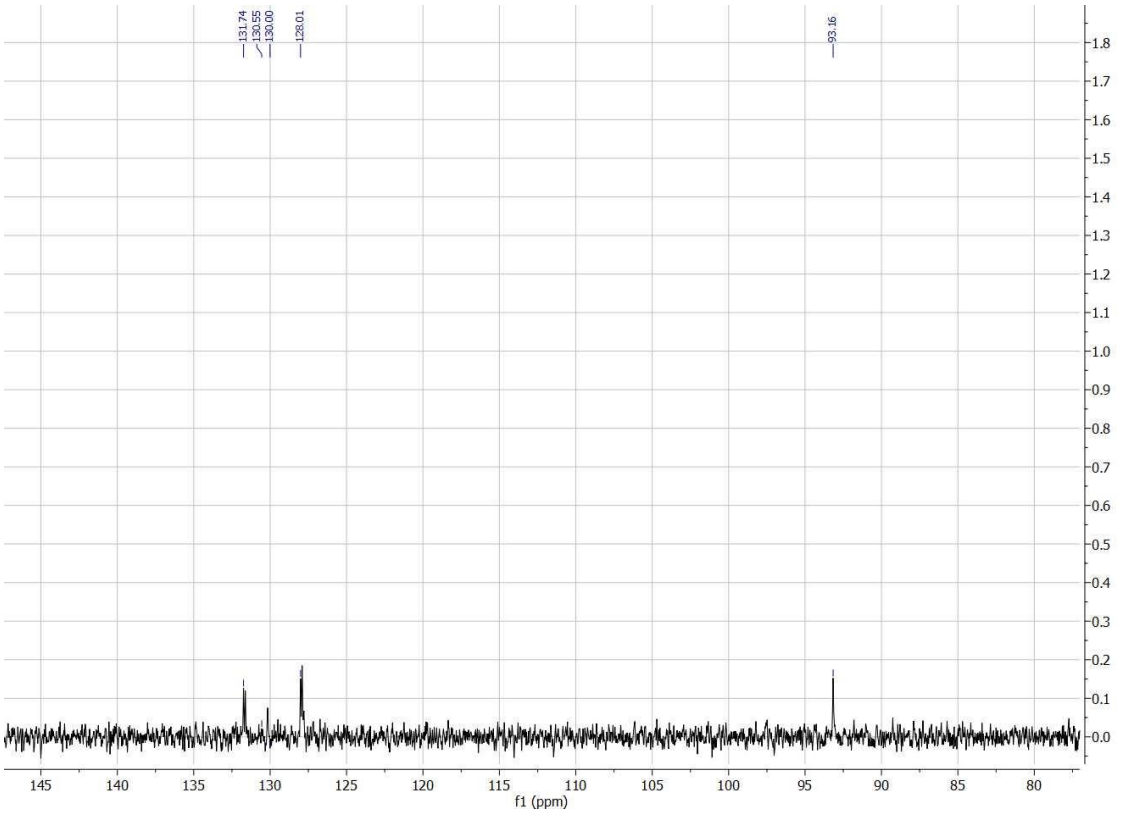

Figure 6.2.12: ^{13}C NMR spectrum of $[Tc^{I}(NO)(Cp)(PPh_3)(PMe_3)](PF_6)$ in $CDCl_3$.

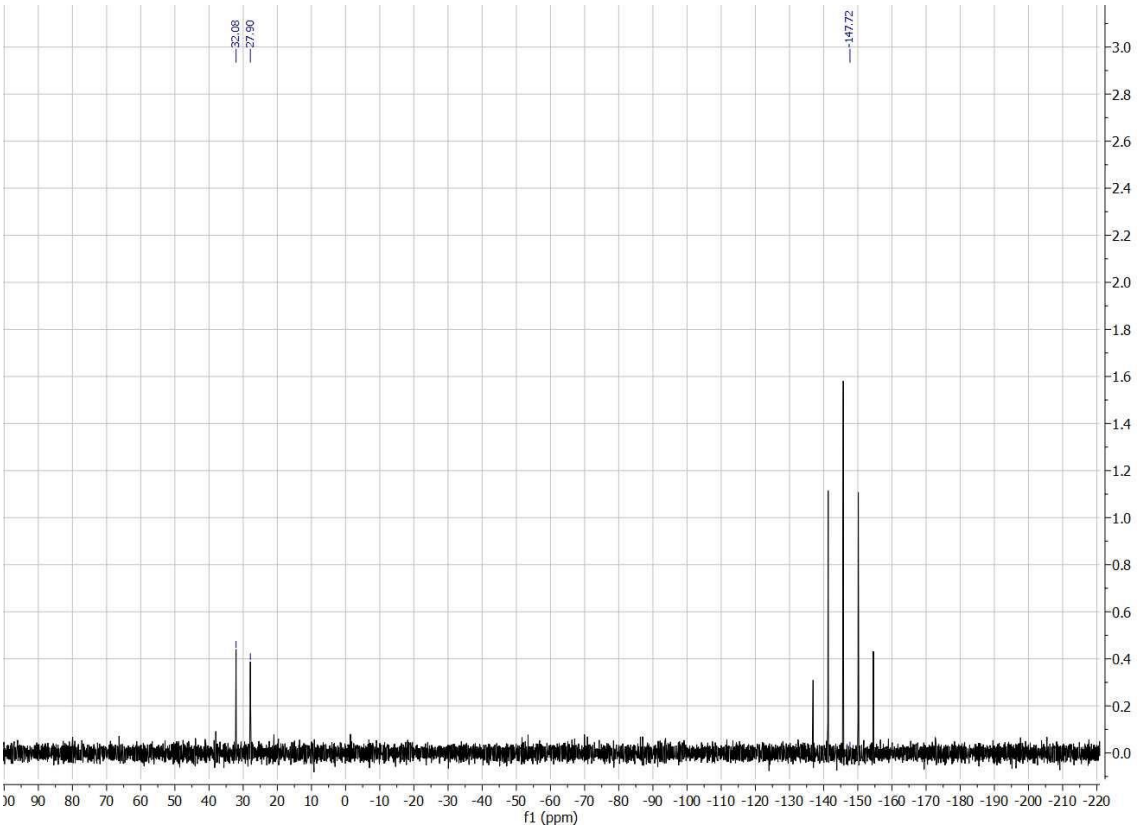

Figure 6.2.13: ^{31}P NMR spectrum of [Tc^{I}(NO)(Cp)(PPh$_3$)(PMe$_3$)](PF$_6$) in CDCl$_3$.

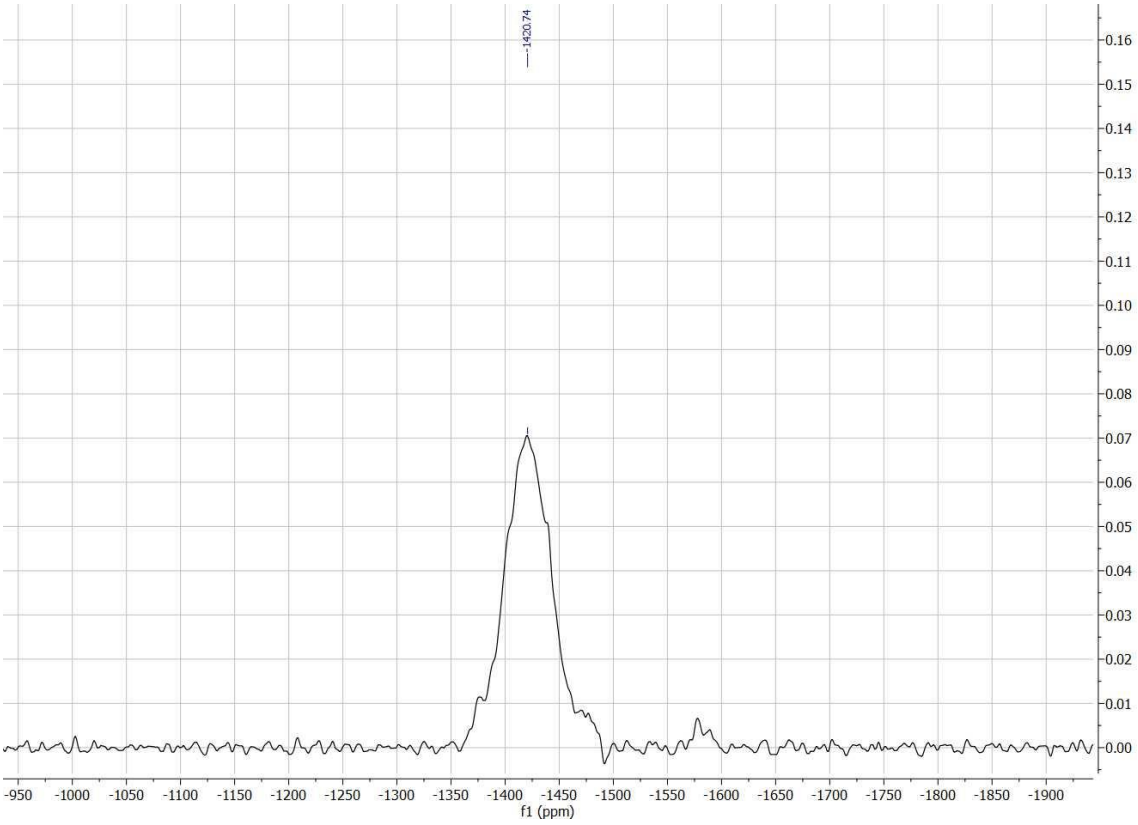

Figure 6.2.14: ^{99}Tc NMR spectrum of [Tc^{I}(NO)(Cp)(PPh$_3$)(PMe$_3$)](PF$_6$) in CDCl$_3$.

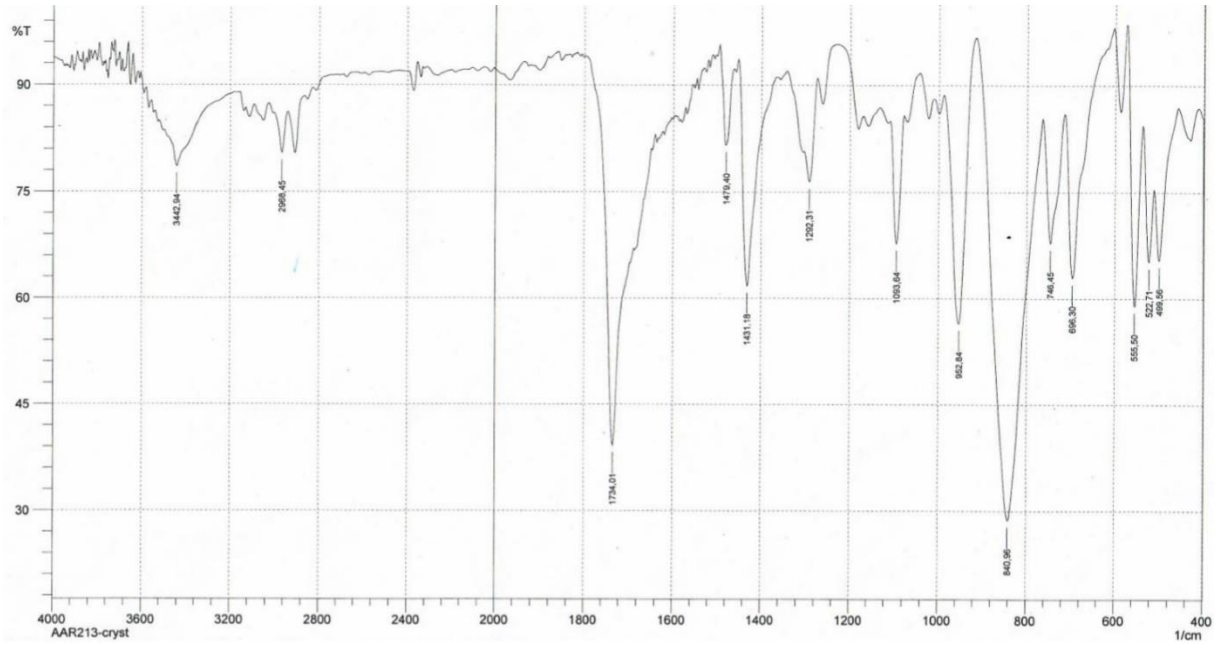

Figure 6.2.15: IR spectrum of $[Tc^{I}(NO)(Cp)(PPh_3)(PMe_3)](PF_6)$.

6.2.5 Spectroscopic data of $[Tc^{I}(NO)(Cp)(PPh_3)_2](PF_6)$

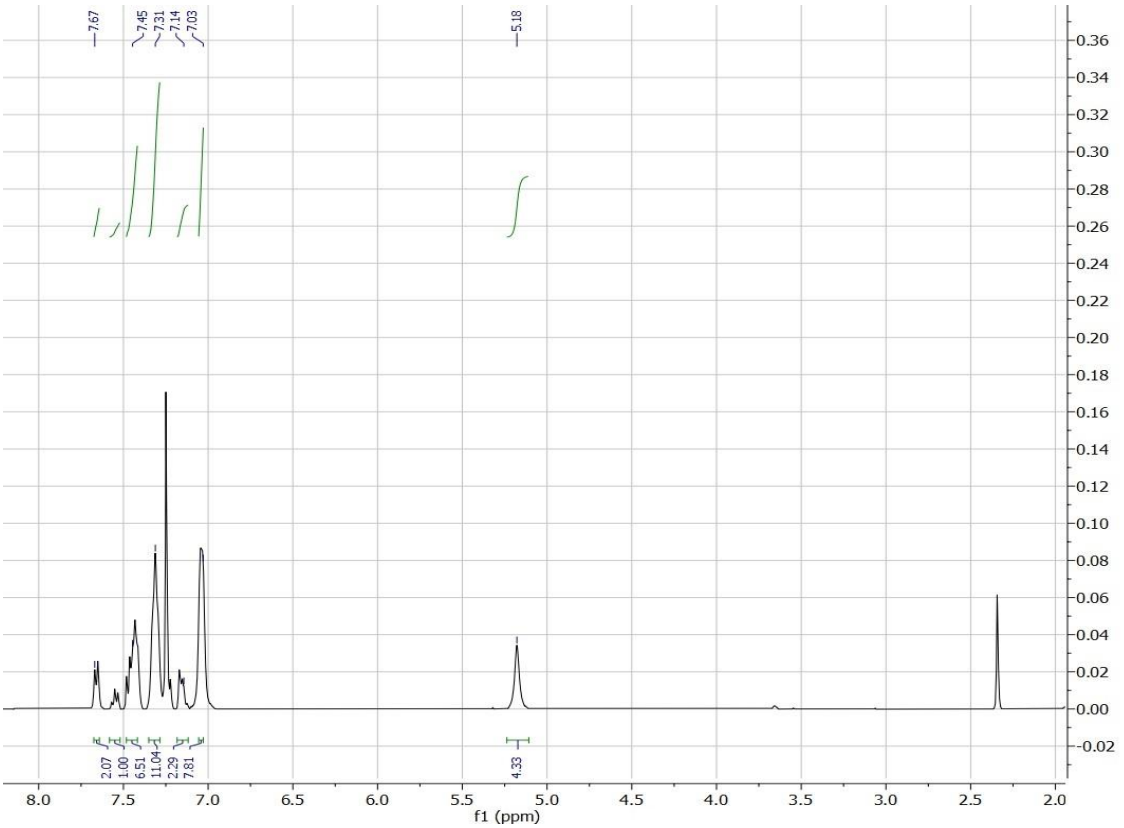

Figure 6.2.16: ^{1}H NMR spectrum of $[Tc^{I}(NO)(Cp)(PPh_3)_2](PF_6)$ in $CDCl_3$.

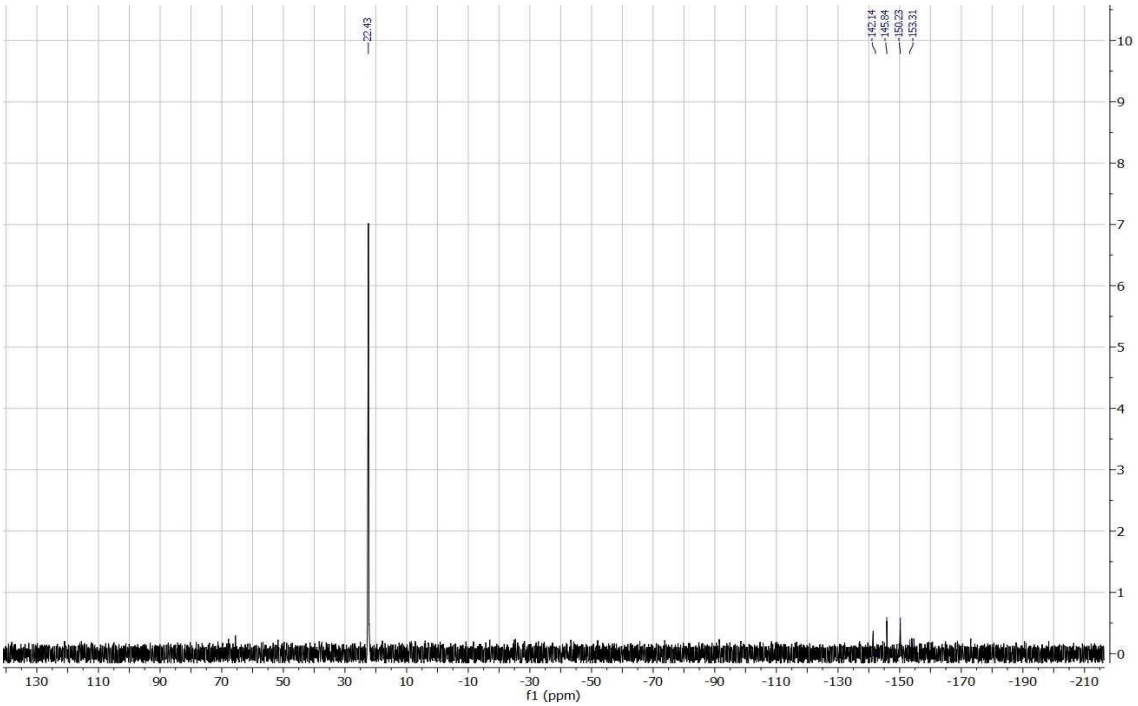

Figure 6.2.17: ^{13}P NMR spectrum of $[Tc^{I}(NO)(Cp)(PPh_3)_2](PF_6)$ in $CDCl_3$.

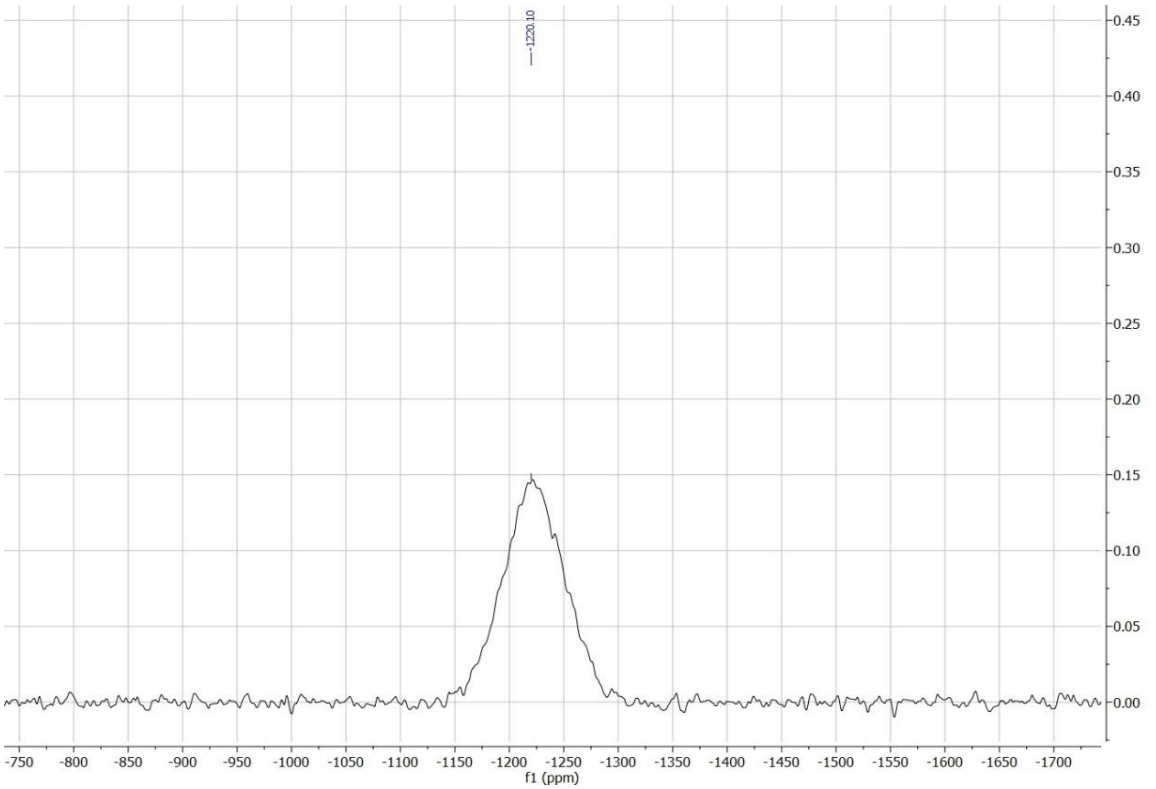

Figure 6.2.18: ^{99}Tc NMR spectrum of $[Tc^{I}(NO)(Cp)(PPh_3)_2](PF_6)$ in $CDCl_3$.

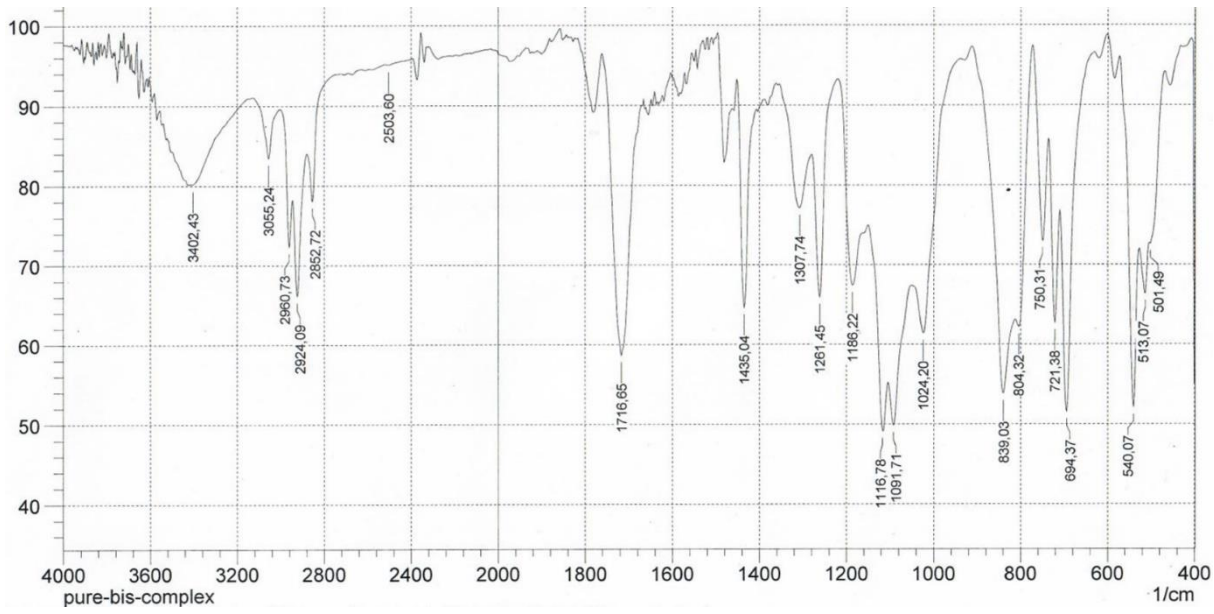

Figure 6.2.19: IR spectrum of $[Tc^{I}(NO)(Cp)(PPh_3)_2](PF_6)$.

6.2.6 Spectroscopic data of $[Tc^{I}(NO)(Cp)(PPh_3)\{C(OMe)C_2H_4PPh_3\}](PF_6)_2$

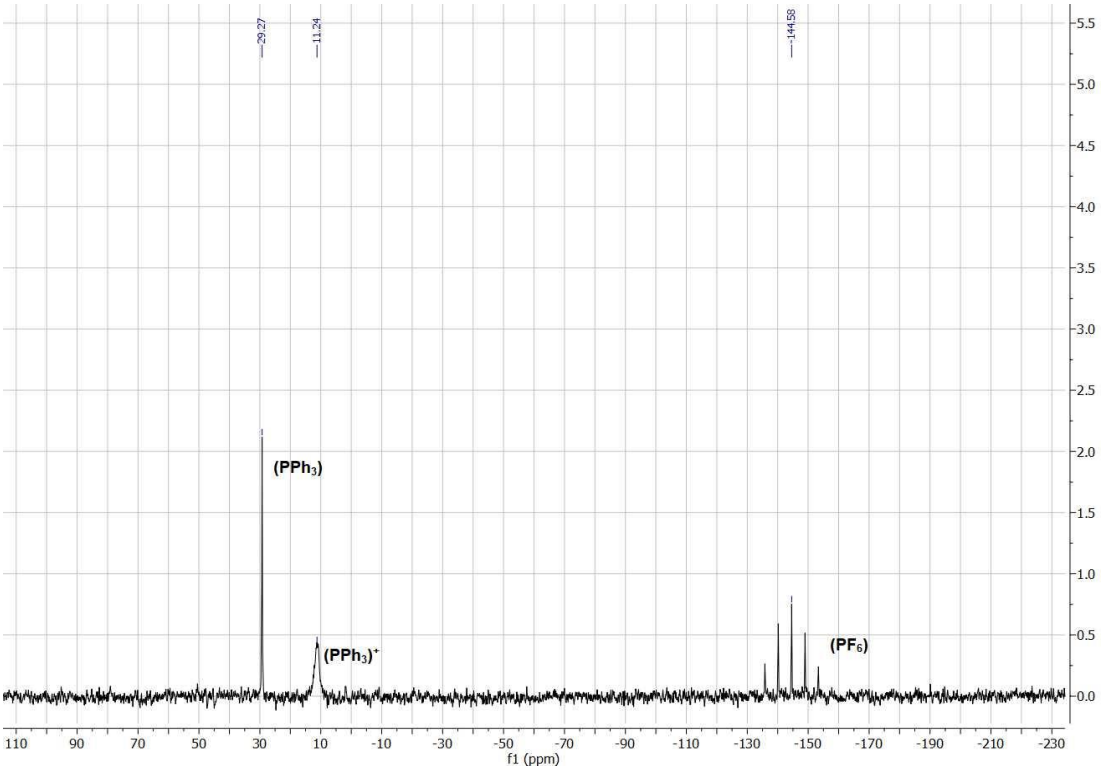

Figure 6.2.20: ^{13}P NMR spectrum of $[Tc^{I}(NO)(Cp)(PPh_3)\{C(OMe)C_2H_4PPh_3\}](PF_6)_2$ in $CDCl_3$.

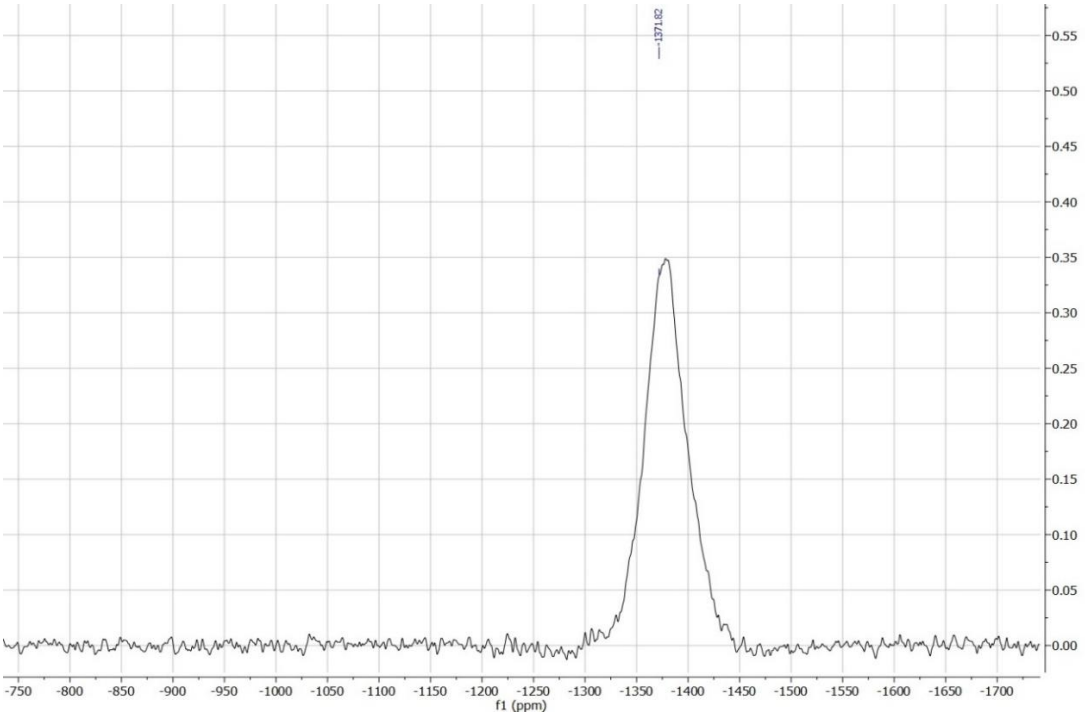

Figure 6.2.21: ^{99}Tc NMR spectrum of $[Tc^{I}(NO)(Cp)(PPh_3)\{C(OMe)C_2H_4PPh_3\}](PF_6)_2$ in $CDCl_3$.

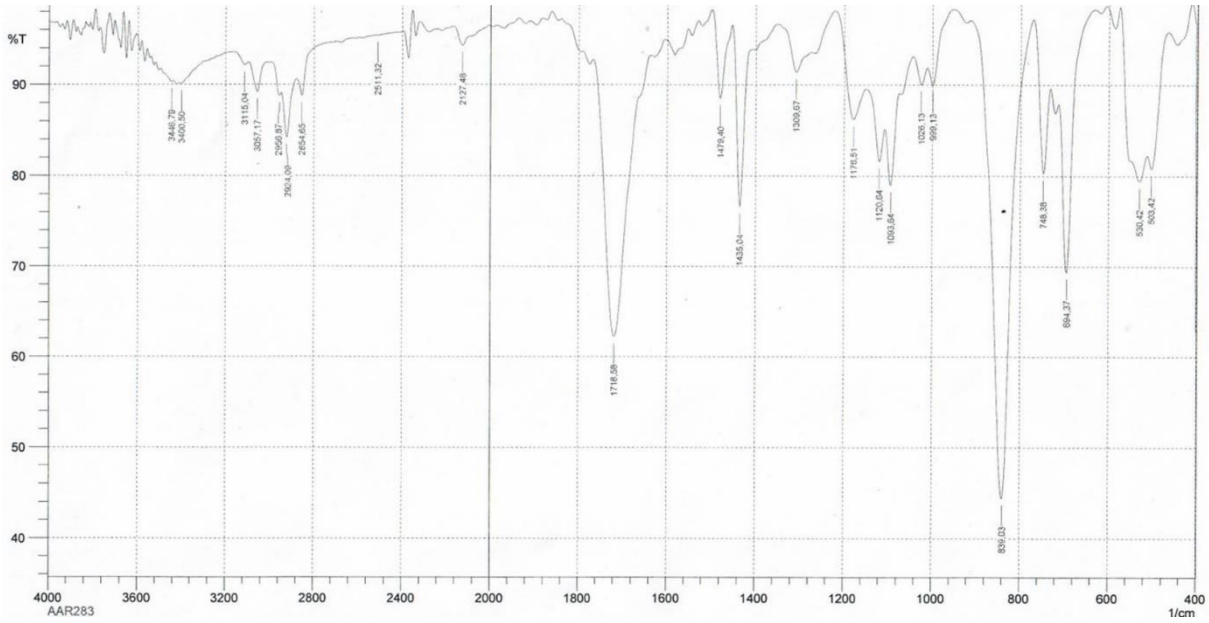

Figure 6.2.22: IR spectrum of $[Tc^{I}(NO)(Cp)(PPh_3)\{C(OMe)C_2H_4PPh_3\}](PF_6)_2$.

6.2.7 Spectroscopic data of $[Tc^{I}(NO)(Cp)(PPh_3)(CH_3CN)](PF_6)$

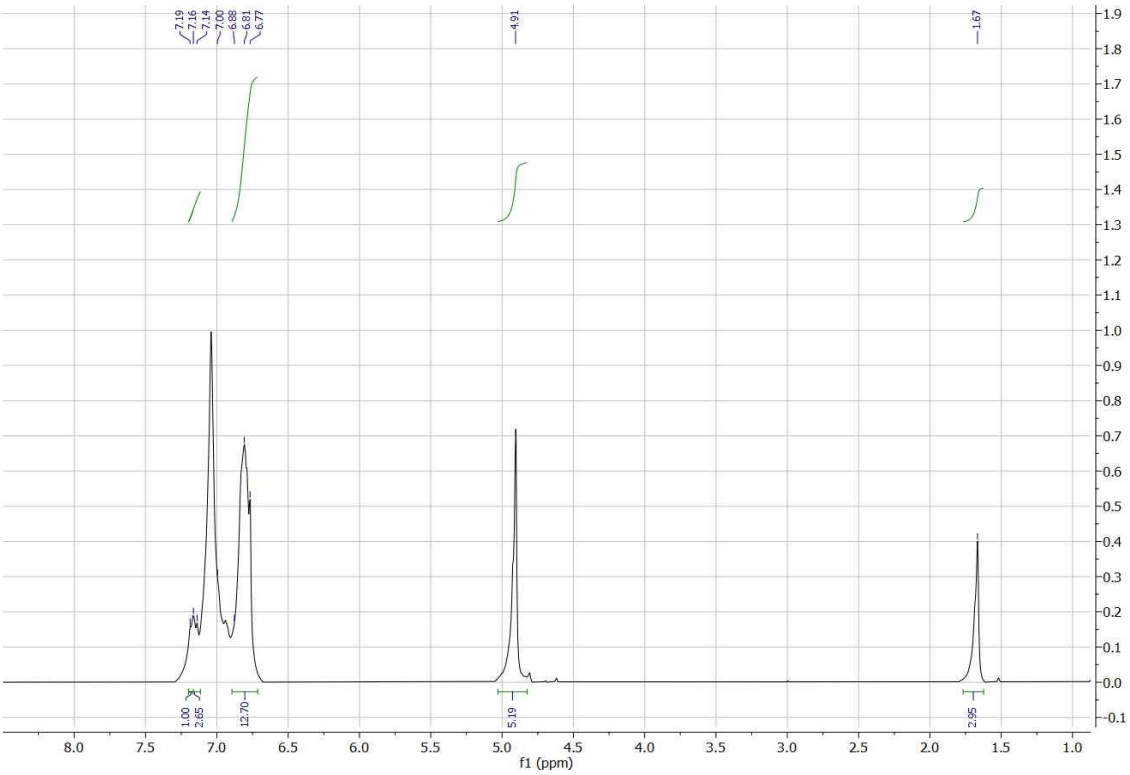

Figure 6.2.23: ^{1}H NMR spectrum of $[Tc^{I}(NO)(Cp)(PPh_3)(CH_3CN)](PF_6)$ in $CDCl_3$.

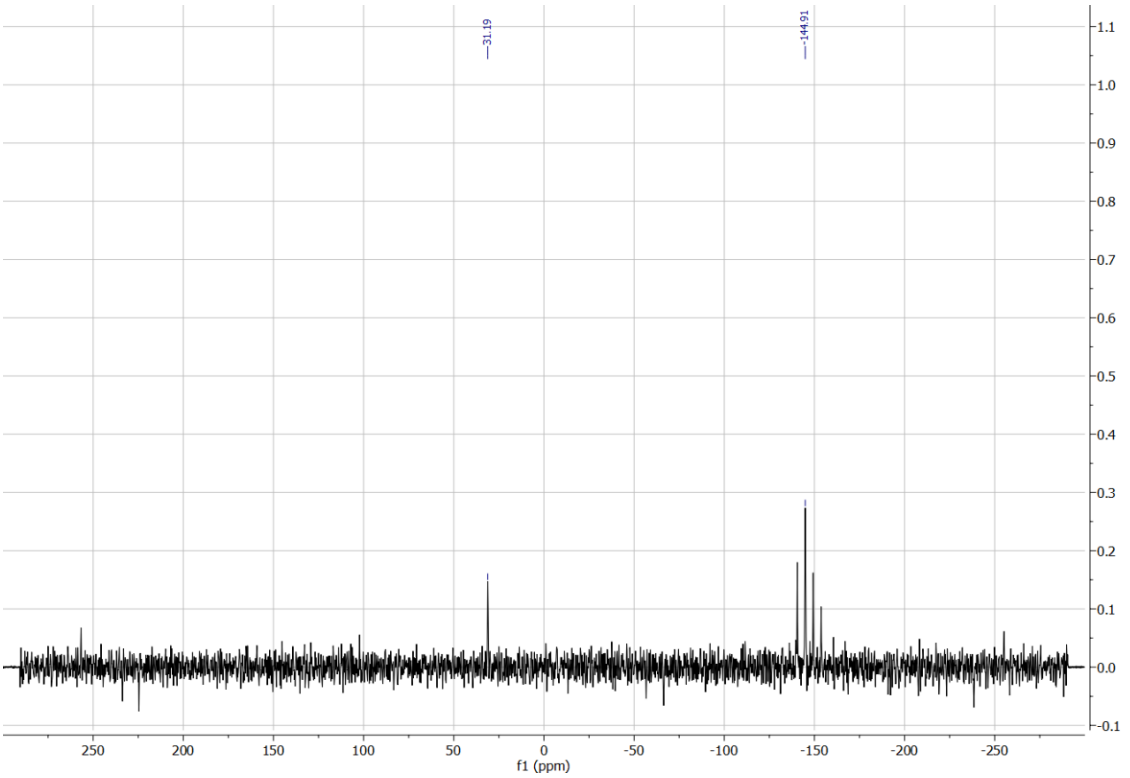

Figure 6.2.24: ^{31}P NMR spectrum of $[Tc^{I}(NO)(Cp)(PPh_3)(CH_3CN)](PF_6)$ in $CDCl_3$.

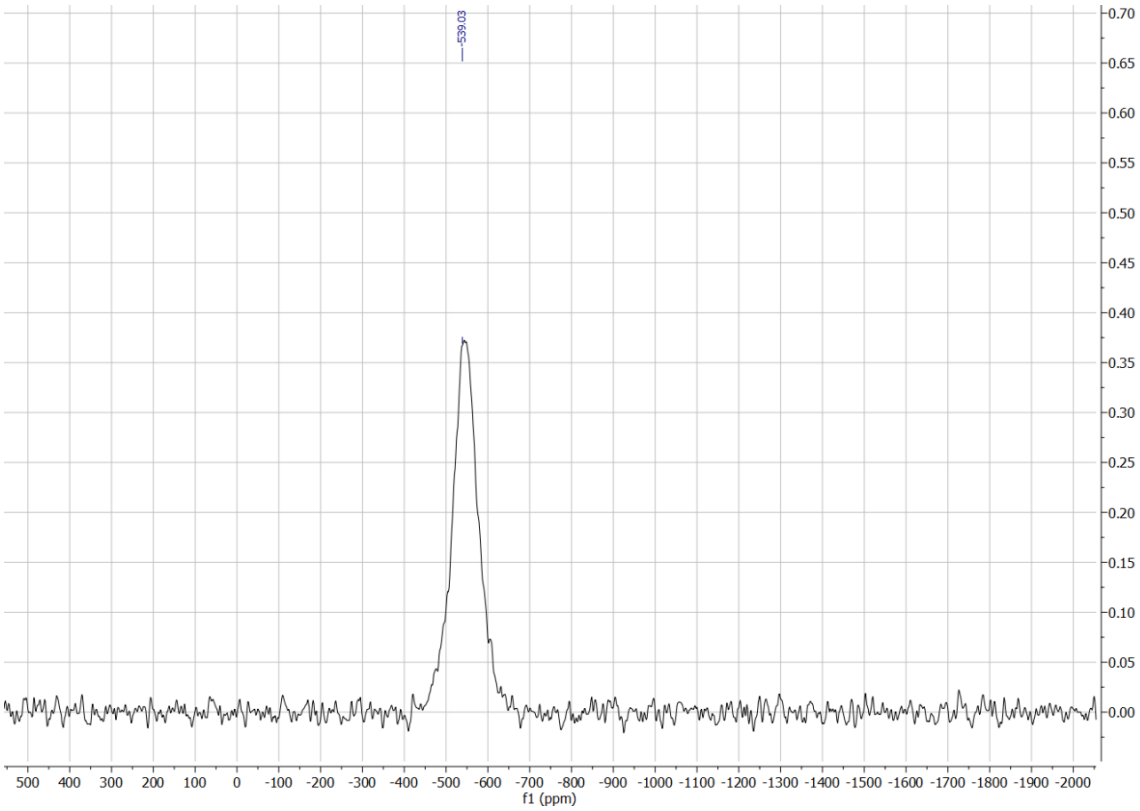

Figure 6.2.25: ^{99}Tc NMR spectrum of [Tc^{I}(NO)(Cp)(PPh$_3$)(CH$_3$CN)](PF$_6$) in CDCl$_3$.

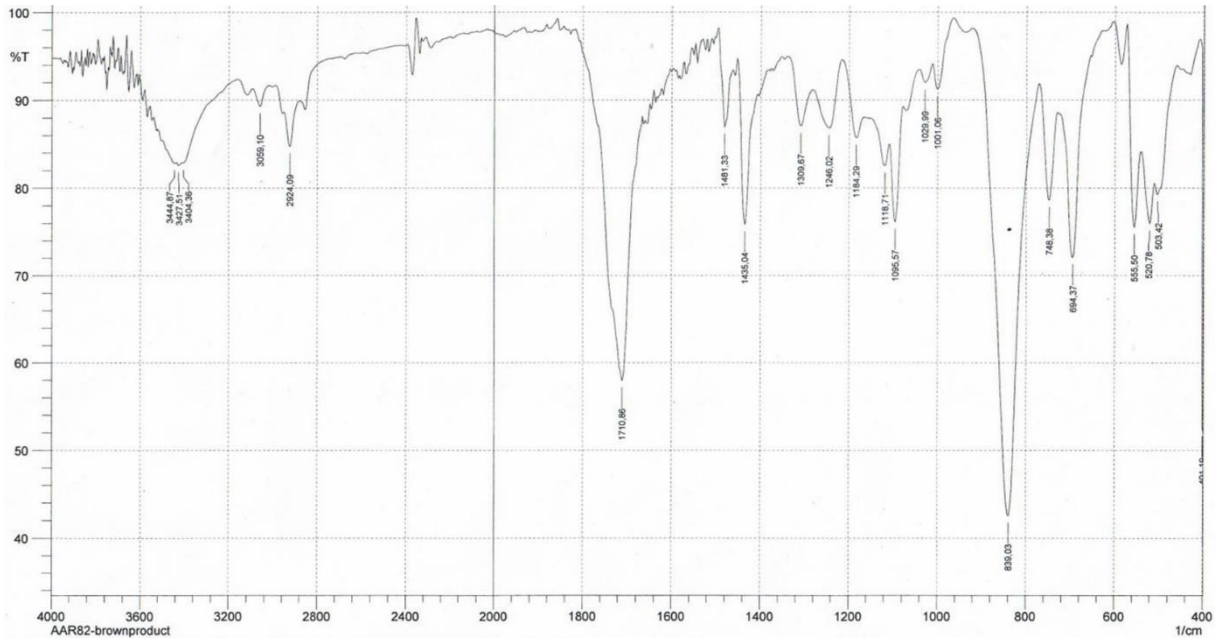

Figure 6.2.26: IR spectrum of [Tc^{I}(NO)(Cp)(PPh$_3$)(CH$_3$CN)](PF$_6$).

6.2.8 Spectroscopic data of $[Tc^{I}(NO)(Cp)(PPh_3)(Py)](PF_6)$

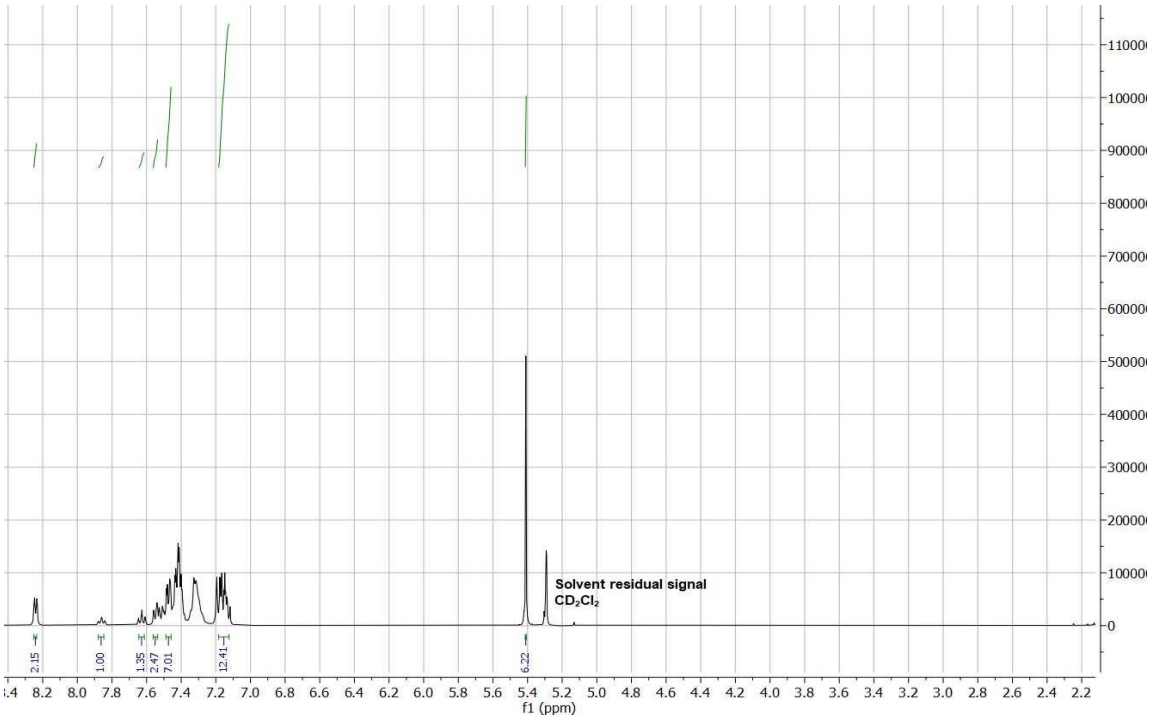

Figure 6.2.27: ^{1}H NMR spectrum of $[Tc^{I}(NO)(Cp)(PPh_3)(Py)](PF_6)$ in $CDCl_3$.

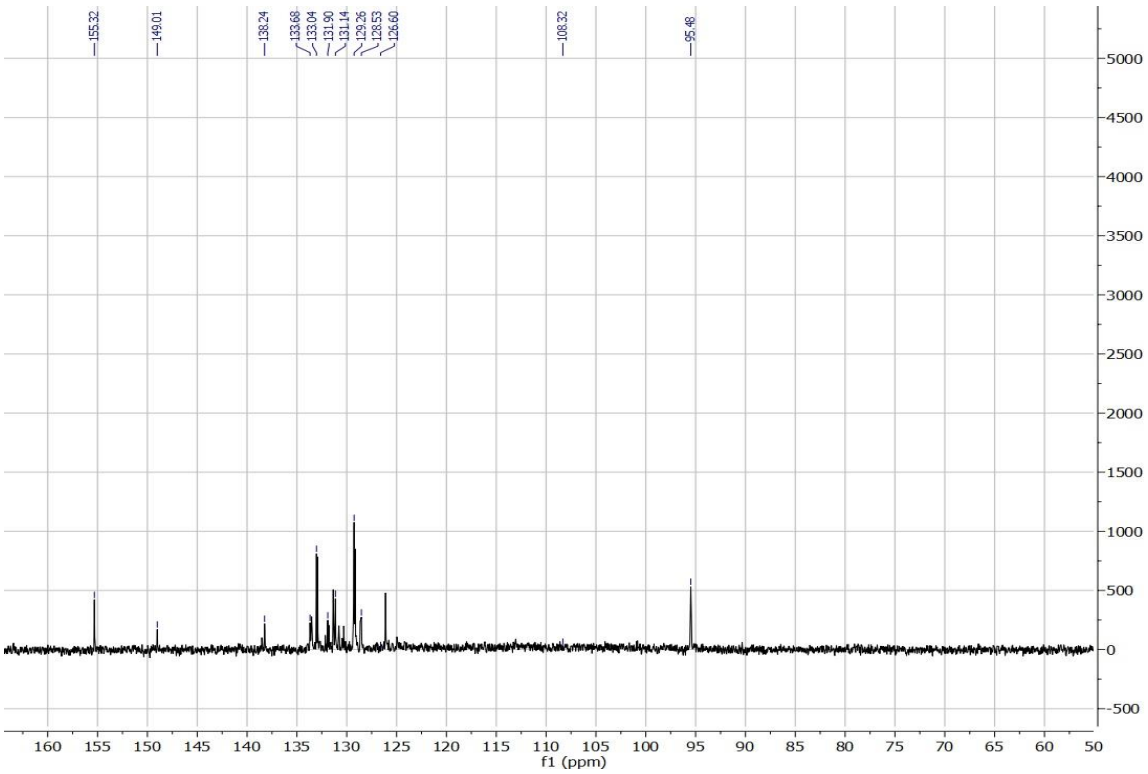

Figure 6.2.28: ^{13}C NMR spectrum of $[Tc^{I}(NO)(Cp)(PPh_3)(Py)](PF_6)$ in $CDCl_3$.

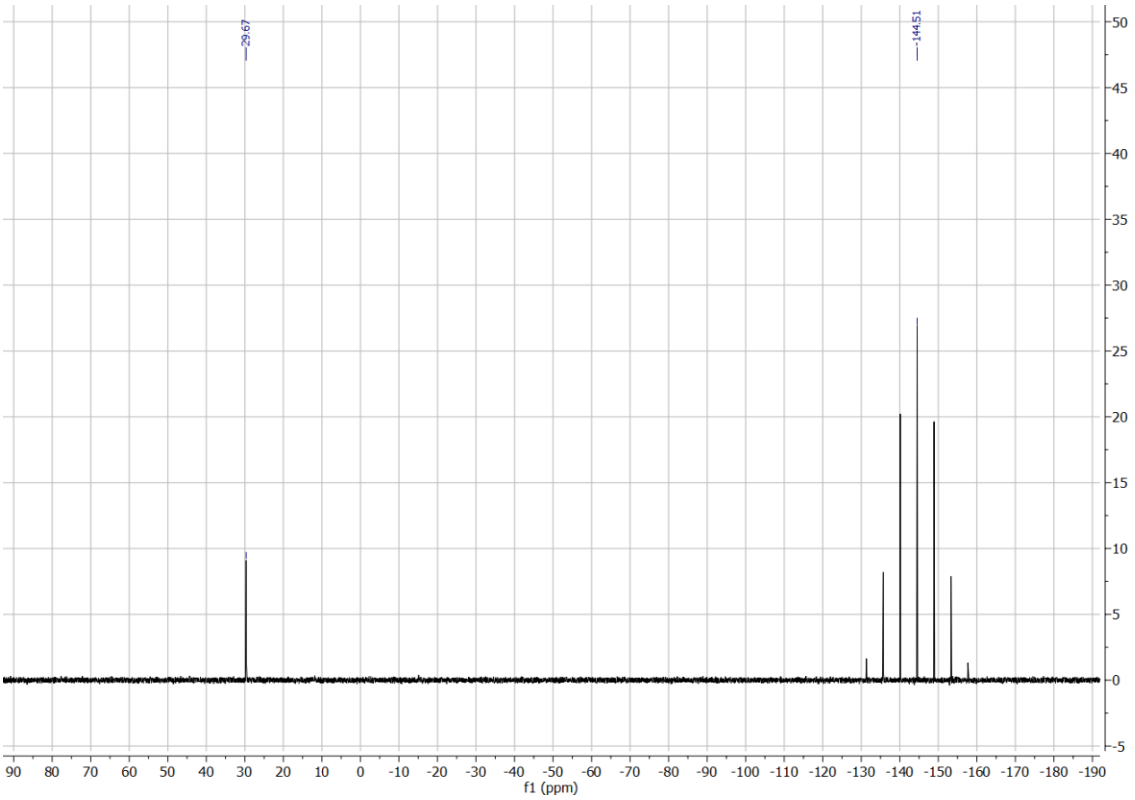

Figure 6.2.29: ^{31}P NMR spectrum of [Tc^{I}(NO)(Cp)(PPh$_3$)(Py)](PF$_6$) in CDCl$_3$.

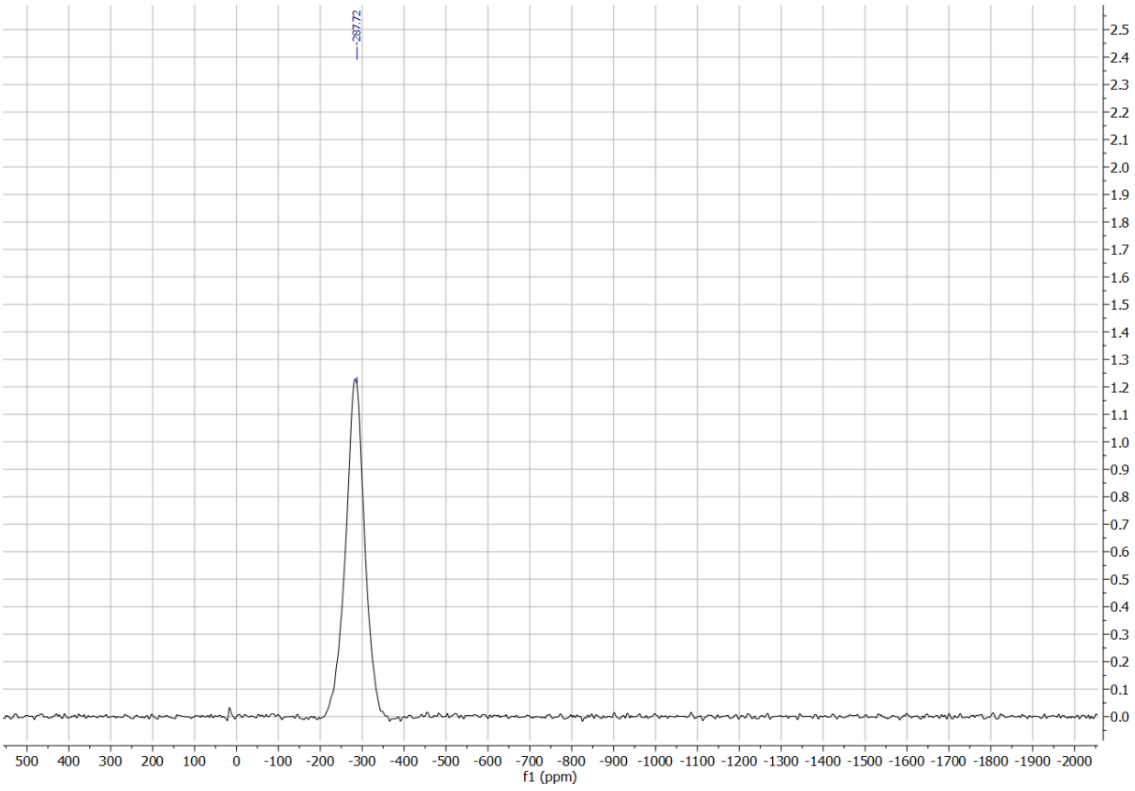

Figure 6.2.30: ^{99}Tc NMR spectrum of [Tc^{I}(NO)(Cp)(PPh$_3$)(Py)](PF$_6$) in CDCl$_3$.

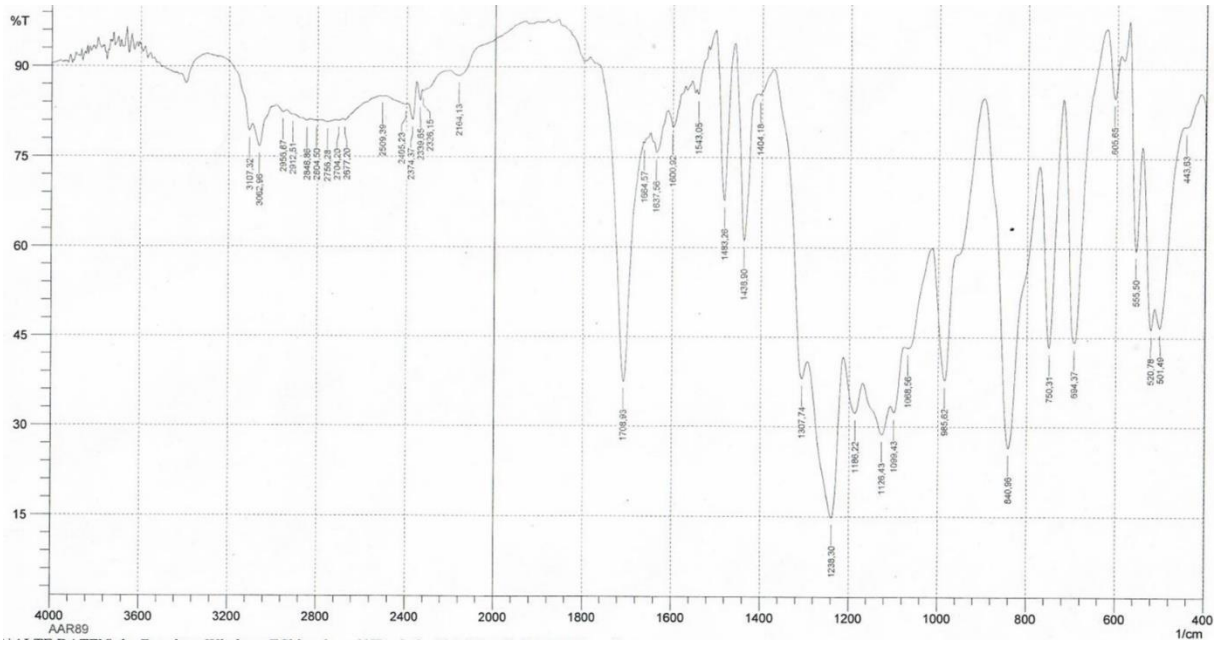

Figure 6.2.31: IR spectrum of $[Tc^{I}(NO)(Cp)(PPh_3)(Py)](PF_6)$.

6.2.9 Spectroscopic data of $[Tc^{I}(NO)(Cp)(PPh_3)(thioxane)](PF_6)$

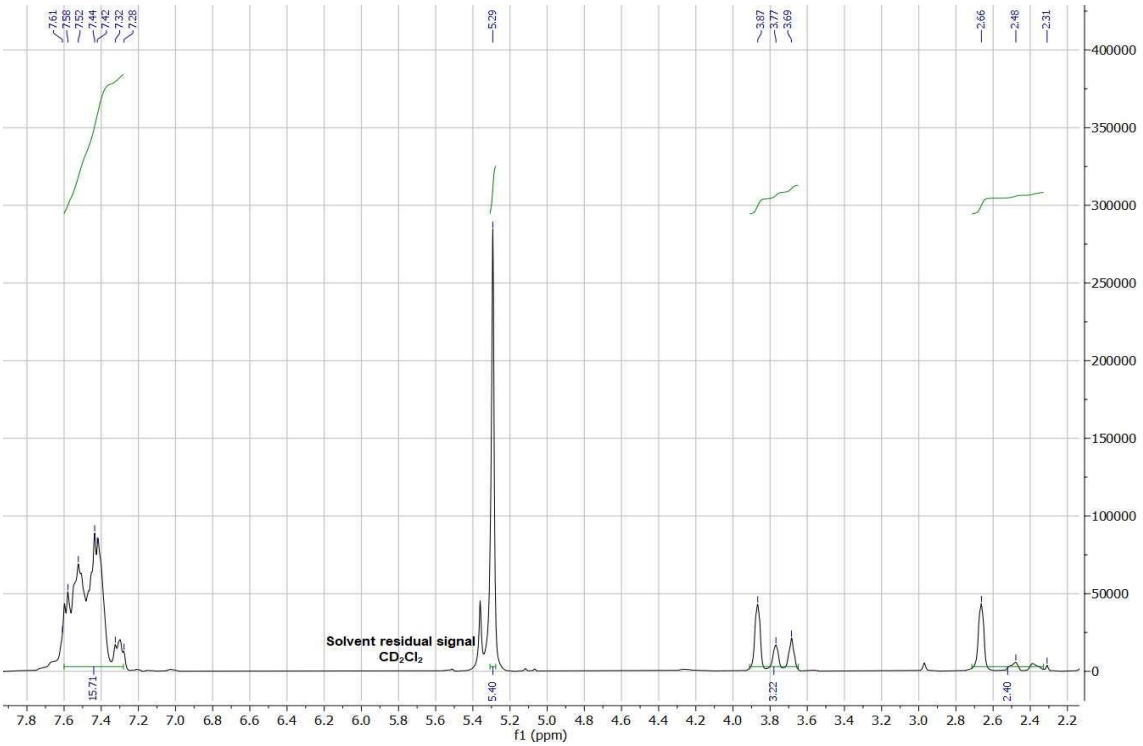

Figure 6.2.32: ^{1}H NMR spectrum of $[Tc^{I}(NO)(Cp)(PPh_3)(thioxane)](PF_6)$ in $CDCl_3$.

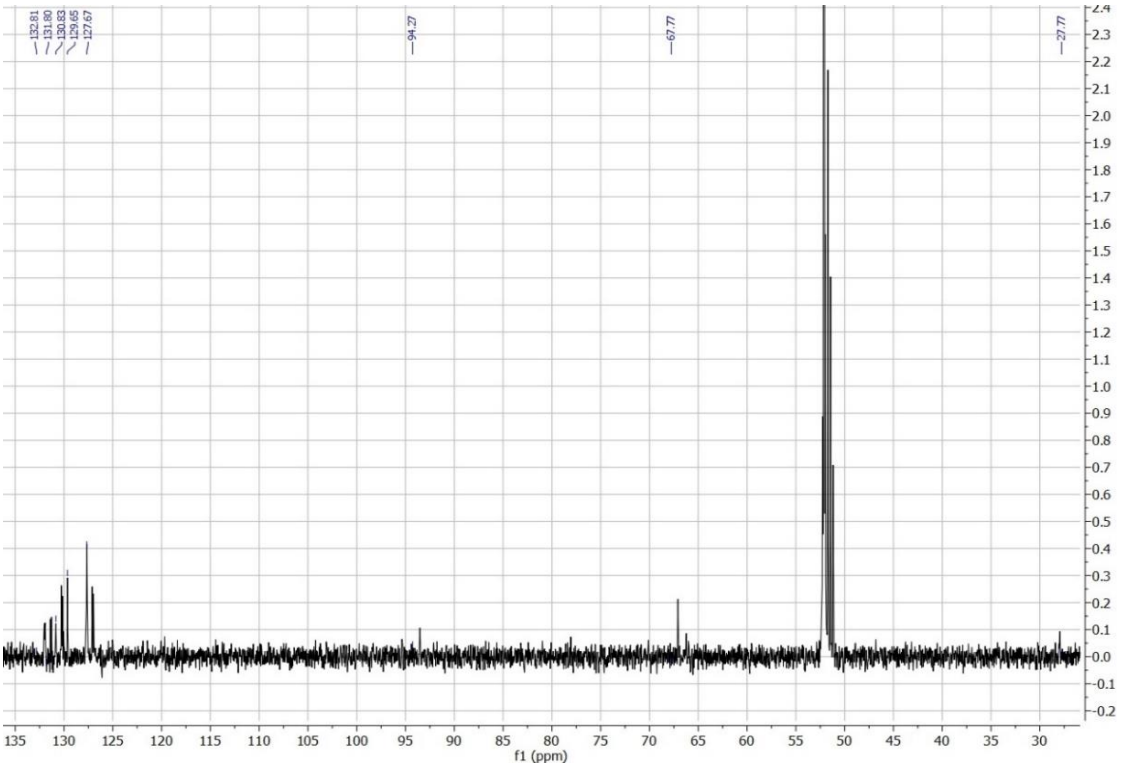

Figure 6.2.33: ^{13}C NMR spectrum of $[Tc^{I}(NO)(Cp)(PPh_3)(thioxane)](PF_6)$ in $CDCl_3$.

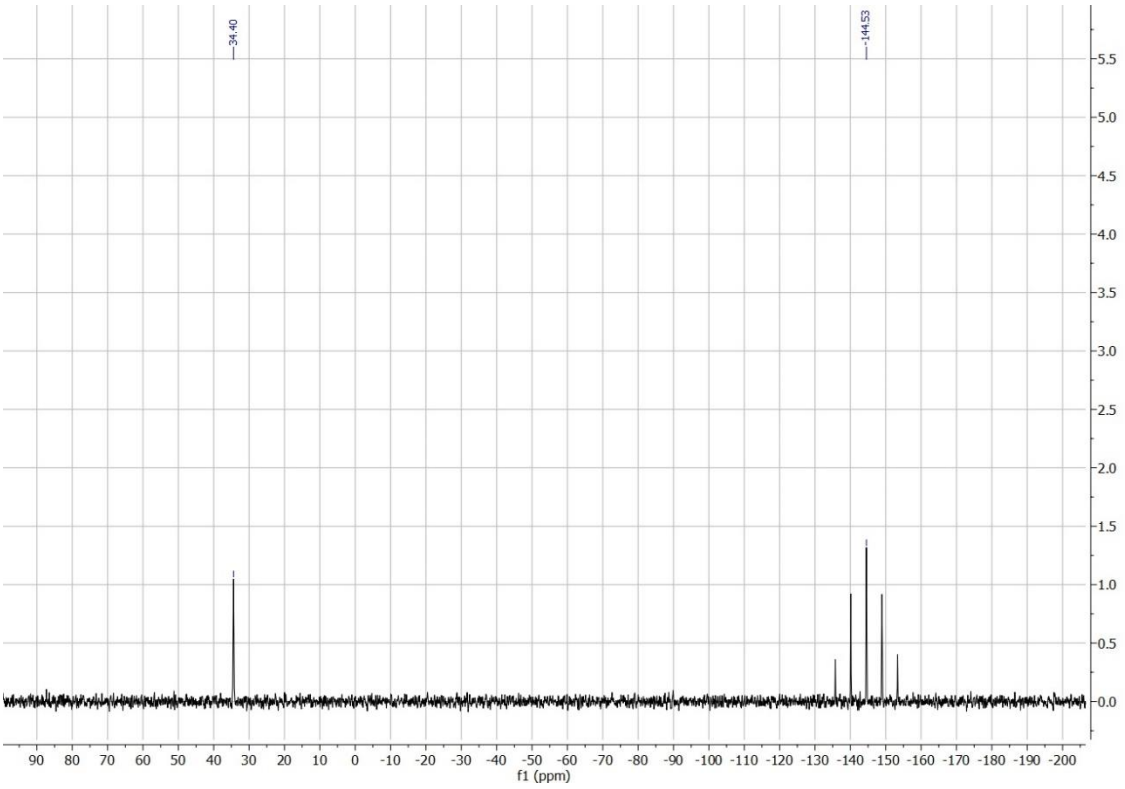

Figure 6.2.34: ^{31}P NMR spectrum of $[Tc^{I}(NO)(Cp)(PPh_3)(thioxane)](PF_6)$ in $CDCl_3$.

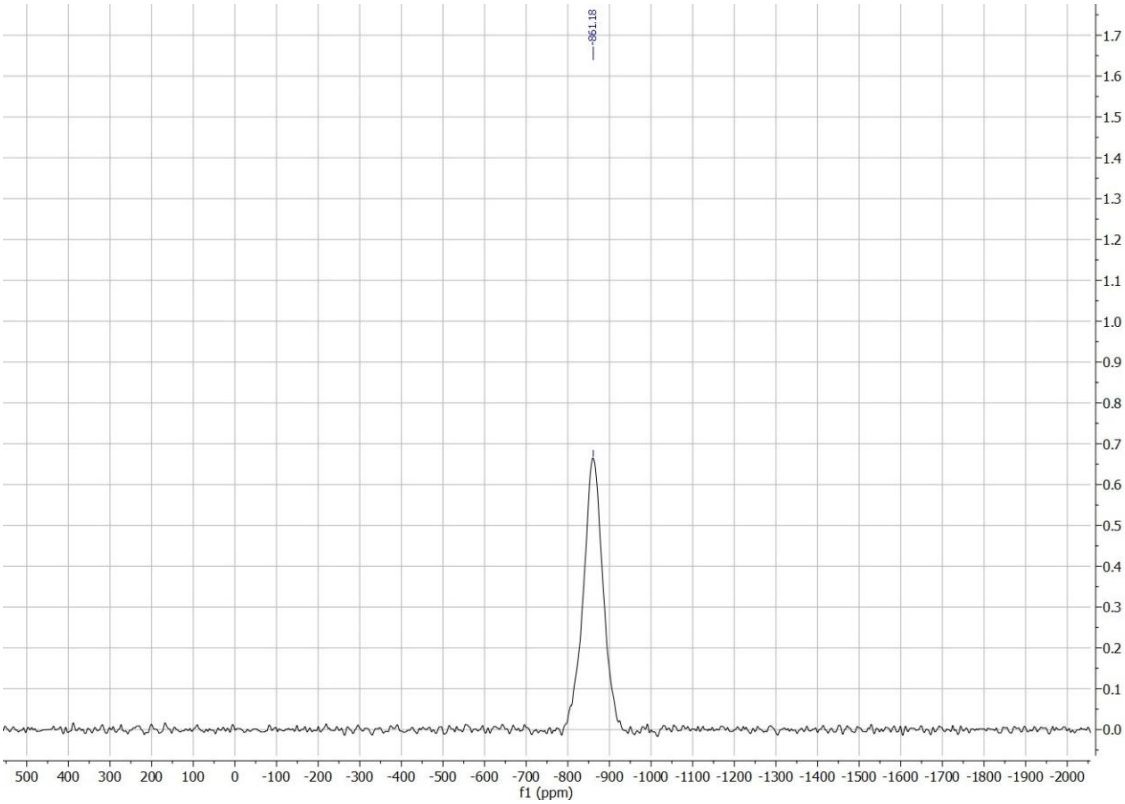

Figure 6.2.35: ^{99}Tc NMR spectrum of $[Tc^{I}(NO)(Cp)(PPh_3)(thioxane)](PF_6)$ in $CDCl_3$.

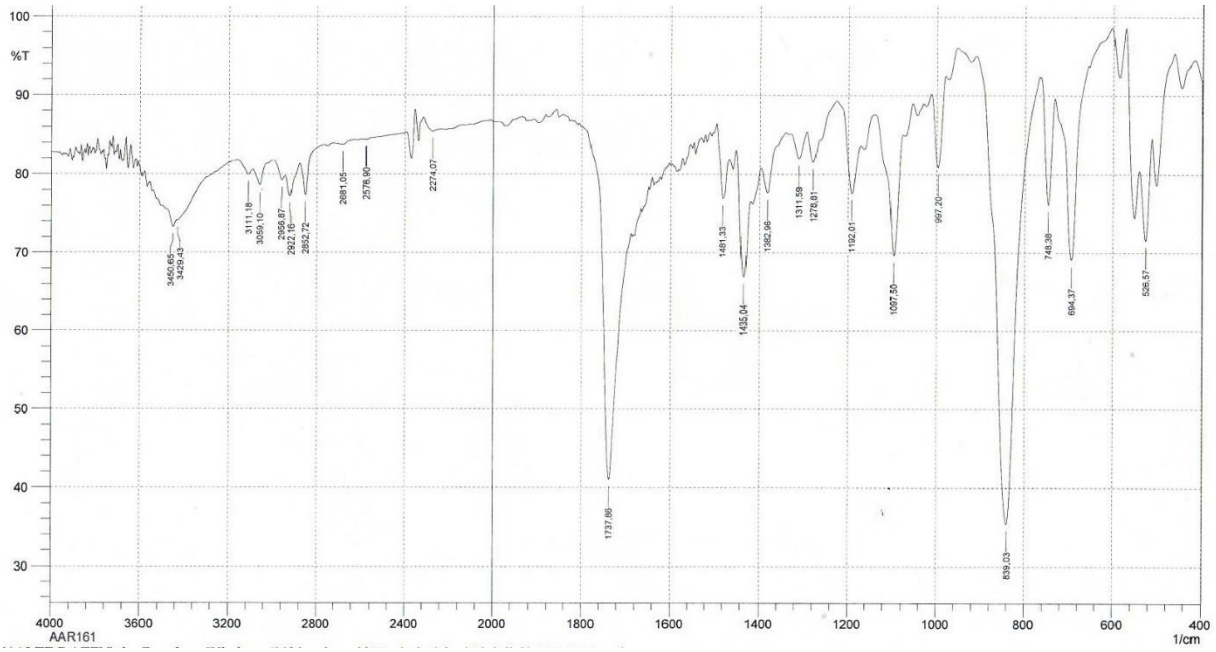

Figure 6.2.36: IR spectrum of $[Tc^{I}(NO)(Cp)(PPh_3)(thioxane)](PF_6)$.

6.2.10 Spectroscopic data of $[Tc^{I}(NO)(Cp)(PPh_3)(OPPh_3)](PF_6)$

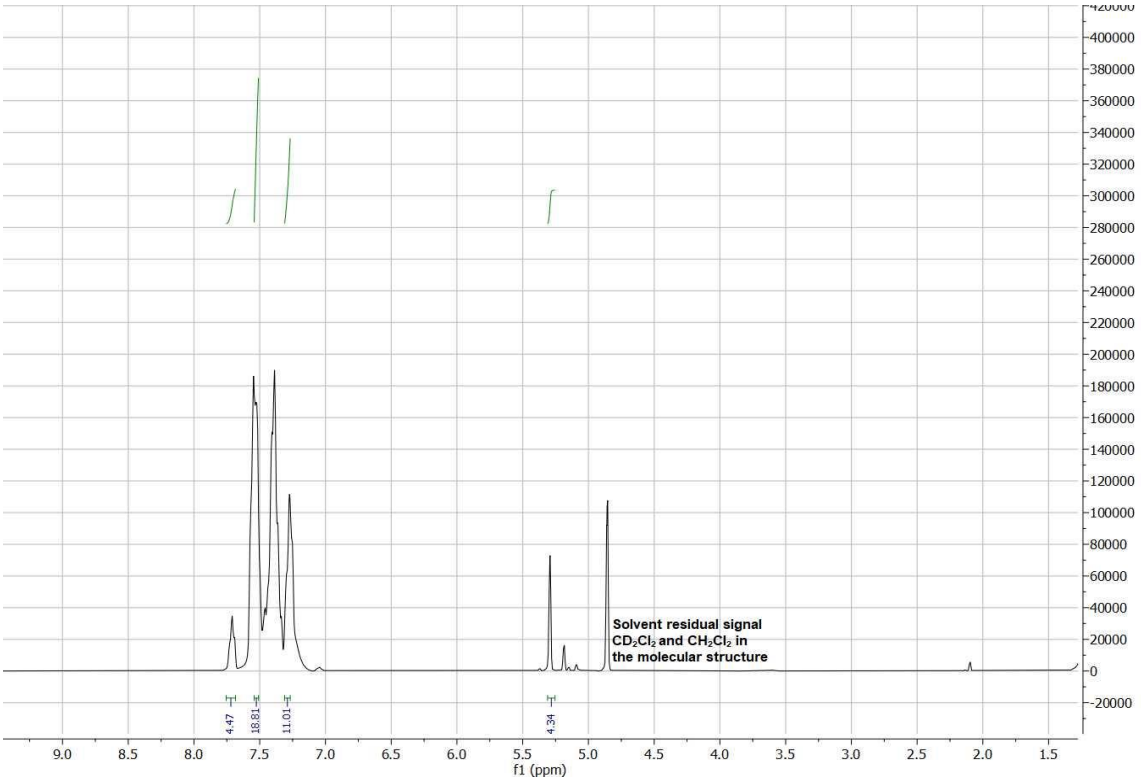

Figure 6.2.37: ^{1}H NMR spectrum of $[Tc^{I}(NO)(Cp)(PPh_3)(OPPh_3)](PF_6)$ in CD_2Cl_2.

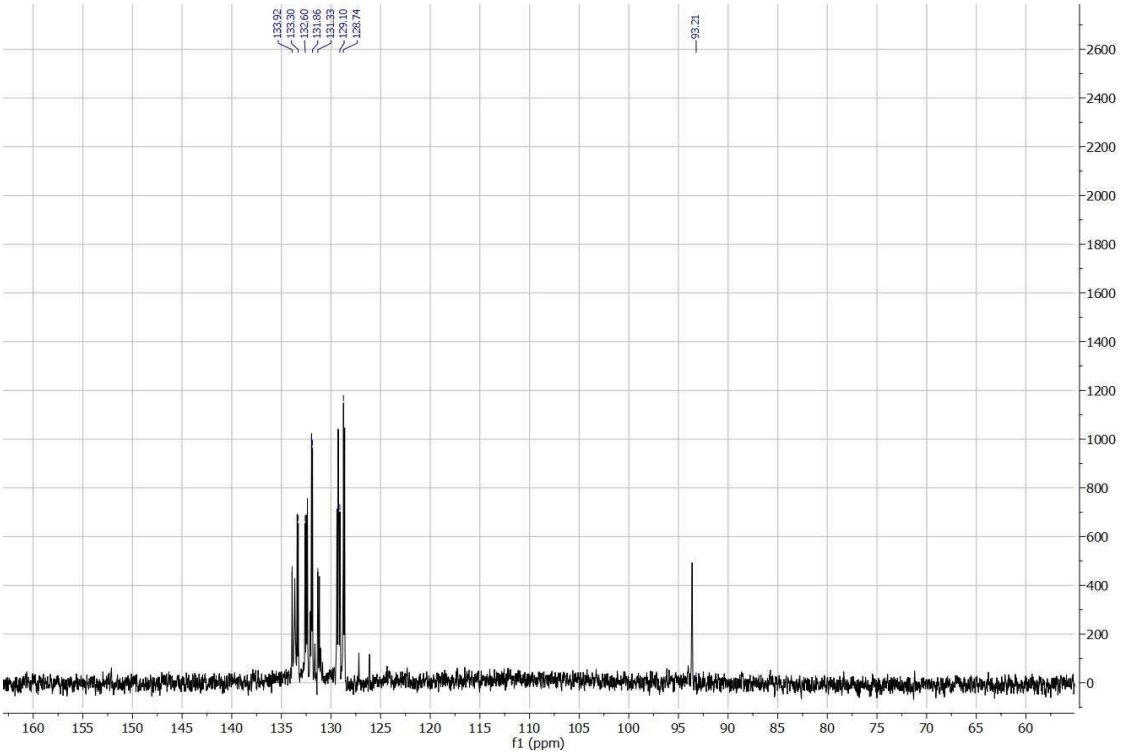

Figure 6.2.38: ^{13}C NMR spectrum of $[Tc^{I}(NO)(Cp)(PPh_3)(OPPh_3)](PF_6)$ in CD_2Cl_2.

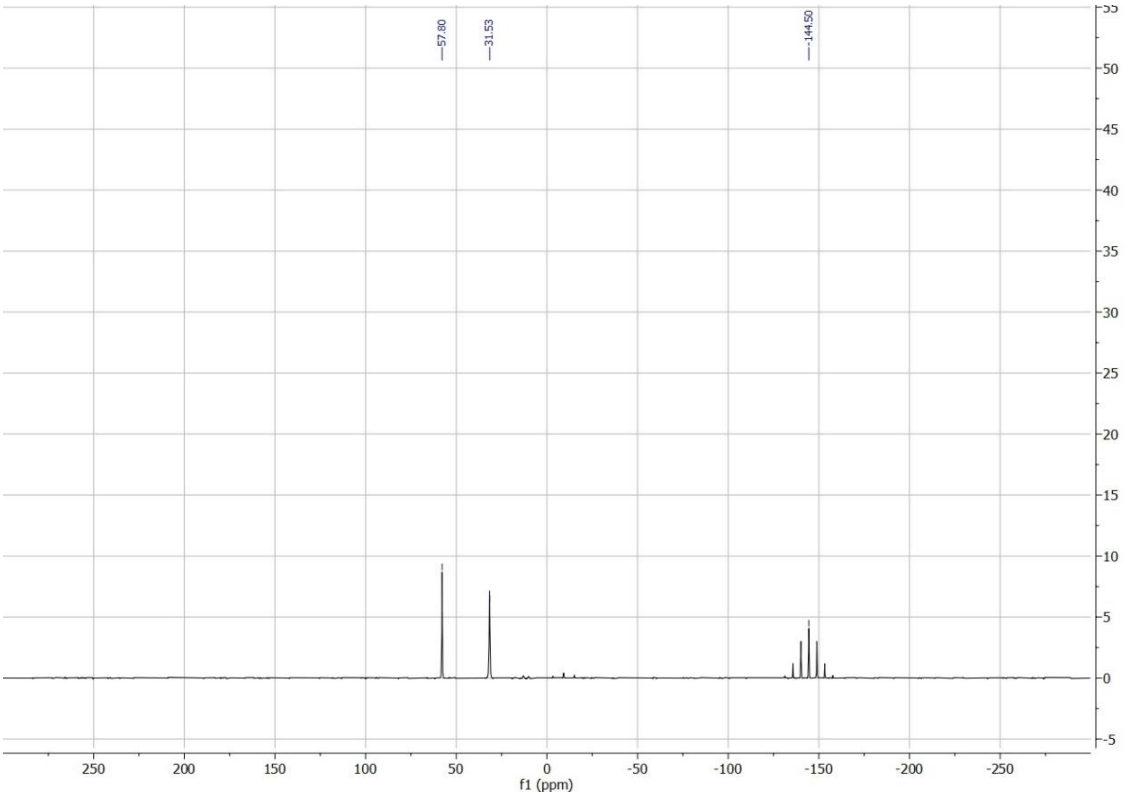

Figure 6.2.39: ^{31}P NMR spectrum of $[Tc^{I}(NO)(Cp)(PPh_3)(OPPh_3)](PF_6)$ in CD_2Cl_2.

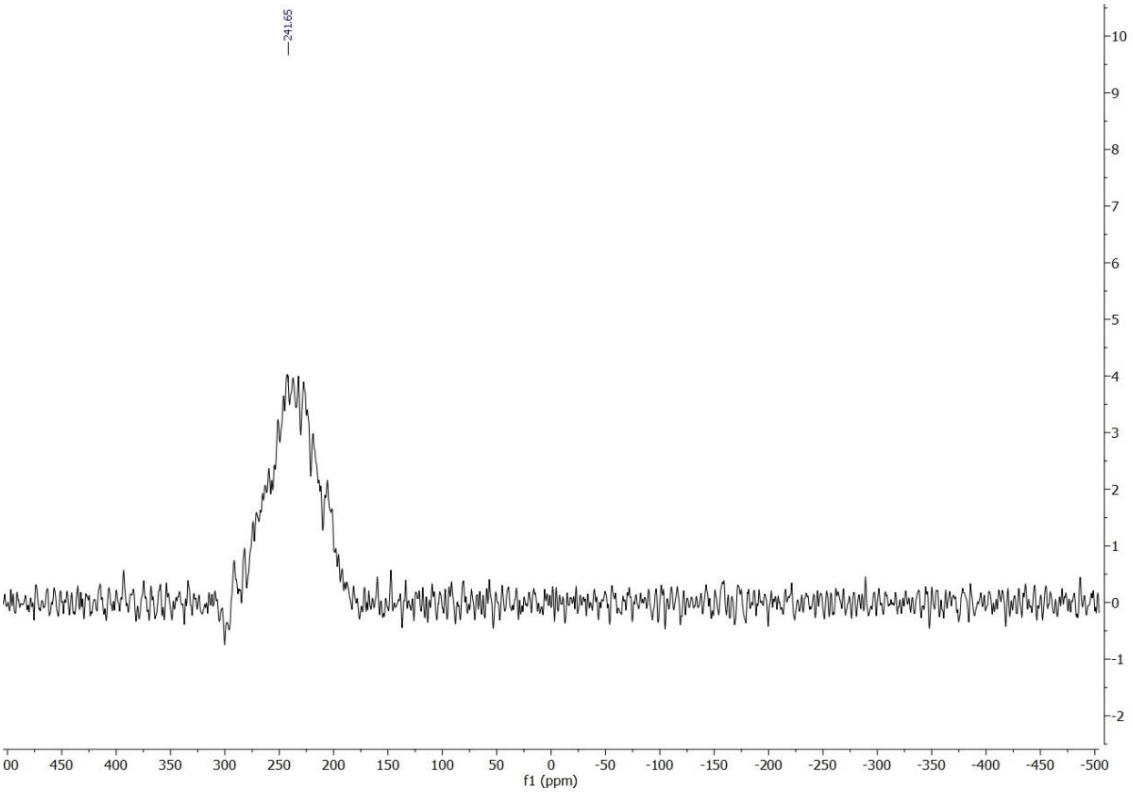

Figure 6.2.40: ^{99}Tc NMR spectrum of $[Tc^{I}(NO)(Cp)(PPh_3)(OPPh_3)](PF_6)$ in CD_2Cl_2.

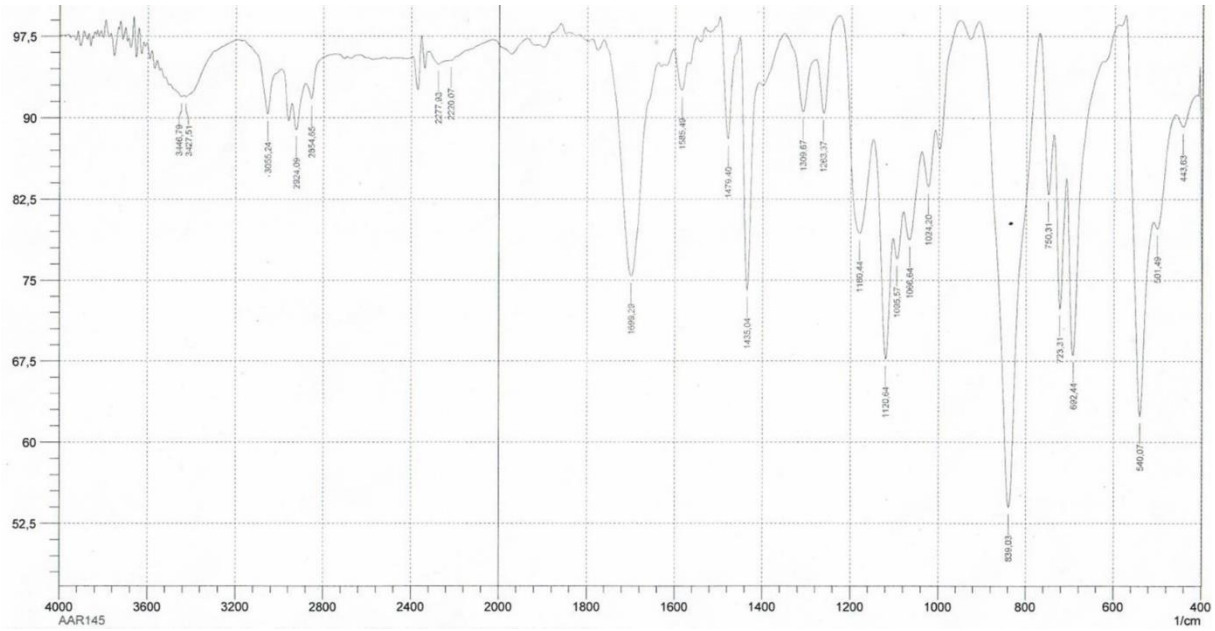

Figure 6.2.41: IR spectrum of $[Tc^{I}(NO)(Cp)(PPh_3)(OPPh_3)](PF_6)$.

6.2.11 Spectroscopic data of $[Tc^{I}(NO)(Cp)(PPh_3)(SPPh_3)](PF_6)$

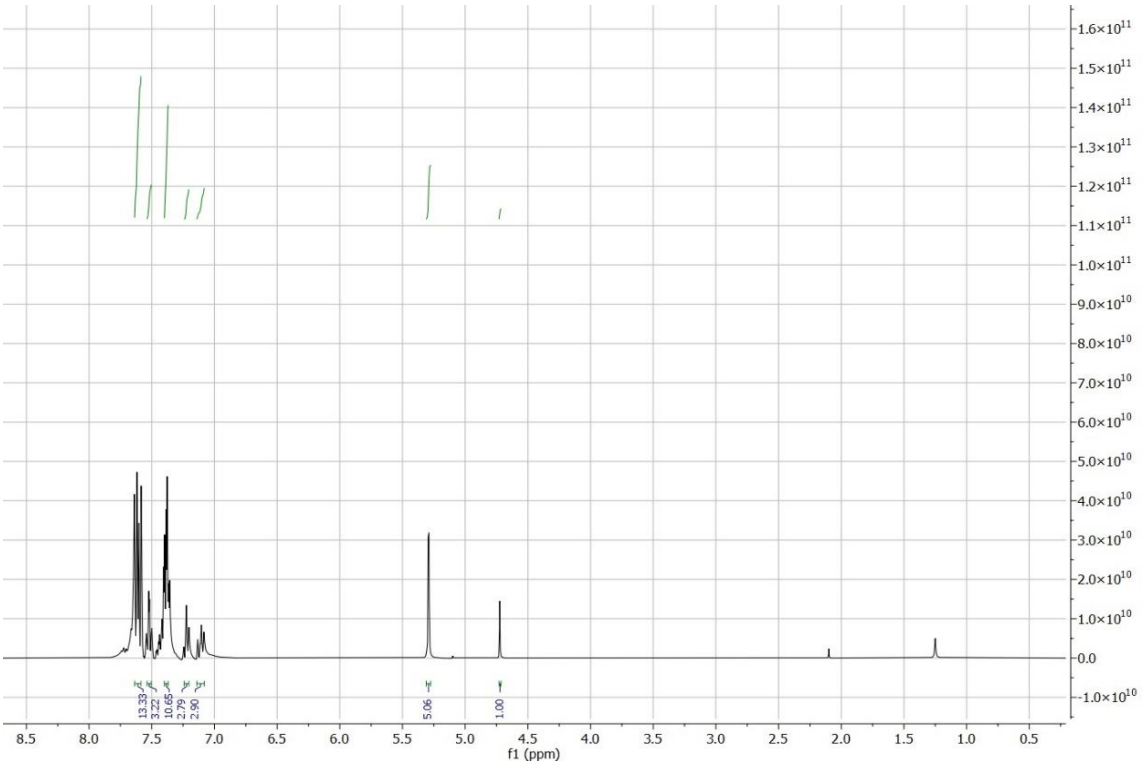

Figure 6.2.42: ^{1}H NMR spectrum of $[Tc^{I}(NO)(Cp)(PPh_3)(SPPh_3)](PF_6)$ in CD_2Cl_2.

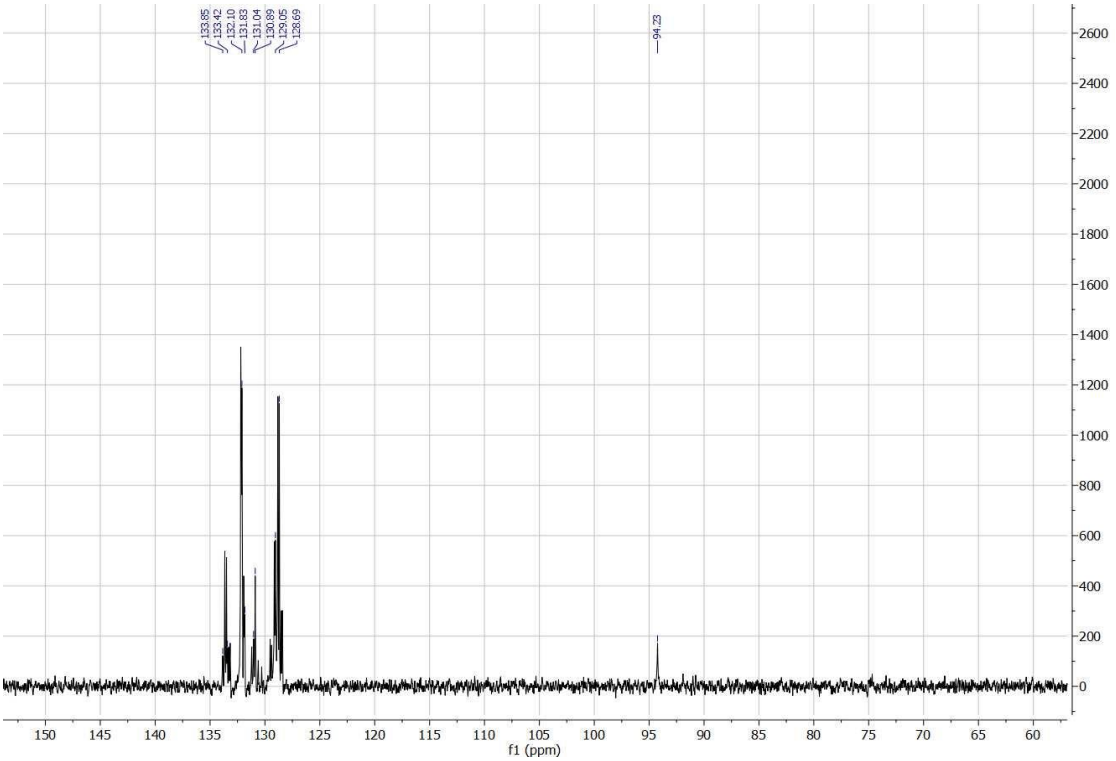

Figure 6.2.43: ^{13}C NMR spectrum of $[Tc^{I}(NO)(Cp)(PPh_3)(SPPh_3)](PF_6)$ in CD_2Cl_2.

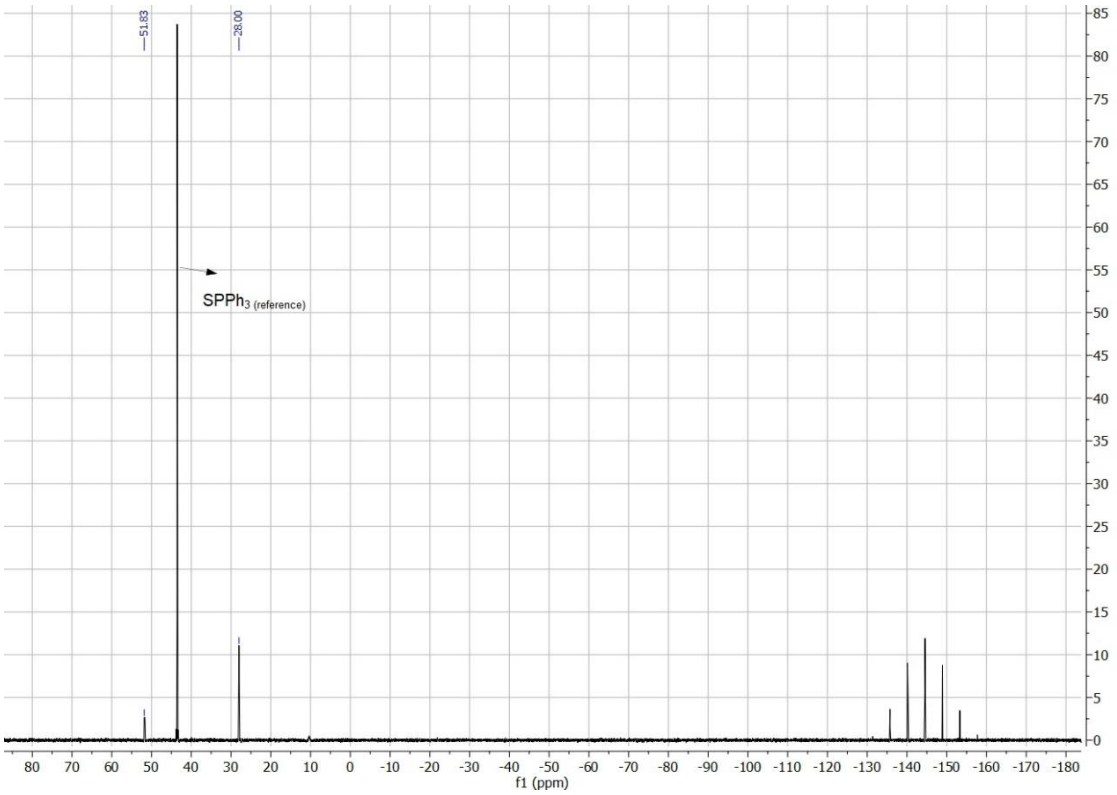

Figure 6.2.44: ^{31}P NMR spectrum of $[Tc^{I}(NO)(Cp)(PPh_3)(SPPh_3)](PF_6)$ in CD_2Cl_2.

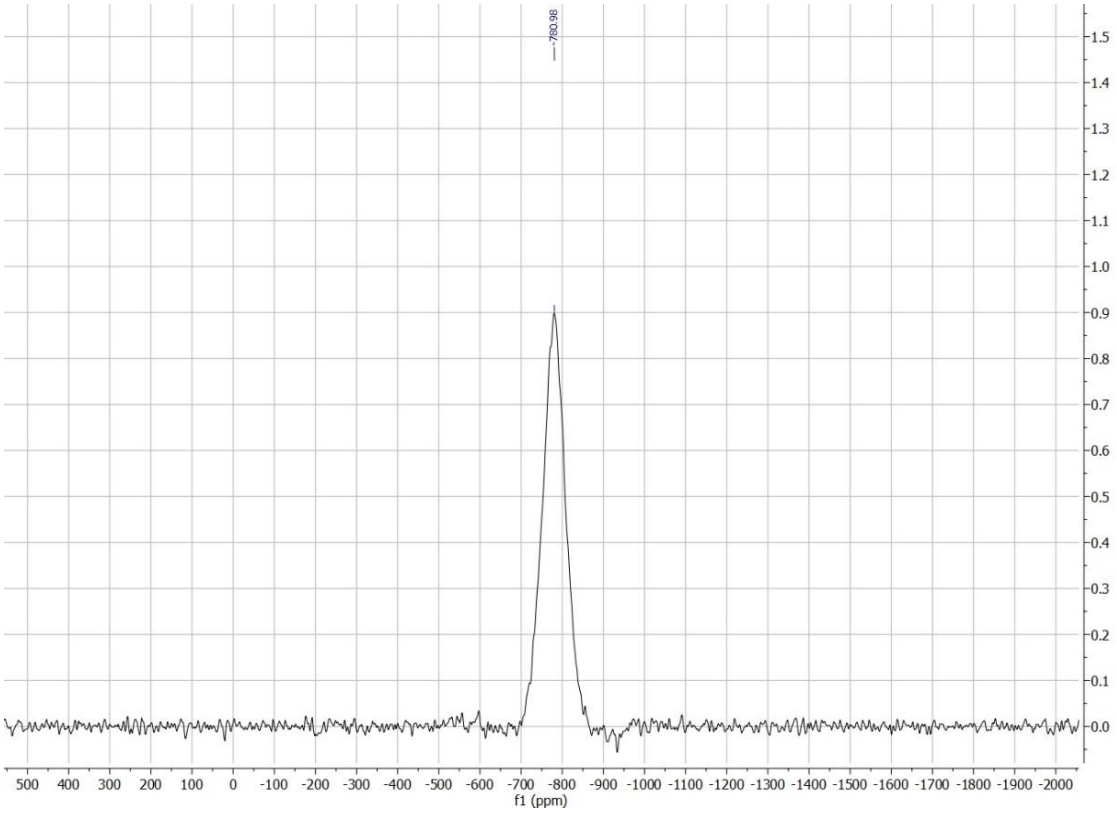

Figure 6.2.45: ^{99}Tc NMR spectrum of $[Tc^{I}(NO)(Cp)(PPh_3)(SPPh_3)](PF_6)$ in CD_2Cl_2.

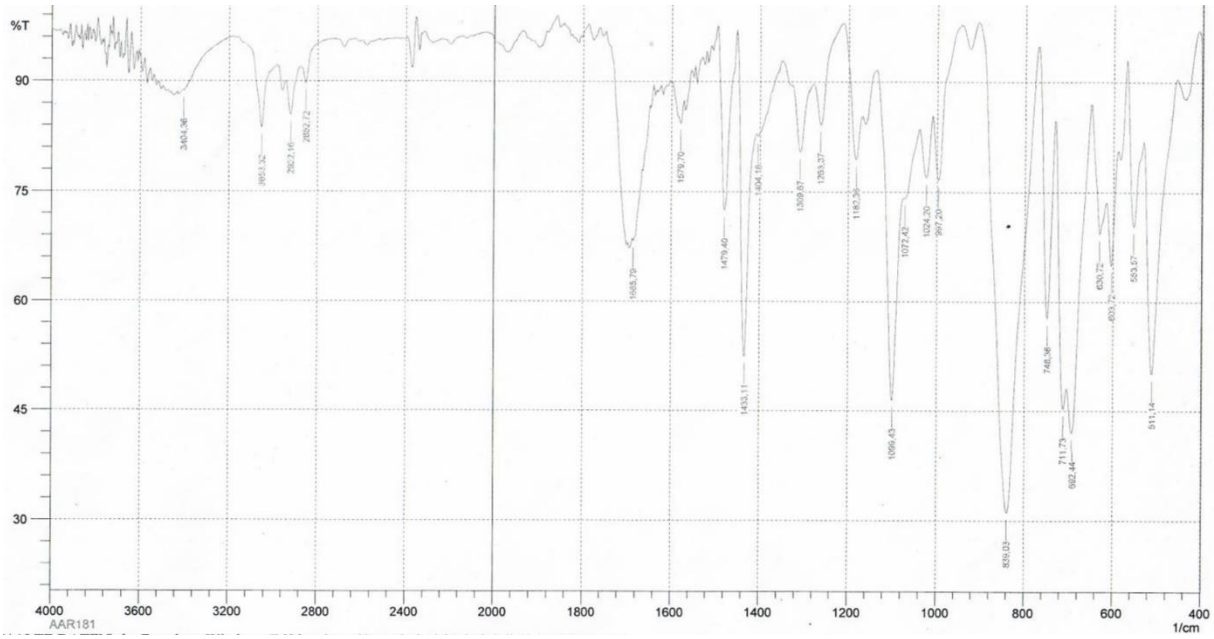

Figure 6.2.46: IR spectrum of $[Tc^{I}(NO)(Cp)(PPh_3)(SPPh_3)](PF_6)$.

6.2.12 Spectroscopic data of $[Tc^{I}(NO)(Cp)(PPh_3)(SePPh_3)](PF_6)$

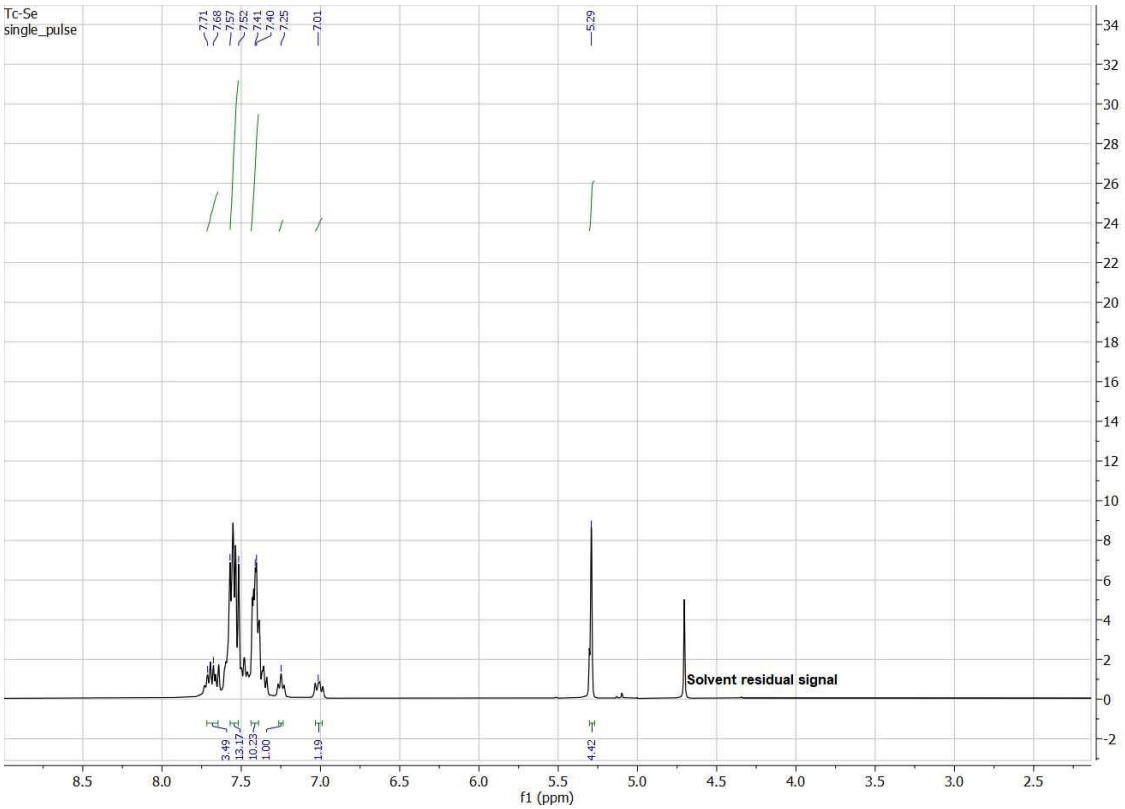

Figure 6.2.47: ^{1}H NMR spectrum of $[Tc^{I}(NO)(Cp)(PPh_3)(SePPh_3)](PF_6)$ in CD_2Cl_2.

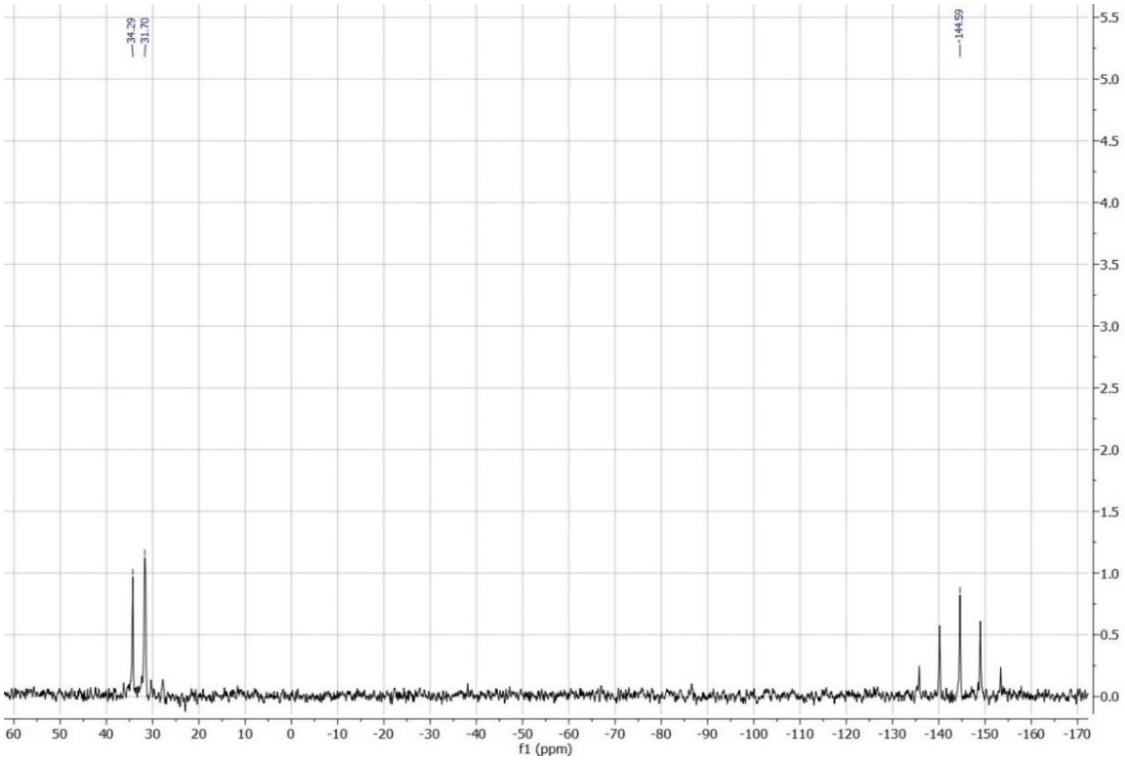

Figure 6.2.48: ^{31}P NMR spectrum of $[Tc^{I}(NO)(Cp)(PPh_3)(SePPh_3)](PF_6)$ in CD_2Cl_2.

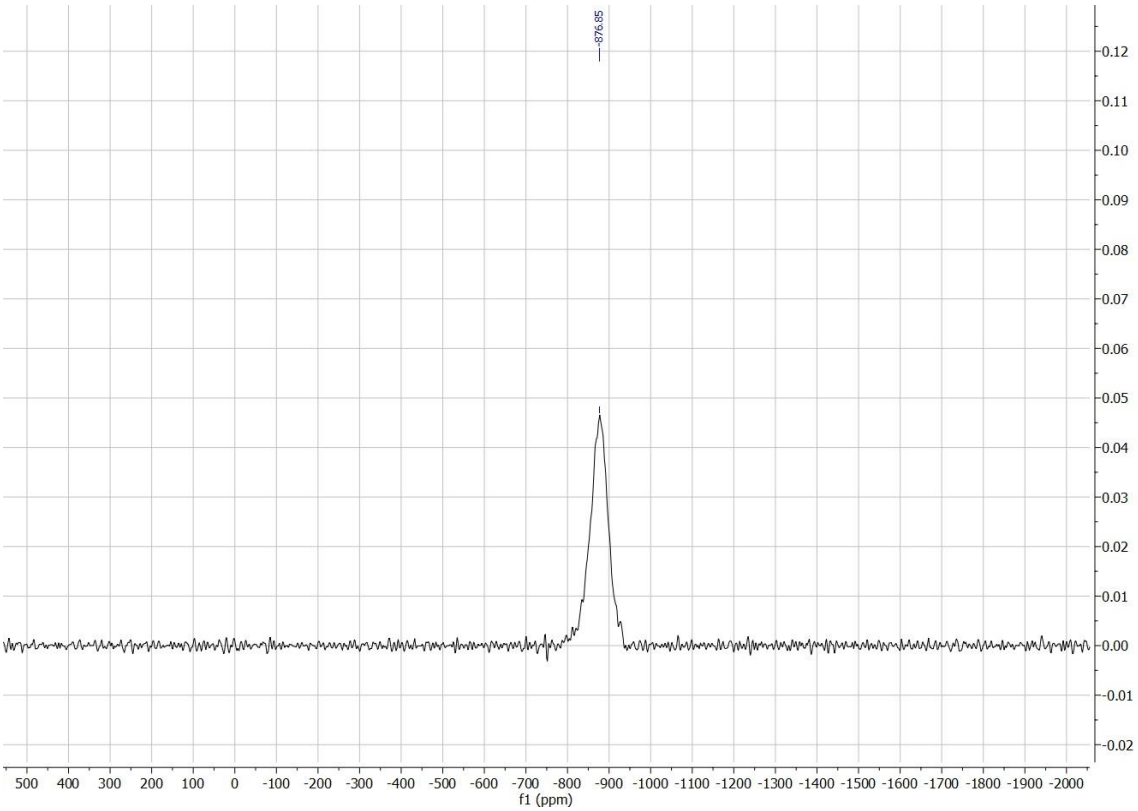

Figure 6.2.49: ^{99}Tc NMR spectrum of $[Tc^{I}(NO)(Cp)(PPh_3)(SePPh_3)](PF_6)$ in CD_2Cl_2.

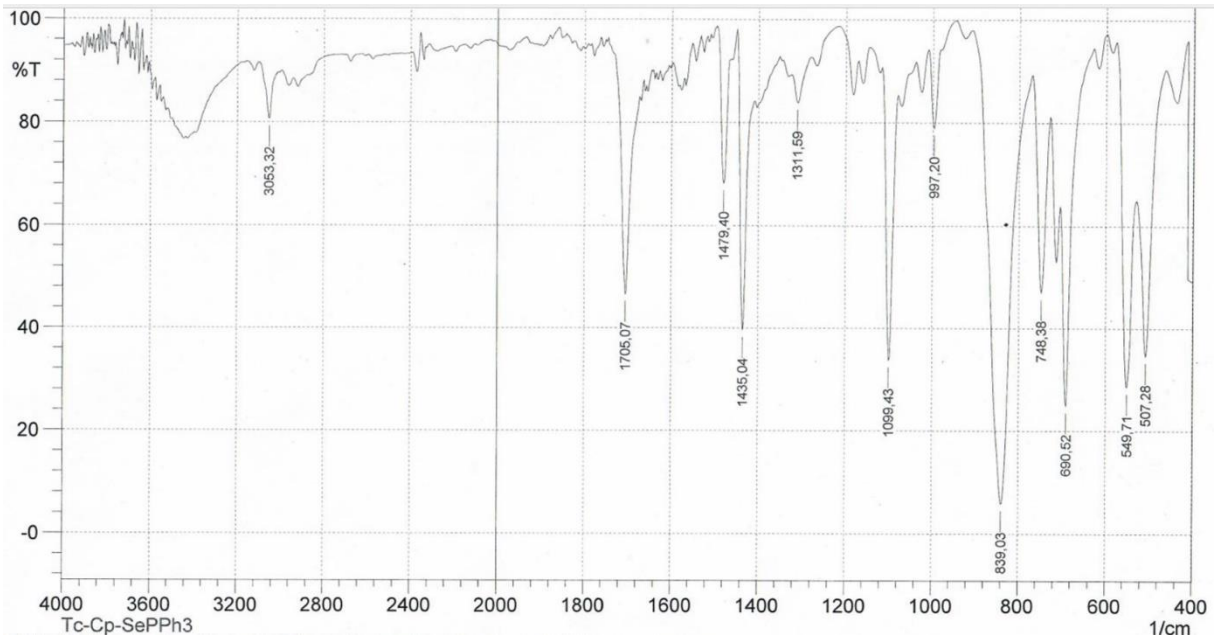

Figure 6.2.50: IR spectrum of $[Tc^{I}(NO)(Cp)(PPh_3)(SePPh_3)](PF_6)$.

6.2.13 Spectroscopic Data of [Tc^{I}(NO)Cl(CpMe)(PPh_3)]

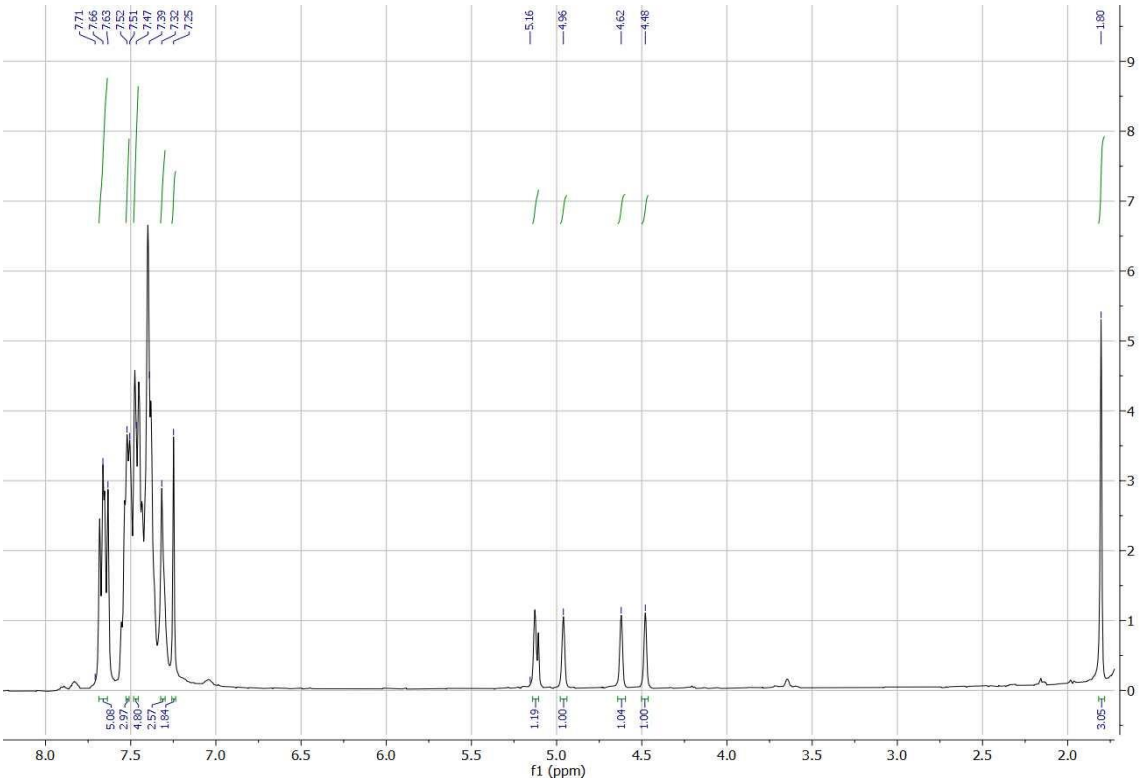

Figure 6.2.51: ^{1}H NMR spectrum of [Tc^{I}(NO)Cl(CpMe)(PPh_3)] in $CDCl_3$.

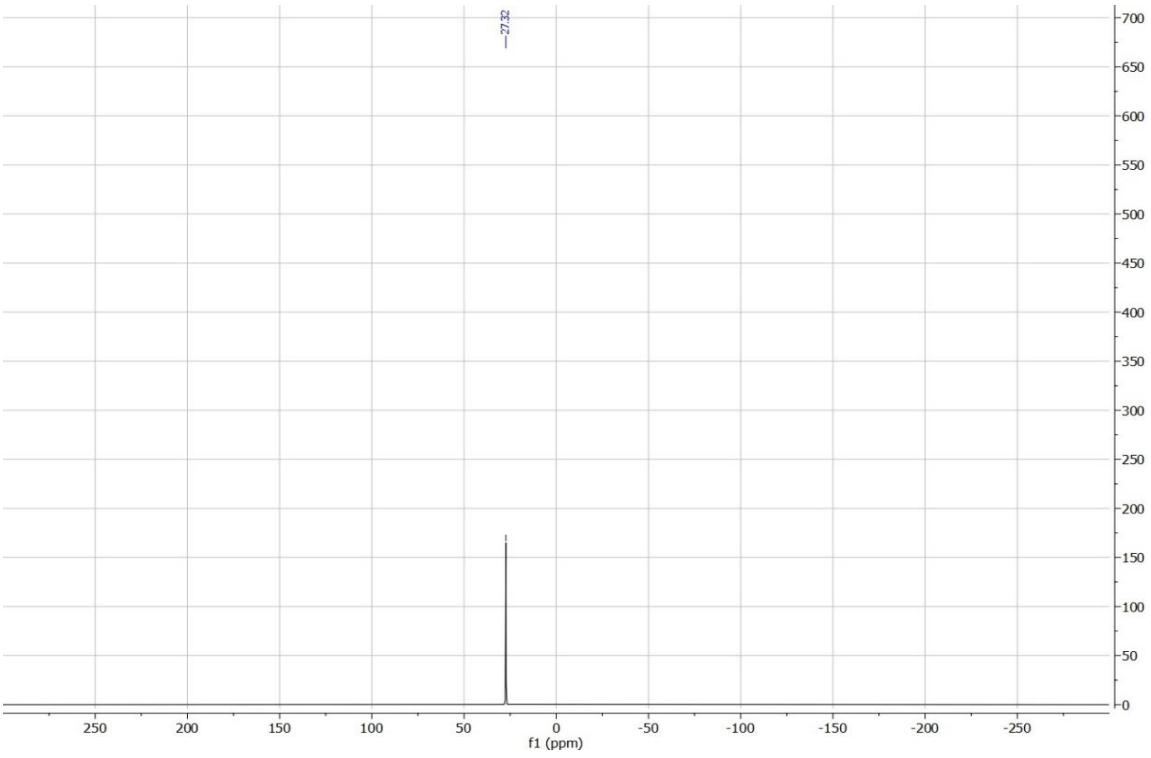

Figure 6.2.52: ^{31}P NMR spectrum of [Tc^{I}(NO)Cl(CpMe)(PPh_3)] in $CDCl_3$.

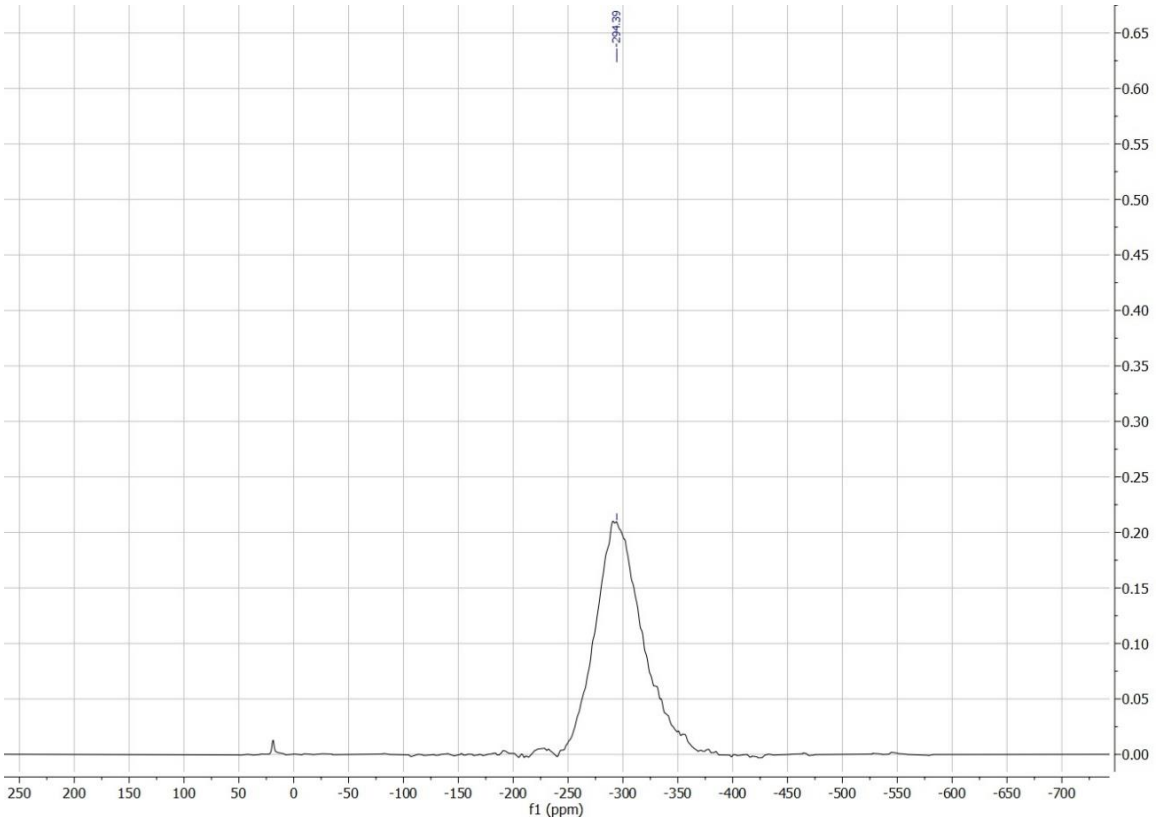

Figure 6.2.53: ^{99}Tc NMR spectrum of [Tc^{I}(NO)Cl(CpMe)(PPh$_3$)] in CDCl$_3$.

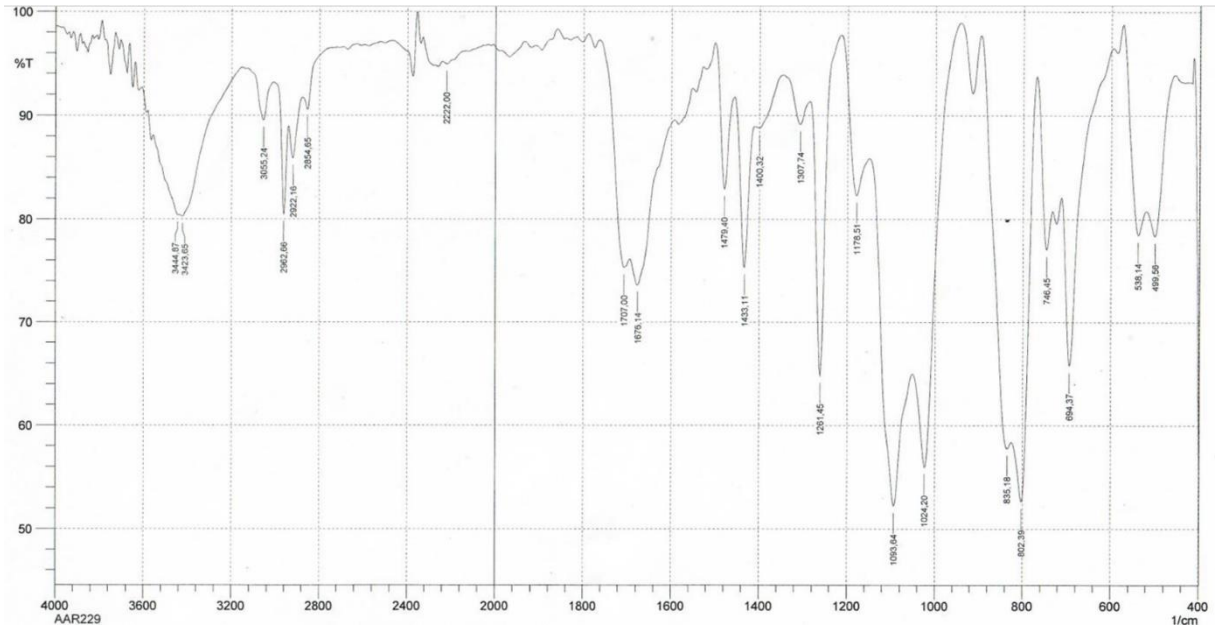

Figure 6.2.54: IR spectrum of [Tc^{I}(NO)Cl(CpMe)(PPh$_3$)].

6.2.14 Spectroscopic Data of $[Tc^{I}(NO)(CpMe)(PPh_3)(Py)](PF_6)$

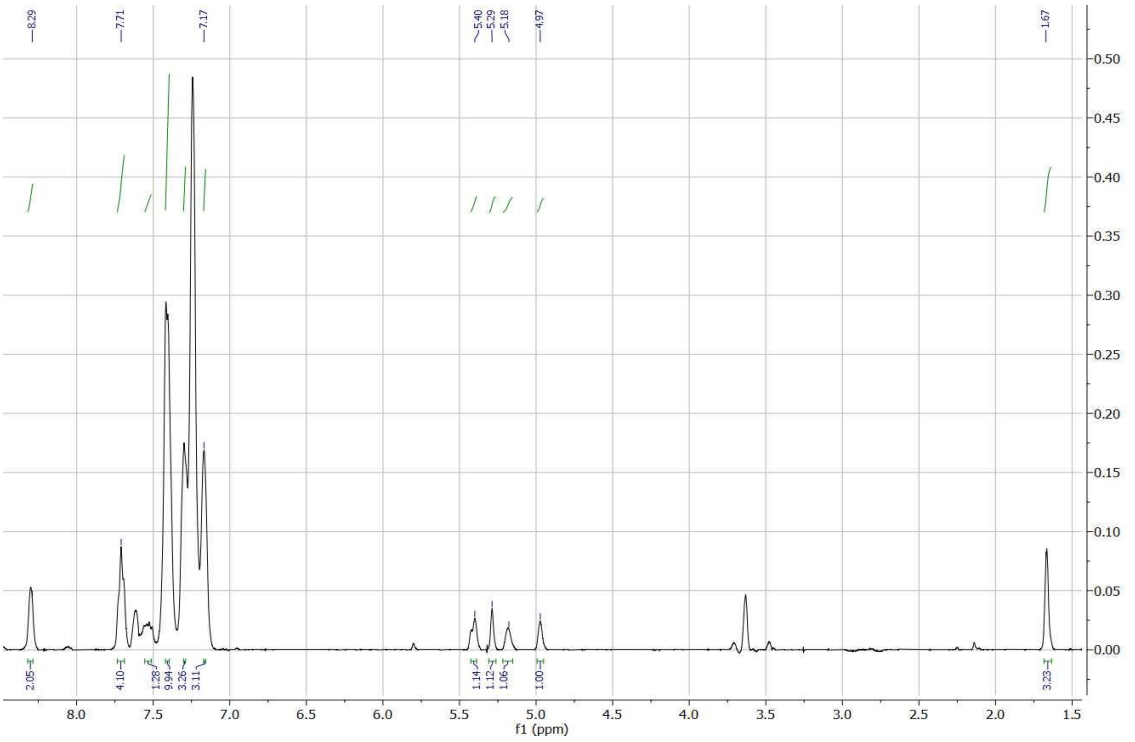

Figure 6.2.55: ^{1}H NMR spectrum of $[Tc^{I}(NO)(CpMe)(PPh_3)(Py)](PF_6)$ in $CDCl_3$.

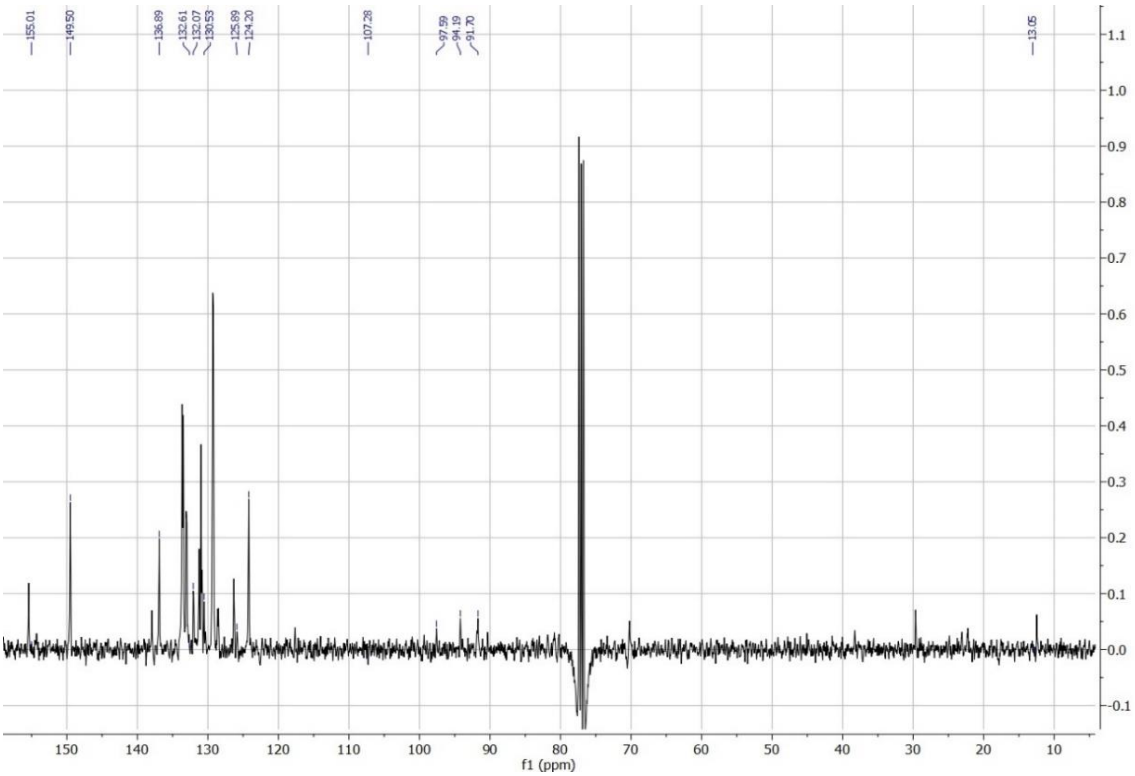

Figure 6.2.56: ^{13}C NMR spectrum of $[Tc^{I}(NO)(CpMe)(PPh_3)(Py)](PF_6)$ in $CDCl_3$.

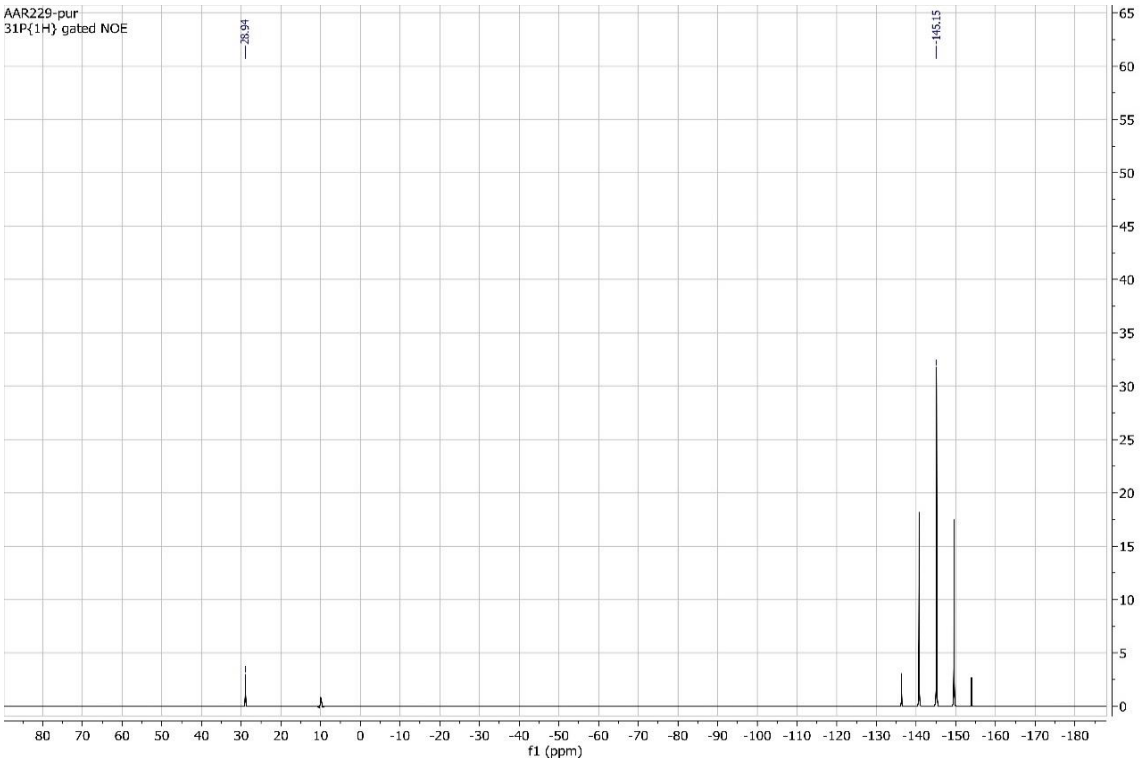

Figure 6.2.57: ^{31}P NMR spectrum of [Tc^{I}(NO)(CpMe)(PPh$_3$)(Py)](PF$_6$) in CDCl$_3$.

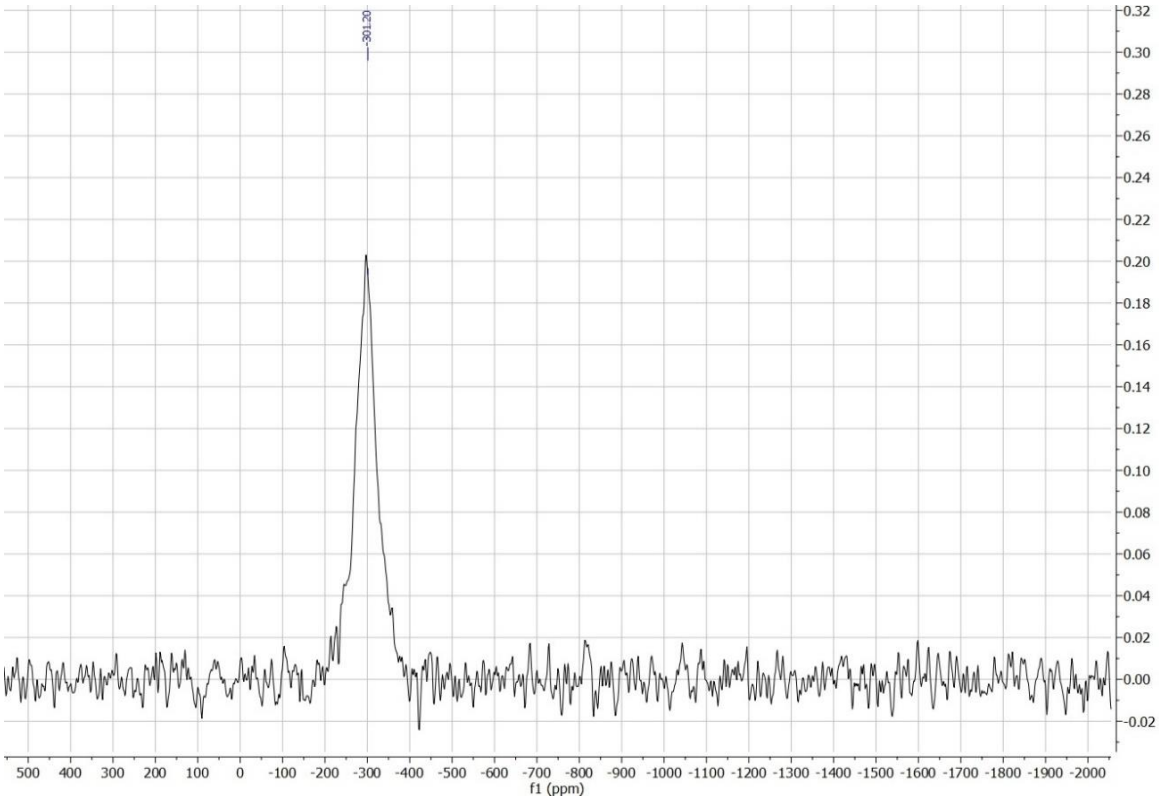

Figure 6.2.58: ^{99}Tc NMR spectrum of [Tc^{I}(NO)(CpMe)(PPh$_3$)(Py)](PF$_6$) in CDCl$_3$.

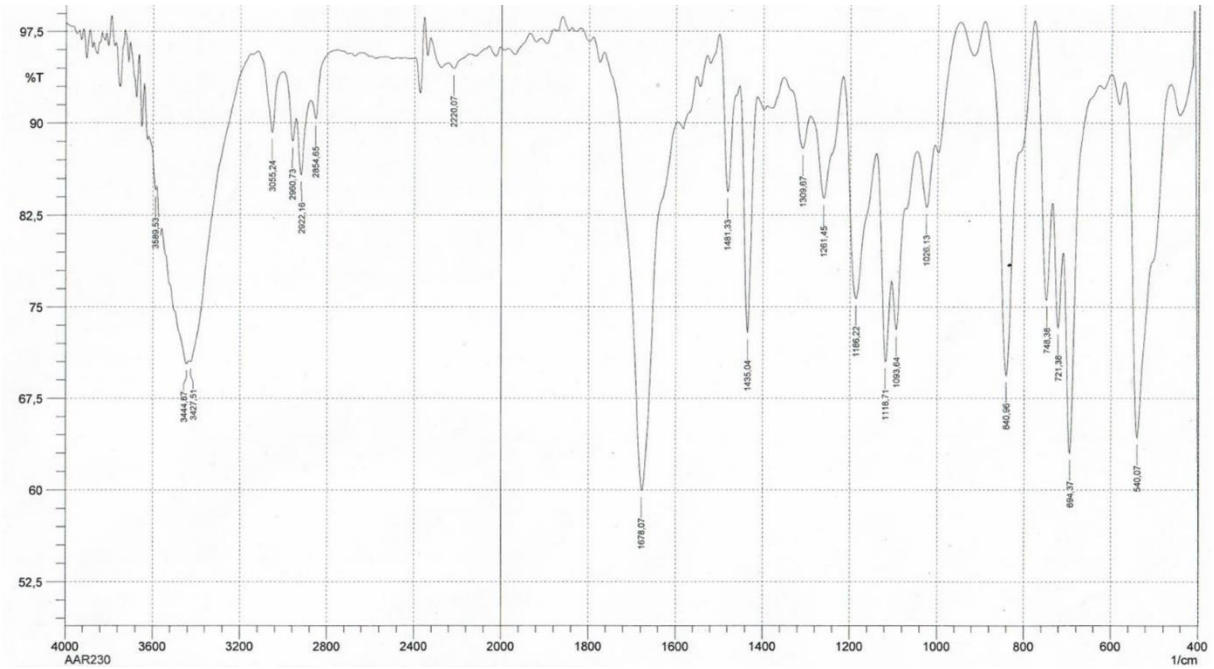

Figure 6.2.59: IR spectrum of $[Tc^{I}(NO)(CpMe)(PPh_3)(Py)](PF_6)$.

6.2.15 Spectroscopic data of [Tc^{I}(NO)Cl(CpCOOMe)(PPh_3)]

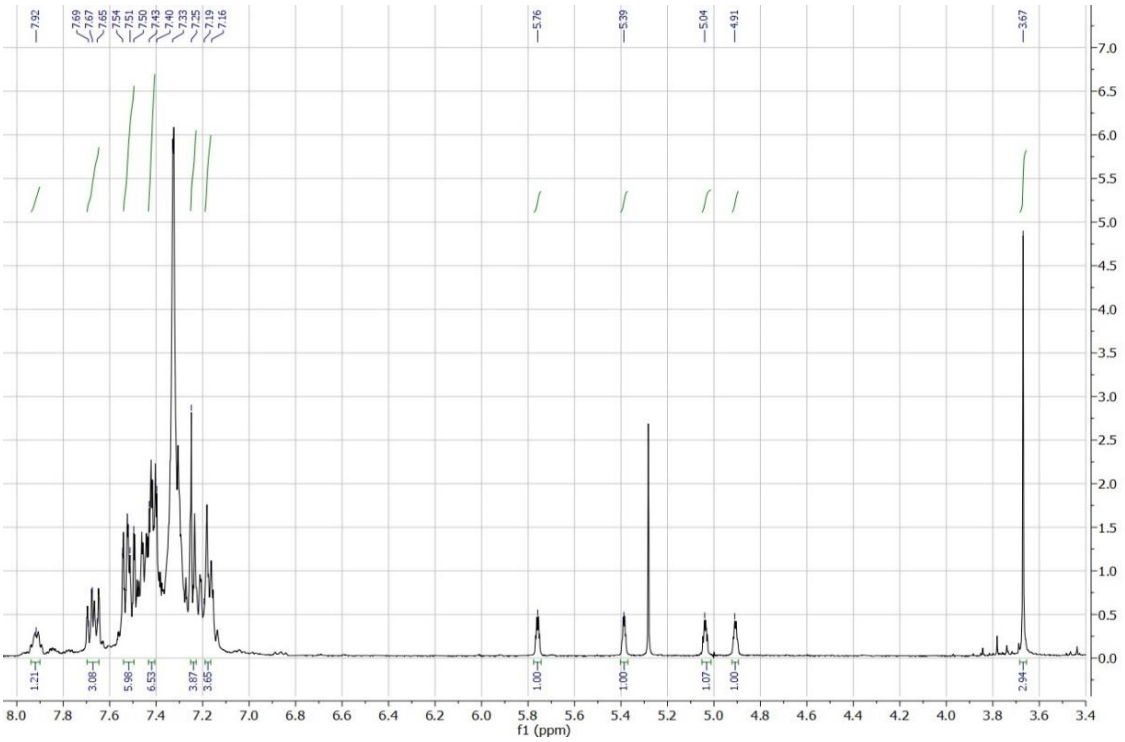

Figure 6.2.60: ^{1}H NMR spectrum of [Tc^{I}(NO)Cl(CpCOOMe)(PPh_3)] in $CDCl_3$.

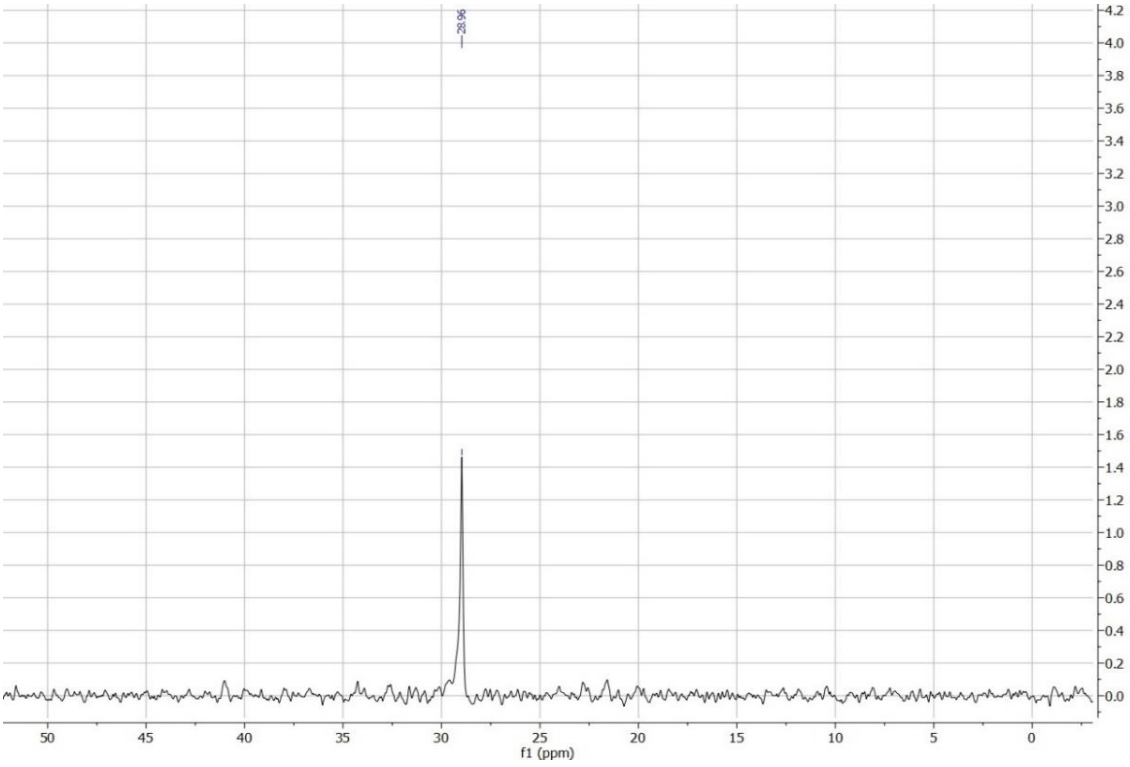

Figure 6.2.61: ^{31}P NMR spectrum of [Tc^{I}(NO)Cl(CpCOOMe)(PPh_3)] in $CDCl_3$.

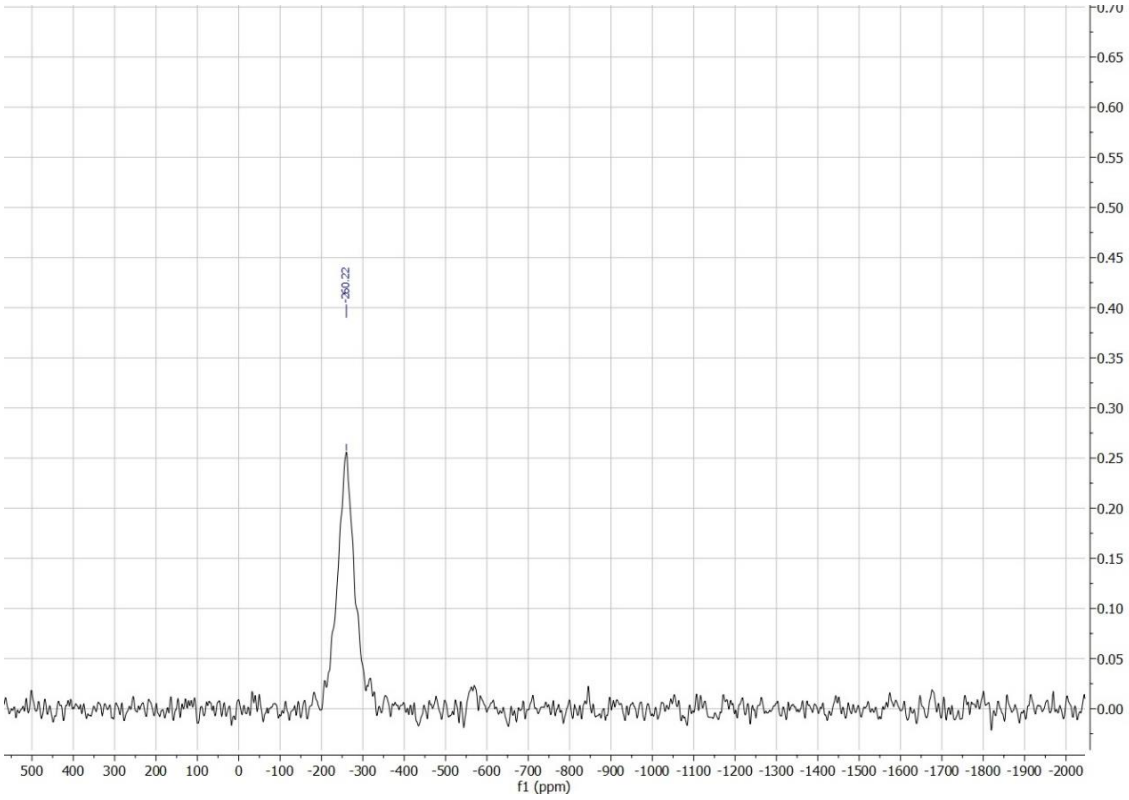

Figure 6.2.62: ^{99}Tc NMR spectrum of [Tc^{I}(NO)Cl(CpCOOMe)(PPh$_3$)] in CDCl$_3$.

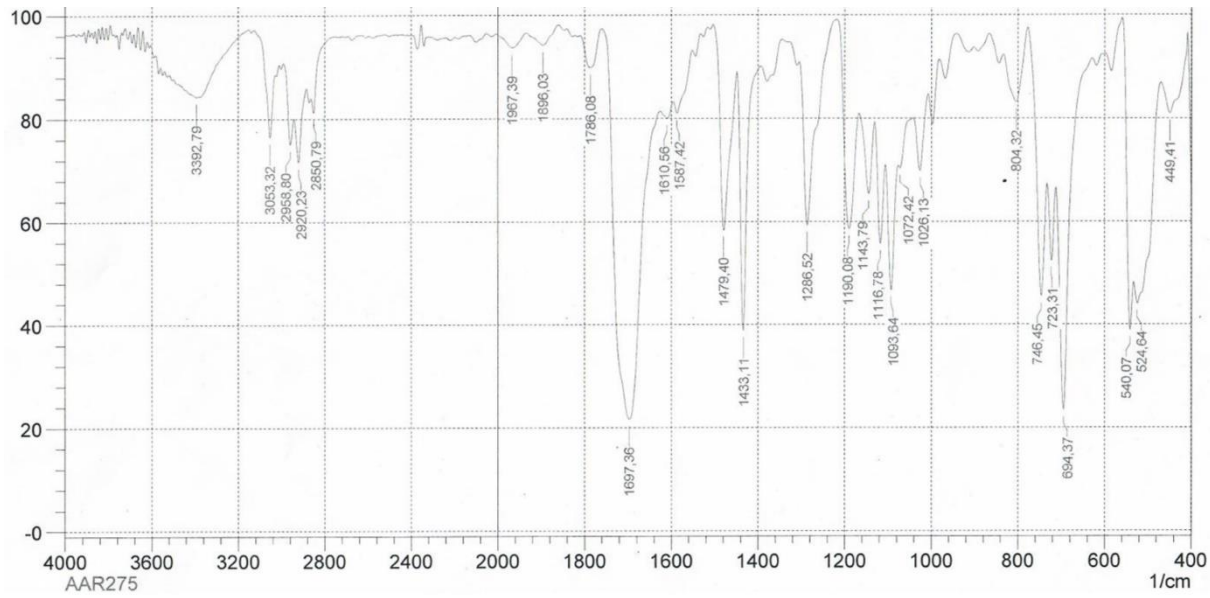

Figure 6.2.63: IR spectrum of [Tc^{I}(NO)Cl(CpCOOMe)(PPh$_3$)].